PALACKÝ UNIVERSITY OLOMOUC

Faculty of Science

Department of Biochemistry

Genetic transformation of fungi from the order Hypocreales

Ph.D. thesis

Author:	**Michaela Králová**
Study programme:	P1406 Biochemistry
Study branch:	Biochemistry
Form of study:	Full-time
Supervisor:	**prof. RNDr. Ivo Frébort, CSc., Ph.D.**
Rok:	2021

I hereby declare that this thesis has been written solely by myself and that all the sources used in this thesis are cited and included in the References.

In Olomouc .....

Michaela Králová

Acknowledgements

I want to thank

- To my supervisor prof. RNDr. Ivo Frébort, CSc. Ph.D. for his help with writing the manuscripts and to doc. Mgr. Petr Galuszka, Ph.D. for giving me the opportunity to work on *Claviceps* and *Fusarium* topics and for his leading during my first two years of the study.
- To Mgr. Josef Vrabka Ph.D. for his valuable advices and help with interpretation and discussion of obtained data.
- To Mgr. Aleš Pěnčík, Ph.D. (Department of Chemical Biology and Genetics, Centre of the Region Haná for Biotechnological and Agricultural Research, Palacký University Olomouc) for measurements of anthranilic acid.
- To Lena Studt (Department of Applied Genetics and Cell Biology, BOKU, Tulln, Austria) for help with *Fusaria* transformation.
- This work was supported by the ERDF project "Plants as a tool for sustainable global development" (No. CZ.02.1.01/0.0/0.0/16_019/0000827) and the grants IGA_PrF_2017 and IGA_PrF_2019_022 from the Palacký University Olomouc, Czech Republic.

Bibliografická identifikace

Jméno a příjmení autora	Michaela Králová
Název práce	Genetická transformace hub z řádu Hypocreales
Typ práce	Disertační
Pracoviště	Oddělení molekulární biologie, Centrum regionu Haná pro biotechnologický a zemědělský výzkum
Vedoucí práce	Prof. RNDr. Ivo Frébort, CSc. Ph.D.
Rok obhajoby práce	2021

Abstrakt

Houby z rodů *Claviceps* a *Fusarium* patřící do říše Hypocreales infikují zejména rostliny včetně ekonomicky významných plodin, jako jsou ječmen, pšenice a žito. Tato práce je zaměřena na námelovou houbu *Claviceps purpurea*, která v pozdějším stádiu infekce tvoří sklerocia obsahující vysoké množství námelových alkaloidů, sekundárních metabolitů, které našly uplatnění ve farmaceutickém průmyslu. Kromě *C. purpurea*, tato práce pojednává také o houbách z rodu *Fusarium, Fusarium graminearum, Fusarium pseudograminearum,* a *Fusarium oxysporum* f. sp. *medicaginis* které způsobují růžovění klasů obilovin, korunní hnilobu, hnilobu kořenů či Fusariové vadnutí. Navíc se v infikovaných částech rostliny tvoří toxické sekundární metabolity, například zearalenon, trichotheceny a fumonisiny.

První část této práce je zaměřena na houbu *C. purpurea* a její transformaci s cílem získat mutanty se zvýšenou produkcí námelových alkaloidů. Za tímto účelem byly v houbě *C. purpurea* P1, která produkuje alkaloidy v submerzních kulturách, exprimovány geny kódující WT formu a Trp-rezistentní formu α podjednotky anthranilát synthasy a gen kódující dimethylallyltryptofan synthasu fúzovaný s gfp. Následně byly v získaných mutantech měřeny primární a sekundární metabolity včetně námelových alkaloidů. Aby bylo potvrzeno, že *TrpE* opravdu kóduje funkční α podjednotku anthranilát synthasy, byl v houbě *C. purpurea* 20.1, jejíž genom byl sekvenován, tento gen deletován; zároveň byl připraven komplementant. U obou získaných mutantů byla popsána Trp auxotrofie a jejich infekčnost na rostlinách žita.

Druhá část této práce je zaměřena na nový nástroj pro úpravu genomu CRISPR/Cas9. Pomocí této metody byly v *C. purpurea* úspěšně mutovány geny *pyr4* kódující orotidin 5´-fosfát dekarboxylasu a *TrpE* kódující α podjednotku anthranilát synthasy. Navíc byla účinnost CRISPR/Cas9 metody porovnána s účinností dvou dalších metod, homologní delece zprostředkované CRISPR/Cas9 a delece založené na homologní rekombinaci. V případě hub s mutací v *TrpE,* byly u všech získaných mutantů sledovány Trp auxotrofie a jejich infekčnost na rostlinách žita.

Třetí část této práce pojednává o genetické transformaci hub z rodu *Fusarium, F. graminearum, F. pseudograminearum,* a *F. oxysporum* f. sp. *medicaginis.* Všechny tyto houby byly transformovány zeleným (*gfp*) a červeným (*dsRED* nebo *mCherry*) markerovým genem. *F.*

oxysporum f. sp. *medicaginis* bylo geneticky transformováno poprvé. Získaní mutanti budou použity na mikroskopické studie interakcí těchto patogenů s rostlinami.

Klíčová slova	*Claviceps purpurea*, CRISPR/Cas9, námelové alkaloidy, dimethylallyltryptofan synthasa, α podjednotka antranilát synthasy, uridin 5´fosfát dekarboxylasa, *Fusarium graminearum*, *Fusarium pseudograminearum*, *Fusarium oxysporum* f. sp. *medicaginis*, gfp, mCherry, dsRED
Počet stran	197
Počet příloh	-
Jazyk	Anglický

Bibliographical identification

Author's first name and surname	Michaela Králová
Title	Genetic transformation of fungi from the order Hypocreales
Type of thesis	Ph.D. thesis
Department	Department of Molecular Biology, Centre of the Region Haná for Biotechnological and Agricultural Research
Supervisor	Prof. RNDr. Ivo Frébort, CSc. Ph.D.
The year of presentation	2021

Abstract

Fungi from the genus *Claviceps* and *Fusarium* belonging to the order Hypocreales parasite predominantly on plants including economically important crops such as barley, wheat, and rye. This work is focused on ergot fungus *Claviceps purpurea*, that produces in the late stages of infection sclerotia containing high amount of ergot alkaloids, secondary metabolites used in pharmacy. In addition to *C. purpurea*, this work also deals with three fungi from the genus *Fusarium*, *Fusarium graminearum*, *Fusarium pseudograminearum*, and *Fusarium oxysporum* f. sp. *medicaginis* that cause Fusarium head blight, crown rot, root rot, and wilting. Moreover, toxic secondary metabolites such as zearalenone, trichothecenes, and fumonisins are formed during the infection.

The first part of this thesis is focused on *C. purpurea* and its transformation to obtain fungal mutants with increased ergot alkaloid production. Thus, genes encoding WT form and Trp-resistant form of α-subunit of anthranilate synthase, and dimethylallyltryptophan synthase fused with gfp were expressed in *C. purpurea* strain P1 that produces ergot alkaloids in submerged cultures. Later, primary and secondary metabolites including ergot alkaloids were measured in all obtained *C. purpurea* P1 transformants. Moreover, to confirm that *TrpE* really encodes a functional α-subunit of anthranilate synthase, knock-out mutant of this gene and complemented strain were prepared in genome-sequenced *C. purpurea* strain 20.1. In both mutants, Trp auxotrophy and pathogenicity on rye plants were described.

The second part of this thesis is focused on a new genome editing technology called CRISPR/Cas9. Using this method, two genes *pyr4* and *TrpE* encoding orotidine 5´-phosphate decarboxylase and α-subunit of anthranilate synthase, respectively were successfully targeted in *C. purpurea*. Moreover, the transformation efficiency of this method was compared to those obtained from CRISPR/Cas9-mediated HDR and the classical gene knock-out approach based on HR. In the case of fungi with a mutation in *TrpE* Trp auxotrophy and pathogenicity on rye plants were assessed.

The third part of this thesis deals with the transformation of three different fungi from the genus *Fusarium*, *F. graminearum*, *F. pseudograminearum*, and *F. oxysporum* f. sp. *medicaginis*. All

fungi were transformed with green (*gfp*) and red (*dsRED* or *mCherry*) reporter marker genes. Moreover, *F. oxysporum* f. sp. *medicaginis* infecting *Medicago* plants was genetically transformed for the first time. Obtained fungi will be used for the microscopic study of plant-pathogen interactions.

Keywords	*Claviceps purpurea*, CRISPR/Cas9, ergot alkaloids, dimethylallyltryptophan synthase, α subunit of anthranilate syntnase, uridine 5´-phosphate decarboxylase, *Fusarium graminearum*, *Fusarium pseudograminearum*, *Fusarium oxysporum* f. sp. *medicaginis*, gfp, mCherry, dsRED
Number of pages	197
Number of appendices	-
Language	English

Content

1 Objectives

1. Genetic transformation of *C. purpurea* to obtain mutants with higher ergot alkaloids production
    - Obtain *C. purpurea* P1 expressing WT form of α-subunit of anthranilate synthase (TrpE), Trp-resistant form of α-subunit of anthranilate synthase (TrpE*S*76L), and dimethylallyltryptophan synthase (DMATS) fused with GFP; measure primary and secondary metabolites
    - Prepare knock-out mutant of *C. purpurea* 20.1 lacking gene encoding α-subunit of anthranilate synthase and its complemented strain; test Trp auxotrophy and pathogenicity

2. Use of CRISPR/Cas9 tool for genetic transformation of *C. purpurea*
    - Prepare *C. purpurea* 20.1 transformants with a mutation in *pyr4* and *TrpE* encoding uridine 5´-monophosphate decarboxylase and α-subunit of anthranilate synthase, respectively using CRISPR/Cas9; check the auxotrophy
        - Remove AMA1-based vector from *CRISPR/Cas9 TrpE C. purpurea* 20.1
    - Compare transformation efficiencies of CRISPR/Cas9 method with CRISPR/Cas9-mediated gene knock-out and classical knock-out approach based on HR
        - Prepare *C. purpurea* 20.1 mutants lacking gene encoding α-subunit of anthranilate synthase by CRISPR/Cas9-mediated gene knock-out and classical knock-out approach based on HR, calculate transformation efficiencies; check Trp auxotrophy and pathogenicity on rye plants

3. Genetic transformation of *F. graminearum*, *F. pseudograminearum*, and *F. oxysporum* f. sp. *medicaginis* with green and red reporter marker genes

2 The current state of knowledge

2.1 Genetic transformation of filamentous fungi

In general, the genetic transformation represents a method by which an exogenous DNA is transferred into a host cell. The first successful transformation of a filamentous fungus, specifically *Neurospora crassa*, has been described in 1973 (Mishra *et al*., 1973) and since this time many different fungal species including *Aspergillus* sp. (Tiburn *et al*., 1983; Christensen *et al*., 1988), *Fusarium* sp. (Kistler and Benny, 1988; Covert *et al*., 2001), and *Claviceps* sp. (van Engelenburg *et al*., 1989; Kozák *et al*., 2018) have been transformed.

2.1.1 Transformation methods

Although many different approaches such as protoplast-mediated transformation (PMT), *Agrobacterium*-mediated transformation (AMT), electroporation, and biolistic transformation have been applied to different filamentous fungi, there are still some strains for which the transformation does not work or the transformation efficiency is very low (Meyer, 2008).

2.1.1.1 Protoplast-mediated transformation

Protoplast-mediated transformation (PMT) is a method that is based on the preparation of fungal protoplasts from young mycelia (Dooijewaard-Kloosterziel *et al*., 1973; Keller *et al*., 1980) or germinating conidia (Moore and Peberdy, 1976; Bos and Slakhorst, 1981). To generate fungal protoplasts, cell wall components have to be removed, usually, enzymes such as lysing enzyme from *Trichoderma harzianum* (Oeser *et al*., 2002), driselase (Ramamoorthy *et al*., 2015), lyticase (Brzezinska-Rodak *et al*., 2016), or yatalase (Matsuzaki *et al*., 2017) are used. Because generated protoplasts are osmotically sensitive, they have to be protected. For this reason, their incubation takes place in solutions containing sodium chloride, magnesium sulphate, sorbitol, mannitol, or sucrose. Once protoplasts are formed, they are incubated together with exogenous DNA, calcium chloride, and polyethylene glycol (PEG). PEG induces fusion of protoplasts, alters the membrane permeability, and thus facilitates the uptake of exogenous DNA, calcium ions form channels or pores in the cell membrane allowing the entry of DNA (Anne and Peberdy, 1975). After the incubation with DNA, calcium

chloride, and PEG, protoplasts are transferred to regeneration media without a selection pressure or containing a low concentration of antibiotics. A few days later, fungal mycelia are transferred to selection agar plates.

2.1.1.2 *Agrobacterium*-mediated transformation

Recently, *Agrobacterium*-mediated transformation (AMT) that provides higher transformation efficiency than commonly used PMT (de Groot *et al*., 1998; Amey *et al*., 2002; Fitzgerald *et al*., 2003) has been successfully applied to various fungal species including *Aspergillus* sp. (Sugui *et al*., 2005; Michielse *et al*., 2008), *Fusarium* sp. (Mullins *et al*., 2001; Sørensen *et al*., 2014), *N. crassa*, *Trichoderma reesei* (de Groot *et al*., 1998), and *C. paspali* (Kozák *et al*., 2018). Compared to PMT, no protoplast preparation and regeneration are required; moreover, by using this approach only a single copy of the T-DNA is inserted into the fungal genome. In contrast to PMT, any material including conidia (Mullins *et al*., 2001), hyphal tissue (Sharma and Kuhad, 2010), fruit body tissue (Chen *et al*., 2000), or even protoplasts (de Groot *et al*., 1998) can be used.

In principle, AMT is based on *Agrobacterium tumefaciens*-mediated transfer of DNA (T-DNA) that is located on bacterial tumor-inducing (Ti) plasmid. Except for T-DNA that is surrounded by 25 bp repeat sequences (so-called left and right borders), Ti plasmid contains *vir* region consisting of *vir* genes that are necessary for successful cleavage, transfer, and integration of T-DNA into a host genome.

2.1.1.3 Electroporation

In addition to PTM and AMT, electroporation has also been used to transform various filamentous fungi, for example, *Aspergillus* sp. (Ozeki *et al*., 1994; Sánchez and Aguirre, 1996; Meyer *et al*., 2003), *Colletotrichum gloeosporioides* (Robinson and Sharon, 1999), and *T. harzianum* (Goldman *et al*., 1990). This relatively simple and rapid technique is based on an electrical pulse that lasts only a few microseconds or milliseconds that is applied to form temporary micropores that allow the uptake of exogenous DNA in the cell membrane. Using this approach factors such as the intensity of the electric field, pulse duration, frequency, capacitance, the composition of buffer solution and the amount of DNA affect the transformation efficiency and usually have to be optimized.

2.1.1.4 Biolistics

Although a biolistic method was originally developed for plants (Klein *et al*., 1987), it has been also used to transform different filamentous fungi (Lorito *et al*., 1993; Barcellos *et al*., 1998). In this approach, an exogenous DNA covered by tungsten or gold particles is delivered into a fungal cell by high pressure created by a gene gun or biolistic particle delivery system. In general, there are many factors such as the type of fungal cells, size of particles, or level of pressure that may influence the transformation efficiency.

2.1.2 Marker genes

As the transformation efficiency of fungal cells is usually quite low, it is necessary to separate fungal transformants containing an exogenous DNA from non-transformed wild type (WT) cells. In general, this selection is achieved by using a marker gene, usually an auxotrophic or drug resistance gene.

2.1.2.1 Auxotrophic markers

Initially, the transformation of fungal strains was based on their reversion toward the WT phenotype (so-called prototroph), thus fungal mutants auxotrophic to different compounds such as uracil or uridine (Berges and Barreau, 1991), methionine (Anaya and Roncero, 1991), or adenine (Alic *et al*., 1989) were complemented by the corresponding WT gene.

Today, many different auxotrophic markers including *argB*, *adeA*, *adeB*, and *trpC* genes are available (Buxton *et al*., 1985; Goosen *et al*., 1989; Jin *et al*., 2004). Briefly, when *argB* encoding ornithine carbamoyltransferase involved in arginine biosynthesis is transformed into the genome of $argB^-$ fungal strain, arginine prototrophs are selected (Buxton *et al*., 1985). Similarly, when a vector containing *adeA* or *adeB* that encode phosphoribosylaminoimidazolesuccinocarboxamide synthase and phosphoribosyl-aminoimidazole carboxylase, respectively, both involved in purine biosynthesis, is transformed into adenine auxotrophs, adenine prototrophs are obtained (Jin *et al*., 2004). Lastly, *TrpC* encoding a trifunctional enzyme involved in Trp biosynthesis is frequently used for the selection of Trp prototrophs (Goosen *et al*., 1989).

Except for auxotrophic markers described above, a special group of markers so-called two-way selection systems that allow both positive and negative selections exist. The most popular two-way selection system *pyr4/pyrG* is based on resistance to

5-fluoroorotic acid (5-FOA), a fluorinated derivative of pyrimidine precursor orotic acid. By using this compound, uracil and/or uridine auxotrophs resistant to 5-FOA that can be further complemented with *pyr4/pyrG* gene encoding orotidine 5´-phosphate decarboxylase (OMPD) can be prepared. Thus, by using this approach, *pyrG/pyr4*$^-$ mutants resistant to 5-FOA and exhibiting auxotrophy to uracil and/or uridine (negative selection) and complemented *pyrG/pyr4*$^+$ mutants sensitive to 5-FOA (positive selection) can be obtained on media supplemented with uracil and/or uridine and 5-FOA, and media deficient in uracil and/or uridine, respectively. As this selection is quite simple, it has already been successfully applied to many different filamentous fungi including *Aspergillus* sp. (Oakley *et al*., 1987; Van Hartingsveldt *et al*., 1987), *Trichoderma* sp. (Cheng *et al*., 1990; Gruber *et al*., 1990), *Penicillium* sp. (Diez *et al.*, 1987; Navarrete *et al*., 2009), and *C. purpurea* (Smit and Tudzynski, 1992). Interestingly, a recyclable *pyrG*-blaster system that is based on using *pyrG* flanked by two small direct repeat sequences derived from the neomycin phosphotransferase gene (*neo*) and 5´ and 3´flanking sequences of the target gene has been developed and applied to *A. fumigatus* (d´Enfert, 1996). Once an *ura*$^-$ strain is transformed with this cassette, *pyrG* becomes excised by homologous recombination between *neo* sequences, returning the transformants to uracil phototrophy. Thus, these transformants can be further selected in the presence of 5-FOA and can be re-transformed with another vector carrying the blaster cassette.

Another example of a two-way selection that has been utilized in *Aspergillus* sp. (Campbell *et al*., 1989; Horng *et al*., 1990), *Penicillium* sp. (Whitehead *et al*., 1989; Navarrete *et al*., 2009), and *Fusarium oxysporum* (Diolez *et al*., 1993) is *niaD* system that is based on resistance to chlorate. Mutants affected in nitrate reductase activity can be then obtained on media supplemented with nitrate. Another two-way selection system that is also frequently used in *Aspergillus* sp. (De Lucas *et al*., 2001; Varadarajalu *et al.*, 2005; Adachi *et al*., 2009) is based on resistance to selenate. In this approach, only mutants lacking *sC* gene encoding ATP-sulphurylase that allows fungi to utilize sulphate can grow on media supplemented with methionine. Except for *pyr4/pyrG*, *niaD,* and *sC* selection systems, fluoroacetate selection of mutants impaired in acetyl CoA synthetase (Garre *et al*., 1996) and fluoroacetamide selection of mutants affected in *amdS* gene (Kelly and Hynes, 1985; Beri and Turner, 1987) are available.

2.1.2.2 Drug resistance markers

Although auxotrophic markers provide high transformation efficiency, their use is quite limited especially when industrial fungal strains are transformed. For this reason, dominant drug selection markers, genes that encode enzymes conferring resistance to different antibiotics, herbicides, or fungicides, are very often used for fungal transformation. In contrast to auxotrophic markers, these genes are usually heterologous, thus they are codon-optimized and placed between a fungal promoter and terminator.

The most commonly used drug resistance markers include *hph* gene providing resistance to aminoglycosidic antibiotic hygromycin B (Punt *et al.* 1987; Kistler and Benny, 1988; Comino *et al*., 1989) and *ble/sh-ble* gene allowing the preparation of mutants resistant to glycopeptide antibiotic bleomycin/phleomycin (van Engelenburg *et al*., 1989; Austin *et al*., 1990). Additionally, *nat1* gene conferring the resistance to antibiotic nourseothricin (Kuck and Hoff, 2006) and *neo* gene that provides resistance to neomycin (Noël *et al*., 1995) can be used for the selection of fungal transformants. Except for these drug resistance markers, *bar* gene encoding resistance to herbicide Bialaphos (Avalos *et al*., 1989; Ma *et al*., 2003), *CbxR* gene providing resistance to fungicide carboxin (Honda *et al*., 2000), and *tub2* gene allowing the selection of fungi resistant to fungicide benomyl (Orbach *et al*., 1986; Panaccione *et al*., 1988) are quite often used.

2.1.2.3 Visual proteins

Besides auxotrophic and drug resistance markers, visual proteins such as β-glucuronidase encoded by *GUS* genes, β-galactosidase encoded by *lacZ* gene, and fluorescent proteins are frequently used in filamentous fungi. For GUS assay that has been successfully applied to various fungal species including *Aspergillus flavus* (Flaherty *et al*., 1995), *T. harzianum* (Bae *et al*., 2000), *F. oxysporum* (Counteaudier *et al*., 1993), and *C. purpurea* (Smit and Tudzynski, 1992), three different substrates can be utilized. While 5-bromo-4-chloro-3-indolyl glucuronide (X-Gluc) allows histochemical staining (Couteaudier *et al*., 1993), *p*-nitrophenyl-β-D-glucuronide (PNPG), and 4-methylumbelliferyl-β-D-glucuronide (MUG) are used for spectrophotometric (Fan *et al*., 2001) and fluorimetric (Smit and Tudzynski, 1992) assays, respectively.

Numerous constructs containing *lacZ* gene have been prepared and successfully transformed into filamentous fungi (Wernars *et al*, 1987; Kolar *et al*., 1988). In colorimetric β-galactosidase assay (so-called blue-white screening), the enzyme

cleaves a glycosidic bond in a chromogenic substrate 5-bromo-4-chloro-3-indolyl-β-D-galactopyranoside (X-gal) and produces galactose and 5-bromo-4-chloro-3-hydroxyindole which dimerizes and oxidizes to a blue product 5,5´-dibromo-4,4´-dichloro-indigo. Moreover, the production of this blue compound is induced by isopropyl β-D-1-thiogalactopyranoside (IPTG) that binds to *lac* repressor and releases it from the *lac* operator, thus allowing the transcription of *lacZ* gene. Except for X-gal, also MUG can be used as a substrate for β-galactosidase. In this case, the production of the fluorophore is monitored.

Furthermore, genes encoding fluorescent proteins can be used to study the plant-pathogen interactions (Maor *et al*., 1998; Oren *et al*., 2003). Alternatively, these genes can be fused to the C- or N- terminus of the target protein, thus allowing the protein localization or specific organelle labelling (Cormack, 1998; Breakspear *et al*., 2007). Today, many different fluorescent proteins including a monomeric green fluorescent protein GFP (Shimomura *et al*., 1962), a tetrameric red fluorescent protein dsRED (Matz *et al*., 1999), mCherry, mOrange, dTomatoor mStrawberry (Shaner *et al*., 2004) are used.

Recently expression vectors containing GFP, mCherry, or dsRED under the control of strong constitutive *OliC* promoter from *A. nidulans* have been prepared and used to transform *Botrytis cinerea* (Schumacher, 2012). Although these vectors were initially developed for this fungus, they have already been successfully transformed also into *F. fujikuroi* (Studt *et al*., 2013a) and *C. purpurea* (Hinsch *et al*., 2016).

2.1.3 Fate of DNA

In fungal transformants exogenous DNA can be inserted into the chromosomes or it can be delivered into a fungal cell as a plasmid containing its origin of replication.

2.1.3.1 Autonomously replicating plasmids

Autonomously replicating plasmids are usually unstable under nonselective conditions and contain autonomously replicating sequences (ARSs). Although it has been demonstrated that vectors containing ARSs provide high transformation efficiencies in yeasts (Boretsky *et al*., 1999), only a few filamentous fungi have been successfully transformed with these vectors (Wright and Philippsen, 1991). Thus, a sequence homologous to ARS of *S. cerevisiae* has been isolated from *U. maydis* (Tsukuda *et al*., 1988) and used for the transformation of this fungus. As expected, the transformation

efficiency was increased; however, almost 20 % of transformed fungal cells after 15 generations still contained this plasmid (Tsukuda *et al.*, 1988). For this reason, ARSs from other fungi, for example, *Mucor circinelloides* (van Heewijck, 1986; Roncero *et al.*, 1989) and *A. nidulans* (Gems *et al.*, 1991) have been isolated. Interestingly, ARS from *A. nidulans* named AMA1 (autonomous maintenance in *Aspergillus*) with a size of 6 kb, has been successfully used for transformation of various filamentous fungi including *Aspergillus* sp. (Khalaj *et al.*, 2007; Nødvig *et al.*, 2015; Weyda *et al.*, 2017; Katayama *et al.*, 2019), *Giberella fujikuroi* (Brücker *et al.*, 1992), and *P. chrysogenum* (Fierro *et al.*, 1996).

2.1.3.2 Integration of exogenous DNA into a fungal genome

In general, two repair mechanisms of double-stranded DNA break (DBS) exist in filamentous fungi, non-homologous end-joining (NHEJ) system, and homologous recombination (HR) (Doherty and Jackson, 2001). As filamentous fungi have employed a powerful NHEJ system, usually an ectopic insertion of exogenous DNA can be observed; however, when exogenous DNA is flanked by regions homologous to the target DNA, HR takes place.

Concerning NHEJ (Fig. 1), DNA-dependent protein kinase (DNA-PK), DNA ligase IV-XRCC4 complex, and Artemis nuclease are involved in this process. The main component, DNA-PK, consists of the catalytic subunit DNA-PKcs and Ku70-Ku80 heterodimer, the first protein that binds the broken DNA ends, probably to prevent the nuclease attack (Walker *et al.*, 2001a; Spagnolo *et al.*, 2006). Then DNA-PKcs is recruited (Hammarsten and Chu, 1998), Ku70-Ku80 heterodimer is translocated into the DNA (Yoo and Dynan, 1999) and DNA-PKcs phosphorylates many other proteins including Artemis that is recruited to the damage site (Ma *et al.*, 2002) and Xrcc4 that stimulates the ligation activity of DNA ligase IV (Grawunder *et al.*, 1997; Sibanda *et al.*, 2001). Finally, DNA ends are re-ligated and a single DNA molecule is formed.

To increase the transformation efficiency, NHEJ-deficient fungal strains lacking *Ku70* or *Ku80* genes have been prepared and used for gene knock-out in filamentous fungi. Interestingly, in *Aspergillus fumigatus* homologous integration frequency (HIF) reached 96 % in *Δku70* (Krappmann *et al.*, 2006) and 80 % in *Δku80* (da Silva Ferreira *et al.*, 2006) compared to only 5-10 % in WT strain. Concerning other *Aspergilli*, HIF in WT strains of *A. nidulans*, *A. oryzae*, and *A. sojae* reaches only 38 %, 11 %, and 1.4 %,

while it increased to 89 %, 63 %, and 75 %, respectively in *Δku70* mutants (Nayak *et al.*, 2006; Takahashi *et al*., 2006).

Except for *Aspergillus* sp., NHEJ-deficient strains have been prepared also in *N. crassa* (Ninomiya *et al*., 2004) and *C. purpurea* (Haarmann *et al*., 2008). While HIF reaches only 1-2 % in *C. purpurea* (Oeser *et al*., 2002), this frequency was increased up to 50-60 % in *Δku70* mutant (Haarmann *et al*., 2008). However, this mutant was found to be affected in the growth and infection rate, thus it has never been used for further transformation (Hinsch and Tudzynski, 2015).

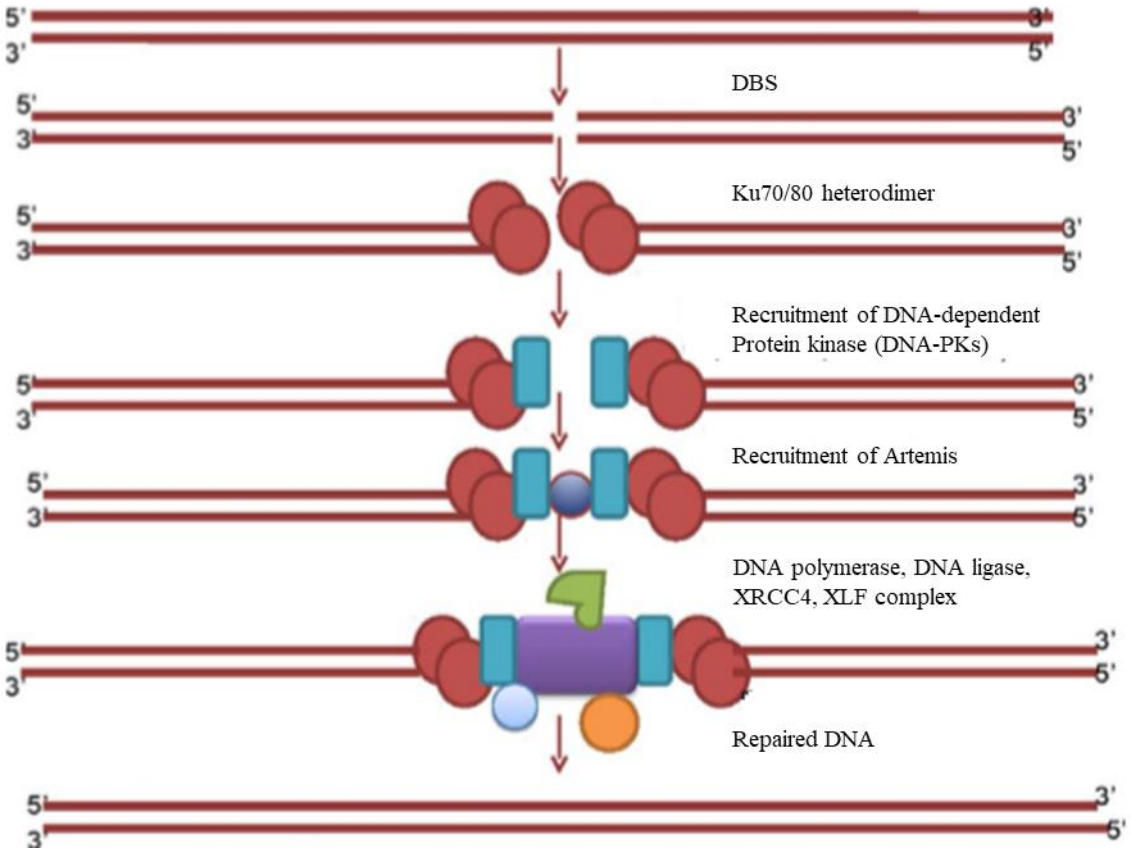

Fig. 1 Repair of double-stranded DNA break by using NHEJ mechanism (Ulaganathan *et al*., 2017).

2.1.3.3 Application of transformation

2.1.3.4 Gene expression

Vectors for gene expression usually contain a promoter, target gene, and terminator; moreover, the marker gene is present. For localization study or purification of the translated protein, a tag such as a gene encoding a fluorescent protein (Lorenz *et al*., 2010; Albermann *et al*., 2013), His-tag (Matuschek *et al*., 2011) or FLAG-tag (Oka *et al*., 2014) can be included. Concerning filamentous fungi, strong constitutive promoters for example P*gpdA* (glyceraldehyde-3-phosphate dehydrogenase), P*oliC* (subunit 9 of mitochondrial ATP synthase), and P*trpC* (a trifunctional enzyme involved in Trp biosynthesis) are frequently used (Lorenz *et al*., 2010; Studt *et al*., 2013b; Jørgensen *et al*., 2014; Hinsch *et al*., 2016). Except for constitutive promoters, inducible promoters P*ben*, P*xyl1*, and P*sorA/B* that can be activated by benzoate, xylan/xylose, and sorbitol, respectively have already been utilized to drive gene expression in filamentous fungi (Blatzer *et al*., 2014; Antunes, 2003; Oda *et al*., 2016).

2.1.3.5 Gene deletion

2.1.3.5.1 Gene replacement mediated by HR

Gene replacement mediated by HR is one of the most used knock-out approaches in filamentous fungi (Rolke and Tudzynski, 2008; Yang *et al*., 2016). In this method, a target gene is replaced by a cassette containing a resistance marker gene together with its promoter and terminator; moreover, this cassette is flanked by approximately 1 kb sequences homologous to 5´and 3´ regions of the target DNA. Although this approach is very often used, HIF is in filamentous fungi usually quite low, thus hundreds of primary transformants have to be screened.

Among the classical knock-out approach described above when many of primary transformants including false-positive fungi containing an ectopic insertion of exogenous DNA have to be screened, a split marker method has gained popularity (Goswami, 2012; Chung and Lee, 2015). In this approach, initially developed for *S. cerevisiae* (Fairhead *et al*., 1996), the resistance cassette is amplified by PCR in two parts, each containing a part of the marker gene fused to one flanking region. After that, both PCR products are transformed into fungal protoplasts, three HR events take place, and only transformants

containing a functional marker gene grow under selection pressure. This approach has already been applied to *Aspergillus* sp. (Gravelat *et al*., 2012; Arentshorst *et al*., 2015), *F. oxysporum* (Liang *et al*., 2014), and *C. purpurea*. Unfortunately, in the case of *C. puepurea*, positive results have been obtained only with hygromycin resistance cassette (Oeser *et al*., 2017; Kind *et al*., 2018).

2.1.3.5.2 Gene editing by CRISPR/Cas9

Recently, new genome editing technology called CRISPR/Cas (Clustered Regularly Interspaced Short Palindromic Repeat/CRISPR Activated System) (Doudna and Charpentier, 2014) has been used for directed mutagenesis in filamentous fungi (Nielsen et al., 2017; Nødvig *et al*., 2015; Schuster *et al*., 2016).

This approach uses only two components, Cas protein, usually Cas9, and guide RNA (gRNA) that consists of two RNAs, crRNA (CRISPR RNA), and tracrRNA (transactivating CRISPR RNA) (Nishimasu *et al*., 2014) (Fig. 2). Alternatively, a chimeric single guide RNA (sgRNA) can be used (Jinek *et al*., 2012). Targeting of the RNA-guided Cas9 is achieved by protospacer sequence (Gasiunas *et al*., 2012) and the cleavage efficiency of double-stranded DNA depends on the presence of 3 bp PAM (Protospacer Adjacent Motifs) sequence (Mojica *et al*., 2009). The double-stranded DNA break can be repaired NHEJ repairing system leading to small insertions/deletions or HR when a donor DNA template is used (Cui *et al*., 2018) (Fig. 3).

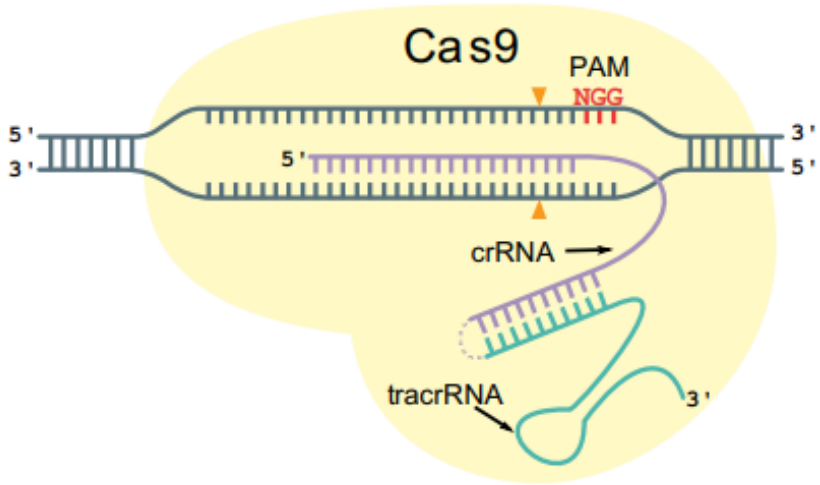

Fig. 2 CRISPR/Cas9consisting of Cas9 and gRNA. This gRNA is composed of two RNAs, tracrRNA and crRNA. The last-mentioned contains 20 bp protospacer that is homologous to the target DNA. Cas9 cleaves usually 3-4 bp before PAM sequence (Vanegas *et al*., 2019).

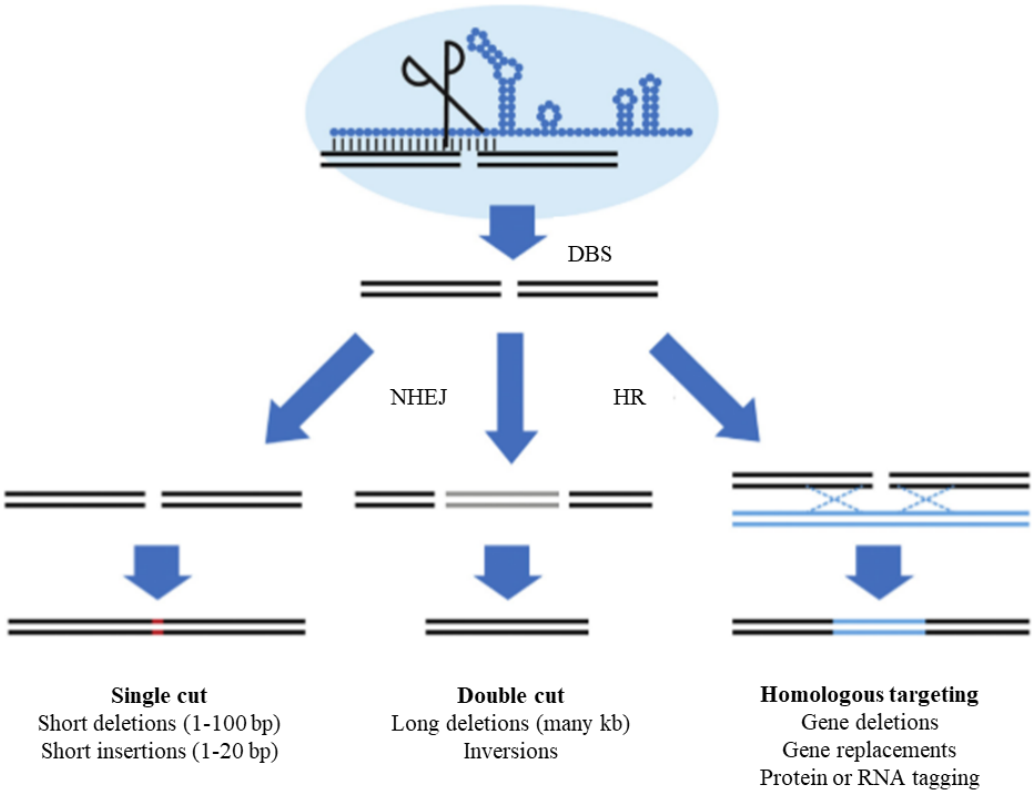

Fig. 3 Repair of double-stranded DNA break caused by CRISPR/Cas9 using NHEJ and HR mechanisms. In the case of NHEJ small insertions/deletions can occur, when the DNA template containing homologous sequences to the broken DNA is used, HR takes place (Bassett and Liu, 2014).

2.1.3.5.2.1 CRISPR/Cas9 components

2.1.3.5.2.1.1 Cas9

Cas9 has been discovered in bacteria and Archea (Ishino *et al*., 1987; Mojica *et al*., 2000), nevertheless human and fungal codon-optimized Cas9 proteins fused to a nuclear localization signal (NLS) have been already used for CRISPR/Cas9 directed mutagenesis in filamentous fungi (Nodvig *et al*., 2015; Fang and Tyler, 2016). Furthermore, GFP is commonly added to the C- or N-terminus (or to both termini) of Cas9 to detect its expression and localization (Liu *et al*., 2017).

In general, constitutive promoters, for example, P*trpC* (Matsu-ura *et al*., 2015), P*gpdA* (Zhang *et al*., 2016; Qin *et al*., 2017), and P*tef1* of gene encoding translation elongation factor 1α (Deng *et al*., 2017; Wenderoth *et al*., 2017), and inducible promoters such as P*xlnA* activated by xylose (Pohl *et al*., 2016), and P*amyB* activated by starch

(Katayama *et al*., 2016) are used to drive the Cas9 expression in fungi. Terminators utilized for Cas9 expression include the T*tef1*, T*CYC1*, and T*nos*.

For CRISPR/Cas9 gene editing, usually SpCas9 isolated from *Streptococcus pyogenes* consisting of two domains, HH and RuvC, is used (Nishimasu *et al*., 2014). Targeting of the RNA-guided SpCas9 is achieved by 20 bp protospacer (Gasiunas *et al*., 2012) and the cleavage efficiency of double-stranded DNA depends on the presence of NGG or less efficient NAG PAM sequences (Hsu *et al*., 2013).

2.1.3.5.2.1.2 Guide RNA

Different types of CRISPR/Cas9 systems in which the expression of gRNA is driven by RNA polymerase type II and III promotors have been utilized in filamentous fungi. Concerning RNA polymerase type III promoters, usually endogenous or exogenous *U6 snRNA* promoters are used (Arazoe *et al*., 2015; Katayama *et al*., 2016; Deng *et al*., 2017). When *U6* promoters are not available or do not work, *SNR52* promoter of *S. cerevisiae*, and the *T7* promoter of bacteriophage are used instead (Fuller *et al*., 2015; Qin *et al*., 2017). Moreover, recently *tRNA* promoters that induced higher or comparable editing efficiencies and *5SrRNA* promoters have been used to drive the expression of gRNA (Schuster *et al*. 2018; Zheng *et al*., 2018)

Although RNA polymerase type III promoters are frequently used (Fang and Tyler, 2016; Schuster *et al*., 2016), they have quite a lot of limitations, for example, the presence of G or A directly upstream the protospacer sequence. However, few such promoters have been identified and used in filamentous fungi (Fuller *et al*., 2015; Matsu-Ura *et al*., 2015). Thus, a self-processing system, where the expression of sgRNA is driven by RNA polymerase II promoters has been developed (Nødvig *et al*., 2015).

One of the most promising self-processing systems seems to be non-integrating AMA1-based plasmids (Nødvig *et al*., 2015). These vectors (Fig. 4a) contain a *Cas9* gene from *S. pyogenes* codon-optimized for expression in *A. niger* fused with nuclear localization signal from Simian virus 40 (SV40NLS) and placed under the control of constitutive *tef1* promoter from *A. nidulans*, a fungal marker, and *Pac*I/*Nt.Bbv*CI restriction sites that allow the insertion of sgRNA (Nødvig *et al*., 2015). Together, four different plasmids containing a hygromycin resistance gene (*hph*) under the control of *TrpC* promoter from *A. nidulans* (*pFC332*), *pyrG* (*pFC330*), *argB* (*pFC331*), and *ble* (*pFC333*) are available (Nødvig *et al*., 2015). As the result, a larger transcript is

synthesized in nucleus by RNA polymerase II and by the action of two ribozymes (Fig. 4b), 5´-end hammerhead (HH) and 3´-end hepatitis delta virus (HDV) that flank the sgRNA, sgRNA is excised (Nødvig *et al.*, 2015). As the cloning of sgRNA into these vectors can be performed in one single USER cloning step, this vector has already been used for CRISPR/Cas9 directed mutagenesis in *Aspergillus* sp., *Penicillium subrubescens*, *Talaromyces atroroseus*, and *Alternatia alternata* (Kuivanen *et al.*, 2016; Nødvig *et al.*, 2015; Nielsen *et al.*, 2017; Wenderoth *et al.*, 2017; van Leeuwe *et al.*, 2019; Kadooka *et al.*, 2020; Salazar-Cerezo *et al.*, 2020).

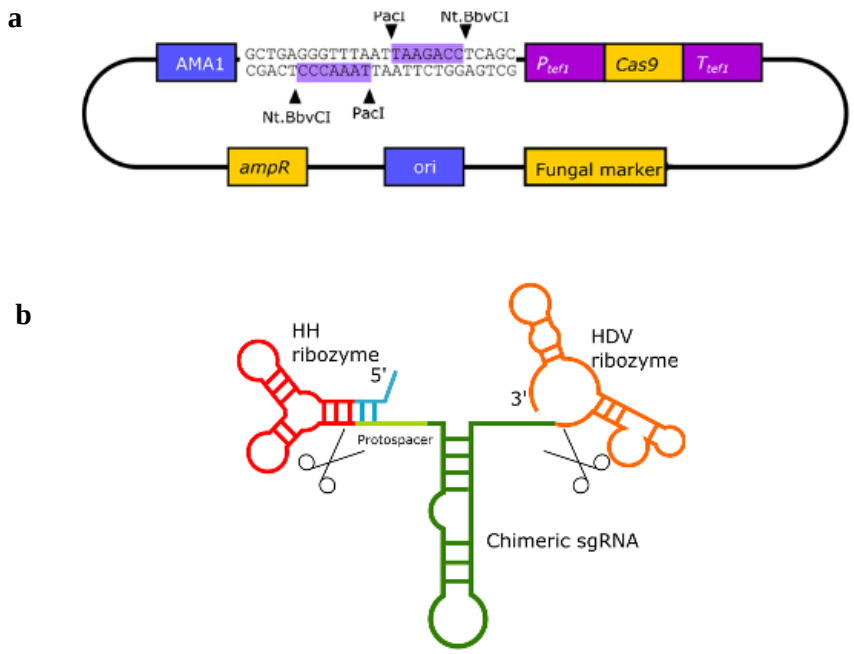

Fig. 4 CRISPR/Cas9 self-processing system that uses a non-integrating AMA1-based plasmid.
(a) AMA1-based plasmid containing Cas9 gene from *S. pyogenes* codon-optimized for expression in *A. niger* driven by P*tef1* from *A. nidulans*, *Pac*I and *Nt.Bbv*CI restriction sites for cloning of sgRNA using USER cloning method and a fungal marker.
(b) SgRNA is excised from a larger transcript synthesized in the nucleus by the action of two ribozymes, HH and HDV (Nødvig *et a*l., 2015).

Moreover, these plasmids contain autonomously replicating sequence AMA1, which enhances the transformation efficiency and can be spontaneously lost without a selection pressure (Aleksenko *et al.*, 1995; Brückner *et al.*, 1992; Gems *et al.*, 1991). As these vectors can be recycled (Katayama *et al.*, 2018), they provide a good way how to deal with a limited number of marker genes available for the selection of filamentous fungi.

Alternatively, gRNA can be synthesized *in vitro*. Such gRNAs have been used for the transformation of *Aspergillus* sp. (Zhang *et al.*, 2016; Kuivanen *et al.*, 2016),

P. chrysogenum (Pohl *et al*., 2016), *T. reesei* (Liu *et al*., 2015a), and *Beauveria bassiana* (Chen *et al*., 2017).

2.1.3.5.2.2 Screening of CRISPR/Cas9 mutants

The easiest approach for screening CRISPR/Cas9 mutations that is based on the amplification of the target sequence around the PAM sequence followed by restriction is so called PCR restriction length polymorphism (PCR-RFLP) analysis. This method is very convenient especially when the gene inactivation does not lead to the obvious change in growth, color, or resistance to compounds that are toxic to WT. This simple method has already been performed in plants (Liu *et al*., 2015b; Osakabe *et al*., 2016; Ueta *et al*., 2017), oomycete *Phytophtora sojae* (Fang and Tyler, 2016), and phytopathogenic fungus *Leptosphaeria maculans* (Idnurm *et al*., 2017). Compared to other advanced methods such as sequencing-based techniques (e.g. amplicon next-generation sequencing, NGS (Bell *et al*., 2014); tracking indels by decomposition, TIDE (Etard *et al*., 2017); indel detection by amplification analysis, IDEAA (Lonowski *et al*., 2017)) or denaturation-based methods (e.g. high-resolution melting, HRM (Samarut *et al*., 2016); single-stranded conformational polymorphism, SSCP (Zheng *et al*., 2016); mismatch-sensitive endonucleases T7/Surveyor (Huang *et al*., 2012)), PCR-RFLP analysis is inexpensive and does not require special equipment, cloning step before sequencing or additional denaturation/renaturation steps. On the other hand, it is quite laborious when hundreds of mutants have to be screened, and most importantly, it requires a suitable restriction site within the target sequence.

To test the functionality of CRISPR/Cas9 system, genes that disruption leads to easily recognized phenotypic change are usually targeted in filamentous fungi. For example, *yA* and *albA* genes encoding *p*-diphenol oxidase and a polyketide synthase, respectively have already been mutated in *Aspergillus* sp. and *Alternaria alternata* (Nodvig *et al*., 2015; Katayama *et al*., 2016; Nielsen *et al*., 2017; Wenderoth *et al*., 2017; Zheng *et al*., 2018). As the products of both genes catalyze the biosynthesis of green conidial pigment, disruption of *yA* results in the yellow colour of conidia compared to green WT conidia (Nødvig *et al*., 2015; Katayama *et al*., 2016) and a mutation in *albA* gene yields an albino phenotype (Nielsen *et al*., 2017; Nødvig *et al*., 2015; Wenderoth *et al*., 2017; Zheng *et al*., 2018). Except for *yA* and *albA* genes, *ade2* gene encoding phosphoribosylaminoimidazole carboxylase that catalyzes the sixth step in *de novo*

biosynthesis of purine nucleotides has been targeted in *Candida albicans* and *Candida glabrata* (Valmik *et al*., 2015; Shapiro *et al*., 2018). In this case, mutants showing red phenotype have been selected. Moreover, Nagy *et al.* (2017) have prepared mutants of *Mucor circinelloides* containing inactivated *carB* gene that encodes phytoene dehydrogenase involved in the biosynthesis of β-carotene. As this enzyme is involved in the biosynthesis of orange-red pigment, mutants were selected based on their albino phenotype.

Concerning auxotrophic markers, genes encoding orotidine 5′-phosphate decarboxylase and orotate phosphoribosyltransferase involved in pyrimidine biosynthesis are frequently mutated by CRISPR/Cas9 in filamentous fungi (Nødvig *et al*., 2015; Chen *et al*., 2017; Qin *et al*., 2017; Wang *et al*., 2018). By disrupting one of these two genes, mutants showing uridine and/or uracil auxotrophy and resistance to 5-FOA can be obtained. Similarly, Gardiner and Kazan (2018) have selected CRISPR/Cas9 fungal mutants impaired in osmosensor histidine kinase resistant to fungicide fludioxonile.

2.1.3.5.3 CRISPR/Cas9-mediated HDR

In this approach, template DNA containing a selection marker is co-transformed together with CRISPR/Cas9 vector, thus any gene regardless of its function can be targeted and mutants can be easily screened by diagnostic PCR. As a selection marker inserted between 5′ and 3′ flanking sequences of the target gene, gene encoding orotidine 5′-phosphate decarboxylase (Kuivanen *et al*., 2016; Chen *et al*., 2017; Nagy *et al*., 2017), *barR* (Arazoe *et al*., 2015; Matsu-ura *et al*., 2015), *hygR* (Nødvig *et al*., 2015; Zhang *et al*., 2016), *amdSR* (Pohl *et al*., 2016) and *neoR* (Zheng *et al*., 2017) have already been used.

2.1.3.5.4 CRISPR/Cas9 and CRISPR/Cas9-mediated HDR application in industrial fungi

Compared to the time-consuming classical gene knock-out approach mediated by HR that provides usually low HIF, CRISPR/Cas9 together with CRISPR/Cas9-mediated HDR represent simple, rapid, and usually efficient systems for genome editing in filamentous fungi. By using these approaches, different novel secondary metabolite (SM) clusters could be discovered; moreover, the role of genes in the regulation of SM biosynthesis or pathogenesis can be studied more easily.

CRISPR/Cas9 and CRISPR/Cas9-mediated HDR have already been established in *A. oryzae* (Katayama *et al*., 2016; Zheng *et al*., 2017), *A. niger* (Nødvig *et al*., 2015; Kuivanen *et al*., 2016), and *A. terreus*, (Itoh *et al*., 2018), fungi that are used for industrial production of amylase, glucoamylase, citric acid, and itaconic acid, respectively. Except for *Aspergillus* sp., CRISPR/Cas9-mediated HDR has already been used to target genes in *P. chrysogenum* (Pohl *et al*., 2016), a fungus that is used in the pharmaceutical industry. Pohl *et al*. (2016) have successfully targeted *pks17* and *lovF* genes in *P. chrysogenum* encoding a polyketide synthetase involved in the biosynthesis of green conidial pigment, and a diketide synthase involved in the biosynthesis of lovastatin, respectively. Moreover, they have successfully mutated both genes simultaneously. Except for these two genes, also *roq*A, *hcp*A, *pcb*AB, and *pen*DE genes encoding two nonribosomal peptide synthases, alpha-aminoadipyl-cysteinyl-valine (ACV) synthetase, and acetyl-CoA:isopenicillin *N*-acetyltransferase involved in the biosynthesis of penicillin have been targeted in this fungus (Pohl *et al*., 2016). Furthermore, the entire penicillin cluster consisting of 3 genes *pcb*AB, *pcb*C, and *pen*DE with a size of 16,155 bp has been deleted in *P. chrysogenum* by CRISPR/Cas9-mediated HDR (Pohl *et al*., 2016). Later, Zheng *et al*. (2018) have shown that even the cluster with a size of 48 kb responsible for the production of mycotoxin fumonisin B1 can be deleted by using this approach.

Another example of the use of CRISPR/Cas9-mediated HDR represents the mutation of several genes in *T. reesei* (Liu *et al*., 2015a). In this fungus, *lae1* gene encoding a methyltransferase involved in the asexual development and pathogenesis has been successfully mutated with editing efficiencies of 93-100 %. Besides, two genes, *lae1* and *vib1* genes encoding a transcription factor involved in cellulose production and even three genes, *lae1*, *vib1*, and *clr2* encoding a transcription factor that regulates xylanase genes have been mutated simultaneously (Liu *et al*., 2015a). Two years later, Liu *et al*. (2017) has successfully deleted even four genes simultaneously in another fungus *Myceliopthora thermophila*. Interestingly, by using CRISPR/Cas9 the biosynthetic pathway leading to the production of different gibberellin acids (GAs) used in industry has been engineered in a strain of *F. fujikuroi* that produces mainly GA3 and small amounts of GA4 and GA7 (Shi *et al*., 2019).

2.2 Representative fungi from order Hypocreales

According to the Dictionary of Fungi (Ainsworth, 2008), the order Hypocreales belonging to the class *Sordariomycetes* (division: *Ascomycota*, kingdom: Fungi) contains 237 genera and 2647 species in 7 families. Since 2008 a family called Stachybotryaceae and new taxa have been identified and characterized (Lombard *et al*., 2016).

In this order, both animal and plant pathogens can be found. For example, fungi from the order *Fusarium* belonging to the family Netriaceae infect a lot of different plant species including economically important crops such as barley (Tekauz *et al*., 2000), wheat (Gilbert and Tekauz, 2000), and oat (Tekauz *et al*., 2004), thus they cause economical losses. Except for *Fusarium* sp., fungi from the genus *Claviceps* belonging to the family Clavicipitaceae also infect crops and cause economic losses (Munkwold *et al*., 1997; Murray and Brennan, 2009). On the other hand, they produce ergot alkaloids, secondary metabolites that are used in the pharmacy (Bigal and Tepper, 2003).

2.2.1 Genus *Claviceps*

Fungi from the genus *Claviceps,* so-called ergot fungi, infect more than 600 plant species including economically important crops such as wheat, rye, and oat, grasses, and sedges (Křen and Cvak, 1999). Until now, approximately 45 *Claviceps* species (sp.) including well-known *Claviceps paspali, Claviceps fusiformis, Claviceps gigantea, Claviceps africana,* and *Claviceps purpurea* have been described and characterized (Pažoutová, 2001; Píchová *et al*., 2018). Although *C. paspali* originally comes from Uruguay or Argentina (Hitchcock, 1951), it has been spread by humans to the USA, Australia, and New Zealand where it colonizes *Paspalum* sp. (Cole *et al*., 1977). On the other hand, *C. fusiformis* can be found in semi-arid areas of Africa and India where it infects pearl millet (Pažoutová *et al*., 2008). *C. gigantea* and *C. africana* colonizing maize (Fuentes *et al*., 1964) and sorghum (Frederickson *et al*., 1991), respectively have been detected in Mexico and Africa. The last mentioned, *C. Africana,* has already been spread to India, Asia, USA, and Australia (Isakeit *et al*., 1998; Bogo and Mantle, 1999; Pažoutová *et al*., 2000; Tsukiboshi *et al*., 2001). In contrast, *C. purpurea* has the widest host range as it infects more than 400 plant species and it can be found especially in Europe (Křen and Cvak, 1999).

Fig. 5 Infection of durum wheat with *C. purpurea* spores.
(a) Production of honeydew at the beginning of the infection process.
(b) Sclerotia containing ergot alkaloids
(Gordon *et al*., 2020).

Once a host is infected by ergot fungus, a purple-black sclerotium containing ergot alkaloids (EAs), physiologically highly active compounds, is formed (Fig. 5) (Krska and Crews, 2008). Although these secondary metabolites are widely used in pharmacy, consumption of contaminated grains led in the Middle ages to vast epidemics of ergotism (so-called St. Anthony´s fire) (Haarmann *et al*., 2009). The industrial production of EAs began with the patent of Arthur Stoll on ergotamine tartrate (Stoll, 1921), which was then produced by Sandoz company. Today many different EAs including ergopeptines, lysergic acid amides, and clavines are used in medicine to treat migraine headaches (Moskowitz, 1992), to prevent the post-partum haemorrhage (Martin and Dumoulin, 1953), as inhibitors of prolactin release (Cassady *et al*., 1974) or in the therapy of Parkinson´s and Alzheimer´s diseases (Lieberman *et al*., 1976; Sharma *et al*., 2016).

2.2.1.1 Primary and secondary metabolites

2.2.1.1.1 Biosynthesis of ergot alkaloids

The EAs biosynthetic cluster was firstly identified in *C. purpurea* strain P1 using a chromosome walking approach with the *dmaW* gene (Tudzynski *et al*., 1999). This cluster consists of 14 genes containing one pseudogene covering over 68.5 kb (Fig. 6a) (Schardl *et al*., 2013).

EAs biosynthesis in *Claviceps* species (Fig. 6b) starts with the prenylation of L-Trp, a precursor, and an inducer of EA biosynthesis (Vining, 1970), by dimethylallyl

diphosphate (DMAPP) leading to the formation of 4-(γ,γ)-dimethylallyltryptophan (4-DMAT). This reaction is catalyzed by DMAT synthase (Metzger *et al.*, 2009) encoded by *dmaW* gene (CPUR_04076.1). DMATS has already been purified from *C. fusiformis* SD 58 (Heinstein *et al.*, 1971; Lee *et al.*, 1976; Cress *et al.*, 1981; Gebler and Poulter, 1992) and the corresponding gene has been characterized both in *C. fusiformis* SD58 (Tsai *et al.*, 1995) and in *C. purpurea*, P1 (Tudzynski *et al.*, 1999). Interestingly, two copies of *dmaW*, one of which was inactivated by 7 bp insertion have been found in *C. purpurea* P1 (Tudzynski *et al.*, 1999). Moreover, binding sites for CREA, a regulatory protein involved in carbon catabolite repression (Ruijter and Visser, 1997; Chulkin *et al.*, 2010; Portnoy *et al.*, 2011), AREA, a regulator of nitrogen metabolism (Arst and Cove, 1973; Chang *et al.*, 2000), pacC, a transcriptional factor that is modulated in response to pH and regulates virulence (Tilburn *et al.*, 1995; Chang *et al.*, 2000), and NUC-1, a transcriptional factor induced by a phosphorus limitation (Kang and Metzenberg, 1990), have been identified in the promoter region of the active *dmaW* (Tudzynski *et al.*, 1999). The next step of EAs biosynthesis, the transfer of the S-methyl group of *S*-adenosylmethionine to the amino group of 4-DMAT, is catalyzed by DMAT *N*-methyltransferase encoded by *easF* gene (CPUR_04078.1) (Otsuka *et al.*, 1980). Subsequent reactions leading to the simplest clavine, chanoclavine-I, are catalyzed by a flavin-dependent oxidoreductase chanoclavine-I synthase, encoded by *easE* gene (CPUR_04079.1) and bifunctional catalase encoded by *easC* gene (CPUR_04081.1) that induces the release of carbon dioxide and subsequent oxidative cyclization on the central C ring (Lorenz *et al.*, 2010; Goetz *et al.*, 2011; Yao *et al.*, 2019). The next step, oxidation of chanoclavine-I to chanoclavine-I aldehyde in the presence of NAD^+, is catalyzed by chanoclavine-I dehydrogenase encoded by *easD* gene (CPUR_04080.1) (Wallwey *et al.*, 2010). Different orthologs of the flavin-dependent oxidoreductase (an old yellow enzyme, encoded by *easA* gene CPUR_04084.1 in *C. purpurea* 20.1) and a reductase catalyzing the next reaction step (encoded by *easG* gene CPUR_04077.1 in *C. purpurea* 20.1) convert chanoclavine I-aldehyde into either festuclavine or agroclavine (Coyle *et al.*, 2010; Matuschek *et al.*, 2011; Matuschek *et al.*, 2012). While festuclavine is formed in *C. africana* that produces dihydroergot alkaloids, agroclavine is produced in *C. paspali*, *C. purpurea*, and *C. fusiformis* (Barrow *et al.*, 1974; Florea *et al.*, 2017). Agroclavine is then converted via elymoclavine into D-lysergic acid in *C. purpurea* or paspalic acid in *C. paspali* (Robinson and Panaccione, 2015). These three rounds of 2-electron oxidations are catalyzed by NADPH-dependent cytochrome P450 encoded by *cloA* gene

(CPUR_04082.1) (Haarmann *et al*., 2006; Robinson and Panaccione, 2014). However, *cloA* variant responsible for the production of elymoclavine in *C. fusiformis* SD 58 that does not produce D-lysergic acid has not yet been identified. In *C. purpurea*, D-lysergic acid is subsequently incorporated into lysergic acid amides and ergopeptines by a process involving nonribosomal lysergyl peptide synthetases (LPSs). In *C. purpurea* 20.1 there are four different LPSs: trimodular LPS1 encoded by *lpsA1* (CPUR_04074.1), monomodular LPS2 encoded by *lpsB* (CPUR_04083.1), monomodular LPS3 encoded by *lpsC* (CPUR_04085.1), and trimodular LPS4 encoded by *lpsA2* (CPUR_04073.1). While the complex LPSB/LPSC catalyzes the production of ergometrine, complex LPSB together with LPS1 or LPS4 catalyzes ergopeptine assembly (Riederer *et al*., 1996; Walzel *et al*., 1997; Haarmann *et al*., 2008; Ortel and Keller, 2009). The final cyclization of EAs is catalyzed by a nonheme iron dioxygenase, encoded by *easH1* gene (CPUR_04075.1) (Havemann *et al*., 2014).

Concerning the regulation of EA biosynthesis, no transcriptional factor has been identified and characterized so far. While the wild type (WT) strain of *C. purpurea* produces EAs only in sclerotia grown on plants, mutants producing EAs in submerged cultures have been generated (Amici *et al*., 1966; Schumann *et al*., 1982; Křen *et al*., 1986). In many of these strains, including the strain P1, EA biosynthesis is regulated by inorganic phosphate (Robbers *et al*., 1972; Lohmeyer *et al*., 1990; Haarmann *et al*., 2005). This regulation has already been described at the transcriptional level (Haarmann *et al*., 2005). Although it can be overcome by the addition of L-Trp (Krupinski *et al*., 1976), the mechanism is still unknown. Besides inorganic phosphate and L-Trp also a chromatin remodelling plays an important role in the regulation of EAs production as the cluster is located in the subtelomeric region (Schardl *et al*., 2013; Lorenz *et al*., 2009; Chen *et al*., 2019a).

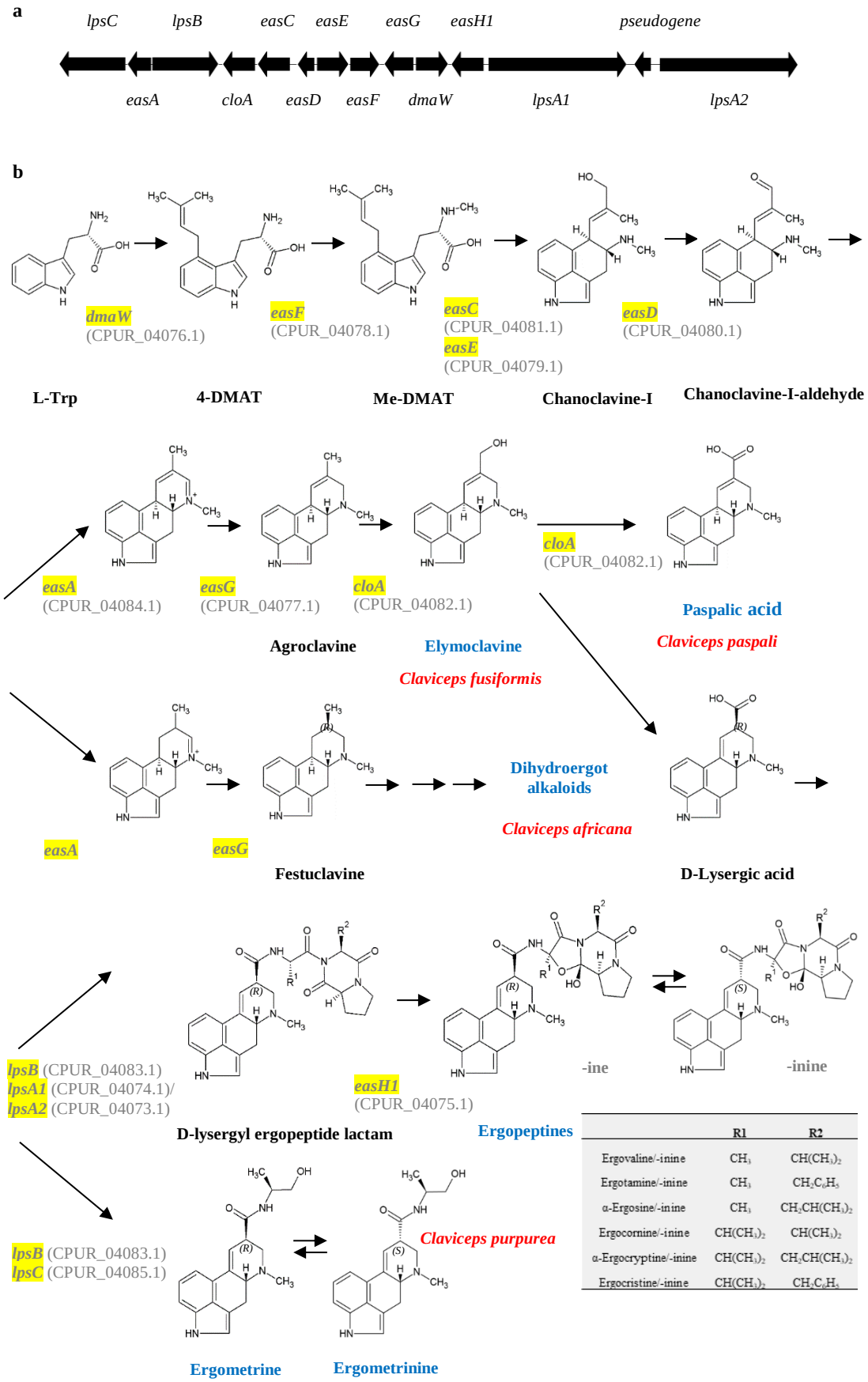

	R1	R2
Ergovaline/-inine	CH_3	$CH(CH_3)_2$
Ergotamine/-inine	CH_3	$CH_2C_6H_5$
α-Ergosine/-inine	CH_3	$CH_2CH(CH_3)_2$
Ergocornine/-inine	$CH(CH_3)_2$	$CH(CH_3)_2$
α-Ergocryptine/-inine	$CH(CH_3)_2$	$CH_2CH(CH_3)_2$
Ergocristine/-inine	$CH(CH_3)_2$	$CH_2C_6H_5$

Fig. 6 Biosynthesis of EAs in *Claviceps* species.
(a) EA biosynthetic cluster containing 13 functional genes and one pseudogene in *C. purpurea* 20.1.
(b) Biosynthetic pathway of EAs in *C. purpurea*, *C. paspali*, *C. fusiformis*, and *C. africana*.

2.2.1.1.2 Biosynthesis of tryptophan

As mentioned above, the biosynthesis of EAs starts with the prenylation of amino acid Trp that is synthesized in filamentous fungi in five enzymatic steps by three separated enzymatic components encoded by four different genes *TrpE, TrpC, TrpD*, and *TrpB* (Hütter and DeMoss, 1967). The first step in Trp biosynthesis (Fig. 7), the conversion of chrorismic acid into anthranilic acid, is catalyzed by anthranilate synthase complex that consists of two subunits, AAS-I (α-subunit encoded by *TrpE* gene) and AAS-II (a trifunctional peptide containing β-subunit of anthranilate synthase, phosphoribosylanthranilate isomerase and indole-3-glycerol-phosphate synthase encoded by *TrpC* gene) (Hütter *et al.*, 1986). While α-subunit containing distinct sites for chorismate substrate binding and Trp-feedback inhibition synthesizes anthranilic acid directly from chorismic acid in the presence of high levels of ammonia, β-subunit catalyzes together with AAS-I the conversion of chorismic acid to anthranilic acid in the presence of glutamine (Crawford and Eberly, 1986). Concerning the second step of the Trp biosynthetic pathway, the conversion of anthranilic acid into *N*-(5-phospho-D-ribosyl) anthranilate, this reaction is catalyzed by anthranilate phosphoribosyltransferase that is encoded by *TrpD* gene (Hütter *et al.*, 1986). Subsequent two reactions that produce indoleglycerol phosphate are catalyzed by phosphoribosylanthranilate isomerase and indole-3-glycerol-phosphate synthase (Schechtman and Yanofsky, 1983; Kos *et al.*, 1985). In the final step, tryptophan synthase encoded by *TrpB* gene catalyzes the formation of Trp (Eckert *et al.*, 2000).

Concerning studies on Trp biosynthesis in *Claviceps* sp. anthranilate synthase has already been purified and characterized only in *C. fusiformis* SD 58 (formerly classified as *C. purpurea* SD 58, ATCC 26245, PRL1980, or DSM 2942; Pažoutová and Tudzynski, 1999) and two strains of *C. purpurea* (Krupinski *et al.*, 1976; Schmauder and Gröger, 1976; Mann and Floss, 1977). Although it has been proved that this enzyme complex is feedback-inhibited by L-Trp (Krupinski *et al.*, 1976; Schmauder and Gröger, 1976; Mann and Floss, 1977), the corresponding *TrpE* gene has not yet been identified.

Interestingly, several studies have shown that the expression of Trp-feedback resistant form of anthranilate synthase, a key enzyme in Trp biosynthesis, leads to Trp accumulation (Matsuda *et al.*, 2005; Tsai *et al.*, 2005; Hong *et al.*, 2006) that in *Aspergillus fumigatus* is even accompanied with increased production of downstream secondary metabolites (Wang *et al.*, 2016).

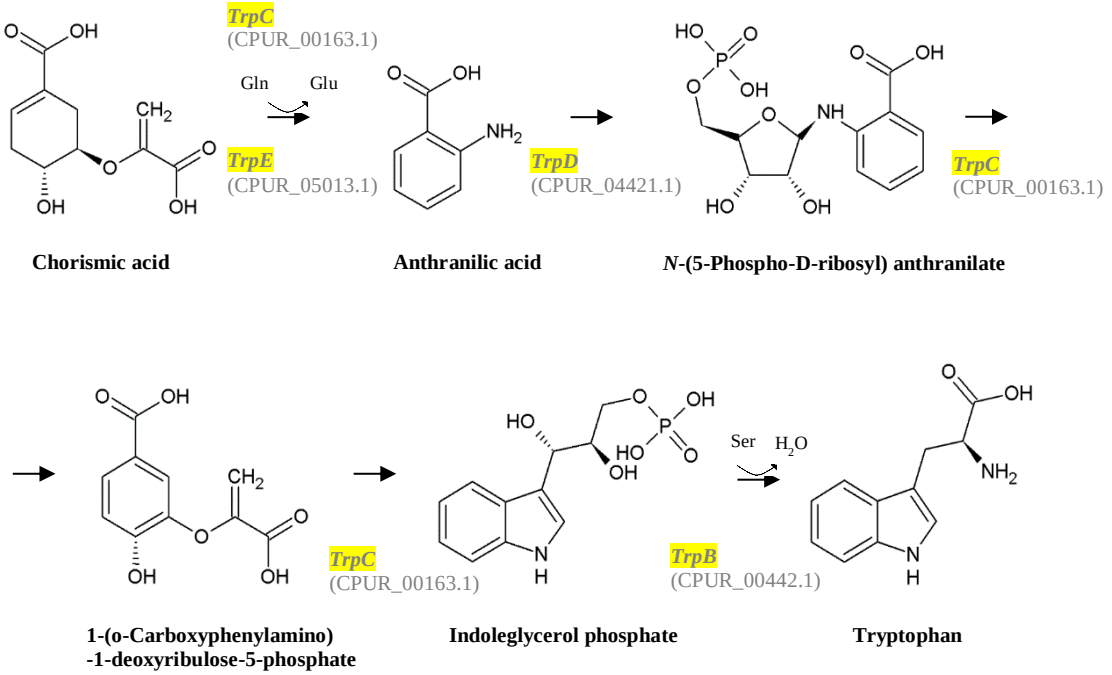

Fig. 7 Trp biosynthesis in *C. purpurea*. *TrpC* (CPUR_00163.1, *TrpE* (CPUR_05013, anthranilate synthase; *TrpD* (CPUR_04421.1), anthranilate phosphoribosyltransferase; *TrpC* (CPUR_00163.1), phosphoribosylanthranilate isomerase; *TrpC* (CPUR_00163.1), indole-3-glycerol-phosphate synthase; *TrpB* (CPUR_00442.1), tryptophan synthase.

2.2.1.1.3 Biosynthesis of auxins

Except for the biosynthesis of EAs, Trp is also involved in the biosynthesis of plant hormones auxins, compounds that play an important role in plant-fungus interactions (Chanclud and Morel, 2016). Although auxins were firstly considered as plant hormones, they have been already detected in phytopathogenic, saprophytic, and symbiotic fungi (Gunasekaran and Weber, 1972; De Battista *et al*., 1990; Fitze *et al*., 2005). Although it is well known that filamentous fungi produce auxins, their role in these organisms is still not fully understood.

In plants, auxins stimulate lateral root initiation, root and shoot apical dominance and promote fruit development (Aloni *et al*., 2006a; Lucas *et al*., 2008; Dorcey *et al*., 2009). Besides, they participate in phototropism, geotropism, and hydrotropism (Muday, 2001); moreover, they are also involved in the regulation of flowering and development of reproductive organs (Aloni *et al*., 2006b). In fungi, the effects of indole-3-acetic acid (IAA) most likely depend on its concentration. For example, the treatment of the pathogenic fungus *Fusarium delphinoides* with a low concentration of IAA led to an increase in its growth; on the other hand, when a higher concentration of IAA was applied, the fungal growth was reduced (Kulkarni *et al*., 2013). Except for the growth

regulation, IAA promotes cellular elongation and spore germination (Nakamura *et al*., 1978; Nakamura *et al*., 1982).

As in plants, IAA is in filamentous fungi synthesized via Trp-dependent and Trp-independent pathways. Concerning Trp-dependent biosynthetic pathway, indole-3-acetamide (IAM), indole-3-pyruvic acid (IPyA), indole-3-acetaldehyde (IAAId), tryptamine (TAM), and indole-3-acetonitrile (IAN), precursors of IAA, have already been detected in *Fusarium* sp., *Colletotrichum* sp., or *Ustilago maydis* (Chung *et al*., 2003; Maor *et al*., 2004; Reineke *et al*., 2008; Tsavkelova *et al*., 2012; Kulkarni *et al*., 2013). Concerning *C. purpurea*, IAA and its precursors have been found in the mycelium of *C. purpurea* strain 20.1 (Mlynarčíková, 2015).

2.2.1.2 Claviceps purpurea

C. purpurea as other fungi from the genus *Claviceps* is a biotrophic fungus that means it does not kill its host during the infection. As no signs of plant defense can be observed, this fungus is classified as a true biotroph (Tudzynski and Scheffer, 2004). It has been already experimentally proved that for the successful infection NADPH oxidases generating ROS (Schürmann *et al*., 2013), MAP kinases (Mey *et al*., 2002a; Mey *et al*., 2002b) and plant hormones cytokinins (Hinsch *et al*., 2015; Hinsch *et al*., 2016; Kind *et al*., 2018) are necessary. Moreover, the involvement of two transcription factors, Cptf1, a homolog of the yeast Ap1, and the small GTPase Cpcdc42 in the pathogenesis has been studied (Nathues *et al*., 2004; Scheffer *et al*., 2005). Interestingly, both deletion mutants were still pathogenic and produced *in plants* massive amounts of ROS (Nathues *et al*., 2004; Scheffer *et al*., 2005).

As this fungus is highly organ-specific it colonizes only unfertilized ovaries (Tudzynski and Scheffer, 2004). Once, the flower of blooming grass ear is infected (Fig. 8, stage 1), *C. purpurea* penetrates the plant cuticle without any physical pressure or creation of specific structures and it grows predominantly intercellularly in thick hyphal bundles almost without any branching following the path of the pollen tube (stage 2). After it reaches a rachilla, a base of the ovary, it starts to branch, mycelium so-called sphacelium is formed. Interestingly, the fungus colonizes the whole ovary, but no hyphae emerge beyond the rachilla tip. The sphacelium produces conidia that are together with plant phloem exudates secreted as honeydew approximately 7 days after infection (stage 3). This honeydew can be transferred by insects, rain splash, or head-to-head contact to

other unfertilized ovaries (stage 4). Approximately five weeks after the infection, sclerotia mature (stage 5) and during the autumn they leave the spike and fall into the soil, where they rest and survive unfavorable winter conditions (stage 6). *C. purpurea* sclerotia germinate in the spring when temperature is 0 °C for at least 25 days. Firstly, usually 6 to 15 stromata that are 15 to 30 mm long with a rounded head at the end are formed (stage 7). Sometimes even up to 50 or 60 stromata can be observed on the germinated sclerotium. Inside the head of stromata perithecia containing ascospores that initiate the infection in the spring are located (8).

Fig. 8 Life cycle of *C. purpurea*. (1) Ascospores infect unfertilized ovaries. (2) Hyphae follow the path of the pollen tube up to the rachilla and colonize the whole ovary. (3) Honeydew containing conidia and phloem sap is produced approximately 7 days after the infection. (4) Conidia in honeydew are transferred by insects, rain splash, or head-to-head contact to other noninfected ovaries. (5) Sclerotia are formed approximately 5 weeks after the infection they mature and fall into the soil, where they overwinter. (7) In the spring when appropriate weather conditions occur sclerotia germinate. (8) Ascospores are released from perithecia (Hulvová *et a*l., 2013).

Concerning the molecular biology of *C. purpurea*, mutants of this fungus were initially generated mostly by UV mutagenesis (Strnadová, 1964; Křen *et al*., 1986) or by treatment with nitrous acid (Strnadová, 1976) or N-methyl-N´-nitro-N-nitrosoguanidine (Brauer and Robbers, 1987). Obtained mutants were usually selected based on their different morphology (Strnadová and Kybal, 1976), auxotrophy (Strnadová 1964, 1967), resistance to fungicides (Tudzynski *et al*., 1982), or qualitative and quantitative changes in EAs production (Kobel and Sanglier, 1973). By these processes for example *C. purpurea* industrial strains Gal012 (90 % α-ergocryptine, 9 % ergometrine, 1 % valinamid), Gal130 (82.8 % ergocristine, rest - α-ergocryptine, ergometrine, and clavins), Gal310 (93.5 % ergocomine:α-ergocryptine:β-ergocryptine = 4.2:1.6:1), and Gal404 (93.5 % ergotamine, 1.1 % ergometrine, 0.5 % ergostine, 0.8 % α-ergocryptine + β-ergocryptine + ergocristine) have been obtained. The content of EAs in sclerotia (% of dry mass) of these industrial strains are 0.78-1.7 %, 0.73-2.66 %, 0.52-1.25 %, and 0.4-2.2 %, respectively (Čudejková *et al*., 2016). Concerning laboratory *C. purpurea* strains whose EAs production is much lower (usually less than 0.01 %), 20.1 and P1 are very often used in experimental studies (Tudzynski *et al*., 1999; Oeser *et al*., 2002; Nathues *et al*., 2004; Haarmann *et al*., 2005; Giesbert *et al*., 2008; Haarmann *et al*., 2008). According to the literature, *C. purpurea* 20.1 produced ergotamine and ergocryptine only *in planta*; moreover, its genome has been fully sequenced and annotated (Schardl *et al*., 2013). In contrast, *C. purpurea* P1 produces ergotamine and α-ergocryptine only in axenic cultures (Haarmann *et al*., 2008).

The first genetic transformation of *C. purpurea* protoplasts using PEG has been performed in 1989 (van Engelenburg *et al*., 1989). In this process, a vector harboring the resistance to antibiotic phleomycin has been used. In the same year, a vector containing the resistance to antibiotic hygromycin has also been used to transform *C. purpurea* (Comino *et al*., 1989). In both cases, exogenous DNA was inserted into the fungal genome in many copies. Thus, Smit and Tudzynski (1992) have performed a transformation that was based on homologous recombination; as a selection marker *pyr4* gene that was transformed into *pyr4* mutants has been used. Later, homologous transformation systems containing resistance to phleomycin (Mey *et al*., 2002b; Giesbert *et al*., 2008), hygromycin (Rolke and Tudzynski, 2008) or phosphinothricin (Haarmann *et al*., 2008) have been established. As already mentioned above, the main boost of molecular analysis of *C. purpurea* was its genome sequencing (Schardl *et al*., 2013). Except for EAS cluster further genome analyses revealed several new clusters such are ergochrome gene cluster

that is responsible for the production of typical purple-black pigment of sclerotia (Neubauer *et al*., 2016), epipolythiodiketopiperazine cluster that produces toxic clapurines (Dopstadt *et al*., 2016), or cluster containing *PKS7* gene responsible for the production of depsides (Lünne *et al*., 2020).

2.2.2 Genus *Fusarium*

Nowadays, the genus *Fusarium* consists of 20 species complexes and nine monotypic lineages (O´Donnell *et al*., 2013). As these fungi are predominantly plant pathogens and are dispersed globally from tropical to arctic areas, they infect numerous plants including economically important crops such as barley, rye, and oat (Leonard and Bushnell, 2003; Tekauz *et al*., 2004). Other *Fusarium* sp. infect animals and humans (Dignani and Anaissie, 2004; Taj-Aldeen *et al*, 2006) or they are non-pathogenic (Forsyth *et al*., 2006).

Concerning plant pathogens, once a host is infected, symptoms such as chlorosis, wilting, stunting, and even necrosis can be observed (Clark *et al*., 1990). Common plant diseases caused by *Fusarium* sp. (Fig. 9) include *Fusarium* head blight or scab (FHB) (Bushnell *et al*., 2003), ear rot (ER) (Sutton, 1982), root rot (RR) (Leath and Kendall, 1978), and crown rot (CR) (Kazan and Gardiner, 2018). *F. graminearum* and *F. pseudograminearum* infect predominantly economically important crops such as barley and wheat. In contrast, fungi from *Fusarium oxysporum* species complex (FOSC) colonize more than 120 plant species including cotton, banana, and tomato causing vascular wilts (Murray *et al*., 2020; Özarslandan and Akgül, 2020; Seo *et al*., 2020), crown rot and root rot (Van Bakel and Kerstens, 1970; Jarvis and Shoemaker, 1978).

Moreover, *Fusarium* fungi produce mycotoxins for example zearalenone (ZEA), trichothecenes (e.g. T-2 toxin, nivalenol (NIV), and deoxynivalenol (DON)) and fumonisins that accumulate in infected crops (Yoshizawa and Jin, 1995; de Saeger and van Peteghem, 1996; Marin *et al*., 1999; Orlando *et al*., 2010; Döll and Dänicke, 2011). As these secondary metabolites can persist during long storage and are heat-resistant, their threshold content in food is usually strictly regulated.

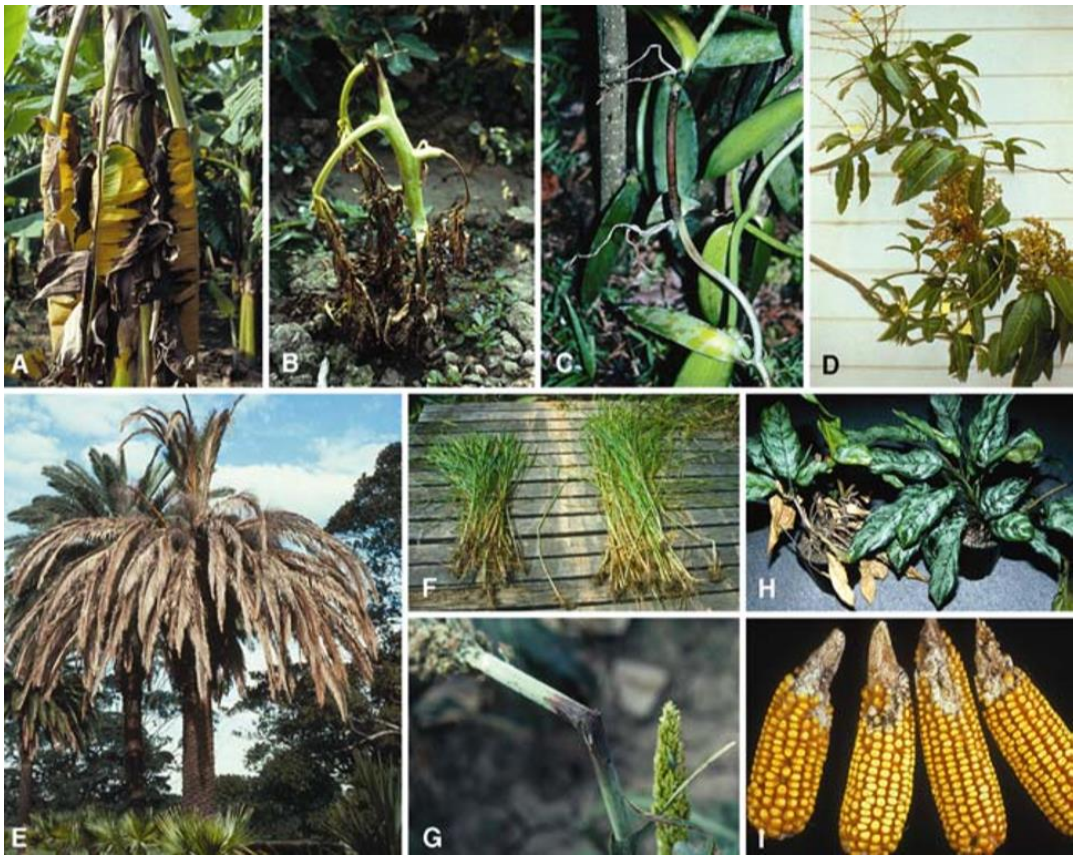

Fig. 9 Disease symptoms caused by *Fusarium* sp.
(a) Fusarium wilt of banana caused by *Fusarium oxysporum* f. sp. *cubense*.
(b) Fusarium wilt of tomato caused by *Fusarium oxysporum* f. sp. *lycopersici*.
(c) Stem rot of vanilla caused by *Fusarium oxysporum*.
(d) Mango malformation caused by *Fusarium manginifera*.
(e) Fusarium wilt of Canary Island date palm caused by *Fusarium oxysporum* f. sp. *canariensis.*
(f) Bakanae disease of rice caused by *Fusarium fujikuroi*.
(g) Stalk rot of sorghum caused by *Fusarium thapsinum.*
(h) Root rot of *Aglaonema commutatum* caused by *Fusarium solani*.
(i) Cob rot of maize caused by *Fusarium verticillioides*.
(Summerell *et al*., 2003).

In general, *Fusarium* fungi produce three types of asexual spores, macroconidia, microconidia, and chlamydospores. Macroconidia are the most important as their characters such as the range and an average number of septa per one spore, their size and length are commonly used for the identification of *Fusarium* sp. (Leslie and Summerell, 2006). For example, macroconidia of *F. graminearum* and *F. pseudograminearum* are thick-walled, slender, and usually possess 3-5 cells that are demarcated by septa (Harris, 2005; Kazan and Gardiner, 2018); on the other hand, *F. oxysporum* contains usually 3- septate macroconidia (Leslie and Summerell, 2006). In contrast to macroconidia, microconidia are not produced by all *Fusarium* sp.; for example, they are not formed by *F. graminearum* and *F. pseudograminearum*; on the other hand, *F. oxysporum* forms

0- septate microconidia (Ruiz-Roldán *et al*., 2010). The last type of spores chlamydospores are produced singly, doubly, in clumps or chains usually after a long time; sometimes a special medium has to be prepared (Leslie and Summerell, 2006). Except for the shape of spores, growth rate, production of mycotoxins or pigmentation can be used to identify *Fusarium* sp. (Leslie and Summerell, 2006). For example, *F. graminearum* and *F. pseudograminearum* produce relatively dense white to red mycelium on PDA agar plates; moreover, a red pigment that is pH sensitive is formed (Pancaldi *et al*., 2010).

2.2.2.1 Important mycotoxins

2.2.2.1.1 Zearalenone

Zearalenone (ZEA), previously called F-2 toxin, is a non-steroidal estrogenic compound (Gromadzka *et al*., 2008) that is produced by *Fusarium* sp. especially by *F. graminearum* (Mirocha *et al*., 1989), *F. culmorum* (Waśkiewicz *et al*., 2008), and *F. moniliforme* (Mirocha *et al*., 1969). Thus, it can be found in infected maize (Pleadin *et al*., 2012), barley (Kim *et al*., 1993), and wheat (Ji *et al*., 2014). As this compound binds to estrogen receptors (Li *et al*., 2012a), it predominantly causes reproductive problems such as abortion (Kallela and Ettala, 1984), infertility (Chang *et al*., 1979), and other breeding problems (Young *et al*., 1990; Gajecka *et al*., 2015). Estrogenic effects of this compound have been observed not only in swine (Chang *et al*., 1979), but also in rats (Maaroufi *et al*., 1996), mice (Yang *et al*., 2007), turkey poults (Allen *et al*., 1981), and broiler chicks (Chi *et al*., 1980).

2.2.2.1.2 Trichothecenes

Trichothecenes are sesquiterpenes that are produced not only by *Fusarium* sp. (Desjardins *et al*., 1993) but also fungi from genus *Myrothecium* (Trapp *et al*., 1998), *Spicellum* (Langley *et al*., 1990), *Stachybotrys*, or *Trichoderma* (Wilkins *et al*., 2003). Together, more than 200 different trichothecenes that contain tricyclic 12,13-epoxytrichothec-9-ene (EPT) core structure have already been identified. Based on the substitution of EPT, these secondary metabolites can be divided into four groups - A, B, C, and D. Groups A, B, and C differ in the substitution of C-8 of EPT. Type A trichothecenes contain ester (e.g. T-2 toxin), hydroxyl (e.g. neosolaniol), or no functional group (e. g. trichodermin) at C-8 of

EPT. Type B trichothecenes have carbonyl group at C-8 of EPT (e.g. nivalenol). Type C trichothecenes contain C-7/C-8 epoxide (e.g. crotocin). In contrast, type D trichothecenes have an extra ring linking C-4 and C-15 (e.g. satratoxin H) (McCormick *et al*., 2011; Cope, 2018).

As trichothecenes are lipophilic, they are predominantly absorbed across the gastrointestinal tract. Alternatively, they can be slowly absorbed through the skin (Kemppainen *et al*., 1988). In general, these secondary metabolites cause polyribosomal disaggregation and inhibition of protein synthesis (Cundliffe *et al*., 1974; Miller and Ewen, 1997); moreover, inhibition of RNA and DNA synthesis can occur (Thompson and Wannemachel, 1990). Except for disruption of reproduction (Yang *et al*., 2020), effects like the disruption of intestinal barrier integrity (van de Walle *et al*., 2010) or dysregulation of energy balance (Lebrun *et al*., 2015) have been observed.

2.2.2.1.3 Fumonisins

Fumonisins are secondary metabolites that are mostly produced by *Fusarium* sp., predominantly by *F. vertillioides*, *F. moniliforme*, *Fusarium nygami*, and *F. proliferatum* (Musser and Plattner, 1997; Seo *et al*., 2001). Except for *Fusarium* sp., these toxins have been detected also in *Aspergillus niger* (Frisvad *et al*., 2007). Thus, fumonisins can be found in maize (Fandohan *et al*., 2003), rye (Fadl-Allah *et al*., 1997), wheat (Stanković *et al*., 2012) or barley (Piacentini *et al*., 2015) infected by *Fusarium* sp. or in peanut (Palencia *et al*., 2014) or grape (Logrieco *et al*., 2009) infected by *A. niger*.

Until now, more than 15 different fumonisins homologs that are divided into four groups A, B, C, and P have been identified and characterized. These secondary metabolites contain one amino, two methyl, one to four hydroxyl, and two tricarboxylic ester groups at different positions along with the linear polyketide-derived backbone.

In general, fumonisins inhibit ceramide synthase (Desai *et al*., 2002), thus disrupting the metabolism of sphingolipids. Concerning the toxicity, they are possible carcinogens (Riley *et al*., 1994); moreover, they are immunosuppressive (Li *et al*., 2017) and nephrotoxic (Suzuki *et al*., 1995).

2.2.2.2 Fusarium graminearum

Fusarium graminearum (teleomorph *Gibberella zeae*), previously also known as *F. graminearum* group 2 is a homothallic pathogenic fungus that can be divided into more

than 16 phylogenetically distinct species (O´Donnell *et al*., 2000; Aoki *et al*., 2012). Although the genome of this fungus has been originally sequenced and annotated in 2005 and 2007 (Gale *et al*., 2005; Cuomo *et al*., 2007) and later refined (Güldener *et al*., 2006), some sequences were still missing. Thus in 2015 genome of this fungus has been sequenced and annotated again (King *et al*., 2015). Based on these results, the size of the genome is 36.6 Mb and it is divided into four chromosomes (King *et al*., 2015).

Concerning the pathogenesis, *F. graminearum* infects predominantly wheat and barley with Fusarium head blight (FHB) disease (Leonard and Bushnell, 2003) and maize with Fusarium stalk (Manstretta and Rossi, 2016) or ear rot disease (Miller *et al*., 2007). These pathogens can be found all over the world including Southern Europe (Somma *et al*., 2014), Australia (Obanor *et al*., 2013), Africa (Lamprecht *et al*., 2011), China (Gale *et al*., 2002), and the USA (Walker *et al*., 2001b). In all cases, grain yield is reduced; moreover, mycotoxins such as ZEA, and trichothecenes deoxynivalenol and acetyldeoxynivalenol that are harmful to animals and humans are produced in infected plants (Mirocha *et al*., 1989).

In the first phase of infection, *F. graminearum* behaves as a biotroph, then the necrotrophic phase takes place (Trail, 2009). The life cycle of *F. graminearum* (Fig. 10) begins in the spring when sexual spores of this fungus called ascospores are released from perithecia that are formed on infected overwintered plant structures. Ascospores land on anthers, stigmas, or lodicules of wheat and other crops; later, they germinate, enter the plant through the natural openings (e. g. stomates), grow, and spread through the xylem. In the case when anthers are infected directly after their formation, the fungus colonizes the whole floret, thus the kernel is not produced. On the other hand, when they are infected later, wilted and shrivelled kernels are formed. Moreover, once the plant is infected, the fungus produces asexual spores called macroconidia that can be transferred by insects, rain splash, or head-to-head contact to other uninfected plants. During the winter, the fungus survives in infected seeds or spike tissues, thus in the spring, the infection process can be repeated.

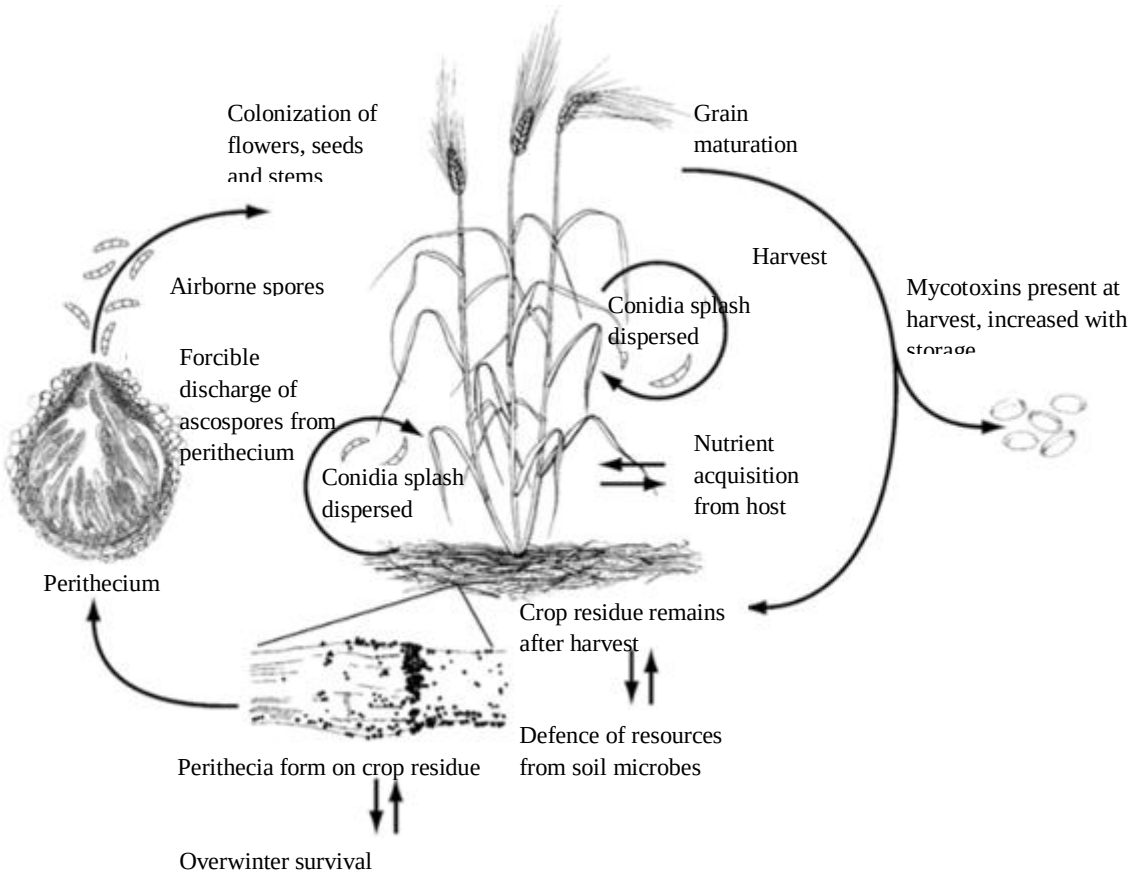

Fig. 10 Life cycle of *Fusarium graminearum* that infects crops with *Fusarium* head blight disease (Trail, 2009).

2.2.2.3 Fusarium pseudograminearum

Fusarium pseudograminearum (teleomorph *Gibberella coronicola*) previously also known as *F. graminearum* group 1 is a haploid heterothallic pathogenic fungus (Aoki and O´Donnell, 1999). The genome of this fungus has been firstly sequenced and annotated in 2012 and 2013 (Gardiner *et al.*, 2012; Moolhuijzen *et al.*, 2013); however, some regions were still missing. As this fungus is heterothallic, Gardiner *et al.* (2018) have crossed this fungus with *F. graminearum*, sequenced and annotated both genomes, and constructed a genetic map. In this map, the genome of *F. pseudograminearum* has been divided into four chromosomes; moreover, genomes of both species have been compared (Gardiner *et al.*, 2018).

As *F. graminearum*, *F. pseudograminearum* causes Fusarium head blight of crops (Ji *et al.*, 2016); moreover, it infects predominantly wheat (Li *et al.*, 2012b) and barley (Xu *et al.*, 2017) with a disease known as crown rot with symptoms such as browning of seedlings´ coleoptiles and white heads of infected plants with no or shriveled grains. The plant infection caused by *F. pseudograminearum* has been detected all over the world

including Australia (Obanor *et al*., 2013), China (Li *et al*., 2012b), and Iran (Saremi *et al*., 2007).

As in the case of *F. graminearum*, both sexual and asexual stages occur during the life cycle of *F. pseudograminearum* (Fig. 11). Interestingly, it has been proposed that only the asexual stage producing conidia plays an important role during the pathogenesis. In the spring, when appropriate weather conditions occur, ascospores of *F. pseudograminearum* are formed in perithecia; nevertheless, their impact on the infection is unknown. Overwintered spores and mycelia in the soil and debris produce asexual spores called conidia that subsequently infect the sub-crown and/or outer leaf sheaths at the tiler bases. Thus, the first sign of infection is usually a brown stem base. White heads can be observed only in wheat, rarely in oat, and not in barley as it matures earlier (Kazan and Gardiner, 2018).

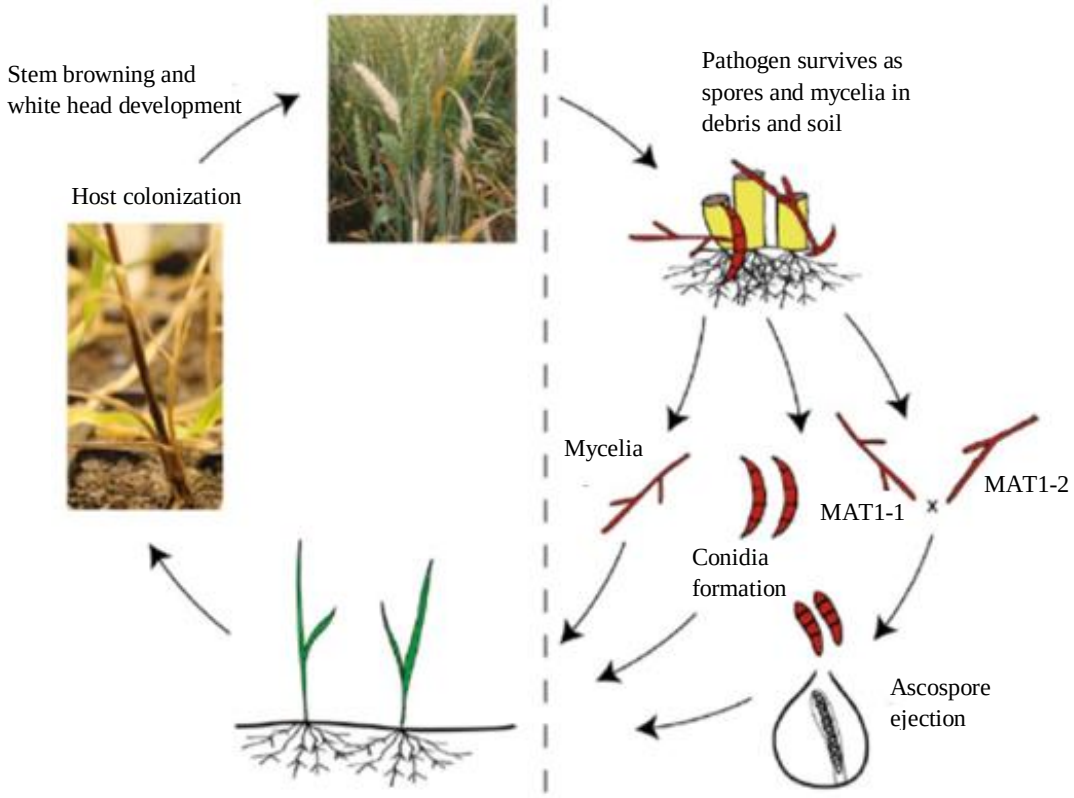

Fig. 11 Life cycle of *Fusarium pseudograminearum* that infects crops with crown rot disease (Kazan and Gardiner, 2018).

2.2.2.4 Fusarium oxysporum

In contrast to *F. graminearum* and *F. pseudograminearum*, fungi from *Fusarium oxysporum* species complex (FOSC) colonize more than 120 plant species including cotton, banana, and tomato and cause vascular wilts (Davis *et al*., 1996; Olivain and Alabouvette, 1999; Ploetz, 2006), crown rot, foot rot and root rot (Van Bakel and Kerstens, 1970; Jarvis and Shoemaker, 1978); moreover, human pathogenic and non-pathogenic strains can be found in this complex (Fuchs *et al*., 1997; O´Donnell *et al*., 2007). In 1981 Armstrong and Armstrong have reported in 1981 based on the host specificity 79 *formae speciales* (f. sp.). As many new *formae speciales* have been identified and characterized since this time, Edel-Hermann and Lecomte have counted them in 2019 again. Together, they have reported 106, 37, and 58 well-documented, insufficiently-documented, and no characterized *formae speciales*. Besides, each *forma specialis* can be divided into races based on the fungal virulence to a set of differential cultivars (Armstrong and Armstrong, 1981; Edel-Hermann and Lecomte, 2019).

Based on current knowledge, *F. oxysporum* has no known sexual stage and as mentioned above it produces three different types of asexual spores – macroconidia, microconidia, and chlamydospores (Nelson *et al*., 1983). This saprophytic fungus that feeds on dead plant and animal remains survives during the winter in the form of mycelium or asexual spores in plant debris in the soil. At the beginning of plant infection, the pathogen recognizes the roots, attaches to the root surface, and colonizes it. Later, *F. oxysporum* penetrates and colonizes the root cortex, and finally, in the case of wilting, its hyphae grow within the xylem vessels. Once the pathogen is in the xylem, it produces microconidia that can move upstream in the plant sap, thus colonizing neighboring vessels. Common symptoms of this disease include pale green to yellow leaves that later wilt and die and dark streaks in the vascular tissue of the roots and lower stem; moreover, roots also die (Hillocks, 1992).

3 Overexpression of Trp-related genes in *Claviceps purpurea* leading to increased ergot alkaloid production

3.1 Introduction

The parasitic fungus *Claviceps purpurea* has been used for decades by pharmaceutic industry as a valuable producer of ergot alkaloids. As the biosynthetic pathway of ergot alkaloids involves a common precursor L-tryptophan, targeted genetic modification of the related genes may improve the production yield.

In this work, S76L mutated version of the gene *trpE* encoding the enzyme anthranilate synthase was constitutively overexpressed in the fungus with the aim to overcome feedback inhibition of the native enzyme by excess of tryptophan. In another approach, *dmaW* gene coding for dimethylallyltryptophan synthase, an enzyme that produces key intermediate for the biosynthesis of ergot alkaloids, was also constitutively overexpressed. Moreover, to confirm that *TrpE* encodes α subunit of anthranilate synthase, knock-out mutant lacking this gene and its complemented strain were prepared and characterized.

3.2 Material

3.2.1 Buffers and solutions

Yeast recombinational cloning

LB agar

- 9.5 g sodium chloride, 15.5 g LB Broth, made up to 1 l with distilled water, pH adjusted to 7.2, 15 g agar, autoclaved for 20 min at 120 °C

LB medium

- 9.5 g sodium chloride, 15.5 g LB Broth, made up to 1 l with distilled water, pH adjusted to 7.2, autoclaved for 20 min at 120 °C

SOC medium

- 20 g of tryptone, 5 g of yeast extract, and 0.5 g of sodium chloride dissolved in 950 ml of distilled water followed by the addition of 10 ml of 250 mM potassium chloride, the mixture was adjusted to pH 7.0, and made up to 1 l with distilled water, after autoclaving for 20 min at 120 °C, 20 ml of 1 M D-glucose and 5 ml of 2 M magnesium chloride were added to the solution

Uracil-free SD agar

- 20 g D-glucose monohydrate, 6.7 g amino acid-free yeast nitrogen base, 0.77 g amino acid mixture and nutrients without uracil, made up to 1 l with distilled water, pH adjusted to 5.8, 16 g agar, autoclaved for 20 min at 120 °C

Uracil-free SD medium

- 20 g D-glucose monohydrate, 6.7 g amino acid-free yeast nitrogen base, 0.77 g amino acid mixture and nutrients without uracil, made up to 1 l with distilled water, pH adjusted to 5.8, autoclaved for 20 min at 120 °C

***C. purpurea* transformation**

0.2 M potassium malate

- 600 ml 0.2 M potassium hydroxide (6.73 g/600 ml) were mixed with 0.2 M maleic acid (13.93 g/600 ml) until pH = 5.2.

BII cultivation medium (Esser *et al.*, 1978)

- 100 g sucrose, 5 g peptone, 5 g L-asparagine monohydrate, 1 g potassium dihydrogen phosphate, 0.5 g magnesium sulphate heptahydrate, 0.01 g ferrous

sulphate heptahydrate, made up to 1 l with distilled water, pH adjusted with potassium hydroxide to 5.8, autoclaved for 20 min at 120 °C

BII selection agar

- 100 g sucrose, 5 g peptone, 5 g L-asparagine monohydrate, 1 g potassium hydrogen phosphate, 0.5 g magnesium sulphate heptahydrate, made up to 1 l with distilled water, pH adjusted with potassium hydroxide to 8.0, 12 g agar, autoclaved for 20 min at 120 °C. Antibiotics hygromycin or phleomycin or both were added.

BII transformation agar

- 200 g sucrose, 5 g peptone, 5 g L-asparagine monohydrate, 1 g potassium hydrogen phosphate, 0.5 g magnesium sulphate heptahydrate, made up to 1 l with distilled water, pH adjusted with potassium hydroxide to 8.0, 12 g agar, autoclaved for 20 min at 120 °C

PEG solution

- 7.5 g PEG 6000, 1.5 ml of 1 M calcium chloride, 3 ml of 1 M Tris-HCl, 19 ml distilled water

Protoplastization solution

- 100 mg of *Trichoderma harzianum* lysing enzyme in 20 ml of SmaC buffer, sterilized through a 0.22 µm pore size filter

SmaC buffer

- 123.88 g sorbitol, 5.88 g calcium chloride, made up to 800 ml with 0.2 M potassium malate, autoclaved for 20 min at 120 °C

STC buffer

- 154.84 g sorbitol, 1.22 g Tris, 7.36 g calcium chloride, made up to 1 l with distilled water, pH adjusted with hydrochloric acid to 7.5, autoclaved for 20 min at 120 °C

Isolation of gDNA from *C. purpurea*

Lysis buffer

- 4.84 g Tris, 2.92 g sodium chloride, 1.86 g EDTA, 1 g SDS, made up to 200 ml with distilled water, pH adjusted with hydrochloric acid to 8.5

Single spore isolation, auxotrophy, pathogenicity assays, hyphal tip dissection

Mantle agar (Mantle and Nisbet, 1976)

- 100 g sucrose, 10 g L-asparagine, 1 g calcium nitrate tetrahydrate, 0.25 g potassium dihydrogen phosphate, 0.125 g potassium chloride, 0.25 g magnesium sulphate heptahydrate, 0.033 g ferrous sulphate heptahydrate, 0.027 g zinc sulphate heptahydrate, 0.01 g L-cysteine, 0.1 g yeast extract, made up to 1 l with distilled water, pH adjusted with sodium hydroxide to 5.2, 20 g agar, autoclaved for 20 min at 120 °C

Western blot analysis

0.1% amidoblack

- 0.1 g amidoblack, 10 ml 80% acetic acid, 40 ml methanol, 50 ml distilled water

Extraction buffer

- 2.42 g Tris pH 8.0, 8.77 g sodium chloride, 500 µl Triton-X100, made up to 1 l with distilled water, pH adjusted with hydrochloric acid to 5.2

4% stacking gel

- 1 ml 30% acrylamide + 0.8% bisacrylamide, 1.25 ml buffer for stacking gel, 5.13 ml distilled water, 0.075 ml 10% (w/v) SDS, 0,0075 ml TEMED, 0.075 ml 100 mg/ml ammonium persulphate

10% separating gel

- 2.5 ml 30% acrylamide + 0.8% bisacrylamide, 1.25 ml buffer for separating gel, 3.63 ml distilled water, 0.075 ml 10% (w/v) SDS, 0,0075 ml TEMED, 0.075 ml 100 mg/ml ammonium persulphate

30% (w/v) acrylamide + 0.8% bisacrylamide

- 7.5 g acrylamide in 17 ml distilled water, then added 0.2 g bisacrylamide and the volume adjusted to 25 ml with distilled water

Buffer for stacking gel

- 9.08 g Tris made up to 100 ml with distilled water, pH adjusted with hydrochloric acid to 6.8

Buffer for separating gel

- 27.25 g Tris made up to 100 ml with distilled water, pH adjusted with hydrochloric acid to 9.2

Running buffer

- 3.03 g Tris, 14.41 g glycine, 10 g SDS, made up to 1 l with distilled water, pH adjusted with hydrochloric acid to 8.3

TBS buffer

- 2.42 g Tris pH 7.0, 29.22 g sodium chloride, made up to 1 l with distilled water, pH adjusted with hydrochloric acid to 7.0

TBS-T buffer

- 2.42 g Tris pH 7.0, 29.22 g sodium chloride, 5 ml Tween-20, made up to 1 l with distilled water, pH adjusted with hydrochloric acid to 7.0

Measurements of anthranilic acid, Trp, and ergopeptines

InoCN preculture medium (Haarmann *et al*., 2008)

- 100 g sucrose, 10 g citric acid monohydrate, 0.12 g potassium chloride, 0.5 g potassium dihydrogen phosphate, 1 g calcium nitrate tetrahydrate, 0.075 g nicotinic acid amide, 0.006 g zinc sulphate heptahydrate, 0.007 g ferrous sulphate heptahydrate, made up to 1 l with distilled water, pH adjusted to 5.2 with ammonia, autoclaved for 20 min at 105 °C

T25N inducing medium with a low level of phosphate (Haarmann *et al*., 2008)

- 300 g sucrose, 15 g citric acid monohydrate, 0.12 g potassium chloride, 0.5 g potassium dihydrogen phosphate, 1 g calcium nitrate tetrahydrate, 0.075 g nicotinic acid amide, 0.006 g zinc sulphate heptahydrate, 0.007 g ferrous sulphate heptahydrate, made up to 1 l with distilled water, pH adjusted to 5.2 with ammonia, autoclaved for 20 min at 105 °C

T25N noninducing medium with a high level of phosphate (Haarmann *et al*., 2008)

- 300 g sucrose, 15 g citric acid monohydrate, 0.12 g potassium chloride, 2 g potassium dihydrogen phosphate, 1 g calcium nitrate tetrahydrate, 0.075 g nicotinic acid amide, 0.006 g zinc sulphate heptahydrate, 0.007 g ferrous sulphate heptahydrate, made up to 1 l with distilled water, pH adjusted to 5.2 with ammonia, autoclaved for 20 min at 105 °C

RNA isolation

Cell lysis solution

- 1.76 g sodium citrate, 2.54 g citric acid, 29.4 g EDTA, 2 g SDS, made up to 100 ml with distilled water, autoclaved for 20 min at 120 °C

DNA-protein precipitation solution

- 23.38 g sodium chloride, 0.41 g sodium citrate, 0.62 g citric acid, made up to 100 ml with distilled water, autoclaved for 20 min at 120 °C

3.2.2 Organisms and plants

- Uracil-auxotrophic strain of *Saccharomyces cerevisiae* FGSC 9721 (Fungal Genetics Stock Center) cultivated in the dark at 28 °C.
- Chemically competent cells of *Escherichia coli* TOP 10 (New England BioLabs) cultivated in the dark at 37 °C.
- *C. purpurea* P1 (1029/N5) (Tudzynski *et al*., 1999) which produces ergotamine, ergotaminine, α-ergocryptine, and α-ergocryptinine in submerged culture (Haarmann *et al*., 2008) cultivated in the dark at 28 °C.
- *C. purpurea* 20.1, a putatively haploid (benomyl-treated) derivative of the standard field isolate T5 (Fr.:Fr.) Tul., obtained from *Secale cereale L*. (Hohenheim, Germany) that produces ergot alkaloids *in planta* (Schardl *et al*., 2013) cultivated in the dark at 28 °C.
- Male-sterile hybrid rye plants (*Secale cereale*), cultivar L62 obtained from Teva Czech Industries

3.2.3 Plasmids

- *pNDH-OGG* (Schumacher, 2012)
- *pRS426* (Christianson *et al*., 1992)
- *pRS426_CpBle*
- *pDRIVE* (Qiagen)

3.3 Methods

3.3.1 Vectors construction

3.3.1.1 Amplification of genes and flanking regions

Together, four different vectors *pNDH-OGG:TrpE*, *pNDH:OGG:TrpE*^{S76L}, *pNDH-OGG:gfp_dmaW*, and *pRS426:ΔTrpE1* were prepared using the yeast recombinational cloning method (Colot *et al.*, 2006).

Amplification of genes *TrpE* (CPUR_05013.1), *TrpE*^{S76L} (*TrpE* containing a point mutation S76L) and *dmaW* (CPUR_04076.1) and 5´and 3´flanking regions of *TrpE* was performed using proofreading Phusion High-Fidelity DNA polymerase (New England BioLabs) (Tab. 1, 2); as a template, genomic DNA isolated from *C. purpurea* 20.1 was used.

Tab. 1 Components of PCR mixture containing Phusion High-Fidelity DNA polymerase.

Component	Final concentration
5x Phusion GC buffer	1x
dNTPS	200 µM
Forward primer	0.5 µM
Reverse primer	0.5 µM
DMSO	3%
Phusion High-Fidelity DNA polymerase	1 unit
Template DNA	< 250 ng

Tab. 2 PCR conditions with Phusion High-Fidelity DNA polymerase.

Step	Temperature (°C)	Time (s)
1. Initial denaturation	98	30
2. Denaturation	98	7
3. Annealing	60	20
4. Extension	72	15-30/kb
5. Final extension	72	300

Steps 2-4 were repeated 34 times

To generate *TrpE* expression vector (Fig. 12), *TrpE* gene (1,369 bp) was amplified with the primers pNDH-OGG_TrpE_fw and pNDH-OGG_TrpE_rev (Tab. 3) containing overlapping sequences toward the yeast shuttle vector *pNDH-OGG* (Schumacher, 2012).

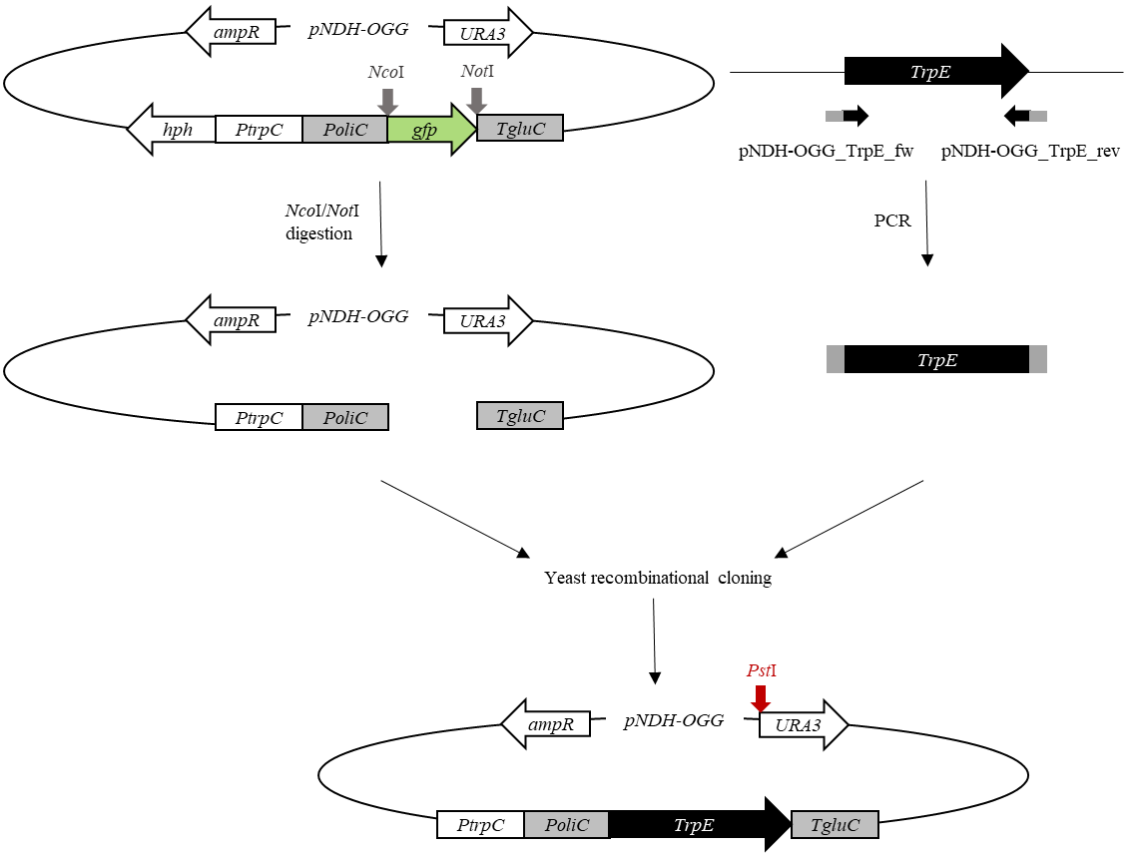

Fig. 12 Construction of *pNDH-OGG:TrpE*.
TrpE gene amplified from gDNA of WT *C. purpurea* strain 20.1 was cloned into *Not*I and *Nco*I-digested *pNDH-OGG* using yeast recombinational cloning method. Then, *Pst*I-linearized *pNDH-OGG:TrpE* was used to transform protoplasts of *C. purpurea* strain P1.

Tab. 3 Sequences of primers used for generation of *pNDH-OGG:TrpE*.

pNDH-OGG_TrpE_fw
5´-CCATCACATCACAATCGATCCAACCATGGCGAGCCCGGTAAGTACTGC-3´
pNDH-OGG_TrpE_rev
5´-CATACATCTTATCTACATACGCTATGTGGTTTTCTCGTTTTGCTGCTGCTGGTA-3´

For expression of mutated *TrpE* (Fig. 13), *TrpE* was amplified in two parts with the following sets of primers harboring a mutation: pNDH-OGG_TrpE_fw and pNDH-OGG_TrpES76L_rev (355 bp), pNDH-OGG_TrpES76L_fw and pNDH-OGG_TrpE rev (1,516 bp) (Tab. 4); primers pNDH-OGG_TrpE_fw and pNDH-OGG_TrpE_rev contained overlapping sequences toward the yeast shuttle vector *pNDH-OGG* (Schumacher, 2012).

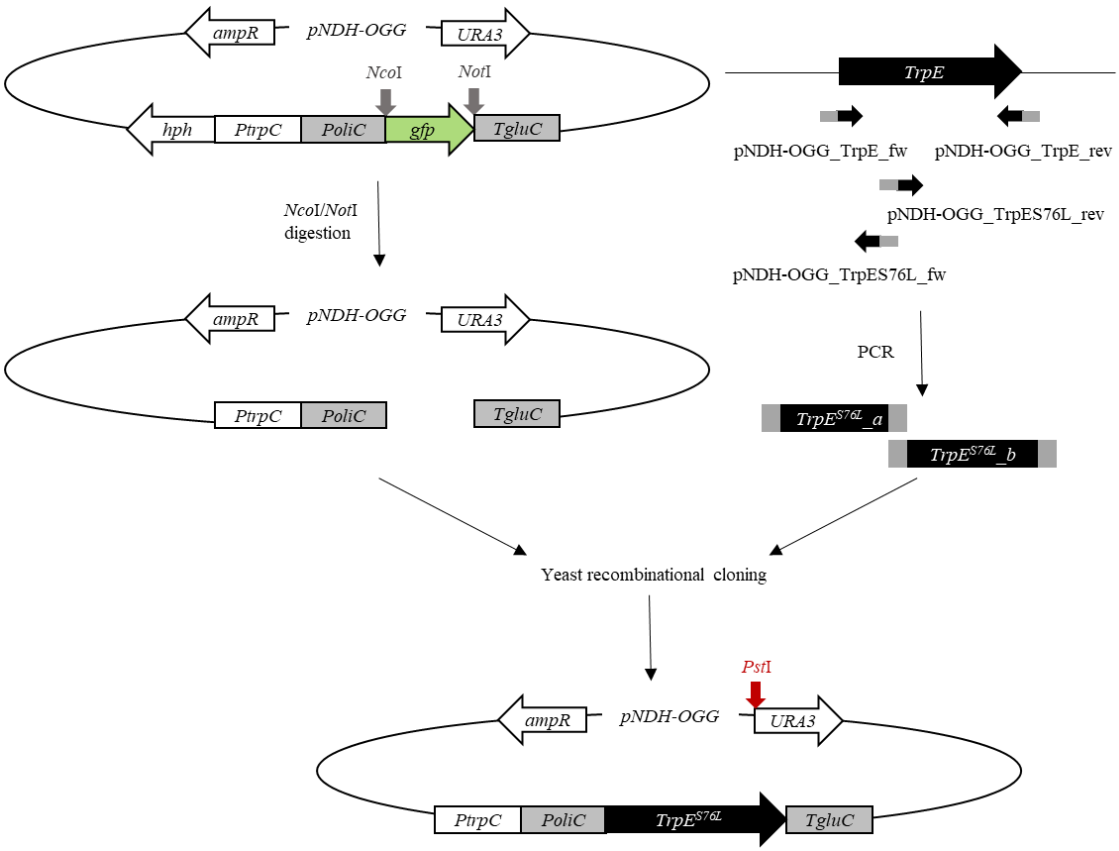

Fig. 13 Construction of *pNDH-OGG:TrpE^{S76L}*.
TrpE gene was amplified from gDNA of WT *C. purpurea* strain 20.1 in two parts using primers containing a mutation S76L. Obtained PCR products were cloned into *Not*I and *Nco*I-digested *pNDH-OGG* using the yeast recombinational cloning method. Then, *Pst*I-linearized *pNDH-OGG:TrpE^{S76L}* was used to transform protoplasts of *C. purpurea* strain P1.

Tab. 4 Sequences of primers used for generation of *pNDH-OGG:TrpE^{S76L}*.

pNDH-OGG_TrpE_fw
5´-CCATCACATCACAATCGATCCAACCATGGCGAGCCCGGTAAGTACTGC-3´
pNDH-OGG_TrpE_rev
5´-CATACATCTTATCTACATACGCTATGTGGTTTTCTCGTTTTGCTGCTGCTGGTA-3´
pNDH-OGG_TrpES76L_rev
5´-TACGAAGAGATACCGGCCGACTTGCTCTGTGGCGGCGGACTCGAA-3´
pNDH-OGG_TrpES76L_fw
5´-CACAGAGCAAGTCGGCCGGTATCTCTTCGTAGGC-3´

For the generation of *dmaW* expression vector (Fig. 14), *dmaW* gene (1,466 bp) was amplified with primers pNDH-OGG_gfp_dmaW_fw and pNDH-OGG_gfp_dmaW_rev (Tab. 5) containing overlapping sequences toward the yeast shuttle vector *pNDH-OGG* (Schumacher, 2012).

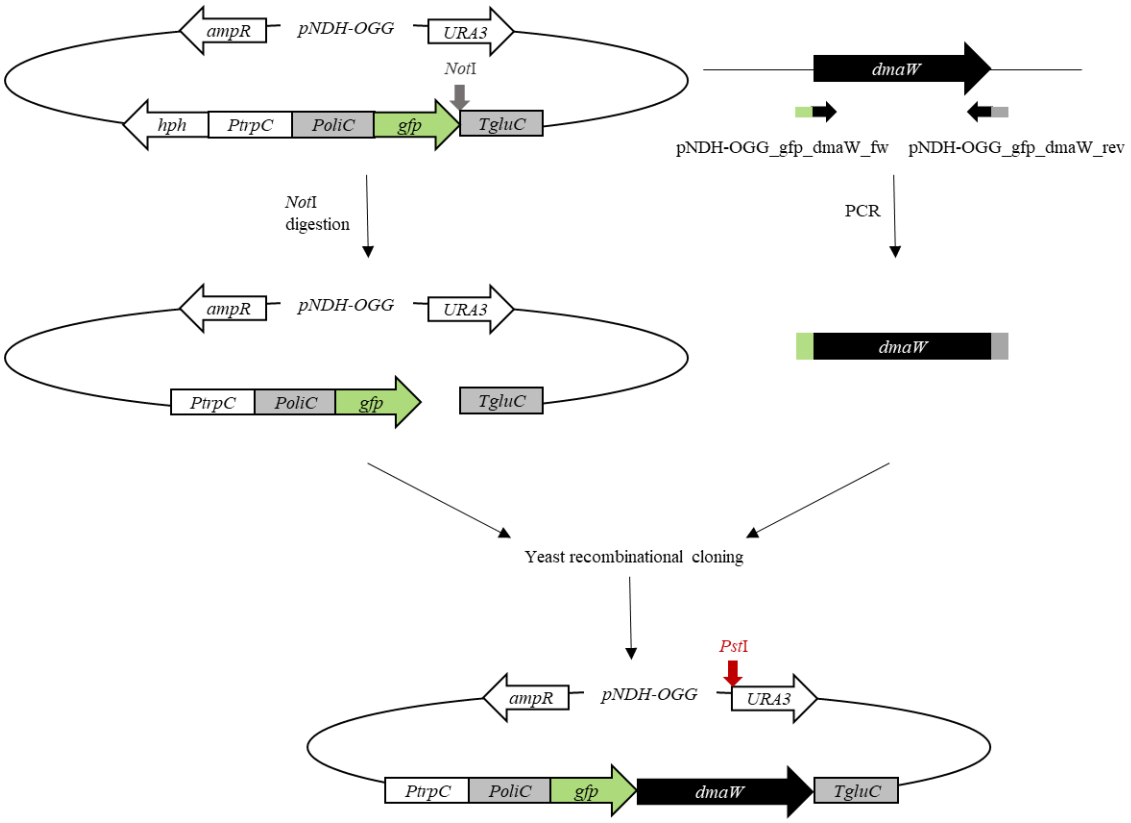

Fig. 14 Construction of *pNDH-OGG:gfp_dmaW*.
DmaW gene amplified from gDNA of WT *C. purpurea* strain 20.1 was cloned into *Not*I-digested *pNDH-OGG* using yeast recombinational cloning method. Then, *Pst*I-linearized *pNDH-OGG:gfp_dmaW* was used to transform protoplasts of *C. purpurea* strain P1.

Tab. 5 Sequences of primers used for generation of *pNDH-OGG:gfp:dmaW*.

pNDH-OGG_gfp_dmaW_fw
5´-GAACTTTACAAAGCGGCCGCTATGTCGACCGCAAAGGACCCAGGAAAC-3´
pNDH-OGG_gfp_dmaW_rev
5´-CCTAATCATACATCTTATCTACATACGCTACTTCGTTGAGAGGTCAC-3´

For the construction of *TrpE* replacement vector (Fig. 15), 5´ (860 bp) and 3´ (488 bp) flanking regions of *TrpE* were amplified with primers *Eco*RI_5F_TrpE and 5R_TrpE, and 3F_TrpE and 3R_TrpE_*Eco*RI (Tab. 6), respectively; primers contained overlapping sequences toward the phleomycin resistance cassette and *pRS426* (Christianson *et al*., 1992). The phleomycin resistance cassette (1,847 bp) was amplified from *pRS426_CpBle* vector with the primers CpBle1F and CpBle1R (Tab. 6).

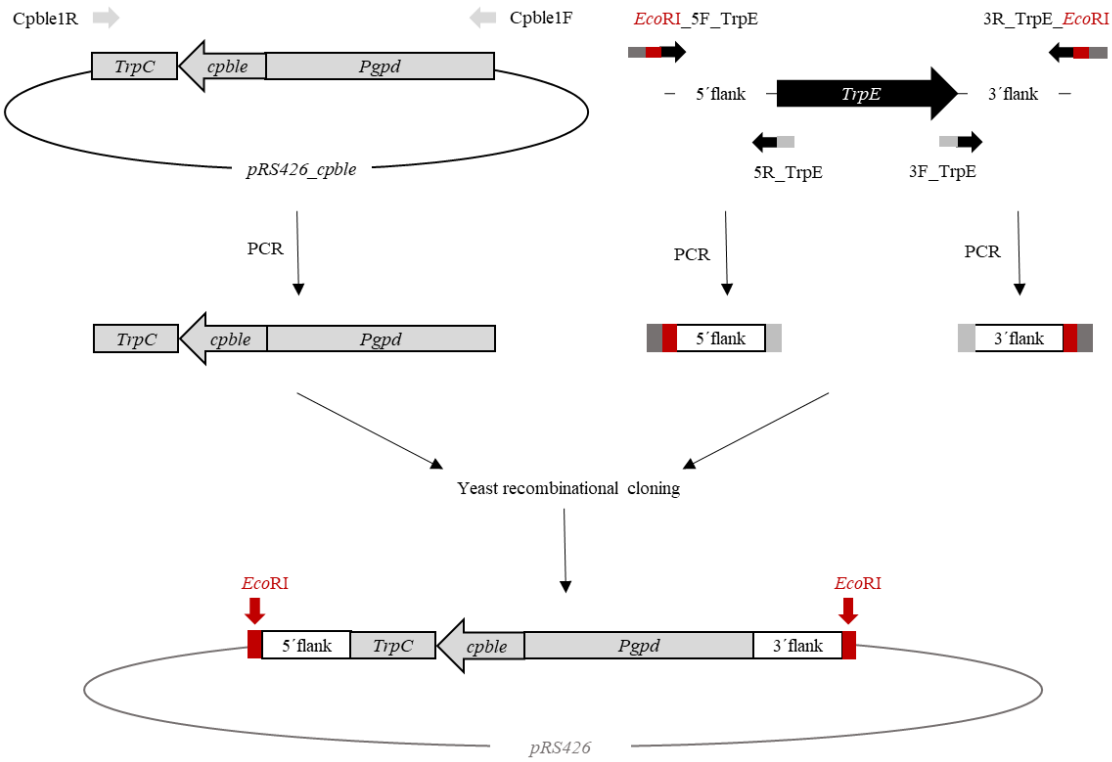

Fig. 15 Construction of *pRS426:ΔTrpE1*.
5´and 3´flanking regions of *TrpE* gene were amplified together with phleomycin resistance cassette from gDNA of WT *C. purpurea* strain 20.1 and *pRS426_CpBle*, respectively, and cloned into *Eco*RI and *Xho*I-digested *pRS426* using yeast recombinational cloning method. Then, *Eco*RI-linearized *pRS426:ΔTrpE1* was used to transform protoplasts of *C. purpurea* strain 20.1.

To check the size of PCR products, DNA fragments were separated in 1% agarose gel containing ethidium bromide. As a buffer, 1x TAE buffer (40 mM Tris, 1 mM EDTA, pH 8.0) was used. As a marker, 1 kb Plus DNA ladder (Thermo Scientific) was used. The gels were documented with a GelDoc™ EZ imager (Bio-Rad).

Tab. 6 Sequences of primers used for generation of *pRS426:ΔTrpE1*.

*Eco*RI_5F_TrpE 5´-TAACGCCAGGGTTTTCCCAGTCGAATTCCATCCCACCTTGGTCACTCT-3´ 5R_TrpE 5´-CACTTAACGTTACTGAAATCTCCAACGGCTTTTTCGTAGGCCTCTTCTAG-3´ 3F_TrpE 5´-GCTCCTTCAATATCATCTTCTGTCTCCGTCTATGCACGGTACGCACTC-3´ 3R_TrpE_*Eco*RI 5´-GATAACAATTTCACACAGGAAACAGCGAATTCTCCGTGCTCCTCGTTTTTAC-3´ Cpble1R 5´-GTTGGAGATTTCAGTAACGTTAAGTGGGCATTGCAGATGAGCTGTATCTG-3´ Cpble1F 5´-CGGAGACAGAAGATGATATTGAAGGAGCGATCGAGACCTAATACAGCCCC-3´

3.3.1.2 Digestion of shuttle vectors

Prior to yeast recombinational cloning, shuttle vectors *pNDH-OGG* (Schumacher, 2012) (Fig. 16) and *pRS426* (Christianson *et al*., 1992) (Fig. 17) were digested according to the manufacturer´s protocol with one or two restriction endonucleases (New England BioLabs) (Tab. 7)

.

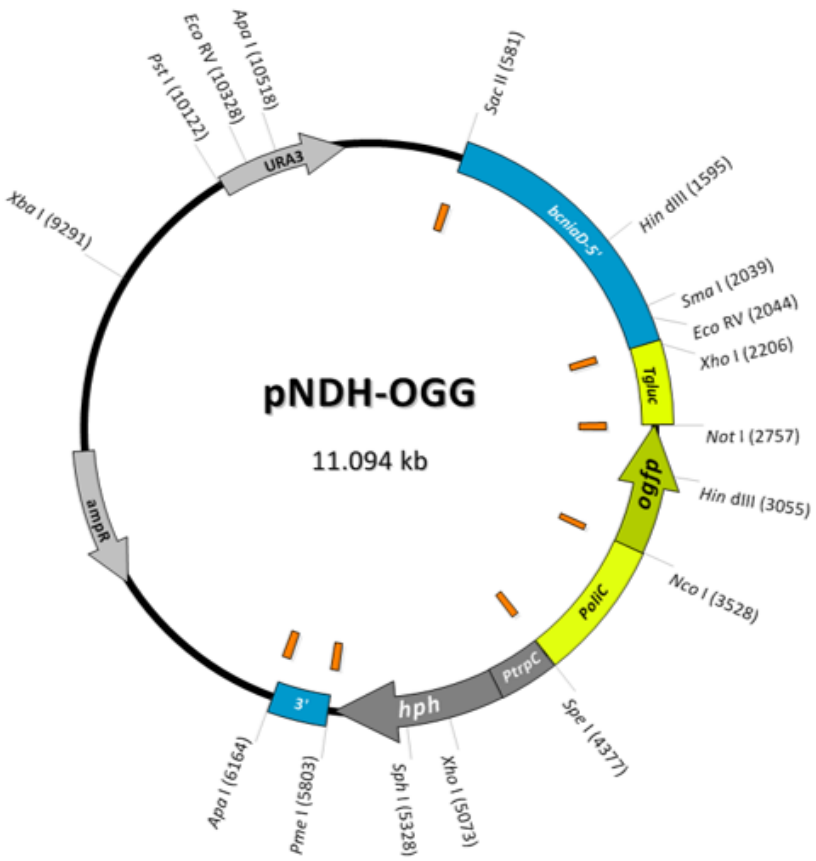

Fig. 16 Shuttle vector *pNDH-OGG* (Schumacher, 2012).

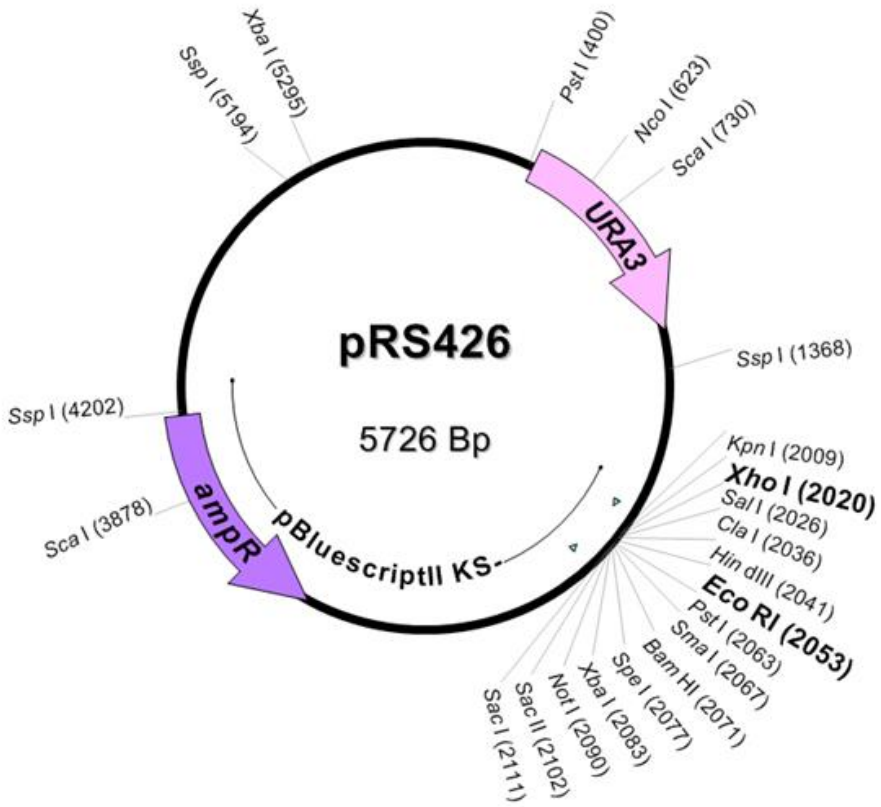

Fig. 17 Shuttle vector *pRS426* (Christianson *et al*., 1992).

Tab. 7 Restriction endonucleases used for digestion of shuttle vectors.

Vector	Restriction endonuclease/s	Final vector
pNDH-OGG	*Nco*I + *Not*I	*pNDH-OGG:TrpE*
pNDH-OGG	*Nco*I + *Not*I	*pNDH-OGG:TrpE*^{S76L}
pNDH-OGG	*Not*I	*pNDH-OGG:gfp_dmaW*
pRS426	*Eco*RI + *Xho*I	*pRS426:ΔTrpE1*

3.3.1.3 Yeast recombinational cloning

The obtained DNA fragments were transformed into a uracil-auxotrophic strain of *Saccharomyces cerevisiae* FGSC 9721 (Fungal Genetics Stock Center). The transformation was performed according to Winston *et al*., 1995.

Briefly, 240 µl of 50% PEG 3350, 36 µl of 1 M lithium acetate, 1.5 µl of the digested *pNDH-OGG* or *pRS426* (100 ng), and 5 µl of each PCR fragment (for gene knock-out: 5´and 3´flanking regions and resistance cassette) were mixed in a microtube; the volume was adjusted to 360 µl with distilled water. Then, 10 µl of denatured salmon sperm DNA (Sigma-Aldrich) was added to the microtube.

Yeast cells, pre-washed with distilled water and 100 mM lithium acetate, and resuspended in 50 µl of 100 mM lithium acetate, were added to this mixture. A microtube with nondigested *pNDH-OGG* or *pRS426* served as a positive control, and the negative control microtube contained only the digested vector without the DNA amplicon. The mixture was incubated 30 min at 30 °C, then 30 min at 42 °C and plated on uracil-free SD agar plates.

After 3 days at 30 °C, the grown colonies of *S. cerevisiae* were harvested from the agar plates and used for isolation of plasmid DNA using the QIAprep Spin Miniprep kit (Qiagen) according to the manufacturer´s protocol. Isolated plasmid DNA was transformed into chemically competent cells of *Escherichia coli* TOP 10 (New England BioLabs) according to the manufacturer´s protocol. After 30 s at 42 °C and 5 min on ice, 950 µl of SOC medium was added to the mixture of *E. coli* and plasmid DNA, and after 1 h at 37 °C, *E. coli* cells were plated on LB agar plates with ampicillin (Sigma-Aldrich) of the final concentration 100 µg/ml. The plates were incubated at 37 °C overnight.

The next day, plasmid DNA was isolated from ampicillin-resistant colonies of *E. coli* using the QIAprep Spin Miniprep kit (Qiagen) according to the manufacturer´s protocol. The resulting constructs were verified by restriction analysis (Tab. 8) and commercial sequencing (SEQme commercial service).

Tab. 8 Restriction analysis of vectors prepared by yeast recombinational cloning

Vector	Restriction endonuclease/s	Expected size of DNA fragments
pNDH-OGG:TrpE	*Eco*RV	7,671 bp; 2,810 bp; 1,673 bp
pNDH-OGG:TrpE^{S76L}	*Eco*RV	7,671 bp; 2,810 bp; 1,673 bp
pNDH-OGG:gfp_dmaW	*Sal*I + *Xho*I	8,227 bp; 2,326 bp; 1,145 bp; 859 bp
pRS426:ΔTrpE1	*Eco*RI	5,756 bp; 3,195 bp

3.3.2 Transformation of *C. purpurea* and selection of obtained fungi

Prepared vectors *pNDH-OGG:TrpE*, *pNDH-OGG:TrpE^{S76L}*, and *pNDH-OGG:gfp_dmaW* were used for transformation of *C. purpurea* P1 (1029/N5) (Tudzynski *et al.*, 1999). Vector *pRS426:ΔTrpE1* was transformed into protoplasts of *C. purpurea* 20.1 (Schardl *et al.*, 2013). Moreover, *pNDH-OGG*:*TrpE* was transformed into *ΔTrpE C. purpurea* 20.1.

The transformation process was done as previously described (Jungehülsing *et al.*, 1994). For transformation of *C. purpurea* P1, 10 µg of purified *Pst*I-digested *pNDH-OGG:TrpE* (12,154 bp), *pNDH-OGG:TrpES^{76L}* (12,154 bp) or

pNDH-OGG:gfp_dmaW (12,557 bp) was used. *Pst*I-digested *pNDH-OGG* (11,094 bp) containing *gfp* was used as a positive control. In the case of transformation of *C. purpurea* 20.1 10 µg of purified *Eco*RI-digested *pRS426:ΔTrpE1* was used. *Eco*RI-restriction of *pRS426:ΔTrpE1* resulted in 3,195 bp and 5,756 bp fragments, of which the former was used for transformation. For the complementation of *ΔTrpE C. purpurea* 20.1 mutant, *Pst*I-digested *pNDH-OGG:TrpE* was used. All restriction mixtures were purified according to the manufacturer´s protocol using a NucleoSpin Gel and PCR Clean-up kit (MACHEREY-NAGEL GmbH and Co. KG).

Transformation of *C. purpurea* protoplasts was performed as follows. After 3 days, the culture of *C. purpurea* 20.1 or P1 in BII cultivation medium was centrifuged and then washed with SmaC buffer. A protoplastization solution was added to the mycelium. After 2 h at 28 °C, the mixture was filtered through a Nytex membrane (Fluka). The filtrate was centrifuged and washed twice with STC buffer, in which the pellet was subsequently resuspended. 10 µl of purified DNA fragment (*Pst*I-digested *pNDH-OGG:TrpE*, *Pst*I-digested *pNDH-OGG:TrpE*^{S76L}, *Pst*I-digested *pNDH-OGG*, *Pst*I-digested *pNDH-OGG:gfp_dmaW*, *ΔTrpE*) (10 µg), 90 µl of STC buffer, 50 µl of PEG solution and 100 µl of *C. purpurea* protoplasts were mixed in 10 ml tube. After 20 min at room temperature, 2 ml of PEG solution were added to the tube. After another 5 min at room temperature, 4 ml of STC buffer were added.

To verify the protoplastization process, 20 ml of BII transformation agar containing 11 µl of *C. purpurea* protoplasts were poured into the first Petri dish. To verify the transformation process, 20 ml of transformation BII agar were together with 690 µl of transformation mixture poured into a second Petri dish. The rest 160 ml of transformation BII agar and transformation mixture were mixed and poured into eight Petri dishes. In the case of vectors containing hygromycin resistance gene (*hph*) (*pNDH-OGG:TrpE*, *pNDH-OGG:TrpE*^{S76L}, *pNDH-OGG*, *pNDH-OGG:gfp_dmaW*) BII transformation agar in Petri dishes was overlaid after 24 h with BII selection agar containing hygromycin (InvivoGen) so that the final antibiotic concentration in the medium was 200 µg/ml. When *pRS426:ΔTrpE* was used for *C. purpurea* transformation, antibiotic phleomycin (InvivoGen) was added directly into BII transformation agar at a final concentration of 33 µg/ml; moreover, 5 mM L-Trp (Sigma-Aldrich) was added into the medium. In the case of transformation of *ΔTrpE C. purpurea* 20.1 with *pNDH-OGG:TrpE* both antibiotics, hygromycin, and phleomycin, were used.

7 days after the transformation, fungi were transferred to the new BII selection medium containing hygromycin at a final concentration of 200 µg/ml or phleomycin at a final concentration of 100 µg/ml or their combination in the case of complementation. The fungi were cultured in the dark at 26 °C.

3.3.3 Transformants derived from *C. purpurea* 20.1

3.3.3.1 Detection of transgenes

3.3.3.1.1 Isolation of gDNA from *C. purpurea*

Genomic DNA (gDNA) was isolated from the mycelia of WT and *C. purpurea* 20.1 transformants according to Cenis, 1992. 600 µl of Lysis buffer was added to the lyophilized mycelia in a microtube. After 15 min at RT, 400 µl of 5 M potassium acetate was added to the mixture. After 20 min at -20 °C, the samples were centrifuged (20 min, 14000 rpm, 4 °C), and the supernatant was mixed with 1 ml of isopropanol. After 45 min at -20 °C, the samples were centrifuged (30 min, 14000 rpm, 4 °C) and the pellet was washed with 300 µl of 70% ethanol (-20 °C). After 10 min centrifugation (14000 rpm, 4 °C), the pellet was dried and resuspended in nuclease-free water.

3.3.3.1.2 Diagnostic PCR

After the transformation, integration of each vector in putative *C. purpurea* transformants was confirmed by diagnostic PCR using GoTaq G2 Flexi DNA polymerase (Tab. 9, 10).

Tab. 9 Components of PCR mixture containing GoTaq G2 Flexi DNA polymerase.

Component	Final concentration
5x GoTaq Flexi buffer	1x
$MgCl_2$	1.5 mM
dNTPS	0.2 mM
Forward primer	0.2 µM
Reverse primer	0.2 µM
GoTaq G2 Flexi DNA polymerase	0.35 U
Template DNA	< 250 ng

Tab. 10 PCR conditions with GoTaq G2 Flexi DNA polymerase.

Step	Temperature (°C)	Time (s)
1. Initial denaturation	95	120
2. Denaturation	95	30
3. Annealing	58	30
4. Extension	72	60/kb
5. Final extension	72	300

Steps 2-4 were repeated 34 times

In the case of *ΔTrpE C. purpurea* 20.1 the integration of *TrpE* replacement vector was confirmed with 3 sets of primers: dia_TrpE_fw and phleohi3f2 (1,410 bp), phleooutHefe3 and dia_TrpE_rev (933 bp), and dia_TrpE_WT_fw and dia_TrpE_rev (847 bp) (Tab. 12). Primers PoliC_fw and TgluC_rev (2,353 bp) (Tab. 13) were used to verify the integration of *pNDH-OGG:TrpE* in $\Delta TrpE^{TrpE}$ *C. purpurea* 20.1.

Tab. 12 Sequences of primers used for diagnostic PCR of ***ΔTrpE C. purpurea* 20.1.**

Primer	Sequence
phleohi3F2	5′-GTGTTCAGGATCTCGATAAGATACG-3′
phleooutHefe3	5′-GAGCTCGGTATAAGCTCTCC-3′
dia_TrpE_fw	5′-ATCCATAGCCGTGAAACTGC-3′
dia_TrpE_WT_fw	5′-CGTATTTGCAGGCAGGTTC-3′
dia_TrpE_rev	5′-CTGCAGCGCCAACATAATAA-3′

Tab. 13 Sequences of primers used for diagnostic PCR of $\Delta TrpE^{TrpE}$ *C. purpurea* 20.1.

Primer	Sequence
PoliC_fw	5′-CCCGGAAACTCAGTCTCCTT-3′
TgluC_rev	5′-GTCTTCCGCTAAAACACCCC-3′

3.3.3.2 Single spore isolation

Homokaryotic mutants of *ΔTrpE* and $\Delta TrpE^{TrpE}$ *C. purpurea* 20.1 were obtained by single spore isolation. Briefly, conidia were collected from Mantle agar plates, filtered through a glass wool (Sigma-Aldrich), and sprayed on BII selection agar plates containing appropriate antibiotics (100 µg/ml phleomycin or its combination with 200 µg/ml hygromycin). After 3 days at 26 °C, germinated spores were transferred on new BII selection agar plates containing appropriate antibiotics. In the case of *ΔTrpE* 5 mM L-Trp was added into the media.

3.3.3.3 Auxotrophy

To test the auxotrophy, a small piece of 7-days old *C. purpurea* 20.1 (WT, *ΔTrpE,* and *ΔTrpE*^{TrpE}) was transferred on minimal Mantle agar plates (Mantle agar without yeast extract) supplemented with 5 µM anthranilic acid (Sigma-Aldrich) or 5 mM L-Trp. The growth of mycelia was documented by EPSON PERFECTION V700 PHOTO scanner after 10 days in the dark at 26 °C. The experiment was performed in six biological replicates.

3.3.3.4 Pathogenicity assays

For pathogenicity assays, male-sterile hybrid rye plants (*Secale cereale*), cultivar L62 cultivated in a soil (Sondermischungen, Gramoflor) under conditions of 16 h light (15 °C)/8 h darkness (12 °C) were used. Prior to planting, rye seeds were vernalized for 8 weeks at 5 °C under conditions of 12 h light/12 h darkness. Infections were performed according to Tenberge *et al*. (1996) by piercing ears with a needle and syringe containing *C. purpurea* conidial suspension (10^6 conidia/ml) harvested from Mantle agar plates supplemented with 5 mM L-Trp. Together, 3-4 spikes per one plant were infected with 2 ml of conidial suspension, and each mutant or WT was inoculated on three rye plants. After the infection, plants were covered with bags from nonwoven fabric and cultivated under conditions of 16 h light (22 °C)/8 h darkness (18 °C). A production of honeydew after 7 dpi (days post-inoculation) and formation of sclerotia after 60 dpi were documented.

3.3.4 Transformants derived from *C. purpurea* P1

3.3.4.1 Detection of transgenes

Genomic DNA was isolated from WT and putative *OE:TrpE, OE:TrpE*^{S76L}, *OE:gfp,* and *OE:gfp_dmaW C. purpurea* P1 mutants transformed with *pNDH-OGG:TrpE, pNDH-OGG:TrepE*^{S76L}, *pNDH-OGG,* and *pNDH-OGG:gfp_dmaW* respectively. The integration of each vector was confirmed by PCR using GoTaq G2 Flexi DNA polymerase (Tab. 10, 11) and primers hph_fw and hph_rev (366 bp), PoliC_fw and TgluC_rev (*OE:TrpE/TrpE*^{S76L} – 2,353 bp, *OE:gfp* – 1,292 bp, *OE:gfp_dmaW* – 3,098 bp) (Tab. 13).

3.3.4.2 Hyphal tip dissection

C. purpurea P1 homokaryotic mutants were obtained by hyphal tip dissection. Briefly, fungi were grown on Mantle agar plates containing hygromycin (200 µg/ml) for 3 days at 26 °C, then hyphal tips adjacent to dichotomous branching were cut off and transferred to new Mantle agar plates containing hygromycin (200 µg/ml). This process was repeated three times to ensure that only true homokaryons were selected.

3.3.4.3 *OE:gfp_dmaW* transformants

3.3.4.3.1 Fluorescence microscopy

WT, *OE:gfp,* and *OE:gfp_dmaW C. purpurea* P1 were each cultivated in 50 ml of BII cultivation medium. After 3 days, the cultures were centrifuged (20 min, 14000 rpm, room temperature), washed with distilled water, and 1 ml samples were transferred into new 50-ml aliquots of BII cultivation medium. After overnight cultivation in the dark at 26 °C (180 rpm), 10 µl of each culture was taken to examine the fluorescence. Fluorescence microscopy was performed with a Zeiss AxioScope microscope equipped with a Zeiss AxioCam 305 camera. GFP fluorescence was examined using an excitation wavelength of 488 nm and an emission wavelength of 509 nm. Image analysis was performed using ZEN 2.6 lite software.

3.3.4.3.2 Western blot analysis

Aliquots of 20 mg of lyophilized *C. purpurea* P1 mycelium (WT, *OE:gfp, OE:gfp_dmaW*) were mixed with 200 µl of Extraction buffer containing 1 µl 20 mM PMSF (Thermo Scientific) and 4 µl 50x Protease inhibitor cocktail (Thermo Scientific). After 10 min on ice, the samples were centrifuged (5 min, 14000 rpm, 4 °C) and protein concentration was determined in the supernatant by Bradford method (Bradford, 1976) with BSA as a standard.

Aliquots of 20 µg of extracted proteins were heated at 95 °C for 10 min in the presence of a loading dye containing 5% β-mercaptoethanol and 2% SDS. After centrifugation (5 min, 14000 rpm, 4 °C), the samples were separated using SDS-PAGE (10% separation gel and 4% stacking gel; Novex Pre-Stained Protein Standard (Thermo Scientific) was used as a molecular mass marker)) in Running buffer and electroblotted

to a 0.45 µm PVDF membrane (Merck) and stained with 0,1% Amido black solution. Then the membrane was rinsed with distilled water and incubated for 90 min at RT in TBS-T buffer containing 5% non-fat dried milk and 2% BSA. Subsequently, the membrane was rinsed with TBS-T and incubated for 90 min with 1:1000 diluted primary monoclonal rabbit antiGFP antibody (Abcam) in TBS buffer. Then the membrane was rinsed twice with TBS-T buffer and finally incubated with a secondary Goat anti-rabbit IgG-HRP antibody (Santa Cruz Biotechnology) (dilution 1:5000). Gfp signal was detected using Clarity^{TM} Western ECL Substrate (Bio-Rad) and ChemiDoc MP software (Bio-Rad).

3.3.4.4 Growth of obtained transformants

To compare the growth of WT and *C. purpurea* P1 mutants (*OE:TrpE*, *OE:TrpE^{S76L}*, *OE:gfp*, and *OE:gfp_dmaW)*, a small piece of 7-days old mycelium was transferred to minimal Mantle agar plates. After 7, 10, and 14 days a colony diameter of each mycelium was measured. The experiment was performed in six biological replicates.

3.3.4.5 Cultivation of fungi in media containing low and high level of inorganic phosphate

For RNA isolation, anthranilic acid and Trp assays, WT and mutants of *C. purpurea* P1 (*OE:TrpE*, *OE:TrpE^{S76L}*, *OE:gfp*, and *OE:gfp_dmaW)* were cultivated in 50 ml of InoCN preculture medium in 250 ml Erlenmeyer flasks for 5 days at 26 °C on a rotary shaker at 180 rpm. The experiment was performed in six biological replicates. After the cultivation, each mycelium was harvested by centrifugation (20 min, 14000 rpm, RT), washed by distilled water, and centrifuged again (20 min, 14000 rpm, RT). The mycelium was resuspended in distilled water (40 ml per 6,97 g), mixed with a stick blender and 2-ml aliquots of this suspension were transferred into 50 ml of T25N inducing medium with a low level of inorganic phosphate and into 50 ml of T25N noninducing medium with a high level of inorganic phosphate. While mutants *OE:TrpE* and *OE:TrpE^{S76L}* were together with WT cultivated for 10 days, *OE:gfp* and *OE:gfp_dmaW* were together with WT cultivated for 14 days on a rotary shaker (180 rpm, 26 °C in the dark).

After the cultivation, the mycelium was separated from the medium by filtration through Miracloth membrane (Calbiochem). Mycelia were frozen in liquid nitrogen and lyophilized in ScanVac Freeze Dryer (Labogene). The lyophilized mycelium was

weighted up and then homogenized by a vibration mill. The separated culture medium was frozen at -20 °C.

3.3.4.5.1 Detection of transgenes at DNA level

Prior to real-time RT-PCR and quantification of primary and secondary metabolites, the presence of transgenes was again confirmed in all induced and non-induced mycelia of WT, *OE:TrpE*, *OE:TrpE*^{S76L}, *OE:gfp*, and *OE:gfp_dmaW C. purpurea* P1 using GoTaq G2 Flexi DNA polymerase (Tab. 9, 10) and two sets of primers hph_fw and hph_rev (366 bp), PoliC_fw and TgluC_rev (*OE:TrpE/TrpE*^{S76L} – 2,353 bp, *OE:gfp* – 1,292 bp, *OE:gfp_dmaW* – 3,098 bp) (Tab. 13).

3.3.4.5.2 Detection of transgenes at RNA level

3.3.4.5.2.1 RNA isolation and its transcription into cDNA

Total RNA was isolated from approximately 60 mg of lyophilized mycelium as described previously (Oñate-Sánchez and Vicente-Carbajosa, 2008). RNA was extracted from all induced and non-induced mycelia of WT, *OE:TrpE*, *OE:TrpE*^{S76L}, *OE:gfp*, and *OE:gfp_dmaW C. purpurea* P1

Briefly, 300 µl of Cell lysis solution were mixed with approximately 60 mg of lyophilized mycelium. After 5 min at RT, 100 µl of DNA-protein precipitation solution were added, samples were mixed by inverting. After 10 min at 4 °C, samples were centrifuged (10 min, 14 000 rpm, 4 °C). 300 µl of supernatant were transferred into a new tube and centrifuged again (10 min, 14 000 rpm, 4 °C). Then, 290 µl of supernatant was transferred into a new tube and mixed with 300 µl of isopropanol, 10 min centrifugation (14 000 rpm, 4 °C). The RNA pellet was twice washed with 70% ethanol, centrifugation 5 min (14 000 rpm, 4 °C). The obtained RNA pellet was resuspended in 200 µl of nuclease-free water. After freezing the pellet at -80 °C and heating at 65 °C, RNA concentration was determined using NanoDrop (Thermo Fisher Scientific).

30 µg of RNA samples were twice treated with DNase I (TURBO DNA-free kit, Thermo Scientific) according to the manufacturer´s protocol, incubation 2 x 45 min at 37 °C. Later, the activity of DNase I was stopped by EDTA at a final concentration of 15 mM, incubation 10 min at 70 °C.

RNA treated with DNase I was purified by LiCl precipitation. 200 µl of RNA were mixed with 100 µl of LiCl Precipitation solution (Thermo Fisher Scientific). After overnight incubation at -80 °C, the mixture was centrifuged (15 min, 14000 rpm, 4 °C). Obtained pellet was rinsed with 70% ethanol and resuspended in 50 µl of nuclease-free water. RNA concentration was determined using NanoDrop (Thermo Fisher Scientific).

For cDNA synthesis, 1 µg of total RNA was transcribed according to the manufacturer´s protocol using RevertAid H Minus First Strand cDNA Synthesis Kit (Thermo Scientific).

3.3.4.5.2.2 RT-PCR

To check the contamination of isolated RNA with gDNA, each RNA was used as a template for amplification of *TrpE* or *gfp* with GoTaq G2 Flexi DNA polymerase (Tab. 9, 10). A part of *TrpE* was amplified with primers PoliC_semiqRT-PCR_fw and TrpE_semiqRT-PCR_rev (cDNA = 598 bp, gDNA = 719 bp); RNA isolated from 10-days old WT, *OE:TrpE*, and *OE:TrpE*^{S76L} was used as a template. A part of *gfp* was amplified with primers PoliC_semiqRT-PCR_fw and gfp_semiqRT-PCR_rev (cDNA = gDNA = 648 bp); RNA isolated from 14-days old WT, *OE:gfp* and *OE:gfp_dmaW* was used as a template. As an endogenous control, a part of *γ-actin* (CPUR_01270.1) was amplified (cDNA = 636 bp, gDNA = 1,082 bp) using primers Actin_semiqRT-PCR_fw and Actin_semiqRT-PCR_rev primers (Tab. 14).

Tab. 14 Sequence of primers used for RT-PCR.

Primer	Sequence
PoliC_semiqRT-PCR_fw	5´-TTCCCATCATCCATCTCCTC-3´
TrpE_semiqRT-PCR_rev	5´-AAGGTCATCAGCTACGTGGC-3´
Gfp_semiqRT-PCR_rev	5´-GGATGGCTCTGTTCAATTGG-3´
Actin_semiqRT-PCR_fw	5´-CGCTCTCGTCATCGACAAT-3´
Actin_semiqRT-PCR_rev	5´-ATTTCACGCTCGGCAGTAGT-3´

3.3.4.5.2.3 Absolute quantification using real-time RT-PCR

3.3.4.5.2.3.1 Cloning into *pDRIVE*

To generate calibration curves, parts of EA biosynthetic genes *easH, dmaW, easG, easF, easE, easD, easC, cloA, lpsB, easA,* and *TrpE* were amplified (Tab. 15, Fig. 18) from cDNA of WT *C. purpurea* P1 using proofreading High-Fidelity Phusion DNA polymerase (Tab. 1, 2) and cloned into *pDRIVE* vector (Fig. 19) (Qiagen) according to the manufacturer´s protocol. For the creation of A-overhangs, GoTaq G2 Flexi DNA polymerase was added to the PCR mixture in the final elongation step. The ligation mixture was transformed into chemically competent cells of *E. coli* TOP10, bacteria were cultivated on LB agar plates containing ampicillin at a final concentration of 100 µg/ml. The next day plasmid DNA was isolated from ampicillin-resistant colonies of *E. coli* TOP10 using QIAprep Spin Miniprep kit (Qiagen). The resulting constructs were verified by restriction analysis (Tab. 16) and commercial sequencing (SEQme commercial service).

Tab. 15 Sequences of primers used for amplification of parts of *TrpE* and EAs genes.

Amplified part of gene	Primer	Sequence
TrpE (CPUR_05013.1)	TrpE_rt_fw	5´-CGAATACGATGAGTGGATCG-3´
	TrpE_rt_rev	5´-TTCTCGTTTTGCTGCTGCT-3´
easH (CPUR_04075.1)	easH_rt_fw	5´-GGTGATTATTGGCTGGGCTA-3´
	easH_rt_rev	5´-GGGCTGTGAAGAAGTTCAGC-3´
dmaW (CPUR_04076.1)	dmaW_rt_fw	5´-TTTGAGTCATTGAACTACCTCCA-3´
	dmaW_rt_rev	5´-GCCAACGACCAGTCTCAAA-3´
easG (CPUR_04077.1)	easG_rt_fw	5´-GCATCTTCCGTCAGACCAAT-3´
	easG_rt_rev	5´-CATAGCCAGACCACGGAAAT-3´
easF (CPUR_04078.1)	easF_rt_fw	5´-CTCTTCCGGTCATCGACATT-3´
	easF_rt_rev	5´-TGATGATTCCAGTGCTCCAG-3´
easE (CPUR_04079.1)	easE_rt_fw	5´-AAGAATACGGGCCATGACAG-3´
	easE_rt_rev	5´-TTTTTGGCACCATGAACGTA-3´
easD (CPUR_04080.1)	easD_rt_fw	5´-GCACCAATTTCACCTCCCTA-3´
	easD_rt_rev	5´-CGTGGGTAGAAACGATGCTT-3´
easC (CPUR_04081.1)	easC_rt_fw	5´-TGGATCTGAGCATTCTGGTG-3´
	easC_rt_rev	5´-CTCGCGATTGAAACGTGATA-3´
cloA (CPUR_04082.1)	cloA_rt_fw	5´-GCTACAATGGCTGCAACAAA-3´
	cloA_rt_rev	5´-AAGGCGTAAAAGTCGGTCAA-3´
lpsB (CPUR_04083.1)	lpsB_rt_fw	5´-TGCGGAATCAAATCTCAACA-3´
	lpsB_rt_rev	5´-TTCTGAGGCCAAAAATCCAC-3´
easA (CPUR_04084.1)	easA_rt_fw	5´-CTTACCAGCCAAGGGTTGAA-3´
	easA_rt_rev	5´-CCCCGTGTACTGCATTCTTT-3´

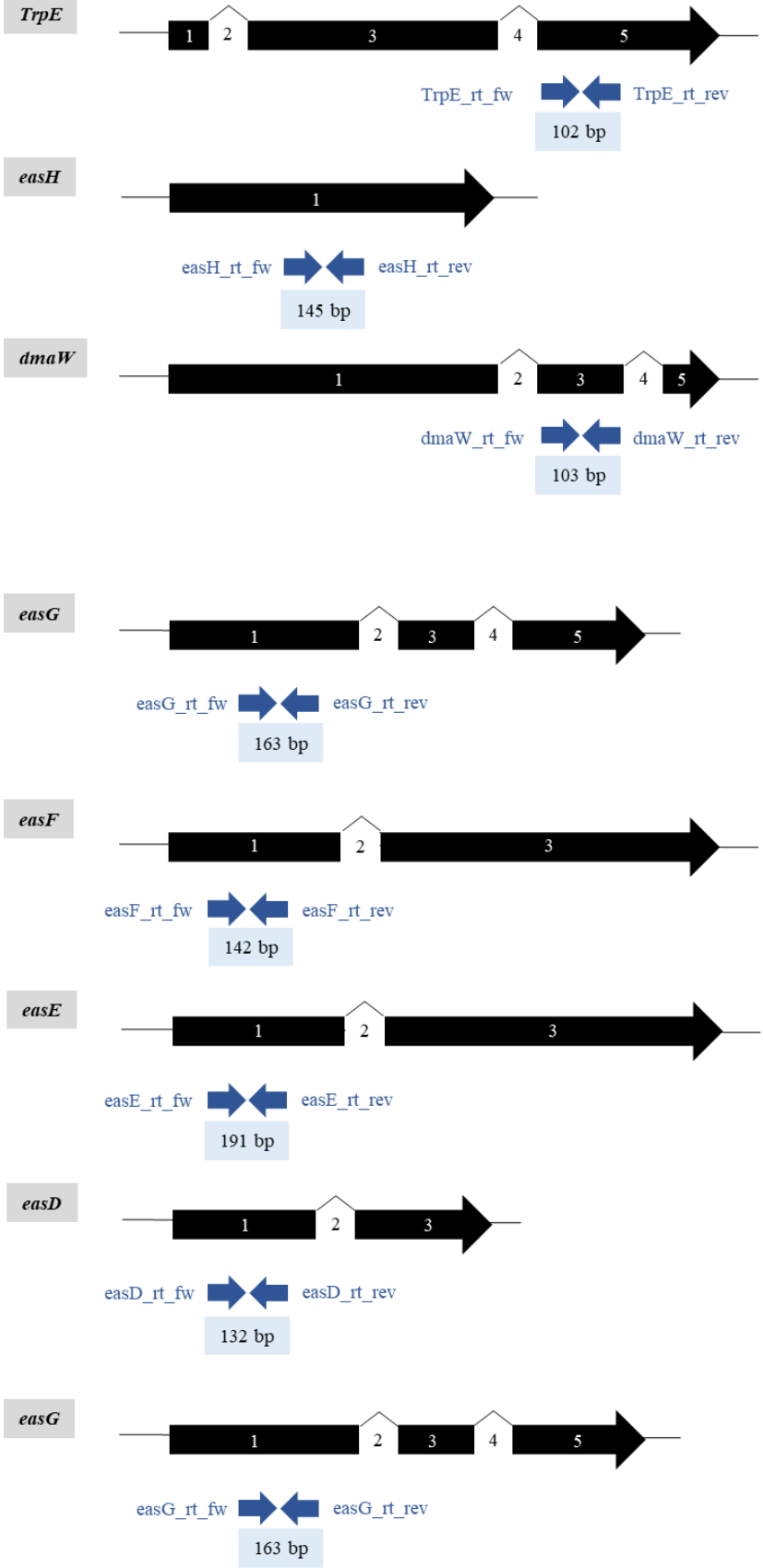

TrpE (gDNA = 1,840 bp)		
1	exon 1	12 bp
2	intron 1	121 bp
3	exon 2	1,417 bp
4	intron 2	153 bp
5	exon 3	137 bp

easH (gDNA = 945 bp)		
1	exon 1	945 bp

dmaW (gDNA = 1,466 bp)		
1	exon 1	1,166 bp
2	intron 1	65 bp
3	exon 2	122 bp
4	intron 2	54 bp
5	exon 3	59 bp

easG (gDNA = 1,079 bp)		
1	exon 1	412 bp
2	intron 1	91 bp
3	exon 2	200 bp
4	intron 2	115 bp
5	exon 3	261 bp

easF (gDNA = 1,150 bp)		
1	exon 1	275 bp
2	intron 1	115 bp
3	exon 2	769 bp

easE (gDNA = 1,503 bp)		
1	exon 1	462 bp
2	intron 1	51 bp
3	exon 2	990 bp

easD (gDNA = 849 bp)		
1	exon 1	589 bp
2	intron 1	63 bp
3	exon 2	197 bp

easG (gDNA = 1,079 bp)		
1	exon 1	412 bp
2	intron 1	91 bp
3	exon 2	200 bp
4	intron 2	115 bp
5	exon 3	261 bp

Fig. 18 Primers used for absolute quantitative qRT-PCR (part A).

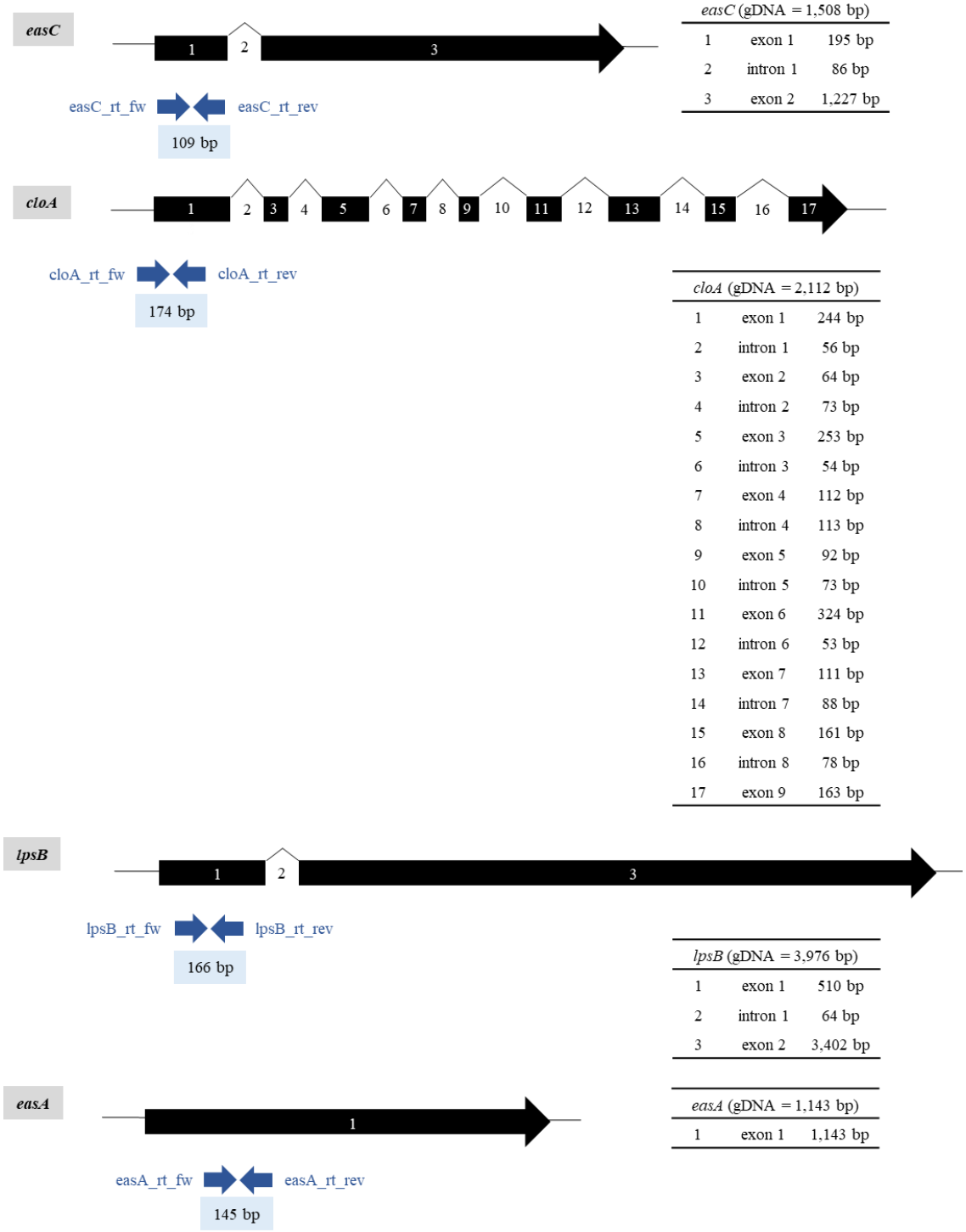

easC (gDNA = 1,508 bp)		
1	exon 1	195 bp
2	intron 1	86 bp
3	exon 2	1,227 bp

cloA (gDNA = 2,112 bp)		
1	exon 1	244 bp
2	intron 1	56 bp
3	exon 2	64 bp
4	intron 2	73 bp
5	exon 3	253 bp
6	intron 3	54 bp
7	exon 4	112 bp
8	intron 4	113 bp
9	exon 5	92 bp
10	intron 5	73 bp
11	exon 6	324 bp
12	intron 6	53 bp
13	exon 7	111 bp
14	intron 7	88 bp
15	exon 8	161 bp
16	intron 8	78 bp
17	exon 9	163 bp

lpsB (gDNA = 3,976 bp)		
1	exon 1	510 bp
2	intron 1	64 bp
3	exon 2	3,402 bp

easA (gDNA = 1,143 bp)		
1	exon 1	1,143 bp

Fig. 18 Primers used for absolute quantitative qRT-PCR (part B).

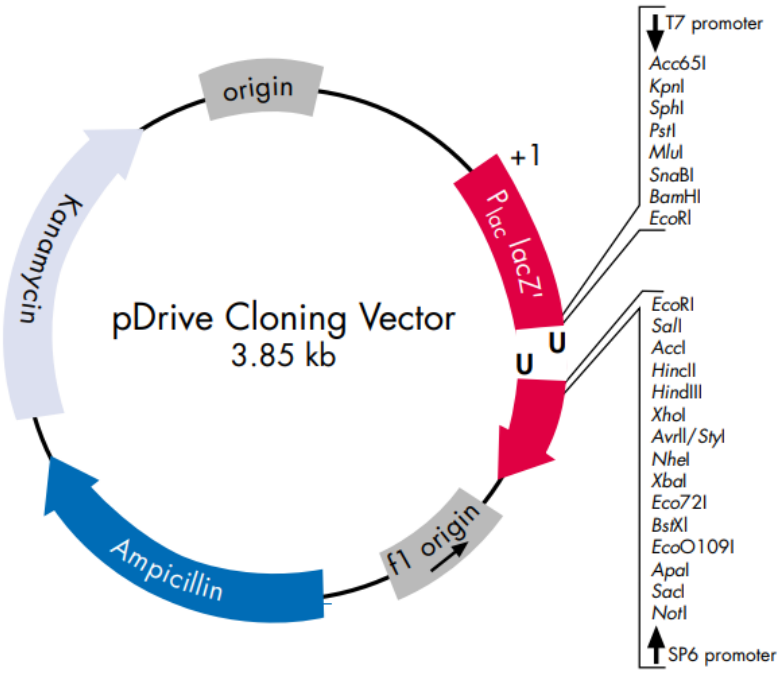

Fig. 19 *pDRIVE* vector (Qiagen).

Tab. 16 Restriction analysis of *pDRIVE* vectors containing parts of *TrpE* or EA biosynthetic genes.

Vector	Restriction endonuclease/s	Expected size of DNA fragments
pDRIVE:part_TrpE	*Eco*RI	3,850 bp; 102 bp
pDRIVE:part_dmaW	*Eco*RI	3,850 bp; 102 bp
pDRIVE:part_easF	*Eco*RI	3,850 bp; 142 bp
pDRIVE:part_easE	*Eco*RI	3,850 bp; 191 bp
pDRIVE:part_easC	*Eco*RI	3,850 bp; 109 bp
pDRIVE:part_easD	*Eco*RI	3,850 bp; 132 bp
pDRIVE:part_easA	*Eco*RI	3,850 bp; 145 bp
pDRIVE:part_easG	*Eco*RI	3,850 bp; 163 bp
pDRIVE:part_cloA	*Eco*RI	3,850 bp; 174 bp
pDRIVE:part_lpsB	*Eco*RI + *Bam*HI	3,850 bp; 166 bp
pDRIVE:part_easH	*Eco*RI + *Bam*HI	3,850 bp; 145 bp

3.3.4.5.2.3.2 Real-time RT-PCR

A SYBR Green qPCR was performed with Gb SG PCR Master mix (2x) together with 100 nM reference dye, ROX (Generi Biotech) in a total volume of 5 µl. As a negative control nuclease-free water was used in triplicates in each run. The analysis was carried out in ViiaTM Real-Time PCR System using a default program (Thermo Scientific). Each analysis was performed in six biological and three technical replicates. The number of transcripts per 1 µg of total RNA was calculated from a standard curve which was

developed using 10-fold serial dilutions of plasmid DNA ranging from 10^9 to 10^1 copies per reaction. To check if only one specific product is amplified, a melting curve analysis was performed at the end of each analysis.

3.3.4.5.3 Quantification of anthranilic acid

Levels of anthranilic acid in mycelia and media were determined according to Novák *et al*., 2012. Briefly, approximately 10 mg of lyophilized mycelia we re-extracted with 1 ml of cold phosphate buffer (50 mM; pH 7.0) containing 0.1% sodium diethyldithiocarbamate. 100 µl of mycelia extract or T25N media samples were diluted with 900 µl of extraction phosphate buffer. To each sample, an aliquot of 5 pmol of [$^2H_4$] anthranilic acid was added as an internal standard. After centrifugation at 20 000 rpm for 10 min, samples were acidified with 1 M HCl to pH 2.7 and purified by solid-phase extraction (SPE) using Oasis™ HLB columns (30 mg, 1 ml; Waters). After evaporation under reduced pressure, samples were analyzed for auxin content using Acquity UHPLC™ (Waters) linked to a triple quadrupole mass detector (Xevo TQ MS™; Waters).

3.3.4.5.4 Quantification of Trp

Levels of Trp in mycelia and media of *C. purpurea* cultures were determined according to the following protocol. Samples of 3 ml of T25N media were applied on Dowex wx50 columns (Sigma-Aldrich). After washing with distilled water, retained amino acids were eluted by 5 ml 10% NH_4OH. Collected samples were evaporated using Speed-Vac concentrator (Thermo Electron Corporation) and obtained residuals resuspended in 50-µl aliquots of distilled water.

Concerning the extraction of Trp from mycelia, samples of approximately 25 mg of lyophilized mycelia were three times extracted by 375 µl 80% MeOH. Pooled supernatants were evaporated using Speed-Vac concentrator and residuals resuspended in 250 µl aliquots of distilled water.

Prior to analysis, all samples were derivatized. Aliquots of 5 µl of resuspended samples were diluted into 50 µl with distilled water and mixed with 50 µl of 10 mM potassium cyanide, 200 µl of 1 mM NDA (naphthalene-2,3-dicarboxaldehyde), and 200 µl of 10 mM sodium borate buffer, pH 9.0. After 10 min incubation at room

temperature, the samples were filtered through 0.22 µm Spin-X® Centrifuge Tube Nylon Filters (Costar).

Quantification of Trp was performed using a Nexera system (Shimadzu) equipped with Kinetex 1.7 µm EVO C18 column (2.1 mm ID x 150 mm, Phenomenex) with monitoring at 450 nm. As a standard, 20 µM Trp (Sigma-Aldrich) was used. The analytes were eluted with mobile phase A (12.5 mM sodium phosphate buffer pH 7.0, and 2% (v/v) tetrahydrofuran) and B (2% (v/v) tetrahydrofuran in 100% acetonitrile) using the following gradient: 0-5 min, 5 % B; 5-10 min, 5-35 % B; 10-25 min, 35-55 % B; 25-28 min, 55-100 % B; 28-30 min, 100 % B; 30-33 min, 100-5 % B. The column temperature was set at 45 °C.

3.3.4.5.5 Quantification of ergopeptines

Levels of ergotamine, ergotaminine, α-ergocryptine, and α-ergocryptinine in mycelia and media of *C. purpurea* cultures were determined as followed. Samples of 2 ml of T25N media with a low level of phosphate or 10 ml of T25N media with a high level of phosphate were each mixed with 1 ml or 5 ml distilled water, respectively, and applied on Spe-ed SPE Cartridges C18/18% (Applied Separations) activated with acetonitrile. After washed with distilled water, the cartridges were eluted with 3 ml of the mixture of 10 mM ammonium carbonate and acetonitrile (1:4) and the eluates evaporated using Speed-Vac concentrator. Finally, the residuals were resuspended in 1 ml 80% MeOH.

Concerning the extraction of ergopeptines from mycelia, approximately 150 mg of lyophilized mycelium was incubated with 500 µl acetone and 500 µl 4% tartaric acid on a rotary shaker in the dark. After overnight incubation, samples were centrifuged and supernatants were evaporated in Speed-Vac concentrator. The residues were resuspended in 500 µl 80% MeOH.

Prior to analysis, the samples were filtered through 0.22 µm nylon filters (Costar). Quantification was performed on a Nexera system equipped with the C18 reverse-phase column (Zorbax RRHD Eclipse Plus, 1.8 µm, 2.1 mm ID x 150 mm, Agilent) with monitoring at 317 nm. As a standard, a mixture of 0.001% ergotamine, ergocornine, α-ergocryptine, ergotaminine, erocristine, β-ergocryptine, ergocorninine, α-ergocryptinine, and ergocristinine in 90 % methanol (Teva Czech Industries) was used. Analytes were eluted with a mobile phase A (0.15 % acetic acid pH 4.4 and acetonitrile, 4:1, v/v) and B (water and acetonitrile, 1:4, v/v) with the following gradient: 0-5 min,

7-9 % B; 5-7 min, 9-13% B; 7-9 min, 13-29 % B; 9-11 min, 29-44 % B; 11-13 min, 44 % B; 13-15 min, 44-59 % B; 15-18 min, 59 % B; 18-19 min, 59-7 % B; and 19-25 min, 7 % B. The column temperature was set at 15 °C.

3.3.4.6 Statistics

All experimental data were processed with Statistica v.13.3 (TIBCO Software Inc.). The non-parametric Kruskal-Wallis ANOVA followed by multiple comparisons of mean ranks was used to compare the differences between groups. All results represent the mean value ± standard error.

3.4 Results

3.4.1 Vectors construction

3.4.1.1 Expression vectors

Together, three vectors *pNDH-OGG:TrpE*, *pNDH-OGG:TrpE*^{S76L} and *pNDH-OGG:gfp_dmaW* for the overexpression of WT form of α subunit of anthranilate synthase (CPUR_05013.1), Trp-resistant form of α subunit of anthranilate synthase, and dimethylallyltryptophan synthase (CPUR_04076.1) fused with gfp, respectively were prepared using yeast recombinational cloning.

TrpE, two parts of *TrpE* with a point mutation, and *dmaW* genes were amplified from gDNA of *C. purpurea* 20.1 (3.2.1.1) (Fig. 20a, 21a, 22a). Obtained DNA amplicons were cloned into *Not*I+*Nco*I-digested *pNDH-OGG* (Fig. 20b, 21b) or *Not*I-digested *pNDH-OGG* (Fig. 22b) (3.2.1.2) using yeast recombinational cloning (3.2.1.3). Plasmid DNAs isolated from *E. coli* TOP10 ampicillin-resistant colonies were confirmed by restriction analysis and then sequenced (Fig. 20c, 21c, 22c).

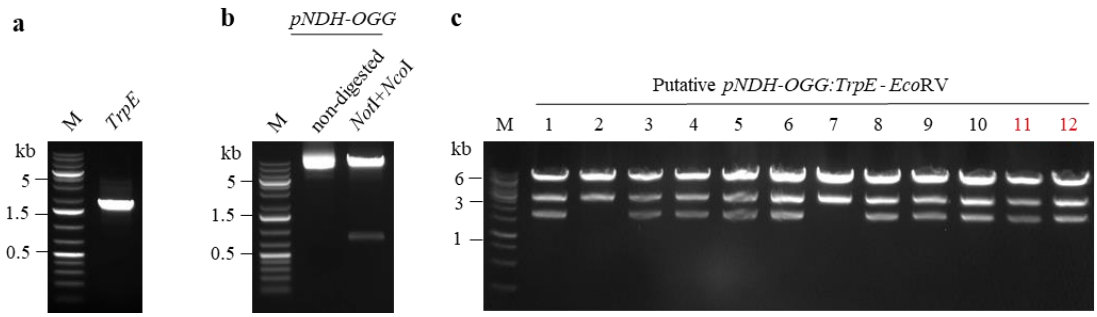

Fig. 20 Cloning of *pNDH-OGG:TrpE*.
(a) Amplification of *TrpE* (1,369 bp) from gDNA of WT *C. purpurea* 20.1 using Phusion High-Fidelity DNA polymerase and primers pNDH-OGG_TrpE_fw and pNDH--OGG_TrpE_rev. M - 1 kb DNA ladder.
(b) Digestion of *pNDH-OGG* with *Not*I and *Nco*I restriction endonucleases (10,314 bp, 780 bp). The non-digested plasmid was used as a control. M - 1 kb DNA ladder.
(c) *Eco*RV-digestion of putative *pNDH-OGG:TrpE* isolated from ampicillin resistant *E. coli* TOP10. (expected bands: 7,671 bp, 2,810 bp, and 1,673 bp). M - 1 kb DNA ladder.
Plasmids 11 and 12 (red) were sequenced.

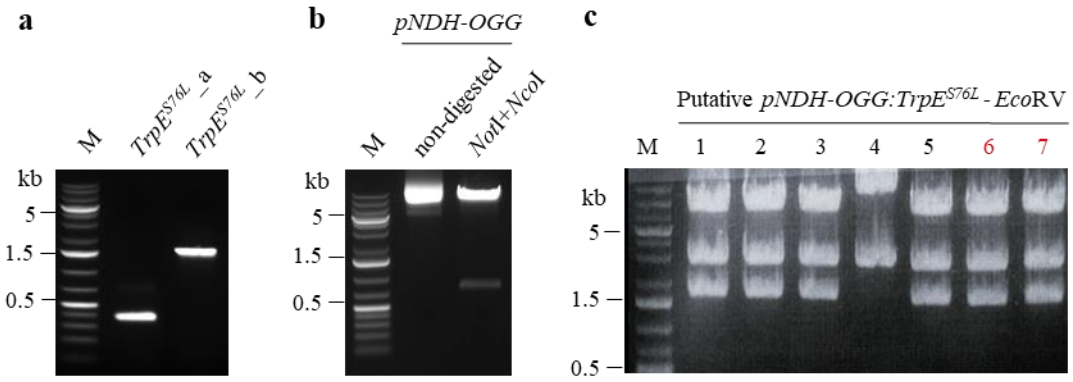

Fig. 21 Cloning of *pNDH-OGG:TrpE^{S76L}*.
(a) Amplification of two parts (355 bp and 1,516 bp) of *TrpE* gene (1,369 bp) from gDNA of WT *C. purpurea* 20.1 using Phusion High-Fidelity DNA polymerase and primers pNDH-OGG_TrpE and pNDH-OGG_TrpES76L_rev and pNDH-OGG_TrpES76L_fw and pNDH-OGG_TrpE_rev, respectively. M - 1 kb Plus DNA ladder.
(b) Digestion of *pNDH-OGG* with *Not*I and *Nco*I restriction endonucleases (10,314 bp and 780 bp). The non-digested plasmid was used as a control. M - 1 kb Plus DNA ladder.
(c) *Eco*RV-digestion of putative *pNDH-OGG:TrpE* isolated from ampicillin-resistant *E. coli* TOP10 (expected bands: 7,671 bp, 2,810 bp, and 1,673 bp). M - 1 kb Plus DNA ladder.
Plasmids 6 and 7 (red) were sequenced.

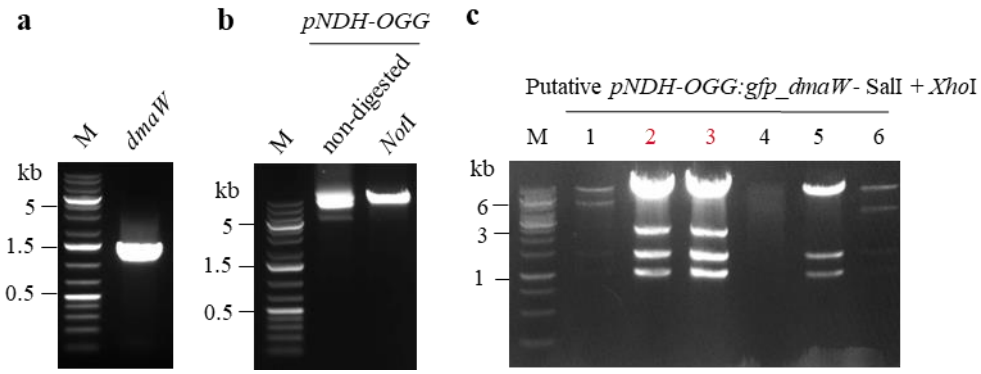

Fig. 22 Cloning of *pNDH-OGG:gfp_dmaW*.
(a) Amplification of *dmaW* gene (1,466 bp) from gDNA of WT *C. purpurea* 20.1 using Phusion High-Fidelity DNA polymerase and primers pNDH-OGG_gfp_dmaW_fw and pNDH-OGG_gfp_dmaW_rev. M - 1 kb Plus DNA ladder.
(b) Digestion of *pNDH-OGG* with *Not*I restriction endonuclease (11,094 bp). The non-digested plasmid was used as a control. M - 1 kb Plus DNA ladder.
(c) *Sal*I and *Xho*I-digestion of putative *pNDH-OGG:gfp_dmaW* isolated from ampicillin-resistant *E. coli* TOP10 (expected bands: 8,227 bp, 2,326 bp, 1,145 bp, and 859 bp). M - 1 kb DNA ladder.
Plasmids 2 and 3 (red) were sequenced.

3.4.1.2 Vector for gene knock-out

Vector *pRS426:ΔTrpE1* for deletion of α subunit of anthranilate synthase (CPUR_05013.1) was also prepared using yeast recombinational cloning method. 5´and 3´flanking regions of *TrpE* and phleomycin resistance cassette were amplified from gDNA of *C. purpurea* 20.1 and *pRS426_CpBle*, respectively (3.2.1.1) (Fig. 23a, b). Subsequently, obtained DNA amplicons were cloned into *Xho*I+*Eco*RI-digested *pRS426* (Fig. 23c) (3.2.1.2, 3.2.1.3). Plasmid DNAs isolated from *E. coli* TOP10 ampicillin-resistant colonies were confirmed by restriction analysis and then sequenced (Fig. 23d).

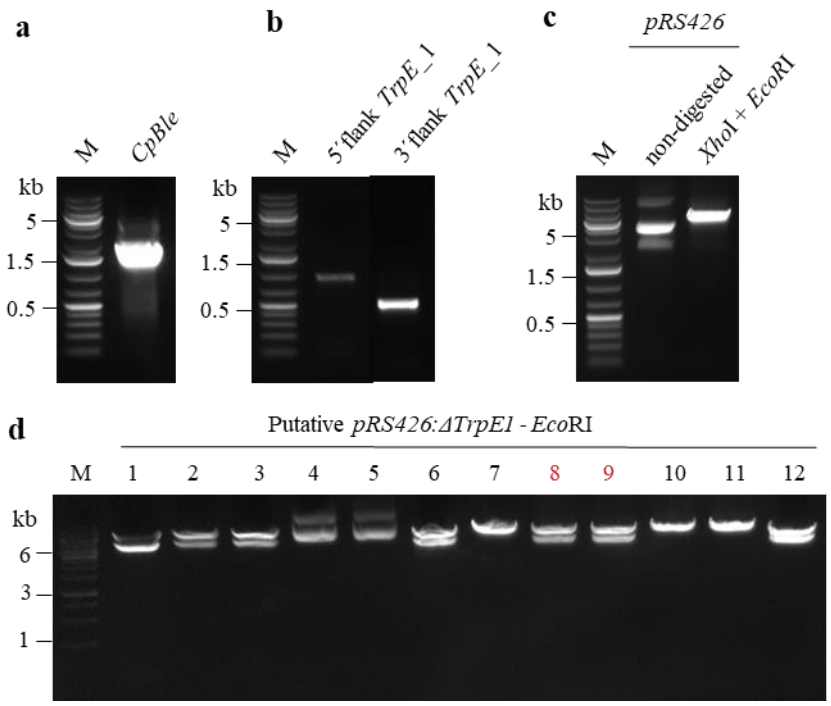

Fig. 23 Cloning of *pRS426:ΔTrpE1*.
(a) Amplification of phleomycin resistance cassette (1,847 bp) from *pRS426_CpBle* using Phusion High-Fidelity DNA polymerase and primers Cpble1F and Cpble1R. M - 1 kb Plus DNA ladder.
(b) Amplification of 5´flanking (860 bp) and 3´flanking (488 bp) regions of *TrpE* from gDNA of WT *C. purpurea* strain using Phusion High-Fidelity DNA polymerase and primers *Eco*RI_5F_TrpE and 5R_TrpE and 3F_TrpE and 3R_TrpE_*Eco*RI, respectively. M - 1 kb Plus DNA ladder.
(c) Digestion of *pRS426* (5,756 bp) with restriction endonucleases *Xho*I and *Eco*RI. The non-digested plasmid was used as a control. M - 1 kb Plus DNA ladder.
(d) *Eco*RI-digestion of putative *pRS426:ΔTrpE1* isolated from ampicillin-resistant *E. coli* TOP10 (expected bands: 5,756 bp and 3,195 bp). M - 1 kb DNA ladder.
Plasmids 8 and 9 (red) were sequenced.

3.4.2 Transformation of *C. purpurea* and selection of obtained fungi

Protoplasts of *C. purpurea* P1 were transformed with *Pst*I-linearized *pNDH-OGG:TrpE* (Fig. 24a), *Pst*I-linearized *pNDH-OGG:TrpE*^{S76L} (Fig. 24b) and *Pst*I-linearized *pNDH-OGG:gfp_dmaW* (Fig. 24c). As a control, protoplasts of *C. purpurea* P1 were transformed with *Pst*I-linearized *pNDH-OGG* (3.2.2).

Protoplasts of *C. purpurea* 20.1 were transformed with DNA fragment of size 3,195 bp obtained after digestion of *pRS426:ΔTrpE1* with *Eco*RI (Fig. 24d) (3.2.2). Moreover, protoplasts of *ΔTrpE C. purpurea* 20.1 were transformed with *Pst*I-linearized *pNDH-OGG:TrpE* (Fig. 24a) (3.2.2).

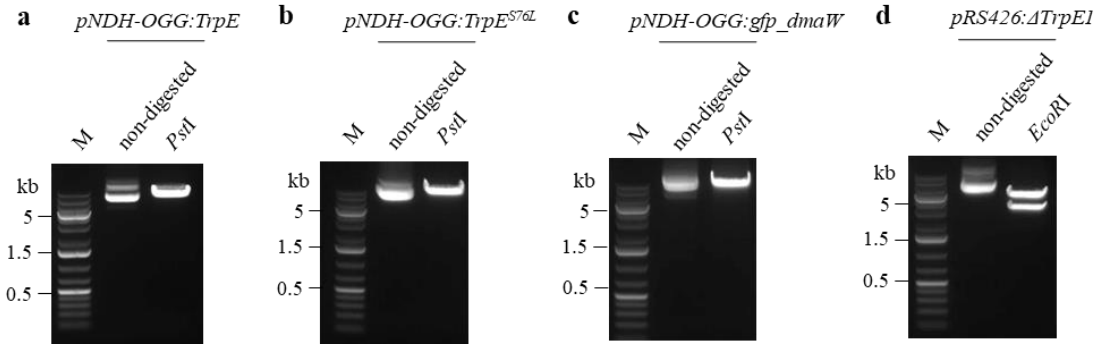

Fig. 24 Plasmid DNAs used for *C. purpurea* transformation.
(a) *Pst*I-linearized *pNDH-OGG:TrpE* (12,154 bp) that was used for transformation of *C. purpurea* P1. Non-digested *pNDH-OGG:TrpE* was used as a control. M - 1 kb Plus DNA ladder.
(b) *Pst*I-linearized *pNDH-OGG:TrpE*^{S76L} (12,154 bp) that was used for transformation of *C. purpurea* P1. Non-digested *pNDH-OGG:TrpE*^{S76L} was used as a control. M - 1 kb Plus DNA ladder.
(c) *Pst*I-linearized *pNDH-OGG:gfp_dmaW* (12,557 bp) that was used for transformation of *C. purpurea* P1. Non-digested *pNDH-OGG:gfp_dmaW* was used as a control. M - 1 kb Plus DNA ladder.
(d) *Eco*RI-restriction of *pRS426:ΔTrpE1*. Band of size 3,195 bp was gel-purified and used for transformation of *C. purpurea* 20.1. Non-digested *pRS426:ΔTrpE1* was used as a control. M - 1 kb Plus DNA ladder.

3.4.3 Transformants derived from *C. purpurea* 20.1

3.4.3.1 Detection of the transgene at DNA level

Together, 780 putative *ΔTrpE C. purpurea* 20.1 resistant to phleomycin were obtained after the transformation of fungal protoplasts with *pRS426:ΔTrpE1*. From all fungi, gDNA was isolated (3.2.3.1.1) and used as a template for diagnostic PCR to confirm the replacement of *TrpE* with phleomycin resistance cassette (3.2.3.1.2) (Fig. 25a). The replacement of *TrpE* was confirmed only in one heterokaryotic transformant;

homokaryon was selected by single spore isolation (3.2.3.2). The deletion of *TrpE* was confirmed in this homokaryon again by diagnostic PCR (Fig. 25b).

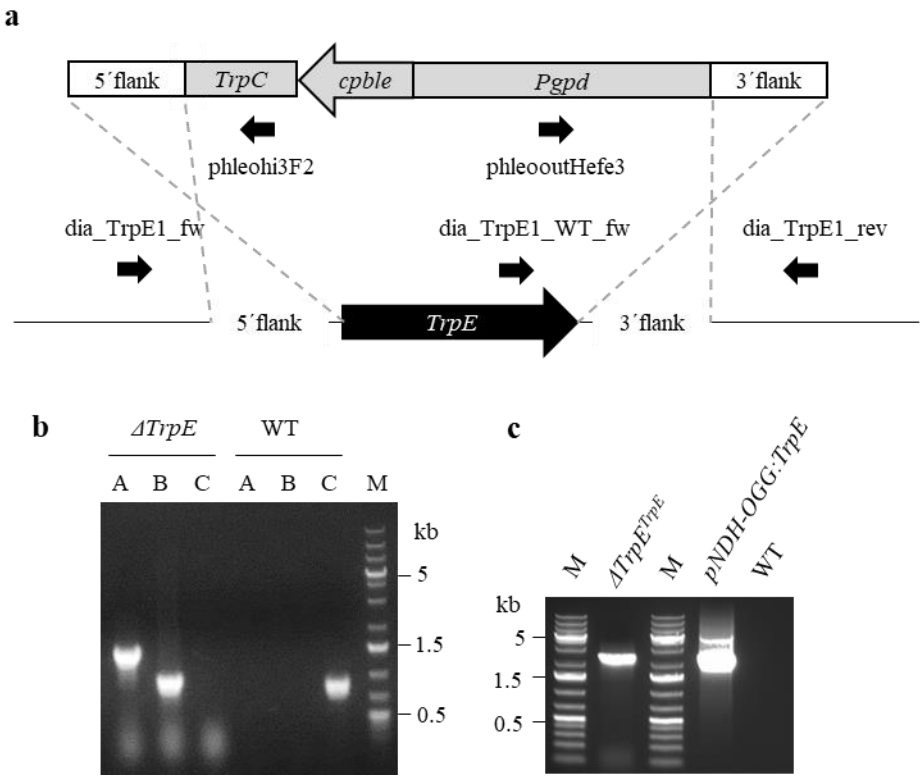

Fig. 25 Confirmation of *ΔTrpE* and *ΔTrpE*^{TrpE} *C. purpurea* 20.1 by diagnostic PCR using GoTaq G2 Flexi DNA polymerase.
(a) Homologous recombination of *TrpE* replacement vector. Three different sets of primers (dia_TrpE_fw and phleohi3F2, phleooutHefe3 and dia_TrpE_rev, dia_TrpE_WT_fw and dia_TrpE_rev) were used for diagnostic PCR.
(b) Integration of *TrpE* replacement vector (*ΔTrpE1*) in a homokaryotic mutant of *ΔTrpE C. purpurea* 20.1 confirmed by diagnostic PCR. A – primers dia_TrpE_fw and phleohi3f2 (1,410 bp), B – primers phleooutHefe3 and dia_TrpE_rev (933 bp), C – primers dia_TrpE_WT_fw and dia_TrpE_rev (847 bp). WT was used as a control. M - 1 kb Plus DNA ladder.
(c) Integration of *Pst*I-linearized *pNDH-OGG:TrpE* vector in a homokaryotic mutant of *ΔTrpE*^{TrpE} *C. purpurea* 20.1 confirmed by diagnostic PCR using primers PoliC_fw a TgluC_rev (2,353 bp), positive control - *pNDH-OGG:TrpE*, negative control – WT, M – 1 kb Plus DNA ladder.

In the case of complementation of *ΔTrpE C. purpurea* 20.1 with *pNDH-OGG:TrpE*, gDNA was isolated (3.2.3.1.1) from 30 putative transformants resistant to both phleomycin and hygromycin, presence of transgene was verified by diagnostic PCR (3.2.3.1.2). For further experiments only one mutant *ΔTrpE*^{TrpE} was selected; homokaryon was obtained by single spore isolation (3.2.3.2) and confirmed again by diagnostic PCR (Fig. 25c).

3.4.3.2 Auxotrophy

To test the auxotrophy, WT, *ΔTrpE,* and *ΔTrpE*^{TrpE} *C. purpurea* 20.1 were cultivated on minimal agar plates containing 5 mM L-Trp or 5 µM anthranilic acid (3.2.3.3) (Fig. 26).

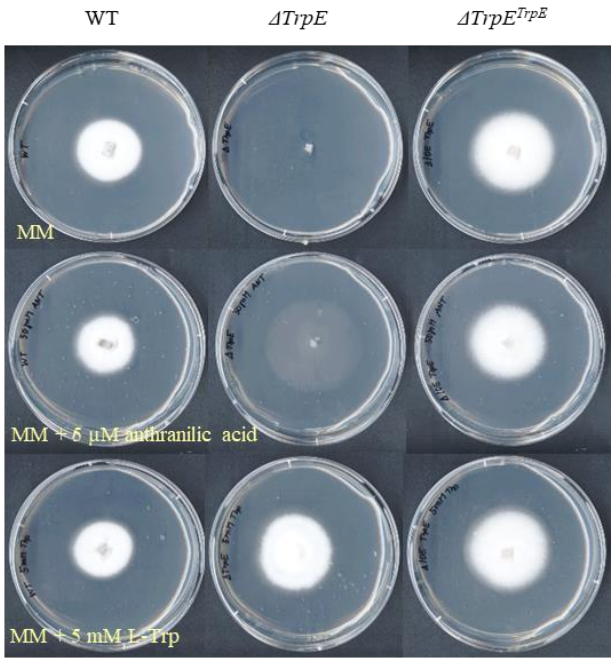

Fig. 26 Growth of WT, *ΔTrpE*, and *ΔTrpE*^{TrpE} *C. purpurea* 20.1 on minimal agar plates supplemented with 5 µM anthranilic acid or 5 mM L-Trp.

3.4.3.3 Pathogenicity assays

To test the pathogenicity, male-sterile rye plants were inoculated with spores of WT, *ΔTrpE*, and *ΔTrpE*^{TrpE} (3.2.3.4) (Fig. 27).

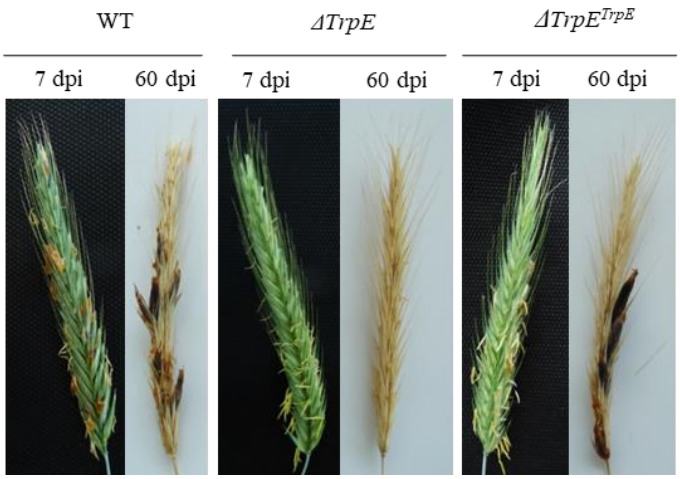

Fig. 27 Rye plants infected with conidia of *ΔTrpE, ΔTrpE*^{TrpE} and WT *C. purpurea* 20.1. Production of honeydew (7 dpi) and sclerotia (60 dpi).

3.4.4 Transformants derived from *C. purpurea* P1

3.4.4.1 Detection of transgenes at DNA level

Genomic DNA was isolated from 20, 30, 35, and 30 hygromycin-resistant putative *OE:TrpE*, *OE:TrpE*^{S76L}, *OE:gfp*, and *OE:gfp_dmaW C. purpurea* P1 containing *pNDH-OGG:TrpE*, *pNDH-OGG:TrpE*^{S76L}, *pNDH-OGG*, and *pNDH-OGG:gfp_dmaW*, respectively. The presence of transgenes was verified by diagnostic PCR with two sets of primers (3.2.4.1).

For further experiments two independent heterokaryons *OE:TrpE* (2, 3), two independent heterokaryons *OE:TrpE*^{S76L} (3, 4), one heterokaryon *OE:gfp*, and two independent heterokaryons *OE:gfp:dmaW* (8, 13) were selected. Homokaryotic mutants were obtained by hyphal tip dissection (3.2.4.2); the presence of transgenes was confirmed in these mutants again using diagnostic PCR (Fig. 28, 29).

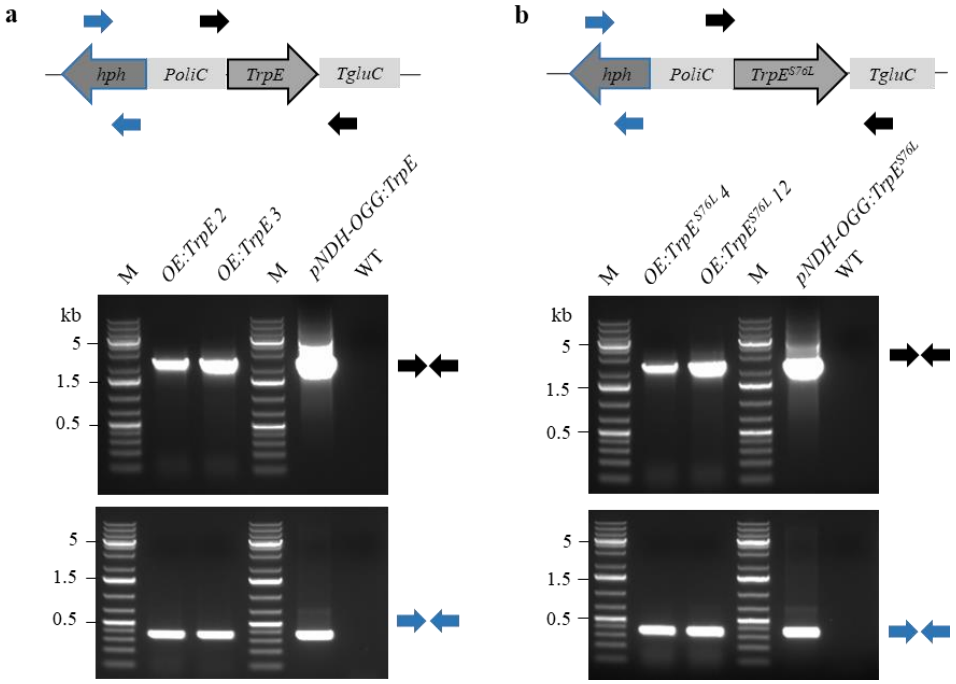

Fig. 28 Confirmation of homokaryotic mutants of *OE:TrpE* and *OE:TrpE*^{S76L} *C. purpurea* P1 by diagnostic PCR using GoTaq G2 Flexi DNA polymerase.
(a) Integration of *Pst*I-linearized *pNDH-OGG:TrpE* in two independent *OE:TrpE C. purpurea* P1 (2, 3) confirmed by diagnostic PCR using primers PoliC_fw and TgluC_rev (2,353 bp) (upper panel) and hph_fw and hph_rev (366 bp) (lower panel), positive control – *pNDH-OGG:TrpE*, negative control - WT, M – 1 kb Plus DNA ladder.

(b) Integration of *Pst*I-linearized *pNDH-OGG:TrpE*^{S76L} in two independent *OE:TrpE*^{S76L} *C. purpurea* P1 (4, 12) confirmed by diagnostic PCR using primers PoliC_fw and TgluC_rev (2,353 bp) (upper panel) and hph_fw and hph_rev (366 bp) (lower panel), positive control – *pNDH-OGG:TrpE*^{S76L}, negative control – WT, M – 1 kb Plus DNA ladder.

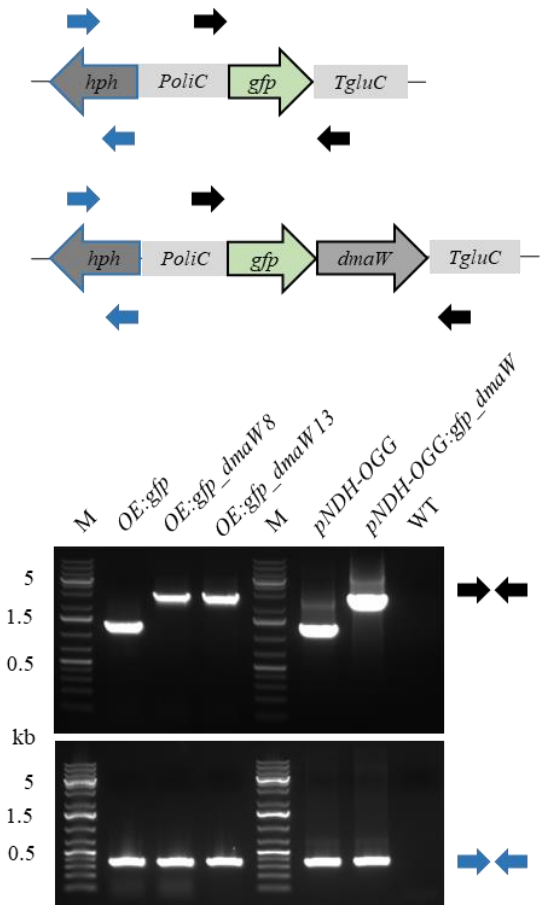

Fig. 29 Confirmation of *OE:gfp_dmaW C. purpurea* P1 by diagnostic PCR using GoTaq G2 Flexi DNA polymerase.
Integration of *Pst*I-linearized *pNDH-OGG* and *Pst*I-linearized *pNDH-OGG:gfp_dmaW* in one *OE:gfp* and two independent *OE:gfp_dmaW C. purpurea* P1 (8, 13), respectively confirmed by diagnostic PCR using primers PoliC_fw and TgluC_rev (*OE:gfp* – 1,292 bp; *OE:gfp_dmaW* - 3,098 bp) (upper panel) and hph_fw and hph_rev (366 bp) (lower panel), positive controls – *pNDH-OGG*, *pNDH-OGG:gfp_dmaW*, negative control – WT, M – 1 kb Plus DNA ladder.

3.4.4.2 *OE:gfp_dmaW* transformants

As *dmaW* was fused with *gfp*, the production of GFP-DMATS in both independent *C. purpurea* P1 mutants (8, 13) was checked by fluorescence microscopy (3.2.4.3.1) (Fig. 30). Moreover, the fused protein was detected by western blot analysis (3.2.4.3.2) (Fig. 31). As a control *OE:gfp C. purpurea* P1 was used.

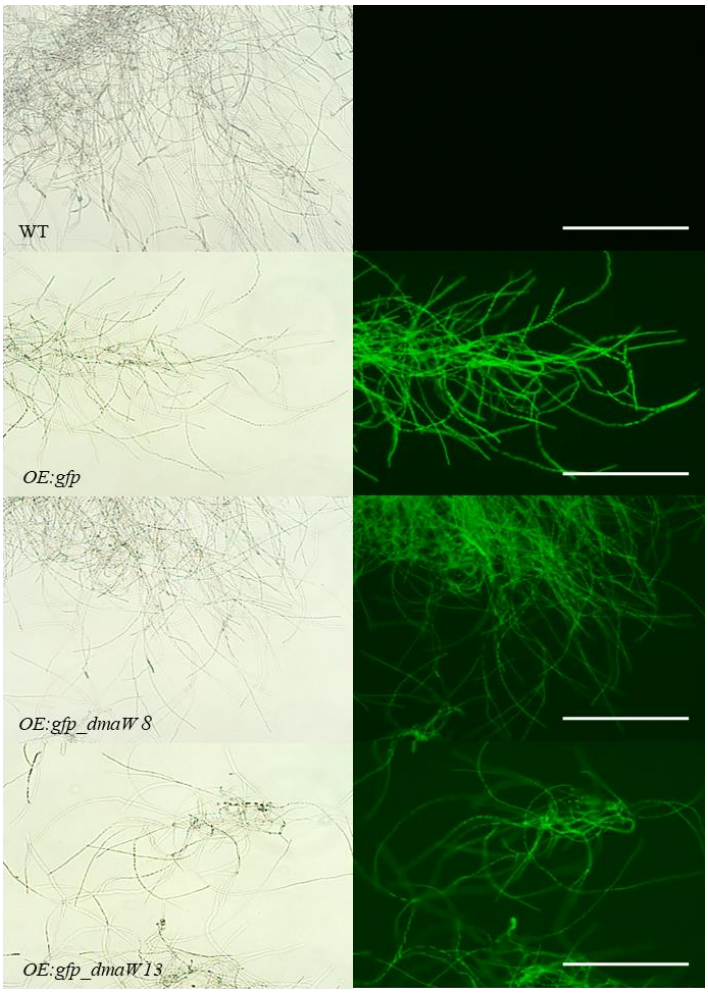

Fig. 30 Detection of GFP signal in *OE:gfp* and *OE:gfp_dmaW C. purpurea* P1 using fluorescence microscopy.
As a negative control, WT *C. purpurea* P1 was used. Bar represents 200 µm.

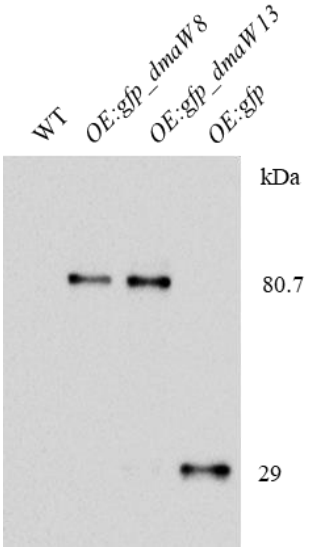

Fig. 31 Detection of GFP in *OE:gfp* and GFP-DMATS in *OE:gfp_dmaW C. purpurea* P1 by western blot analysis.
GFP (29 kDa) and GFP-DMATS (80.7 kDa) were detected using an antiGFP antibody. As a negative control, WT *C. purpurea* P1 was used.

3.4.4.3 Growth of obtained transformants

To compare the growth of all obtained *C. purpurea* P1 mutants with WT, transformants *OE:TrpE*, *OE:TrpE*^{S76L}, *OE:gfp*, and *OE:gfp_dmaW* were together with WT cultivated on minimal Mantle agar plates, the diameter of each colony was measured after 7, 10, and 14 days (3.2.4.4) (Fig. 32).

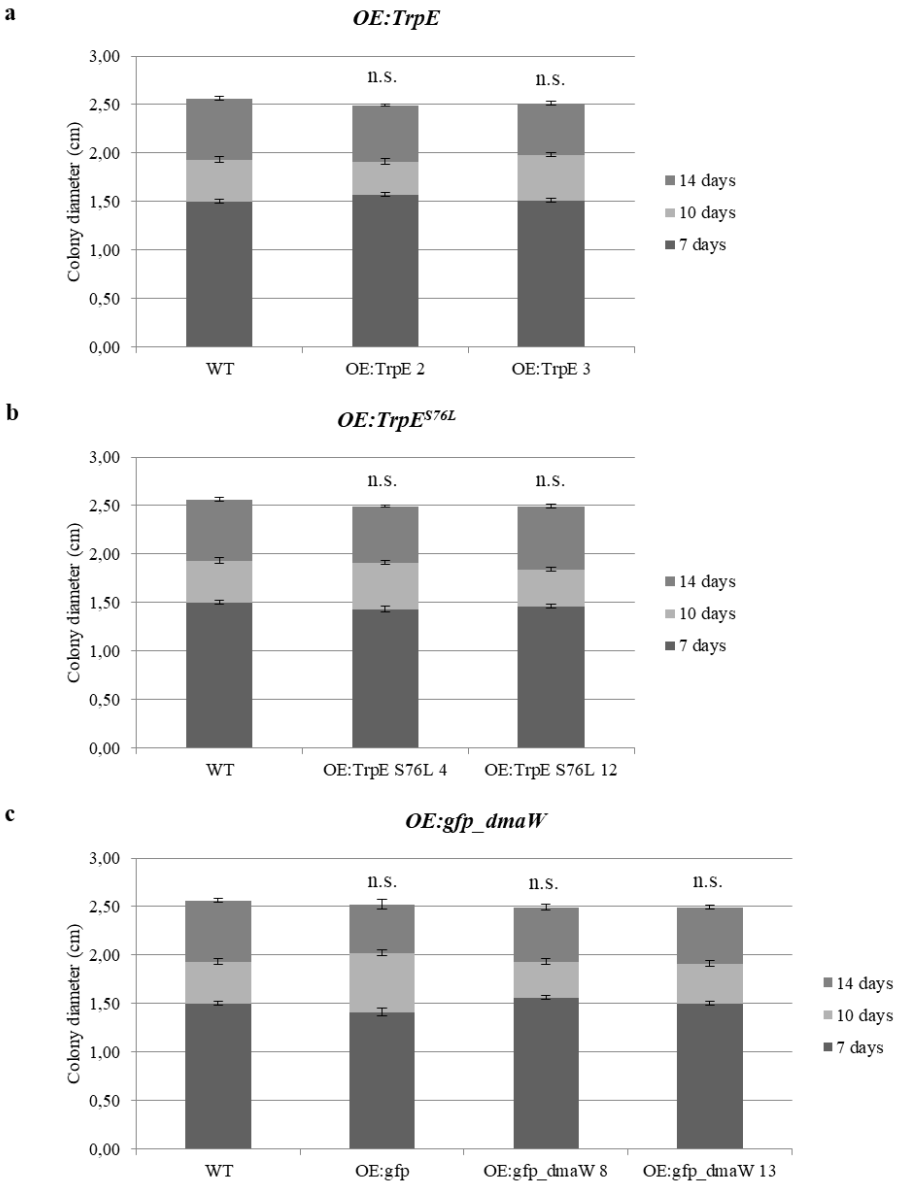

Fig. 32 Growth of *C. purpurea* mutants P1 on minimal Mantle agar plates without yeast extract.
Colony diameters after 7, 10, and 14 days were measured.
(a) WT and *OE:TrpE*
(b) WT and *OE:TrpE*^{S76L}
(c) WT, *OE:gfp*, and *OE:gfp_dmaW*.
The non-parametric Kruskal-Wallis ANOVA followed by multiple comparisons of mean ranks was used to compare the differences between groups. Data comparing differences between WT and individual transformants are shown n.s. – not significant).

3.4.4.4 Cultivation of fungi in media containing low and high level of inorganic phosphate

WT, *OE:TrpE*, *OE:TrpE*^{S76L}, *OE:gfp*, and *OE:gfp_dmaW C. purpurea* P1 were firstly cultivated in InoCN media, then in T25N inducing media with a low level of inorganic phosphate and T25N non-inducing media with a high level of inorganic phosphate; the experiment was performed in six biological replicates (3.2.4.5). 10-days old mycelia of WT, *OE:TrpE* and *OE:TrpE*^{S76L} and 14-days old mycelia of WT, *OE:gfp* and *OE:gfp_dmaW* were separated from media, lyophilized, and stored together with media at -20 °C.

3.4.4.4.1 Detection of transgenes at DNA level

Genomic DNA was isolated from all lyophilized 10-days old mycelia of WT, *OE:TrpE*, and *OE:TrpE*^{S76L} *C. purpurea* P1 and 14-days old mycelia of WT, *OE:gfp*, and *OE:gfp_dmaW C. purpurea* P1; the presence of transgenes was confirmed in all samples by diagnostic PCR using two sets of primers (3.2.4.5.1) (Fig. 33 - 36).

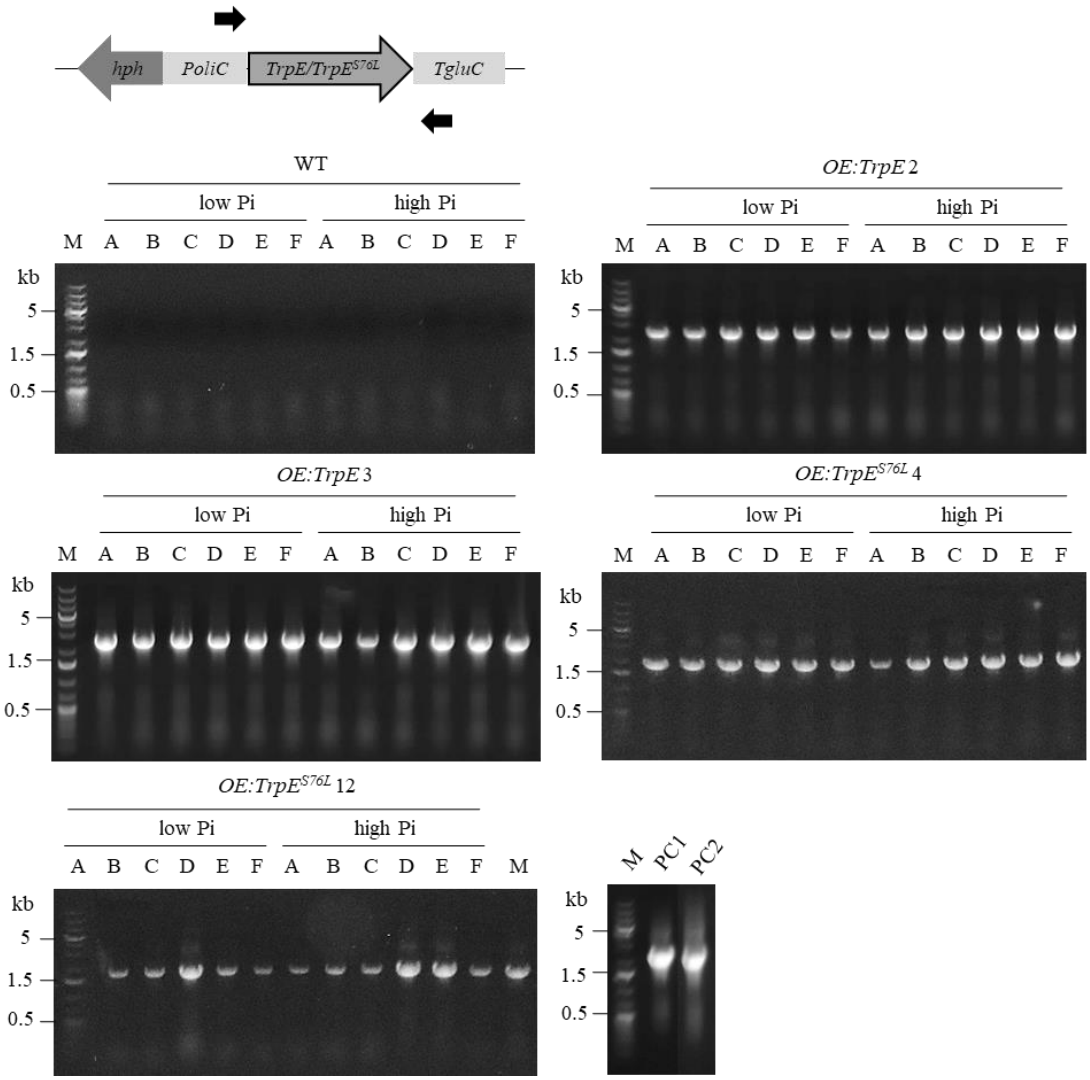

Fig. 33 Diagnostic PCR of WT, *OE:TrpE* and *OE:TrpE^{S76L}* *C. purpurea* P1 that were cultivated in T25N inducing media containing low level of inorganic phosphate (low Pi) and T25N non-inducing media containing high level of inorganic phosphate (high Pi) using GoTaq G2 Flexi DNA polymerase and primers PoliC_fw and TgluC_rev.

Integration of *Pst*I-linearized *pNDH-OGG:TrpE* and *pNDH-OGG:TrpE^{S76L}* in six biological replicates of two independent *OE:TrpE* (2, 3) and two independent *OE:TrpE^{S76L}* (3, 12) *C. purpurea* P1, respectively confirmed by diagnostic PCR using primers PoliC_fw and TgluC_rev (2,353 bp), positive controls: PC1 - *pNDH-OGG:TrpE* and PC2 - *pNDH-OGG:TrpE^{S76L}*, negative controls – six biological replicates of WT *C. purpurea* P1, M – 1 kb Plus DNA ladder.

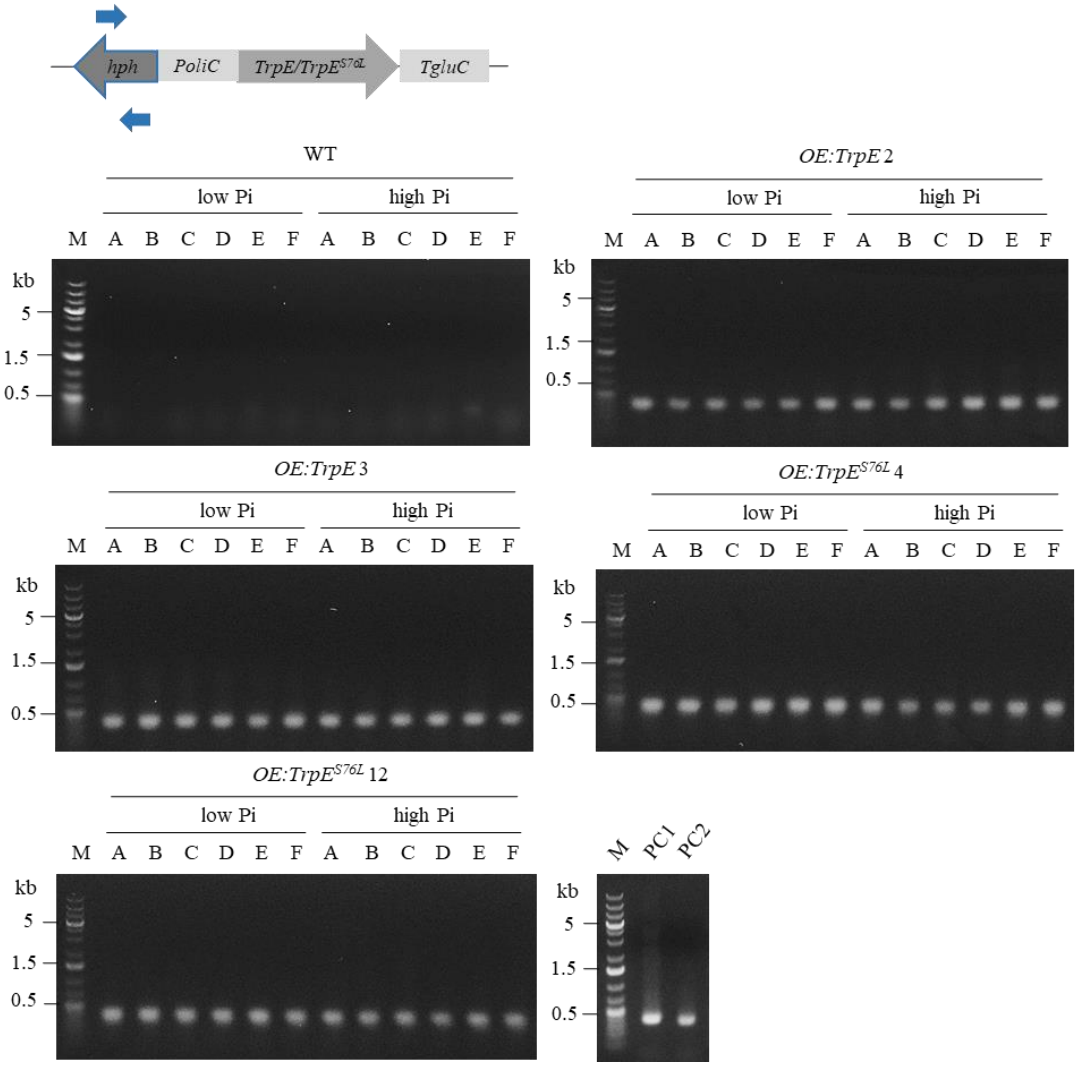

Fig. 34 Diagnostic PCR of WT, *OE:TrpE* and *OE:TrpE*^{S76L} *C. purpurea* P1 that were cultivated in T25N inducing media containing low level of inorganic phosphate (low Pi) and T25N non-inducing media containing high level of inorganic phosphate (high Pi) using GoTaq G2 Flexi DNA polymerase and primers hph_fw and hph_rev.

Integration of *Pst*I-linearized *pNDH-OGG:TrpE* and *pNDH-OGG:TrpE*^{S76L} in six biological replicates of two independent *OE:TrpE* (2, 3) and two independent *OE:TrpE*^{S76L} (3, 12) *C. purpurea* P1, respectively confirmed by diagnostic PCR using primers hph_fw and hph_rev (366 bp), positive controls: PC1 - *pNDH-OGG:TrpE* and PC2 - *pNDH-OGG:TrpE*^{S76L}, negative controls – six biological replicates of WT *C. purpurea* P1, M – 1 kb Plus DNA ladder.

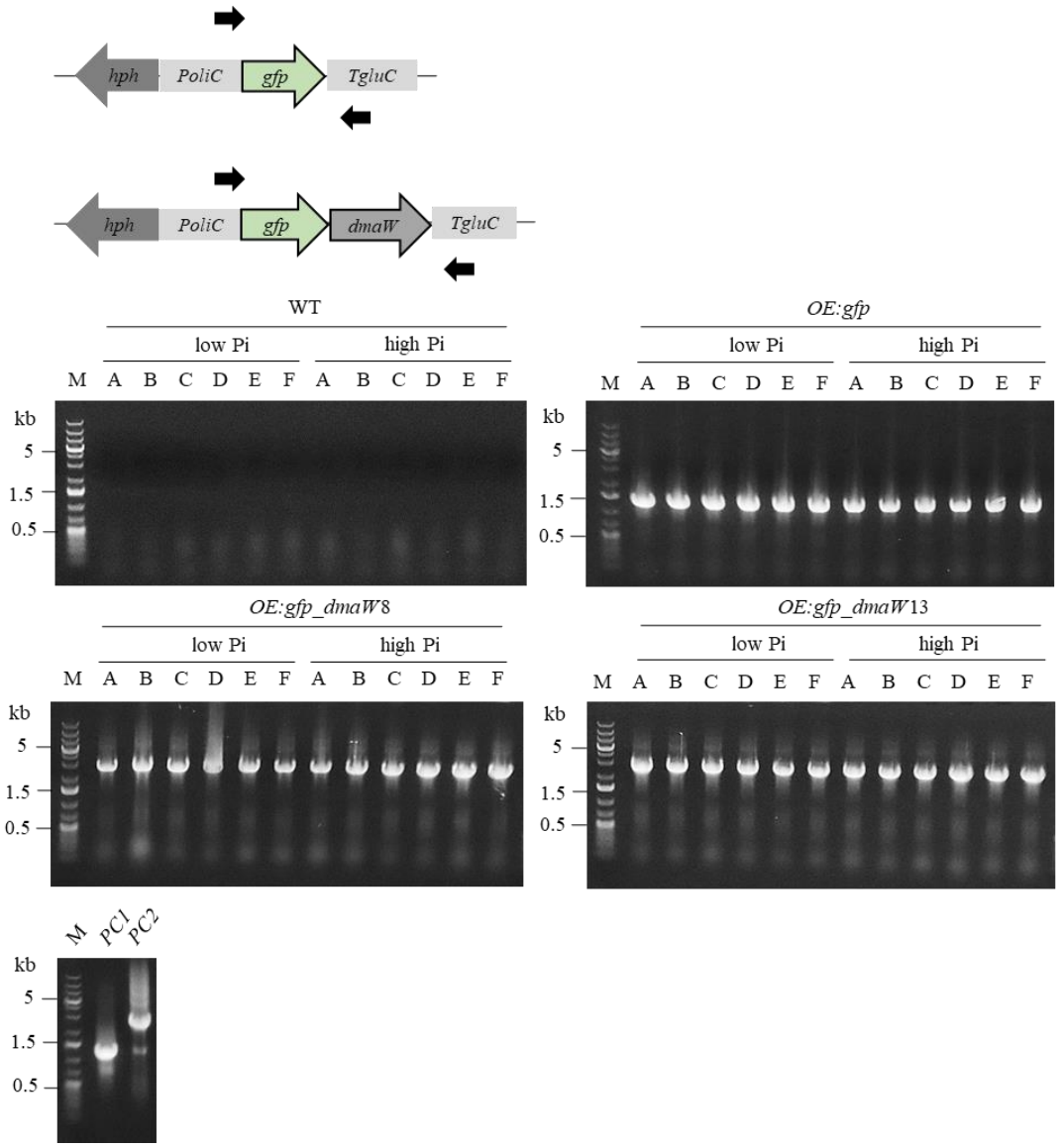

Fig. 35 Diagnostic PCR of WT, *OE:gfp,* and *OE:gfp_dmaW C. purpurea* P1 that were cultivated in T25N inducing media containing low level of inorganic phosphate (low Pi) and T25N non-inducing media containing high level of inorganic phosphate (high Pi) using GoTaq G2 Flexi DNA polymerase and primers PoliC_fw and TgluC_rev.

Integration of *Pst*I-linearized *pNDH-OGG:gfp* and *pNDH-OGG:gfp_dmaW* in six biological replicates of *OE:gfp* and two independent *OE:gfp_dmaW* (8, 13) *C. purpurea* P1, respectively confirmed by diagnostic PCR using primers PoliC_fw and TgluC_rev (*OE:gfp* – 1,292 bp; *OE:gfp_dmaW* – 3,098 bp), positive controls: PC1 - *pNDH-OGG* and PC2 - *pNDH-OGG:gfp_dmaW*, negative controls – six biological replicates of WT *C. purpurea* P1, M – 1 kb Plus DNA ladder.

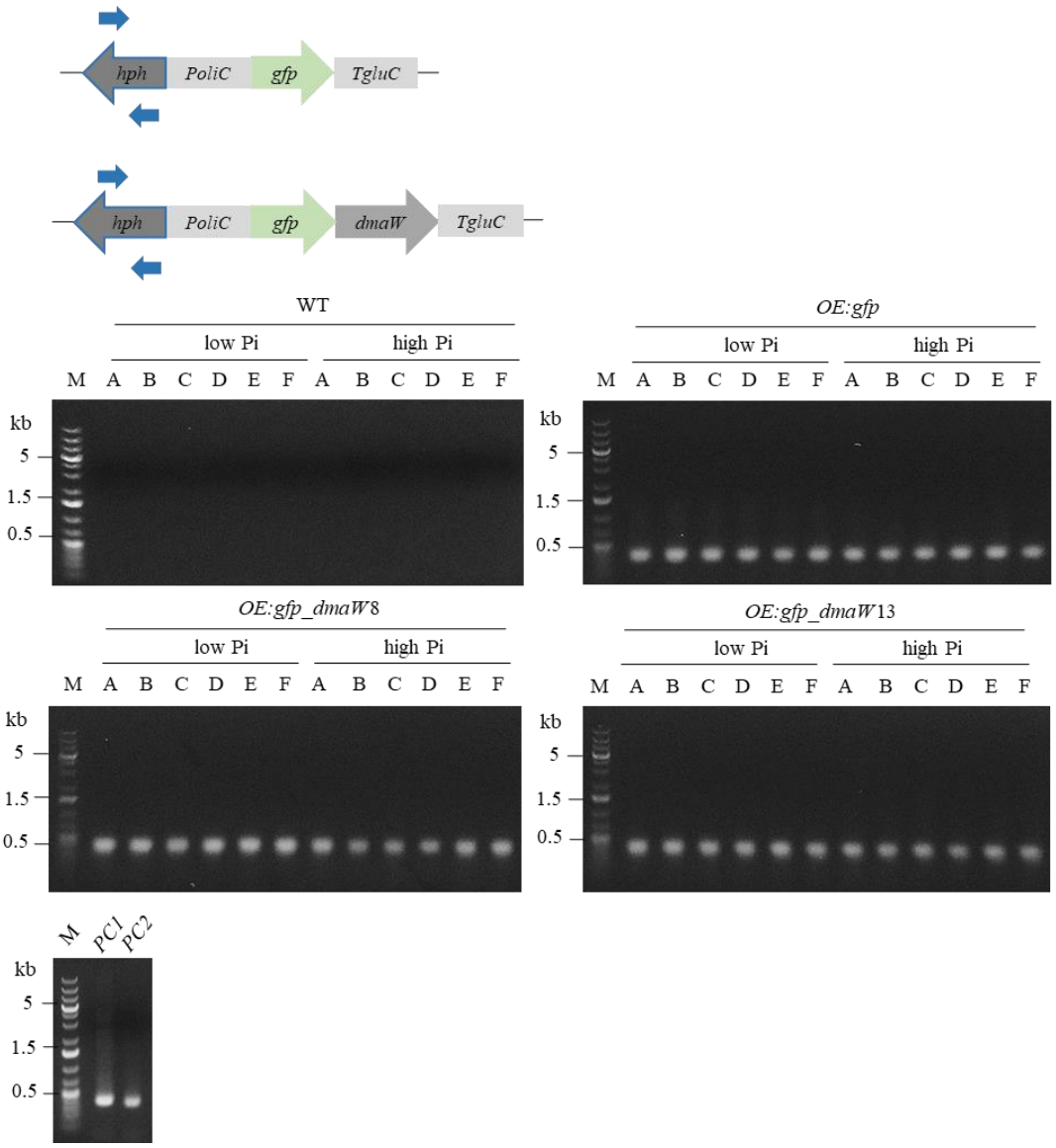

Fig. 36 Diagnostic PCR of WT, *OE:gfp,* and *OE:gfp_dmaW C. purpurea* P1 that were cultivated in T25N inducing media containing low level of inorganic phosphate (low Pi) and T25N non-inducing media containing high level of inorganic phosphate (high Pi) using GoTaq G2 Flexi DNA polymerase and primers hph_fw and hph_rev.

Integration of *Pst*I-linearized *pNDH-OGG:gfp* and *pNDH-OGG:gfp_dmaW* in six biological replicates of *OE:gfp* and two independent *OE:gfp_dmaW*(8, 13) *C. purpurea* P1, respectively confirmed by diagnostic PCR using primers hph_fw and hph_rev (366 bp), positive controls: PC1 - *pNDH-OGG* and PC2 - *pNDH-OGG:gfp_dmaW*, negative controls – six biological replicates of WT *C. purpurea* P1, M – 1 kb Plus DNA ladder.

3.4.4.4.2 Detection of transgenes at RNA level

3.4.4.4.2.1 RT-PCR

RNA was isolated from all lyophilized 10-days old mycelia of WT, *OE:TrpE,* and *OE:TrpE*^{S76L} *C. purpurea* P1 and 14-days old mycelia of WT, *OE:gfp,* and *OE:gfp_dmaW C. purpurea* P1 (3.2.4.5.2.1); the expression of transgenes (*TrpE*, *gfp,* and *gfp_dmaW*) was confirmed in the samples by RT-PCR (3.2.4.5.2.2) (Fig. 37, 38). As an endogenous control γ-actin was amplified.

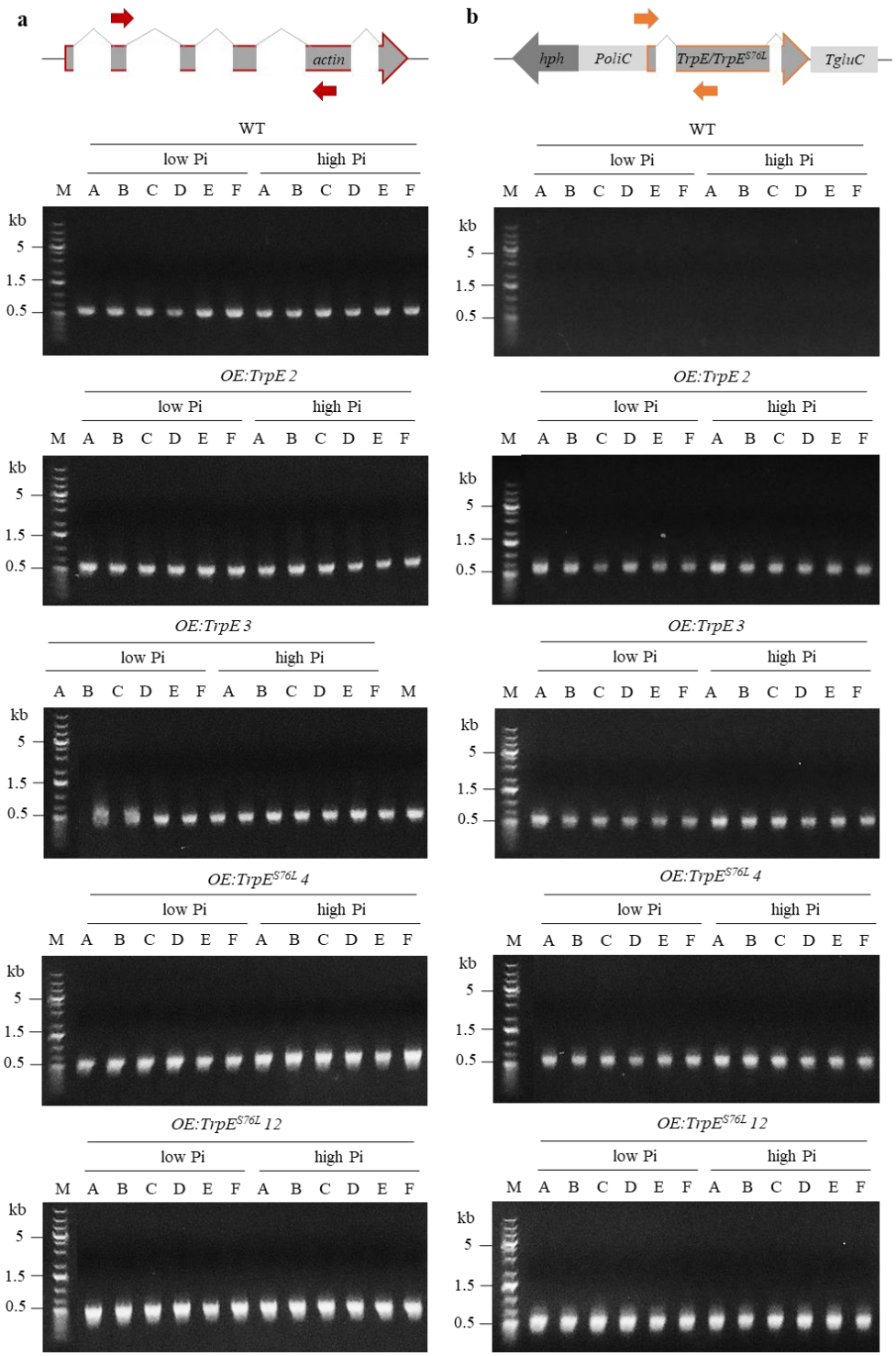

Fig. 37 RT-PCR of WT, *OE:gfp*, and *OE:gfp_dmaW C. purpurea* P1 that were cultivated in T25N inducing media containing a low level of inorganic phosphate (low Pi) and T25N non-inducing media containing a high level of inorganic phosphate (high Pi).

(a) Amplification of housekeeping gene γ-actin in six biological replicates of two independent *OE:TrpE* (2, 3) and two independent *OE:TrpE*^{S76L} (3, 12) *C. purpurea* P1using primers Actin_semiqRT-PCR_fw and Actin_semiqRT-PCR_rev (cDNA = 636 bp, gDNA = 1,082 bp), negative control – six biological replicates of WT *C. purpurea* P1, M – 1 kb Plus DNA ladder.

(b) Amplification of PoliC-TrpE/TrpE^{S76L} in six biological replicates of two independent *OE:TrpE* (2, 3) and two independent *OE:TrpE*^{S76L} (3, 12) *C. purpurea* P1 using primers PoliC_semiqRT-pCR_fw and TrpE_semiqRT-PCR_rev (cDNA = 598 bp, gDNA = 719 bp), negative control – six biological replicates of WT *C. purpurea* P1, M – 1 kb Plus DNA ladder.

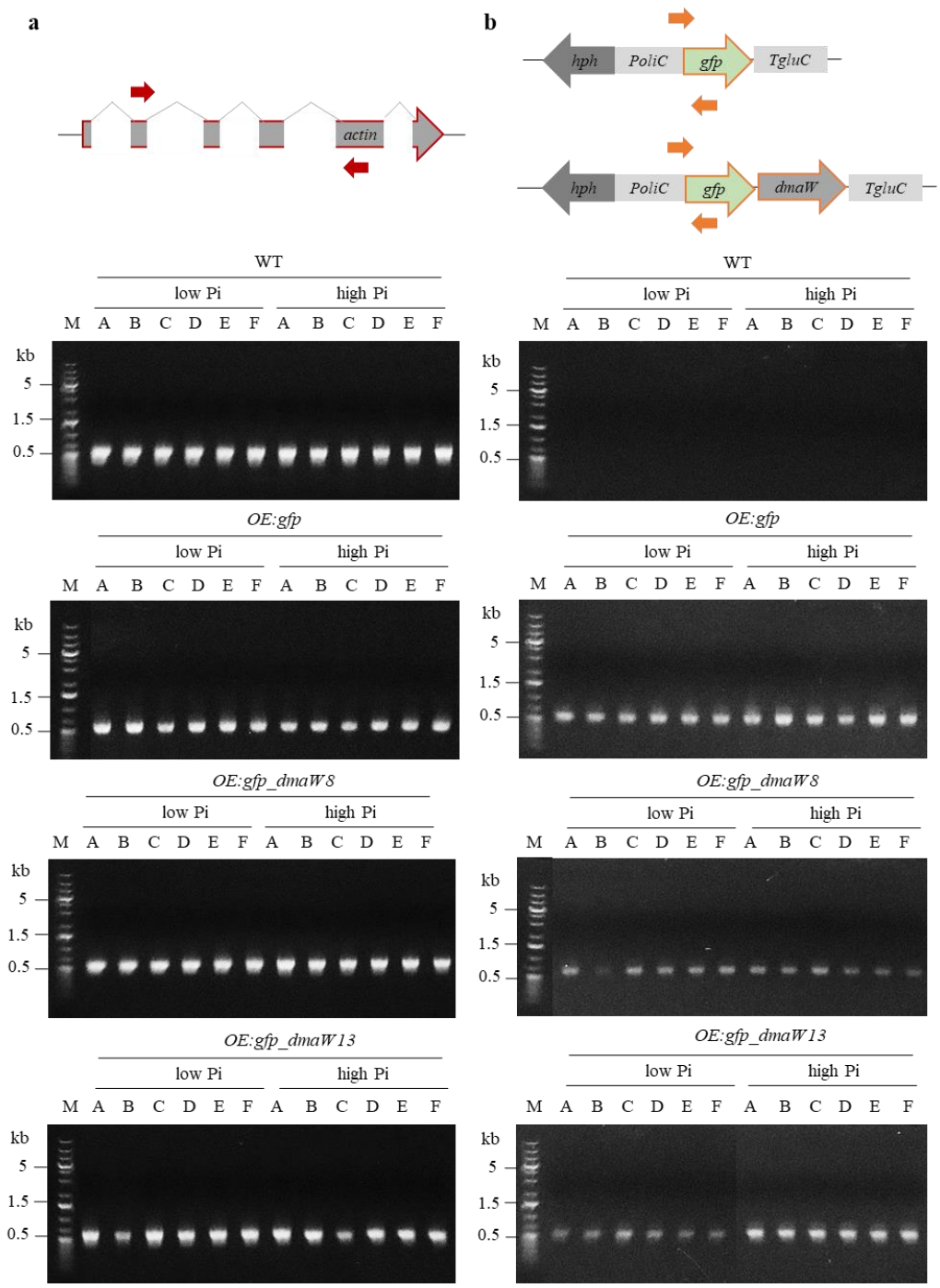

Fig. 38 RT-PCR of WT, *OE:gfp*, and *OE:gfp_dmaW C. purpurea* P1 that were cultivated in T25N inducing media containing a low level of inorganic phosphate (low Pi) and T25N non-inducing media containing a high level of inorganic phosphate (high Pi).

(a) Amplification of housekeeping gene γ-actin in six biological replicates of *OE:gfp* and two independent *OE:gfp_dmaW* (8, 13) *C. purpurea* P1 using primers Actin_semiqRT-PCR_fw and Actin_semiqRT-PCR_rev (cDNA = 636 bp, gDNA = 1,082 bp), negative control – six biological replicates of WT *C. purpurea* P1, M – 1 kb Plus DNA ladder.

(b) Amplification of PoliC-gfp/gfp_dmaW in six biological replicates of *OE:gfp* and two independent *OE:gfp_dmaW* (8, 13) *C. purpurea* P1 using primers PoliC_semiqRT-pCR_fw and TrpE_semiqRT-PCR_rev (cDNA = gDNA = 648 bp), negative control – six biological replicates of WT *C. purpurea* P1, M – 1 kb Plus DNA ladder.

3.4.4.4.2.2 Absolute quantification using real-time RT-PCR

3.4.4.4.2.2.1 Cloning into *pDRIVE*

To construct calibration curves, parts of *TrpE* and EAs genes (*easH, dmaW, easG, easF, easE, easD, easC, cloA, lpsB, easA*) were amplified from cDNA of *C. purpurea* P1 (Fig. 39). Obtained PCR amplicons were cloned into *pDRIVE* and the ligation mixture was transformed into *E. coli* TOP10. Prior to sequencing, plasmids isolated from ampicillin resistant bacteria were digested with restriction endonucleases (Fig. 40) (3.2.4.5.2.3.1).

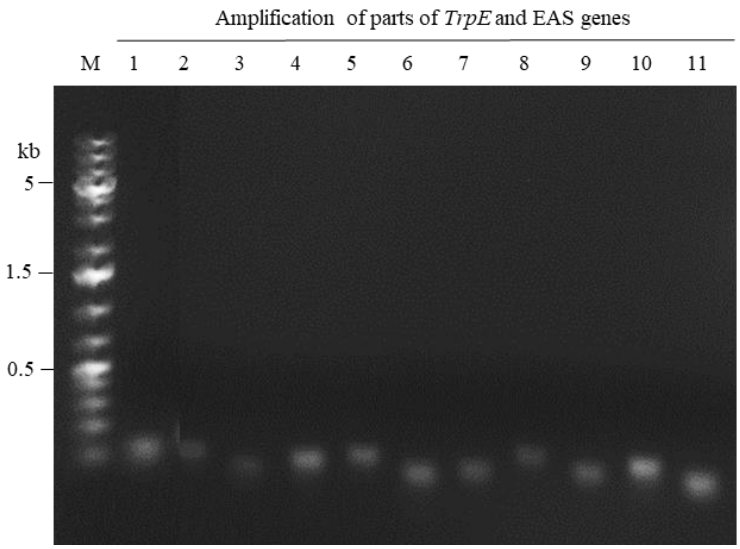

Fig. 39 Amplification of partial regions of *TrpE* and 10 EA biosynthetic genes from cDNA WT *C. purpurea* P1 using Phusion High-Fidelity DNA polymerase.
1 - part of *TrpE* (102 bp) amplified using primers TrpE_rt_fw and TrpE_rt_rev
2 - part of *easH* (145 bp) amplified using primers easH_rt_fw and easH_rt_rev
3 - part of l*psB* (166 bp) amplified using primers lpsB_rt_fw and lpsB_rt_rev
4 - part of *easA* (145 bp) amplified using primers easA_rt_fw and easA_rt_rev
5 - part of *cloA* (174 bp) amplified using primers cloA_rt_fw and cloA_rt_rev
6 - part of *easC* (109 bp) amplified using primers easC_rt_fw and easC_rt_rev
7 - part of *easD* (132 bp) amplified using primers easD_rt_fw and easD_rt_rev
8 - part of *easE* (191 bp) amplified using primers easE_rt_fw and easE_rt_rev
9 - part of *easF* (142 bp) amplified using primers easF_rt_fw and easF_rt_rev
10 - part of *easG* (163 bp) amplified using primers easG_rt_fw and easG_rt_rev
11 - part of *dmaW* (103 bp) amplified using primers dmaW_rt_fw and dmaW_rt_rev.
M – 1 kb Plus DNA ladder.

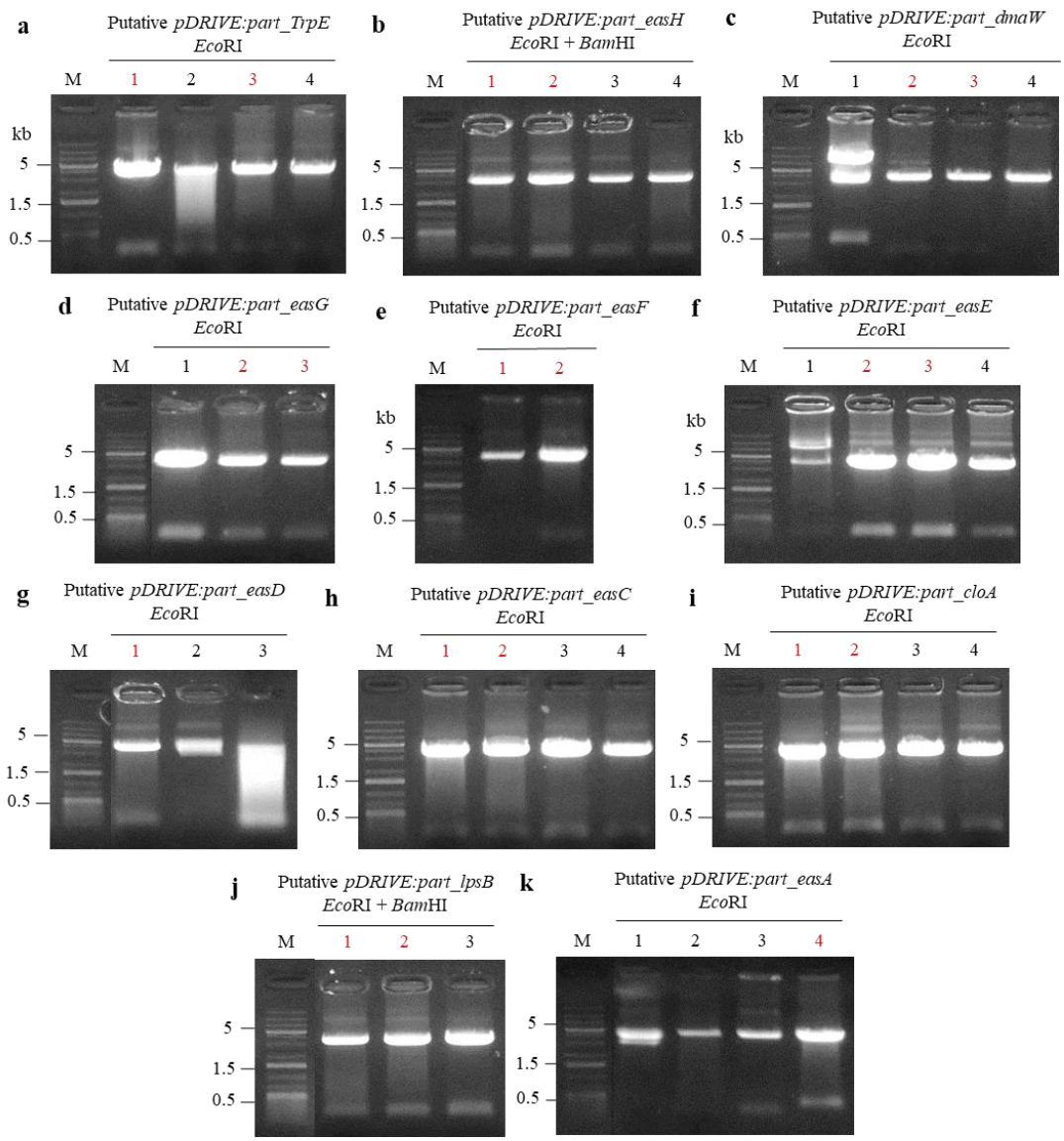

Fig. 40 Restriction of putative *pDRIVE* vectors containing parts of *TrpE* gene or EAS genes.
(a) *pDRIVE:part_TrpE* digested with *Eco*RI (expected bands: 3.85 kb, 102 bp).
Plasmids 1 and 3 (red) were sequenced.
(b) *pDRIVE:part_easH* digested with *Eco*RI and *Bam*HI (expected bands: 3.85 kb, 145 bp).
Plasmids 1 and 2 (red) were sequenced.
(c) *pDRIVE:part_dmaW* digested with *Eco*RI (expected bands: 3.85 kb, 102 bp).
Plasmids 2 and 3 (red) were sequenced.
(d) *pDRIVE:part_easG* digested with *Eco*RI (expected bands: 3.85 kb, 163 bp).
Plasmids 2 and 3 (red) were sequenced.
(e) *pDRIVE:part_easF* digested with *Eco*RI (expected bands: 3.85 kb, 142 bp).
Plasmids 1 and 2 (red) were sequenced.
(f) *pDRIVE:part_easE* digested with *Eco*RI (expected bands: 3.85 kb, 191 bp).
Plasmids 2 and 3 (red) were sequenced.
(g) *pDRIVE:part_easD* digested with *Eco*RI (expected bands: 3.85 kb, 132 bp).
Plasmid 1 (red) was sequenced.
(h) *pDRIVE:part_easC* digested with *Eco*RI (expected bands: 3.85 kb, 109 bp).
Plasmids 1 and 2 (red) were sequenced.
(i) *pDRIVE:part_cloA* digested with *Eco*RI (expected bands: 3.85 kb, 174 bp).
Plasmids 1 and 2 (red) were sequenced.
(j) *pDRIVE:part_lpsB* digested with *Eco*RI and *Bam*HI (expected bands: 3.85 kb, 166 bp).
Plasmids 1 and 2 (red) were sequenced.
(k) *pDRIVE:part_easA* digested with *Eco*RI (expected bands: 3.85 kb, 145 bp).
Plasmid 1 (red) was sequenced.
M – 1 kb Plus DNA ladder.

Results from sequencing (Tab. 17) were compared with corresponding sequences from *C. purpurea* 20.1 which genome has been already sequenced (Schardl *et al*., 2013).

Part of *TrpE* (102 bp) **Cp 20.1** 5´- CGAATACGATGAGTGGATCGAGACGATCAACAAGCTCGGCAGCAACATGACGTGCATCA AGTCAGCAGAGGAGATGTATTACCAGCAGCAGCAAAACGAGAA -3´ **Cp P1** 5´- CGAATACGATGAGTGGATCGAGACGATCAACAAGCTCGGCAGCAACATGACGTGCATCA AGTCAGCAGAGGAGATGTATTACCAGCAGCAGCAAAACGAGAA -3´
Part of *easH* (145 bp) **Cp 20.1** 5´- GGTGATTATTGGCTGGGCTACGGAGCTGTCATCGAAAACGGCCCGGGAACAACGGAGCA GAAATGGCACCGCGACCAGCCCAGATATCCCTTGGTCAAGGAAGGTCCGGACGCGCCTGAA GGCATGCTGAACTTCTTCACAGCCC -3´ Cp P1 5´- GGTGATTATTGGCTGGGCTACGGAGCTGTCATCGAAAACGGTCCGGGAACAACGGAGCA GAAATGGCACCGCGACCAGCCCAGATATCCCTTGGTCAAGGAAGGTCCGGACGCGCCTGAA GGCATGCTGAACTTCTTCACAGCCC -3´
Part of *dmaW* (103 bp) **Cp 20.1** 5´-TTTGAGTCATTGAACTACCTCCACGCATATATCTCATTCTCTTACCGTCGAAACAAGCCGT ATTTGAGCGTATATTTGCATACGTTTGAGACTGGTCGTTGGC -3´ **Cp P1** 5´-TTTGAGTCATTGAACTACCTCCACGCATATATCTCATTCTCTTACCGTCGAAACAAGCCGT ATTTGAGCGTATATTTGCATACATTTGAGACTGGTCGTTGGC -3´
Part of *easG* (163 bp) **Cp 20.1** 5´- GCATCTTCCGTCAGACCAATGTTCCTTTTTTGGTCGCATCGCGTTCCAGCAGCGCAGGAA CAGCTGAAAACCATCGCAAATTTGATTGGCTGGACGAAGAGACGTTTCCGAATGCCCTGTCA GTCGATCAAGGCATGAAGCCTATTTCCGTGGTCTGGCTATG -3´ **Cp P1** 5´- GCATCTTCCGTCAGACCAATGTTCCTTTTTTGGTCGCATCGCGTTCCAGCAGCGCAGGAA CAGCTGAAAACCATCGCAAATTTGATTGGCTGGACGAAGAGACGTTTCCGAATGCCCTGTCA GTCGATCAAGGCATGAAGCCTATTTCCGTGGTCTGGCTATG -3´
Part of *easF* (142 bp) **Cp 20.1** 5´- CTCTTCCGGTCATCGACATTCGCTCGAATCATGTGGAAGATTCCCTTCCCGAACAAATTAT CAAGGGCTTAACGAGCCAACCGAAAACTCTCCCCCCTCTTCTTTTCTACTCCAACGAAGGAC TGGAGCACTGGAATCATCA -3´ **Cp P1** 5´- CTCTTCCGGTCATCGACATTCGCTCGAATCATGTGGAGGATTCCCTTCCCGAACAAATTAT CAAGGGCTTAACGAGCCAACCGAAAACTCTCCCCCCTCTTCTTTTCTACTCCAACGAAGGAC TGGAGCACTGGAATCATCA -3´

Tab. 17 Comparison of DNA sequences (parts of *TrpE* and EA biosynthetic genes) amplified from cDNA *C. purpurea* P1, cloned into *pDRIVE*, and sequenced and sequenced from *C. purpurea* 20.1 (GCA_000347355) (part A).
Grey – fw primer used for amplification, blue – rev primer used for amplification, yellow – SNPs.

Part of *easE* (191 bp)

Cp 20.1

5´- AAGAATACGGGCCATGACAGCGCGGGACGATCAAGTGCTCCTCATTCGTTCCAGATACA
TACCAGCCTGCTCCAGAACATATCCTTGCACAAGAATTTCATTGCGAGAGGATCGACCACGG
GCCGCGGGCCTGCCGTCACATTGGGTGCTGGGGTCATGCAGTGGCAAGCATACGTTCATGGT
GCCAAAAA -3´

Cp P1

5´- AAGAATACGGGCCATGACAGCGCGGGACGATCAAGTGCTCCTCATTCGTTCCAGATACA
TACCAGCCTGCTCCAGAACATATCCTTGCACAAGAATTTCATTGCGAGAGGATCGACCACGG
GCCGCGGGCCTGCCGTCACATTGGGTGCTGGGGTCATGCAGTGGCAAGCATACGTTCATGGT
GCCAAAAA -3´

Part of *easD* (132 bp)

Cp 20.1

5´- GCACCAATTTCACCTCCCTACAAGAGTCCATCGCCAAAAGCAACCCATCTACTCTTGTCC
ATTGCACCGAATTAGACGTAAGATCGGCCGACAAGGTGGACCAGTGGCTACAAAGCATCGT
TTCTACCCACG -3´

Cp P1

5´- GCACCAATTTCACCTCCCTACAAGAGTCCATCGCCAAAAGCAACCCATCTACTCTTGTCC
ATTGCACCGAATTAGACGTCAGATCGGCCGACAAGGTGGACCAGTGGCTACAAAGCATCGT
TTCTACCCACG -3´

Part of *easC* (109 bp)

Cp 20.1

5´- TGGATCTGAGCATTCTGGTGCTCAAAAATGTCCTTTTCAAGATCCGGGTTTGTCTTCAATG
GACCAAGACTCACGTTTGCGTGATATCTTATCACGTTTCAATCGCGAG -3´

Cp P1

5´- TGGATCTGAGCATTCTGGTGCTCAAAAATGTCCTTTTCAAGATCCGGGTTTGTCTTCAATG
GACCAAGACTCACGTTTGCGTGATATCTTATCACGTTTCAATCGCGAG -3´

Part of *cloA* (174 bp)

Cp 20.1

5´- GCTACAATGGCTGCAACAAACTCGGCACGAACTTTCTTGGACTTGGATTTTACTGACCAC
ATGTATTGCTCTCATATCTCCACTGGTTCTTAAAGGCATCTATAATGTCTATTTTCATCCTCTT
CGCAACATTCCGGGGCCCAAGCTTGCCGCATTGACCGACTTTTACGCCTT -3´

Cp P1

5´- GCTACAATGGCTGCAACAAACTCGGCACGAACTTTCTTGGACTTGGATTTTACTGACCAC
ATGTATTGCTCTCACATCTCCACTGGTTCTGAAAGGCATCTATAATGTCTATTTTCATCCTCTT
CGCAACATTCCGGGGCCCAAGCTTGCCGCATTGACCGACTTTTACGCCTT -3´

Part of *lpsB* (166 bp)

Cp 20.1

5´- TGCGGAATCAAATCTCAACATCAGACCCTGCCGAATTCGATTCACTTCCGACAAAGTTGT
ATCTGACATTCTTTCCGCGTGCCAAAGCCCTTGCGGCGAGAAAACTGGTGATCATGACATTC
CTGCGTCACATTTGTCTCAAGATGGTGGATTTTTGGCCTCAGAA-3´

Cp P1

5´- TGCGGAATCAAATCTCAACATCAGACCCTGCCGAATTCGATTCACTTCCGACAAAGTTGT
ATCTGACATTCTTTCCGCGTGCCAAAGCCCTTGCAGCGAGAAAACTGGTGATCATGACATTC
CTGCGTCACATTTGTCTCAAGATGGTGGATTTTTGGCCTCAGAA -3´

Part of *easA* (145 bp)

Cp 20.1

5´- CTTACCAGCCAAGGGTTGAAACTCGAATCAAGCAGCGAAGTACCGGTCGCACCGGGGGA
GCCTACGCCACGAGCGCTGGACGAGGACGAGATTCAGCAGTACATACTCGATTATGTCCAA
GGAGCAAAGAATGCAGTACACGGGG -3´

Cp P1

5´- CTTACCAGCCAAGGGTTGAAACTCGAATCAAGCAGCGAAGTACCGGTCGCACCGGGGGA
GCCTACGCCACGAGCGCTGGACCAGGACGAGATTCAGCAGTACATACTCGATTATGTCCAA
GGAGCAAAGAATGCAGTACACGGGG -3´

Tab. 17 Comparison of DNA sequences (parts of *TrpE* and EA biosynthetic genes) amplified from cDNA *C. purpurea* P1, cloned into *pDRIVE*, and sequenced and sequenced from *C. purpurea* 20.1 (GCA_000347355) (part B).

Grey – fw primer used for amplification, blue – rev primer used for amplification, yellow – SNPs.

3.4.4.4.2.2.2 Real-time RT-PCR

RNA isolated from 10-days old mycelia of WT, *OE:TrpE* and *OE:TrpE*^{S76L} and 14-days old mycelia of WT, *OE:gfp* and *OE:gfp_dmaW* was used for absolute quantitative real time RT-PCR (Tab. 18 - 20). As calibration curves, different dilutions of *pDRIVE* vectors with cloned parts of *TrpE* or EA biosynthetic genes were used. From the slope of curves, primer efficiencies were calculated (Tab. 21) (3.2.4.5.2.3.2).

Tab. 18 Expression levels of 10 selected EA biosynthetic genes in 10-days old and 14-days old induced (low Pi) and non-induced (high Pi) mycelia of WT *C. purpurea* P1 determined by absolute quantification using real-time RT-PCR.
Results are expressed as the number of transcripts per 1 ng of total RNA ± SE of six biological replicates. The non-parametric Kruskal-Wallis ANOVA followed by multiple comparisons of mean ranks was used to compare the differences between groups. Data comparing differences between inducing (low Pi) and non-inducing (high Pi) conditions are shown (* $p<0.05$, ** $p<0.01$, *** $p<0.001$). *DmaW*, DMAT synthetase; *easF*, DMAT N-methyltransferase; *easE*, chanoclavine-I synthase; *easC*, catalase; *easD*, chanoclavine-I dehydrogenase; *easA*, chanoclavine-I aldehyde oxidoreductase; *easG*, reductase; *cloA*, NAPDH-dependent cytochrome P450; *lpsB*, nonribosomal lysergyl peptide synthetase LPS2; *easH1*, dioxygenase.

		WT (10 days)	WT (14 days)
dmaW	low Pi	8965 ± 336 ***	5018 ± 317 ***
	high Pi	136 ± 11	183 ± 27
easF	low Pi	1947 ± 162 ***	1520 ± 149 ***
	high Pi	266 ± 26	376 ± 38
easE	low Pi	638 ± 40 ***	357 ± 34 ***
	high Pi	50 ± 6	42 ± 4
easC	low Pi	3305 ± 219 ***	1677 ± 178
	high Pi	656 ± 108	882 ± 151
easD	low Pi	3702 ± 214 ***	2790 ± 263 ***
	high Pi	134 ± 12	177 ± 12
easA	low Pi	7183 ± 374 ***	4843 ± 364 ***
	high Pi	635 ± 45	838 ± 150
easG	low Pi	3573 ± 130 ***	1903 ± 159 ***
	high Pi	12 ± 2	31 ± 5
cloA	low Pi	1427 ± 172 ***	748 ± 60 ***
	high Pi	130 ± 17	156 ± 16
lpsB	low Pi	1494 ± 84 ***	961 ± 72 ***
	high Pi	642 ± 66	640 ± 91
easH1	low Pi	7103 ± 367 ***	4734 ± 380 ***
	high Pi	490 ± 108	260 ± 57

Tab. 19 Expression levels of 10 selected EA biosynthetic genes and *TrpE* in 10-days old induced (low Pi) and non-induced (high Pi) mycelia of *OE:TrpE*, *OE:TrpE*^{S76L} and WT *C. purpurea* P1 determined by absolute quantification using real-time RT-PCR.

Results are expressed as the number of transcripts per 1 ng of total RNA ± SE of six biological replicates. The non-parametric Kruskal-Wallis ANOVA followed by multiple comparisons of mean ranks was used to compare the differences between groups. Data comparing differences between WT and individual transformant are shown (* $p<0.05$, ** $p<0.01$, *** $p<0.001$). *TrpE*, α-subunit of anthranilate synthase; *dmaW*, DMAT synthetase; *easF*, DMAT N-methyltransferase; *easE*, chanoclavine-I synthase; *easC*, catalase; *easD*, chanoclavine-I dehydrogenase; *easA*, chanoclavine-I aldehyde oxidoreductase; *easG*, reductase; *cloA*, NAPDH-dependent cytochrome P450; *lpsB*, nonribosomal lysergyl peptide synthetase LPS2; *easH1*, dioxygenase.

		WT	*OE:TrpE 2*	*OE:TrpE 3*	*OE:TrpE*^{S76L} *4*	*OE:TrpE*^{S76L} *12*
TrpE	low Pi	752 ± 46	13273 ± 1235 ***	28456 ± 2419 ***	7222 ± 339 *	7880 ± 862 **
	high Pi	583 ± 40	12825 ± 447 ***	33382 ± 1486 ***	6531 ± 717 **	12894 ± 1091 ***
dmaW	low Pi	8965 ± 336	22892 ± 2951 ***	17525 ± 1752 ***	12699 ± 809	7223 ± 560
	high Pi	136 ± 11	660 ± 120 ***	433 ± 62 ***	266 ± 22 ***	329 ± 31 ***
easF	low Pi	1947 ± 162	3361 ± 422 *	4660 ± 509 ***	3809 ± 467	2844 ± 307
	high Pi	266 ± 26	554 ± 104	453 ± 73	398 ± 36	450 ± 59
easE	low Pi	638 ± 40	1678 ± 260 ***	1104 ± 99 **	1199 ± 118	797 ± 73
	high Pi	50 ± 6	221 ± 62 *	95 ± 18	104 ± 8 **	106 ± 14 *
easC	low Pi	3305 ± 219	4970 ± 517	5947 ± 745 **	3801 ± 358	2680 ± 247
	high Pi	656 ± 108	28284 ± 7778 ***	7387 ± 2259 ***	7816 ± 1106 ***	9660 ± 1508 ***
easD	low Pi	3702 ± 214	9133 ± 912 ***	8841 ± 425 ***	5530 ± 401	3790 ± 327
	high Pi	134 ± 12	511 ± 77 ***	287 ± 40 **	351 ± 38 ***	277 ± 15 ***
easA	low Pi	7183 ± 374	22475 ± 1994 ***	16514 ± 874 ***	16176 ± 1044 ***	14337 ± 370 ***
	high Pi	635 ± 45	1335 ± 201 **	1056 ± 77 *	1659 ± 145 ***	1237 ± 87 ***
easG	low Pi	3573 ± 130	11763 ± 2323 ***	7232 ± 1200	4895 ± 346	1964 ± 170 *
	high Pi	12 ± 2	278 ± 58 ***	111 ± 22 ***	89 ± 15 **	99 ± 15 ***
cloA	low Pi	1427 ± 172	1466 ± 216	1570 ± 131	1335 ± 112	808 ± 74 *
	high Pi	130 ± 17	195 ± 32	186 ± 17	315 ± 77	148 ± 19
lpsB	low Pi	1494 ± 84	1329 ± 108	1378 ± 85	2382 ± 136 **	1921 ± 212
	high Pi	642 ± 66	406 ± 28	633 ± 60	370 ± 33 *	672 ± 91
easH1	low Pi	7103 ± 367	23315 ± 2596 ***	16616 ± 1788 ***	12810 ± 987 **	8039 ± 676
	high Pi	490 ± 108	646 ± 81	632 ± 121	757 ± 156	401 ± 55

Tab. 20 Expression levels of 10 selected EA biosynthetic genes in 14-days old induced (low Pi) and non-induced (high Pi) mycelia of *OE:gfp, OE:gfp_dmaW,* and WT *C. purpurea* P1determined by absolute quantification using real-time RT-PCR.

Results are expressed as the number of transcripts per 1 ng of total RNA ± SE of six biological replicates. The non-parametric Kruskal-Wallis ANOVA followed by multiple comparisons of mean ranks was used to compare the differences between groups. Data comparing differences between WT and individual transformant are shown (* p<0.05, ** p<0.01, *** p<0.001). *DmaW*, DMAT synthetase; *easF*, DMAT N-methyltransferase; *easE*, chanoclavine-I synthase; *easC*, catalase; *easD*, chanoclavine-I dehydrogenase; *easA*, chanoclavine-I aldehyde oxidoreductase; *easG*, reductase; *cloA*, NAPDH-dependent cytochrome P450; *lpsB*, nonribosomal lysergyl peptide synthetase LPS2; *easH1*, dioxygenase.

		WT	*OE:gfp*	*OE:gfp_dmaW 8*	*OE:gfp_dmaW 13*
dmaW	low Pi	5018 ± 317	8380 ± 536	109927 ± 7774 ***	24357 ± 1800 ***
	high Pi	183 ± 27	207 ± 15	12877 ± 977 ***	13907 ± 918 ***
easF	low Pi	1520 ± 149	1887 ± 95	1707 ± 168	2042 ± 226
	high Pi	376 ± 38	413 ± 42	581 ± 59	480 ± 76
easE	low Pi	357 ± 34	347 ± 15	275 ± 24	353 ± 25
	high Pi	42 ± 4	50 ± 5	94 ± 12 **	71 ± 9
easC	low Pi	1677 ± 178	1880 ± 87	1496 ± 107	1671 ± 98
	high Pi	882 ± 151	789 ± 1008	4127 ± 1098 **	2751 ± 524 *
easD	low Pi	2790 ± 263	3515 ± 306	3249 ± 326	3264 ± 207
	high Pi	177 ± 12	135 ± 8	258 ± 41	201 ± 18
easA	low Pi	4843 ± 364	6811 ± 257	9106 ± 527 ***	8314 ± 368 ***
	high Pi	838 ± 150	855 ± 48	1250 ± 110 ***	1060 ± 93 *
easG	low Pi	1903 ± 159	2575 ± 192	2100 ± 201	1525 ± 230
	high Pi	31 ± 5	27 ± 7	105 ± 24 *	86 ± 15
cloA	low Pi	748 ± 60	869 ± 52	774 ± 79	650 ± 69
	high Pi	156 ± 16	212 ± 18	237 ± 22 *	222 ± 22
lpsB	low Pi	961 ± 72	886 ± 36	881 ± 89	1030 ± 98
	high Pi	640 ± 91	618 ± 43	991 ± 121 **	566 ± 57
easH1	low Pi	4734 ± 380	6287 ± 352	5007 ± 542	5153 ± 555
	high Pi	260 ± 57	214 ± 42	253 ± 29	326 ± 47

Tab. 21 Efficiencies of primers used for absolute quantification by qRT-PCR.

Gene	R^2	Efficiency (%)
TrpE (CPUR_05013.1)	0.9952	103.54
easH (CPUR_04075.1)	0.9948	114.24
dmaW (CPUR_04076.1)	0.9903	107.66
easG (CPUR_04077.1)	0.9972	105.72
easF (CPUR_04078.1)	0.9890	86.99
easE (CPUR_04079.1)	0.9722	95.79
easD (CPUR_04080.1)	0.9897	90.44
easC (CPUR_04081.1)	0.9904	105.58
cloA (CPUR_04082.1)	0.9959	90.42
*lpsB (*CPUR_04083.1)	0.9847	98.47
easA (CPUR_04084.1)	0.9929	88.40

3.4.4.4.3 Quantification of anthranilic acid

Levels of anthranilic acid were measured in 10-days old induced (low Pi) and non-induced (high Pi) media and mycelia of WT, *OE:TrpE,* and *OE:TrpE*^{S76L} (Tab. 22) (3.2.4.5.3).

Tab. 22 Anthranilic acid in 10-days old mycelia and media of *OE TrpE, OE TrpE*^{S76L} and WT *C. purpurea* P1 under inducing (low Pi) and non-inducing (high Pi) conditions.
Presented are means ± SE of six biological replicates, n.d. - not detected. The non-parametric Kruskal-Wallis ANOVA followed by multiple comparisons of mean ranks was used to compare the differences between groups. Data comparing differences between WT and individual transformant are shown (* p<0.05, ** p<0.01, *** p<0.001).

Anthranilic acid (ng/culture)	WT	*OE:TrpE 2*	*OE:TrpE 3*	*OE:TrpE*^{S76L} *4*	*OE:TrpE*^{S76L} *12*
Low Pi					
Mycelium	60.34 ± 11.53	61.48 ± 7.37	64.43 ± 35.75	352.89 ± 85.07	494.93 ± 82.28*
Medium	n.d.	n.d.	n.d.	8889.73 ± 3476.98	16463.49 ± 8935.26
High Pi					
Mycelium	75.23 ± 14.59	73.10 ± 17.24	56.95 ± 19.98	12145.19 ± 6975.73*	3379.84 ± 1974.59
Medium	n.d.	n.d.	n.d.	47306.30 ± 23308.29	18790.46 ± 10966.14

3.4.4.4.4 Quantification of Trp

Levels of Trp were measured in 10-days old induced (low Pi) and non-induced (high Pi) media and mycelia of WT, *OE:TrpE,* and *OE:TrpE*^{S76L} (Tab. 23) (3.2.4.5.4).

Tab. 23 Tryptophan in 10-days old mycelia and media of *OE TrpE, OE TrpE*^{S76L} and WT *C. purpurea* P1 under inducing (low Pi) and non-inducing (high Pi) conditions.
Presented are means ± SE of six biological replicates, n.d. - not detected. The non-parametric Kruskal-Wallis ANOVA followed by multiple comparisons of mean ranks was used to compare the differences between groups. Data comparing differences between WT and individual transformant are shown (* p<0.05, ** p<0.01, *** p<0.001).

Tryptophan (µg/culture)	WT	*OE:TrpE 2*	*OE:TrpE 3*	*OE:TrpE*^{S76L} *4*	*OE:TrpE*^{S76L} *12*
Low Pi					
Mycelium	119.62 ± 14.06	125.01 ± 12.84	102.55 ± 7.77	210.89 ± 24.62	305.16 ± 33.04*
Medium	97.90 ± 18.84	118.29 ± 11.52	179.26 ± 33.47	519.72 ± 172.03*	1208.42 ± 172.89***
High Pi					
Mycelium	126.02 ± 16.75	100.40 ± 32.39	105.68 ± 17.57	402.67 ± 39.93	378.00 ± 39.19
Medium	835.50 ± 69.61	318.02 ± 154.28	544.54 ± 170.75	1320.51 ± 251.02	1377.31 ± 88.62

3.4.4.4.5 Quantification of ergopeptines

Levels of ergopeptines ergotamine, ergotaminine, α-ergocryptine, and α-ergocryptinine were measured in 10-days old induced (low Pi) and non-induced (high Pi) media and mycelia of WT, *OE:TrpE* and *OE:TrpE*^{S76L} (Tab. 24) and 14-days old induced (low Pi) and non-induced (high Pi) media and mycelia of WT, *OE:gfp*, and *OE:gfp_dmaW* (Tab. 25) (3.2.4.5.5).

Tab. 24 Content of ergopeptines in 10-days old mycelia and media of *OE TrpE, OE TrpE*^{S76L} and WT *C. purpurea* P1 under inducing (low Pi) conditions, ERG – ergotamine and ergotaminine, α-ERC – α-ergocryptine and α-ergocryptinine.
Presented are means ± SE of six biological replicates. The non-parametric Kruskal-Wallis ANOVA followed by multiple comparisons of mean ranks was used to compare the differences between groups. Data comparing differences between WT and individual transformants are shown (* p<0.05, ** p<0.01, *** p<0.001).

Ergopeptines (µg/culture)	WT	*OE:TrpE 2*	*OE:TrpE 3*	*OE:TrpE*^{S76L} *4*	*OE:TrpE*^{S76L} *12*
Low Pi					
Mycelium					
ERG	485.22 ± 78.89	1840.68 ± 342.63	1314.59 ± 171.29	2510.98 ± 291.54***	1548.63 ± 187.16
α-ERC	77.65 ± 8.57	225.16 ± 38.79	177.44 ± 13.98	411.22 ± 48.41***	238.27 ± 56.87
Medium					
ERG	2332.88 ± 183.70	7939.22 ± 919.15	8527.90 ± 1288.66	17580.90 ± 3615.42**	10461.46 ± 977.75*
α-ERC	325.42 ± 29.32	1175.69 ± 170.39	1226.83 ± 167.84	2587.85 ± 589.77**	1164.58 ± 104.16
High Pi					
Mycelium					
ERG	n.d.	166.01 ± 29.26	81.91 ± 27.53	318.41 ± 112.89	229.43 ± 25.67
α-ERC	n.d.	13.06 ± 2.01	10.78 ± 2.72	42.46 ± 4.04	10.68 ± 2.40
Medium					
ERG	n.d.	864.78 ± 172.68	468.67 ± 159.89	2329.21 ± 983.36	795.01 ± 186.34
α-ERC	n.d.	69.44 ± 14.63	41.96 ± 13.34	184.97 ± 79.25	83.17 ± 27.38

Tab. 25 Content of ergopeptines in 14-days old mycelia and media of *OE:gfp, OE:gfp_dmaW* and WT *C. purpurea* P1 under inducing (low Pi) conditions, ERG – ergotamine and ergotaminine, α-ERC – α-ergocryptine and α-ergocryptinine.
Presented are means ± SE of six biological replicates. The non-parametric Kruskal-Wallis ANOVA followed by multiple comparisons of mean ranks was used to compare the differences between groups. Data comparing differences between WT and individual transformants are shown (* p<0.05, ** p<0.01, *** p<0.001).

Ergopeptines (µg/culture)	WT	*OE:gfp*	*OE:gfp_dmaW 8*	*OE:gfp_dmaW 13*
Mycelium				
ERG	813.46 ± 56.73	963.94 ± 71.52	2243.67 ± 242.43**	1729.42 ± 111.87**
α-ERC	101.48 ± 11.64	103.30 ± 15.75	229.10 ± 23.95*	234.22 ± 40.71*
Medium				
ERG	3867.91 ± 279.15	4469.86 ± 360.55	14785.92 ± 1709.82	10380.08 ± 1162.45**
α-ERC	314.06 ± 58.96	408.13 ± 47.04	1413.19 ± 151.10	1315.23 ± 235.21*

3.5 Discussion

3.5.1 Generation of vectors for *C. purpurea* transformation using yeast recombinational cloning

Since the expression of Trp feedback-resistant form of *TrpE* in *A. fumigatus* had been previously reported to increase Trp levels and production of secondary metabolites (Wang *et al*., 2016), *C. purpurea* mutants expressing Trp feedback-resistant form of *TrpE* (CPUR_05013.1) were generated. Firstly, the protein sequence of AAS-I from genome-sequenced *C. purpurea* 20.1 (Schardl *et al*., 2013) was aligned with the AAS-I sequence from *A. fumigatus*. Since the highly conserved amino acid sequence element LLES is involved in Trp regulation (Graf *et al*., 1993) and only a mutation S77L in *A. nidulans* led to an increase in fumiquinazolines (Wang *et al*., 2016), the same point mutation was designed in *C. purpurea*. The serine residue from the LLES element was identified in *C. purpurea* 20.1 at a position 76 thus this mutation was named S76L. For comparison, also a non-mutated, Trp-sensitive version of *TrpE* was used for *C. purpurea* P1 transformation. Together, two vectors *pNDH-OGG:TrpE*^{S76L} and *pNDH-OGG:TrpE* for expression of Trp-resistant and WT form of α-subunit of anthranilate synthase, respectively were prepared (Fig. 20 - 21).

To confirm that the gene CPUR_05013.1 encodes α-subunit of anthranilate synthase involved in Trp biosynthesis, *TrpE* replacement vector *pRS426:ΔTrpE1* (Fig. 23) was prepared.

In addition to *TrpE*^{S76L} and *TrpE* vectors, a plasmid expressing *dmaW* encoding DMATS that catalyzes the first pathway-specific step leading to EAs biosynthesis (Unsöld and Li, 2005; Ding *et al*., 2008; Metzger et al., 2009; Fernández-Bodega *et al*., 2017), was prepared. In this case, DMATS was N-terminally fused to *Botrytis cinerea* codon-optimized *gfp* gene (Schumacher, 2012) (Fig. 22).

Both genes, *TrpE*, and *dmaW* were amplified from gDNA of *C. purpurea* 20.1 and transformed into *C. purpurea* P1. Although strain 20.1 produces EAs only *in planta* (Schardl *et al*., 2013) on contrary to the strain P1 that produces EAs only in submerged cultures, the same EAs, ergotamine, ergotaminine, ergocryptine, and ergocryptinine, have been detected in both strains (Tudzynski *et al*., 1999; Correia *et al*., 2003). Genes were expressed under the control of the strong constitutive *oliC* (subunit 9 of mitochondrial ATP synthase) promoter from *A. nidulans* (Bailey *et al*., 1989)

3.5.2 Generation and characterization of *C. purpurea* mutants

3.5.2.1 Deletion and complementation of *TrpE* in *C. purpurea* 20.1

By the transformation of *C. purpurea* 20.1 protoplasts with *TrpE* replacement vector *pRS426:Δ,TrpE1* knock-out mutant of this gene was prepared. Due to the low efficiency of homologous recombination in *C. purpurea* (Oeser *et al*., 2002), only one heterokaryotic mutant out of 780 primary transformants was obtained. The replacement of *TrpE* gene with phleomycin resistance cassette was confirmed in this mutant by diagnostic PCR (Fig. 25a). Homokayon *ΔTrpE* was selected by single spore isolation and confirmed with diagnostic PCR again (Fig. 25b). Moreover, a complemented homokaryon $\Delta TrpE^{TrpE}$ was prepared and confirmed by diagnostic PCR (Fig. 25c).

As shown in Fig. 26 only *ΔTrpE* exhibited Trp auxotrophy, its growth was restored by the addition of 5 µM anthranilic acid or 5 mM L-Trp. Concerning the inoculation of rye plants (Fig. 27), only *ΔTrpE* was non-infectious, most probably due to decreased level of auxins, plant hormones previously detected in *C. purpurea* that are synthesized via Trp-dependent and Trp-independent pathways and play a crucial role in plant-pathogen interactions (Jameson, 2000; Kazan and Manners, 2009).

3.5.2.2 *C. purpurea* P1 mutants expressing $TrpE^{S76L}$, *TrpE*, and *dmaW*

Concerning *C. purpurea* P1 mutants expressing Trp-resistant form of α-subunit of anthranilate synthase ($OE{:}TrpE^{S76L}$), WT Trp-feedback sensitive form of α-subunit of anthranilate synthase (*OE:TrpE*), and dimethylallyltryptophan synthase fused with gfp (*OE:gfp_dmaW*), the presence of vectors was confirmed in heterokaryotic mutants by diagnostic PCR Subsequently, homokaryons were selected by hyphal tip dissection and confirmed again with diagnostic PCR (Fig. 28, 29). In the case of *OE:gfp_dmaW C. purpurea* P1, the production of GFP-DMATS was confirmed by fluorescence microscopy (Fig. 30) and also detected by western blot analysis using antiGFP antibody (Fig. 31). As a control, *C. purpurea* mutant expressing *gfp* gene was used in all analyses. Moreover, the overexpression of *TrpE* and *dmaW* in *C. purpurea* P1 mutants was confirmed by qRT-PCR (Tab. 19, 20). The growth of all *C. purpurea* P1 mutants showed no significant changes when compared with that of WT (Fig. 32).

As the EAs biosynthesis in *C. purpurea* P1 is regulated by inorganic phosphate (Robbers *et al*., 1972; Lohmeyer *et al*., 1990), all mutants and WT were grown for

comparison under inducing (low level of inorganic phosphate, EAs producing) and non-inducing (high level of inorganic phosphate, EAs not produced) conditions. All mutants were cultivated in six biological replicates, the presence of transgenes was confirmed in all samples at DNA level using diagnostic PCR (Fig. 33 - 36) and RNA level using RT-PCR (Fig. 37, 38).

To investigate whether the expression of Trp feedback-sensitive or resistant form of *TrpE* in *C. purpurea* led to the accumulation of Trp, a precursor, and inducer of EAs biosynthesis (Floss *et al*., 1964; Erge *et al*., 2007), firstly the content of anthranilic acid was measured (Tab. 22). While anthranilic acid was not detected in the medium of WT *C. purpurea* P1, it was readily detected in the medium of *OE:TrpE*^{S76L} *C. purpurea* P1 but not in the medium of *OE:TrpE*. Hence, the expression of Trp feedback-resistant form of *TrpE* led to the accumulation of anthranilic acid in such amounts that it started to be secreted into the medium.

Next, Trp content in *C. purpurea* P1 cultures was determined (Tab. 23). As expected, only the expression of Trp feedback-resistant form of *TrpE* led to a significant increase. Interestingly, inducing conditions for EAs biosynthesis (low phosphate level) did not change Trp level in WT mycelium but led to the 8-fold accumulation of Trp in the medium compared to non-inducing conditions. Thus, Trp synthesis clearly proceeds even under non-inducing conditions in WT *C. purpurea* P1, however for an unknown reason its excess is secreted into the medium instead of being used for EAs biosynthesis.

3.5.3 Changes in the production of ergopeptines in *C. purpurea* P1 mutants

Although WT of *C. purpurea* P1 is known to release ergopeptines ergotamine and α-ergocryptine into the medium and thus these EAs have been previously assayed only in the media (Haarmann *et al*., 2008; Lorenz *et al*., 2009; Lorenz *et al*., 2010), we decided to quantify these metabolites also in the mycelium. As both ergopeptines are derivatives of $\Delta^{9,10}$-ergolene, they form 8S (or α) and 8R (or β) stereoisomers. Whereas 8R ergopeptines are considered inactive (suffix –inine), members of the 8S group are biologically active (suffix –ine) (Pierri *et al*., 1982; Kidrič *et al*., 1986). Moreover, the interconversion of the forms has also been described (Hellberg, 1957; Smith and Shappell, 2002). Since both forms of ergopeptines were measured, levels of ergotamine

and ergotaminine, and α-ergocryptine and α-ergocryptinine were summed and are expressed as ERG and α-ERC, respectively.

At inducing conditions, higher ergopeptine production was detected in the media of *OE:TrpE*^{S76L} (Tab. 24) and *OE:gfp_dmaW* mutants (Tab. 25). The highest increase (7-fold) was observed in *OE:TrpE*^{S76L} line 4. As expected, ERG and α-ERC that were detected in all media were also found in all mycelia under inducing conditions. No qualitative changes in ergopeptine spectrum between WT and mutants were observed.

Under non-inducing conditions, no EAs production was detected in WT of *C. purpurea* P1. On the other hand, both ergopeptines were still present in the mycelia and media of *OE:TrpE* and *OE:TrpE*^{S76L} mutants (Tab. 24). On the contrary, no ergopeptines were detected in the mycelia and media of *OE:gfp_dmaW* mutant lines under these conditions. Therefore, the inhibition of EAs production by high levels of inorganic phosphate in *C. purpurea* P1 can be overcome not only by the addition of Trp or its analogs into the growth medium as described previously (Robbers *et al*., 1972; Krupinski *et al*., 1976) but also by the overexpression of *TrpE*, a gene encoding anthranilate synthase, a key enzyme in Trp biosynthesis that is feedback-regulated by Trp. Concerning the mechanism of phosphate starvation response, a global regulatory mechanism called the phosphate (Pho) regulon containing a transcriptional factor Nuc-1 and its homologs have already been characterized in filamentous fungi (Peleg *et al*., 1996; de Gouvêa *et al*., 2008), yeasts (Magbanua *et al*., 1997) and bacteria (Tommassen *et al*., 1982). Although the Pho regulon has not yet been identified and characterized in *C. purpurea* P1, a binding site for a regulator Nuc-1 is present in the promoter region of *dmaW* gene, which suggests that a similar regulatory mechanism may trigger the induction of ergot alkaloid biosynthesis under low phosphate conditions (Tudzynski *et al*., 1999).

3.5.4 Expression of EA biosynthetic cluster genes

As the biosynthesis of EAs in *C. purpurea* P1 mutants resulted in increased and modified production under inducing and non-inducing conditions, the expression of 10 related genes (*dmaW, easF, easE, easC, easD, easA, easG, cloA, lpsB,* and *easH*) involved in EAs formation and the *TrpE* gene was investigated. Genes *lpsA1* and *lpsA2* encoding nonribosomal lysergyl peptide synthetases were omitted as unique primers could not be designed due to high DNA sequence identity. Furthermore, *lpsC* gene involved in the

biosynthesis of ergometrine was excluded. Although *lpsC* transcript has been previously detected in *C. purpurea* P1, none LPS3 has been purified from this fungus (Ortel and Keller, 2009). Thus the role of *lpsC* gene in strain P1 is still questionable.

Firstly, parts of *TrpE* and EAS genes were amplified from gDNA of *C. purpurea* P1 (Fig. 39) and cloned into *pDRIVE* vector (Fig. 40). Obtained plasmids were sequenced and sequences were compared with those from *C. purpurea* 20.1 (Tab. 17). As only a few SNPs were found and these differences were not present in the sequences of primers used for amplification, these primers were used, after a calculation of primer efficiencies (Tab. 21) for absolute quantification by qRT-PCR (Tab. 19, 20).

In correlation with results obtained previously by Northern blot analyses (Arntz and Tudzynski, 1997; Tudzynski *et al*., 1999; Haarmann *et al*., 2005), all 10 EA biosynthetic genes were significantly upregulated in WT under inducing compared to non-inducing conditions (Tab. 18). Under inducing conditions, *dmaW* that encodes the enzyme catalyzing the prenylation of L-Trp by dimethylallyl diphosphate (Heinstein *et al*., 1971; Lee *et al*., 1976; Cress *et al*., 1981; Gebler and Poulter, 1992; Tsai *et al*., 1995) was the highest expressed gene in WT of *C. purpurea* P1. On the other hand, *easE*, a flavin-dependent oxidoreductase catalyzing together with *easC* formation of the simplest clavine alkaloid chanoclavine-I (Lorenz *et al*., 2010; Goetz *et al*., 2011) was expressed the least. Under non-inducing conditions, *easC* was the most expressed gene in WT compared to the least expressed *easG* gene encoding an imine reductase involved in the formation of agroclavine (Matuschek *et al*., 2011). Interestingly, the biggest change in gene expression between induced and non-induced mycelia was detected in *dmaW* and *easG* genes that share a single bidirectional promoter containing binding sites for homologs of transcriptional factors that have been characterized in other filamentous fungi including Nuc-1, a transcriptional factor that is activated under conditions of phosphate starvation (Tudzynski *et al*., 1999).

Under both inducing and non-inducing conditions, a significant increase compared to WT in *TrpE* and *dmaW* expression levels was detected for the overexpressor mutants *OE:TrpE*, *OE:TrpE*^{S76L} and *OE:gfp_dmaW*, respectively. Under inducing conditions, only *easA* gene encoding a protein involved together with easG reductase in agroclavine synthesis (Coyle *et al*., 2010; Matuschek *et al*., 2011) was upregulated in *OE:TrpE*^{S76L} and *OE:gfp_dmaW* mutants that produced significantly higher amounts of ergopeptines than WT under these conditions. Even if no detectable amounts of EAs were formed in WT under non-inducing conditions, all analyzed genes involved in EAs

biosynthesis were weakly expressed. Expression of five genes (*dmaW, easC, easD, easA,* and *easG*) significantly increased both in *OE:TrpE* and *OE:TrpE*^{S76L} mutants, which were readily producing ergotamine and α-ergocryptine. Concerning *OE:gfp_dmaW* mutants, except for *dmaW* itself, only two genes (*easC,* and *easA)* were upregulated compared to WT under non-inducing conditions. As the constitutive *OliC* promoter was used for *dmaW* overexpression instead of the bidirectional promoter from *C. purpurea*, *easG* was not overexpressed by this mutation. Taken together the constitutive overexpression of *dmaW* resulted in the upregulation of *easC* and *easA*, whereas the overexpression of Trp feedback-resistant and Trp-sensitive forms of *TrpE* led to an increase in *dmaW*, *easD*, *easG*, *easC*, and *easA* expression under non-inducing conditions.

Although the regulation of EA biosynthesis in *C. purpurea* has been studied for many years, it is not yet fully understood. Nevertheless, being very complex it strongly depends on the specific strain, and most probably other factors in addition to Trp, inorganic phosphate, and chromatin remodeling are involved (Lorenz *et al*., 2009).

4 CRISPR/Cas9 genome editing in ergot fungus *Claviceps purpurea*

4.1 Introduction

Claviceps purpurea is a filamentous fungus well known as a widespread plant pathogen, but it is also an important ergot alkaloid producer exploited by the pharmaceutic industry. For this reason, different fungal strains with altered EAs production were initially generated mostly by UV mutagenesis or by treatment with nitrous acid or N-methyl-N´-nitro-N-nitrosoguanidine. The first genetic transformation of *C. purpurea* protoplasts using PEG has been performed in 1989. From this time only three different resistance genes encoding resistance to phleomycin, hygromycin, and phosphinothricin have been used for selection of *C. purpurea* transformants.

As a new genome editing tool CRISPR/Cas has been established not only in human cells, plants, and mammals, but also in filamentous fungi and *C. purpurea* genome was already sequenced in 2013, we decided to demonstrate that CRISPR/Cas9 can be a tool for directed mutagenesis in *C. purpurea*. In this work, two genes *pyr4* and *TrpE* encoding the orotidine 5´-phosphate decarboxylase involved in pyrimidine biosynthesis and the α-subunit of the anthranilate synthase involved in tryptophan biosynthesis, respectively were successfully targeted; mutations were sequenced and analyzed. Moreover, we wanted to compare the CRISPR/Cas9 transformation efficiency with those from CRISPR/Cas9-mediated HDR and gene knock-out approach based on HR.

4.2 Material

4.2.1 Buffers and solutions

Minimal MM1 agar

- 100 g sucrose, 10 g L-asparagine, 1 g calcium nitrate tetrahydrate, 0.25 g potassium dihydrogen phosphate, 0.125 g potassium chloride, 0.25 g magnesium sulphate heptahydrate, 0.033 g ferrous sulphate heptahydrate, 0.027 g zinc sulphate heptahydrate, made up to 1 l with distilled water, pH adjusted to 5.2 with sodium hydroxide, 20 g agar, autoclaved for 20 min at 120 °C

Minimal MM2 agar

- 100 g sucrose, 10 g L-asparagine, 1 g calcium nitrate tetrahydrate, 0.25 g potassium dihydrogen phosphate, 0.125 g potassium chloride, 0.25 g magnesium sulphate heptahydrate, 0.033 g ferrous sulphate heptahydrate, 0.027 g zinc sulphate heptahydrate, 0.01 g L-cysteine, made up to 1 l with distilled water, pH adjusted to 5.2 with sodium hydroxide, 20 g agar, autoclaved for 20 min at 120 °C

Other buffers and solutions are listed in 3.1.1.

4.2.2 Organisms and plants

Organisms and plants are listed in 3.1.2.

4.2.3 Plasmids

pFC332 (Nødvig *et al*., 2015)

pFC334 (Nødvig *et al*., 2015)

Other plasmids are listed in 3.1.3.

4.3 Methods

4.3.1 Vectors construction

4.3.1.1 USER cloning

Vectors for CRISPR/Cas9 directed mutagenesis, *pFC332:pyr4*, and *pFC332:TrpE*, were constructed using USER cloning method (Fig. 41, 42) according to a published protocol (Hoof *et al*., 2018).

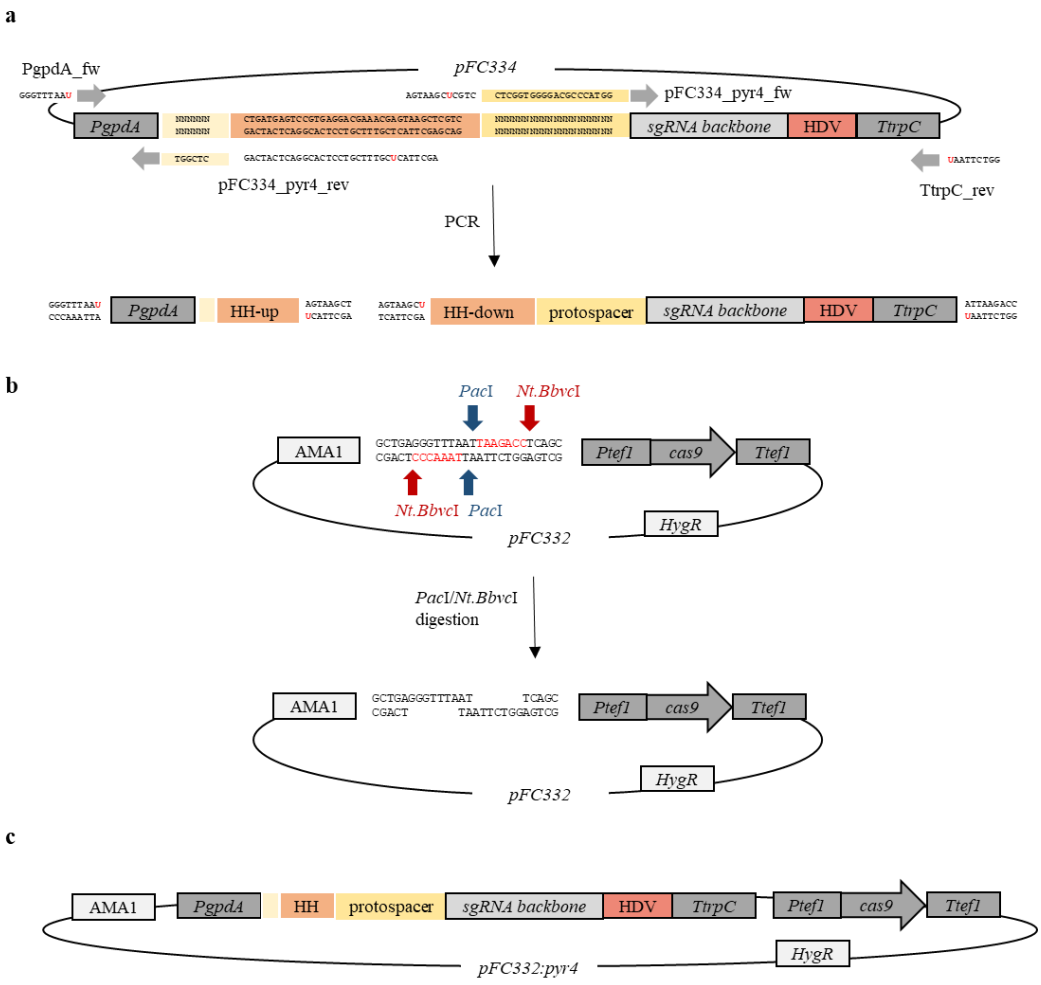

Fig. 41 Construction of *pFC332:pyr4*.
(a) SgRNA containing protospacer targeting *pyr4*, and ribozymes HH and HDV, was amplified together with *GpdA* promoter and *TrpC* terminator from *pFC334* in two parts using primers PgpdA_fw and pFC334_pyr4_rev, pFC334_pyr4_fw and TrpC_rev. Primer pFC334_pyr4_rev contained NN region that corresponds to the 6 bp inverted sequence of the 5´-end of the protospacer, primer pFC334_TrpE_fw contained protospacer
(b) *pFC332* digested with *Pac*I and *Nt.Bbvc*I.
(c) *pFC332:pyr4* that was used for transformation of *C. purpurea* strain 20.1. To create this vector, two PCR products from (a) were cloned into digested *pFC332* using USER cloning method,

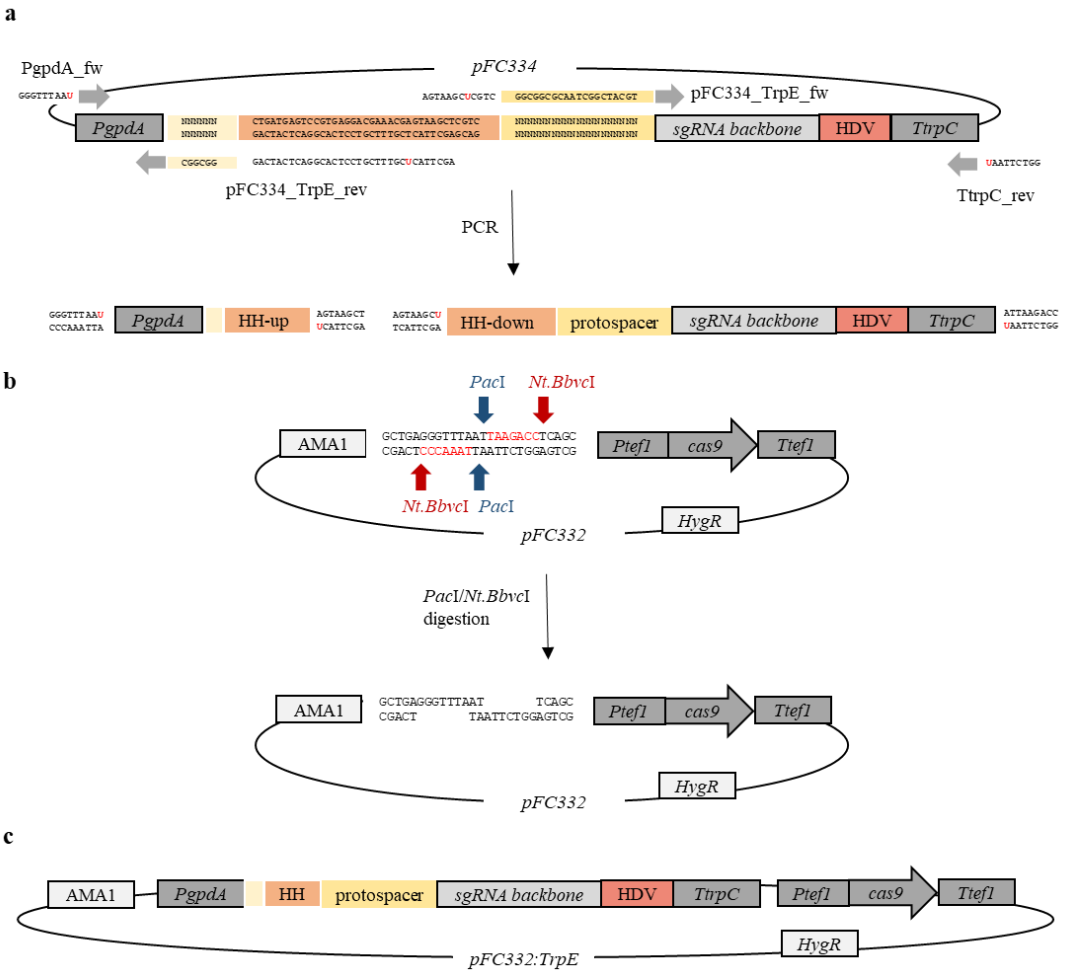

Fig. 42 Construction of *pFC332:TrpE*.
(a) SgRNA containing protospacer targeting *TrpE*, and ribozymes HH and HDV was amplified together with *GpdA* promoter and *TrpC* terminator from *pFC334* in two parts using primers PgpdA_fw and pFC334_TrpE_rev, pFC334_TrpE_fw, and TrpC_rev. Primer pFC334_TrpE_rev contained NN region that corresponds to the 6 bp inverted sequence of the 5′-end of the protospacer, primer pFC334_TrpE_fw contained protospacer.
(b) *pFC332* digested with *Pac*I and *Nt.Bbvc*I.
(c) *pFC332:TrpE* that was used for transformation of *C. purpurea* strain 20.1. To create this vector, two PCR products from (a) were cloned into digested *pFC332* using USER cloning method,

As a genome sequence of *C. purpurea* 20.1 (GCA_000347355) has been shared via the Benchling database (www.benchling.com), protospacers targeting *pyr4* (CPUR_06934.1) and *TrpE* (CPUR_05013.1) could be designed using CRISPR Guide RNA design tool. Finally, two protospacer sequences (*pyr4*: 5′-CTCGGTGGGGACGCCCATGG-3′;*TrpE*: 5′-GGCGGCGCAATCGGCTACGT-3′) having the highest on-target score and a suitable restriction site around the PAM sequence were amplified together with the rest of sgRNA backbone using Phusion U Hot Start DNA Polymerase (Tab. 26, 27); *pFC334* was used as a template (Nødvig *et al.*, 2015).

Primers PgpdA_fw, pFC334_pyr4_rev (545 bp) and pFC334_pyr4_fw, TtrpC_rev (424 bp) (Tab. 28) were used to amplify *pyr4* protospacer and construct *pFC332:pyr4*, while primers PgpdA_fw, pFC334_TrpE_rev (545 bp) and pFC334_TrpE_fw, TtrpC_rev (424 bp) (Tab. 29) were used for amplification of *TrpE* protospacer and construction of *pFC332:TrpE*.

Tab. 26 Components of PCR mixture containing Phusion U Hot Start DNA polymerase.

Component	Final concentration
5x Phusion GC buffer	1x
dNTPS	200 µM
Forward primer	0.5 µM
Reverse primer	0.5 µM
Phusion High-Fidelity DNA polymerase	1 unit
Template DNA	< 250 ng

Tab. 27 PCR conditions with Phusion U Hot Start DNA polymerase.

Step	Temperature (°C)	Time (s)
1. Initial denaturation	98	30
2. Denaturation	98	7
3. Annealing	60	20
4. Extension	72	15-30/kb
5. Final extension	72	300

Steps 2-4 were repeated 34 times

Tab. 28 Sequences of primers used for amplification of sgRNA targeting *pyr4*.

PgpdA_fw
5´- GGGTTTAAUGCGTAAGCTCCCTAATTGGC-3´
pFC334_pyr4_rev
5´-AGCTTACUCGTTTCGTCCTCACGGACTCATCAGCTCGGTCGGTGATGTCTGCTCAAGCG-3´
pFC334_pyr4_fw
5´-AGTAAGCUCGTCCTCGGTGGGGACGCCCATGGGTTTTAGAGCTAGAAATAGCAAGTTAAA
TtrpC_rev
5´- GGTCTTAAUGAGCCAAGAGCGGATTCCTC-3´

Tab. 29 Sequences of primers used for amplification of sgRNA targeting *TrpE*.

PgpdA_fw
5´- GGGTTTAAUGCGTAAGCTCCCTAATTGGC-3´
pFC334_TrpE_rev
5´-AGCTTACUCGTTTCGTCCTCACGGACTCATCAGGGCGGCCGGTGATGTCTGCTCAAGCG-3´
pFC334_TrpE_fw
5´-AGTAAGCUCGTCGGCGGCGCAATCGGCTACGTGTTTTAGAGCTAGAAATAGCAAGTTAAA
TtrpC_rev
5´- GGTCTTAAUGAGCCAAGAGCGGATTCCTC-3´

To check the size of all PCR products, DNA fragments were separated in 1% agarose gel containing ethidium bromide, 1x TAE buffer (40 mM Tris, 1 mM EDTA, pH 8.0) was used. As a marker, 1 kb Plus DNA ladder (Thermo Scientific) was used. The gels were documented with a GelDoc^{TM} EZ imager (Bio-Rad).

Subsequently, *pFC332* (Fig. 43) containing the hygromycin resistance gene (Nødvig *et al*., 2015) was digested with *Nt.Bbvc*I and *Pac*I according to the manufacturer´s protocol (New England BioLabs). Digested vector was together with both PCR products purified according to the manufacturer´s protocol using a NucleoSpin Gel and PCR Clean-up kit (MACHEREY-NAGEL GmbH and Co. KG); purified PCR amplicons were cloned into *pFC332* using USER® cloning method (Bitinaite *et al*., 2007).

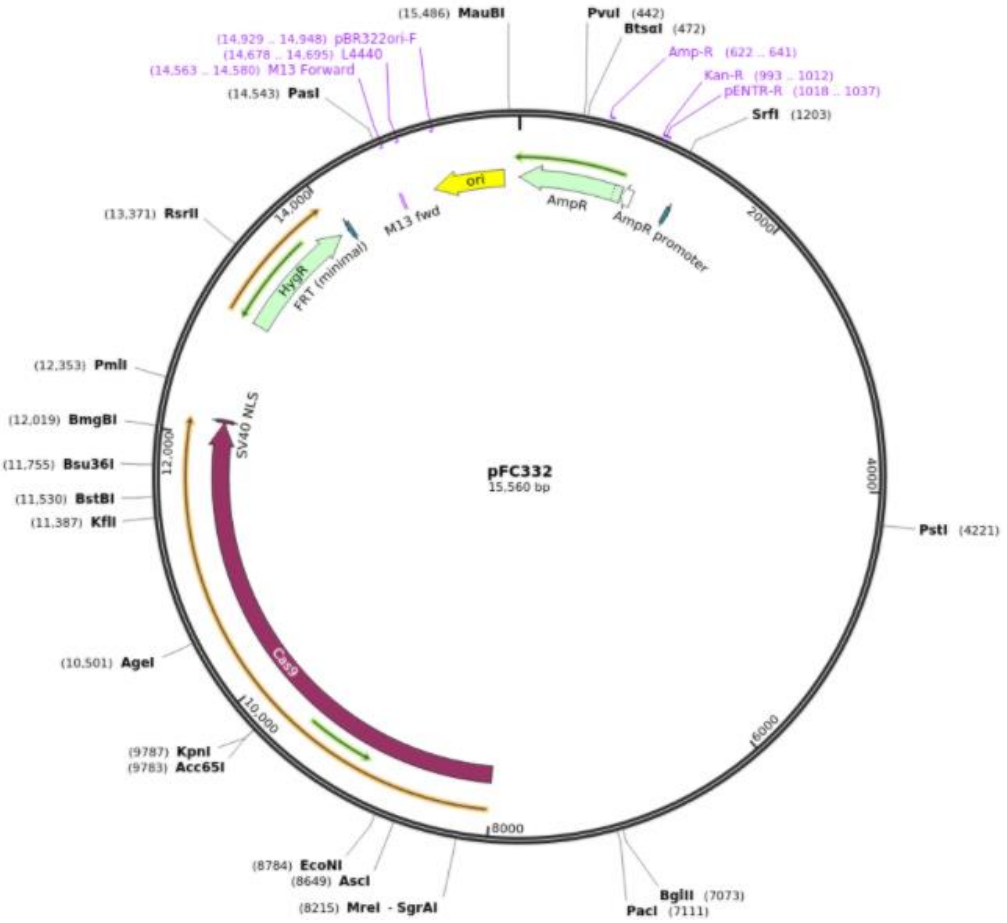

Fig. 43 Vector *pFC332* (Nødvig *et al*., 2015).

Briefly, USER cloning mix (Tab. 30) containing USER enzyme (New England BioLabs) was incubated for 35 min at 37 °C. After 25 min at RT, it was placed on ice and transformed into chemically competent cells of *E. coli* strain TOP10 (see 3.3.1.3). After the transformation, *E. coli* TOP10 cells were plated on LB agar plates containing ampicillin (Sigma-Aldrich) in the final concentration of 100 µg/ml.

The next day, plasmid DNA was isolated from ampicillin-resistant bacterial colonies according to the manufacturer´s protocol using the QIAprep Spin Miniprep kit (Qiagen). The resulting constructs were verified by restriction analysis (Tab. 31) and commercial sequencing (SEQme commercial service).

Tab. 30 Components of USER cloning mix.

Component	Amount (concentration)
Digested and purified pFC332	1 µl (5 ng/µl)
Purified PCR fragment	4 µl (> 20 ng/µl)
10x Cut Smart buffer	0.5 µl
USER enzyme (1 U/µl)	0.5 µl
dH_2O	up to 10 µl

Tab. 31 Restriction analysis of vectors prepared by USER cloning method.

Vector	Restriction endonuclease	Expected size of DNA fragments
pFC332:pyr4	*Sal*I	9,297 bp; 3,945 bp; 2,761 bp; 465 bp
pFC332:TrpE	*Sal*I	9,297 bp; 3,945 bp; 2,761 bp; 465 bp

4.3.1.2 Yeast recombinational cloning

To knock-out *TrpE* (CPUR_05013.1), vector *pRS426:ΔTrpE2* (Fig. 44) was constructed using the yeast recombinational cloning method (see 3.3.1.3). 5´and 3´flanking regions of *TrpE* were amplified using proofreading Phusion High-Fidelity DNA polymerase (Tab. 1, 2) and the primers *Eco*RI_5F_TrpE2, 5R_TrpE2 (1,547 bp) and 3F_TrpE2, 3R_TrpE2_*Eco*RI (1,500 bp) (Tab. 32); as a template, gDNA isolated from *C. purpurea* 20.1 was used. Phleomycin resistance cassette was amplified with the primers CpBle1F and CpBle1R (1,847 bp) (Tab. 6). All generated PCR products were subsequently cloned using the yeast recombinational method (Colot *et al.*, 2006) into the *Xho*I-*Eco*RI-digested *pRS426* vector (Christianson *et al.*, 1992).

Plasmid DNA isolated from *S. cerevisiae* FGSC 9721 was transformed into chemically competent cells of *E. coli* TOP10, the mixture was plated on LB agar plates containing ampicillin (Sigma-Aldrich) in the final concentration of 100 µg/ml. The

resulting constructs were verified by restriction analysis using *EcoR*I and *Xba*I (expected bands: 4,900 bp; 3,131 bp, and 2,375 bp) and commercial sequencing (SEQme commercial service).

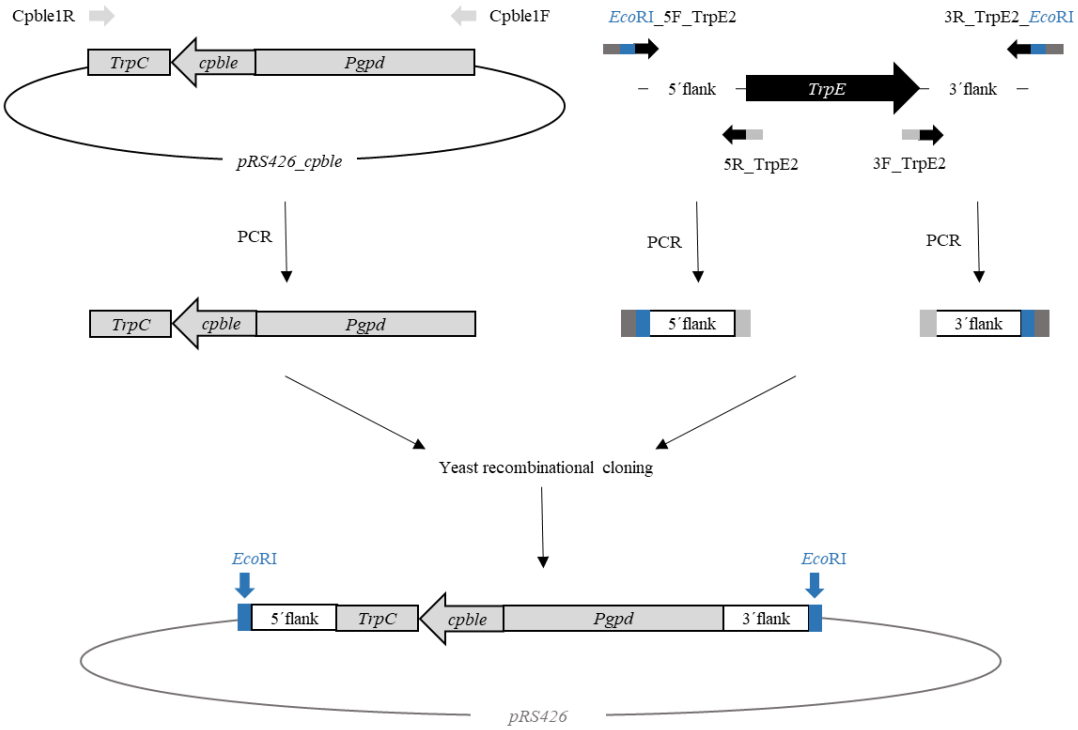

Fig. 44 Cloning of *pRS426:ΔTrpE2*.
5´and 3´flanking regions of *TrpE* gene were amplified together with phleomycin resistance cassette from gDNA of WT *C. purpurea* strain 20.1 and *pRS426_CpBle*, respectively, and cloned into *Eco*RI and *Xho*I-digested *pRS426* using yeast recombinational cloning method. Then, *Eco*RI-linearized *pRS426:ΔTrp21* was used to transform protoplasts of *C. purpurea* strain 20.1.

Tab. 32 Sequences of primers used for generation of *pRS426:ΔTrpE2*.

*Eco*RI_5F_TrpE2
5´-AACGCCAGGGTTTTCCCAGTCGAATTCGGCTCTACCACATGCCTCTT-3´
5R_TrpE2
5´-TGCCCACTTAACGTTACTGAAATCTCCAACTTTTTCTTGCTCCCGTTTTG-3´
3F_TrpE2
5´-TTGTAGGGGCTGTATTAGGTCTCGATCGTCCCTTGAAAAGTGGGAGTTT-3´
3R_TrpE2_*EcoR*I
5´-CAATTTCACACAGGAAACAGCGAATTCTTCACAGCATTCTTCGCAAT-3´

4.3.2 Transformation of *C. purpurea* 20.1 and selection of obtained fungi

Transformation of *C. purpurea* 20.1 protoplasts was performed according to 3.2.2 according to a published protocol (Jungehülsing *et al.*, 1994). *OE:Cas9 C. purpurea* 20.1 transformants were prepared as follows: 10 µg of *pFC332* vector was used. Concerning CRISPR/Cas9 directed mutagenesis, *pyr4* and *TrpE* mutants were prepared by transforming the fungus with 10 µg of *pFC332:pyr4* or *pFC332:TrpE*, respectively. To generate *ΔTrpE* mutants prepared by HR-mediated gene knock-out and *Δ+CRISPR/Cas9 TrpE* mutants prepared by CRISPR/Cas9-mediated HDR, 10 µg of purified 4,900 bp fragment of *pRS426:ΔTrpE2* digested with *Eco*RI alone or in combination with 10 µg of *pFC332:TrpE*, respectively, were used to transform *C. purpurea* 20.1 protoplasts.

While phleomycin (InvivoGen) in the final concentration of 33 µg/ml was added directly to BII transformation agar plates during the process of transformation, Hygromycin B Gold (InvivoGen) in the final concentration of 200 µg/mL was added to BII transformation agar that was used to overlay BII transformation agar plates with regenerated protoplasts 24 h after transformation. In both cases, *C. purpurea* 20.1 mutants were transferred 7 days after the transformation to BII selection agar plates containing 100 µg/ml phleomycin (in the case of *ΔTrpE C. purpurea* 20.1 mutants) or 200 µg/ml hygromycin (in the case of *CRISPR/Cas9 TrpE* and *CRISPR/Cas9 pyr4 C. purpurea* 20.1 mutants) or their combination (in the case of *Δ+CRISPR/Cas9 TrpE C. purpurea* 20.1 mutants).

C. purpurea 20.1 transformants with a mutation in *pyr4* were grown on BII selection agar plates supplemented with 10 mM uridine (Sigma-Aldrich) (Smit and Tudzynski, 1992) and hygromycin, transformants with a mutation in *TrpE* gene were grown on BII selection agar plates supplemented with 5 mM L-Trp (Sigma-Aldrich) and appropriate antibiotic (hygromycin, phleomycin or both).

4.3.3 *C. purpurea* 20.1 transformants expressing Cas9

4.3.3.1 Detection of Cas9 at DNA level

The presence of *pFC332* in *OE:Cas9 C. purpurea* 20.1 mutants was confirmed by diagnostic PCR using GoTaq G2 Flexi DNA polymerase (Tab. 9, 10) and two sets of primers: dia_Cas9_fw and dia_Cas9_rev (1,203 bp), hph_fw and hph_rev (366 bp) (Tab. 33).

Tab. 33 Sequences of primers used for diagnostic PCR of *OE:Cas9 C. purpurea 20.1*.

Primer	Sequence
hph_fw	5´-GAATTCAGCGAGAGCCTGAC-3´
hph_rev	5´-ACATTGTTGGAGCCGAAATC-3´
dia_Cas9_fw	5´-AGTACGTGACGGAGGGAATG-3´
dia_Cas9_rev	5´-TTTGTGATCTGTCGCGTCTC-3´

4.3.3.2 Single spore isolation

Homokaryons of *OE:Cas9 C. purpurea* 20.1 were obtained by single spore isolation (see 3.2.3.2). Fungal spores were harvested from Mantle agar and plated on BII selection agar plates containing hygromycin. After 3 days, germinated spores were transferred to new BII selection agar plates containing hygromycin.

4.3.3.3 Detection of Cas9 at RNA level

RNA was isolated from approximately 60 mg of lyophilized mycelium according to Oňate-Sánchez and Vicente-Carbajosa (2008) (see 3.2.4.5.2.1). After the treatment of RNA samples with DNase I (TURBO DNA-free kit, Thermo Scientific) and purification by LiCl precipitation, 1 µg of total RNA was transcribed into cDNA using RevertAid H Minus First Strand cDNA Synthesis Kit (Thermo Scientific). Prepared cDNAs of WT and *OE:Cas9 C. purpurea* 20.1 were used as templates for amplification of *Cas9* (869 bp), hygromycin resistance gene (366 bp), and γ-actin (636 bp) using GoTaq G2 Flexi DNA polymerase (Tab. 9, 10) and primers Cas9_RT-PCR_fw and Cas9_RT-PCR_rev, hph_fw and hph_rev, γ-actin_RT-PCR_fw and γ-actin_RT-PCR_rev. respectively (Tab. 33, 34).

Tab. 34 Sequences of primers used for RT-PCR to detect Cas9 and γ-actin in *OE:Cas9 C. purpurea*.

Primer	Sequence
Cas9_RT-PCR_fw	5´-GCCAATGGAGAAATCCGTAA-3´
Cas9_RT-PCR_rev	5´-ATCGCTTACGGTCGATTGTC-3´
γ-actin_RT-PCR_fw	5´-CGCTCTCGTCATCGACAAAT-3´
γ-actin_RT-PCR_rev	5´-ATTTCACGCTCGGCAGTAGT-3´

4.3.3.4 Stress assays

To compare the growth of WT and *Cas9* expressing mutants, a small piece of 7-days old mycelium was transferred to minimal MM2 agar plates supplemented with fungin (1, 2, 4, and 8 µg/ml), Congo red (50, 100, 200, and 400 µg/ml) and hydrogen peroxide (1, 2, 4, and 8 mM) according to a published protocol (Fuller *et al*., 2015). The experiment was performed in six biological replicates; after 7, 10, and 14 days, the colony diameter was measured with a ruler to the nearest mm. The data were analyzed using the non-parametric Kruskal-Wallis ANOVA followed by multiple comparisons of mean ranks in Statistica v.13.3 (TIBCO Software Inc.). Results are expressed as a mean value ± standard error.

4.3.3.5 Pathogenicity assays

Pathogenicity assays were performed according to Tenberge *et al*. (1996) (see 3.2.3.4). Infections were performed by piercing ears with a needle and syringe containing WT and *OE:Cas9 C. purpurea* 20.1 conidial suspension (10^6 conidia/mL) harvested from Mantle agar plates.

4.3.4 *C. purpurea* 20.1 transformants with a mutation in *pyr4* generated by CRISPR/Cas9

4.3.4.1 PCR-RFLP analysis

CRISPR/Cas9 pyr4 mutants of *C. purpurea* 20.1 were selected using PCR restriction fragment length polymorphism (PCR-RFLP) analysis. Briefly, a part of *pyr4* was amplified from the gDNA using GoTaq G2 Flexi DNA polymerase (Tab. 9, 10) and primers PCR_pyr4_fw and PCR_pyr4_rev (705 bp) (Tab. 35); PCR amplicon was digested with *Nco*I according to the manufacturer´s protocol (New England BioLabs). While a restriction of WT should provide two bands (482 bp, 223 bp), a restriction of

pyr4 hetero- and homo-karyons should result in three bands (706 bp, 482 bp, 223 bp) and a single band (706 bp), respectively.

Tab. 35 Sequences of primers used for PCR-RFLP analysis in the case of CRISPR/Cas9 *pyr4*.

Primer	Sequence
PCR_pyr4_fw	5´-CCATGGGTTCCTGATATTCG -3´
PCR_pyr4_rev	5´-TTTTGCGGCGTATTGTACTG-3´

4.3.4.2 Single spore isolation

Homokaryons of *CRISPR/Cas9 pyr4 C. purpurea* 20.1 were obtained by single spore isolation (see 3.2.3.2). Fungal conidia were harvested from Mantle agar plates supplemented with 10 mM uridine (Sigma-Aldrich) (Smit and Tudzynski, 1992). Obtained spores were grown on BII selection agar plates containing 10 mM uridine and hygromycin. After 3 days, germinated spores were transferred to new BII selection agar plates containing 10 mM uridine. Subsequently, each mycelium was transferred on minimal MM1 agar plates with and without uridine, allowing thus putative *pyr4* homokaryons to be selected based on uridine auxotrophy (Fig. 45).

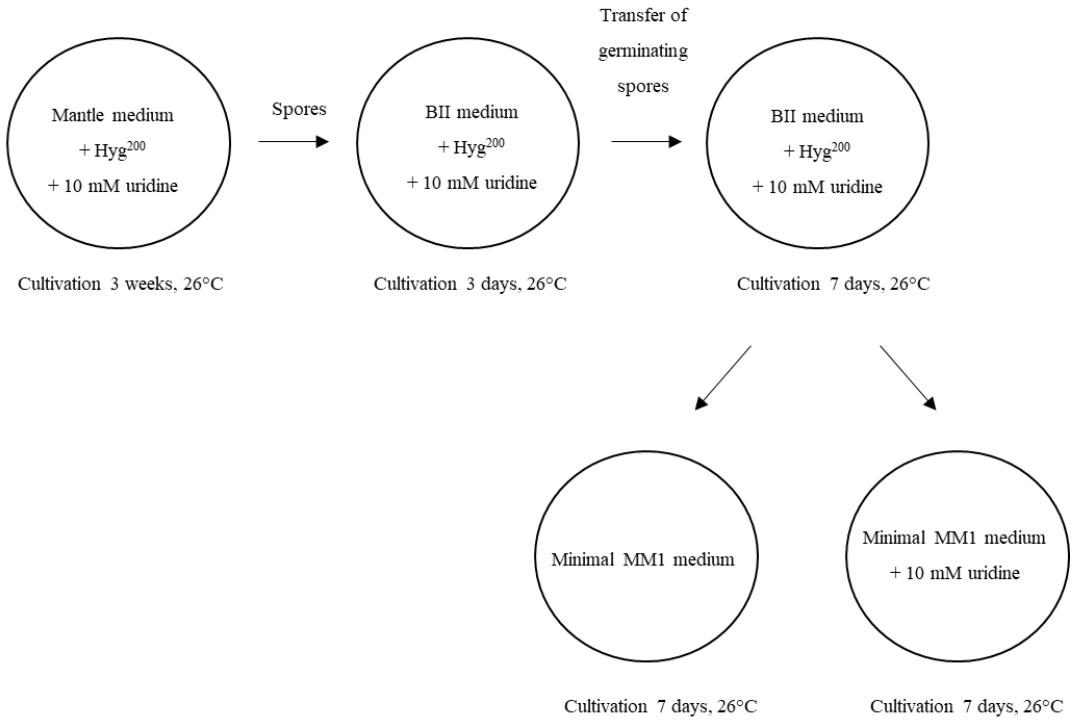

Fig. 45 Schema of the selection of CRISPR/Cas9 *pyr4* homokaryons.
CRISPR/Cas9 pyr4 heterokaryons of *C. purpurea* 20.1 were selected by single spore isolation on media containing uridine and hygromycin, and then cultivated on minimal MM1 agar plates with or without uridine.

4.3.5 *C. purpurea* 20.1 transformants with a mutation in *TrpE* generated by CRISPR/Cas9, HR, and CRISPR/Cas9-mediated HDR

4.3.5.1 Detection of mutations in *TrpE* transformants

As *CRISPR/Cas9 pyr4* mutants, *CRISPR/Cas9 TrpE* mutants of *C. purpurea* 20.1 were selected using PCR-RFLP analysis. Briefly, a part of *pyr4* was amplified from the gDNA using GoTaq G2 Flexi DNA polymerase (Tab. 9, 10) and primers PCR_TrpE_fw and PCR_TrpE_rev (631 bp) (Tab. 36); PCR amplicon was digested with *Bsa*AI according to the manufacturer´s protocol (New England BioLabs). While a restriction of WT should provide two bands (504 bp, 127 bp), a restriction of *TrpE* hetero- and homo-karyons should result in three bands (631 bp, 504 bp, 127 bp) and a single band (631 bp), respectively.

Tab. 36 Sequences of primers used for PCR-RFLP analysis in the case of CRISPR/Cas9 *TrpE*.

Primer	Sequence
PCR_TrpE_fw	5´-GAGCCCGGTAAGTACTGCA-3´
PCR_TrpE_rev	5´-ATGCCGTAGAAGCGATCAAA-3´

The replacement of WT *TrpE* allele with phleomycin resistance cassette in *ΔTrpE* mutants obtained by HR-mediated gene knock-out and CRISPR/Cas9-mediated HDR was confirmed by diagnostic PCR using GoTaq G2 Flexi DNA polymerase (Tab. 9, 10) and three sets of primers (Tab. 37) producing fragments of the following size: dia_TrpE2_fw and phleohi3F2 (2,075 bp), phleooutHefe3 and dia_TrpE2_rev (1,740 bp) dia_TrpE_WT2_fw and dia_TrpE2_rev (1,622 bp).

Tab. 37 Sequences of primers used for diagnostic PCR of ***ΔTrpE C. purpurea* 20.1.**

Primer	Sequence
phleohi3F2	5´-GTGTTCAGGATCTCGATAAGATACG-3´
phleooutHefe3	5´-GAGCTCGGTATAAGCTCTCC-3´
dia_TrpE2_fw	5´-CGGTCAGGGTCACAGCAG-3´
dia_TrpE_WT2_fw	5´-AGCAGCAAAACGAGAAAACC-3´
dia_TrpE2_rev	5´-AGGACTGCCTTTGCATGCTC-3´

4.3.5.2 Single spore isolation

Homokaryons of *C. purpurea* 20.1 with a mutation in *TrpE* were obtained by single spore isolation (see 3.2.3.2). Fungal conidia were harvested from Mantle agar plates supplemented with 5 mM L-Trp (Sigma-Aldrich). Obtained spores were grown on BII selection agar plates containing 5 mM L-Trp and hygromycin (*CRISPR/Cas9 TrpE*), phleomycin (*ΔTrpE*), or both (*Δ+CRISPR/Cas9 TrpE*). After 3 days, germinated spores were transferred to new BII agar plates containing 5 mM L-Trp and appropriate antibiotics. Subsequently, each mycelium was transferred on minimal MM2 agar plates with and without L-Trp, allowing thus putative *TrpE* homokaryons to be selected based on tryptophan auxotrophy (Fig. 46).

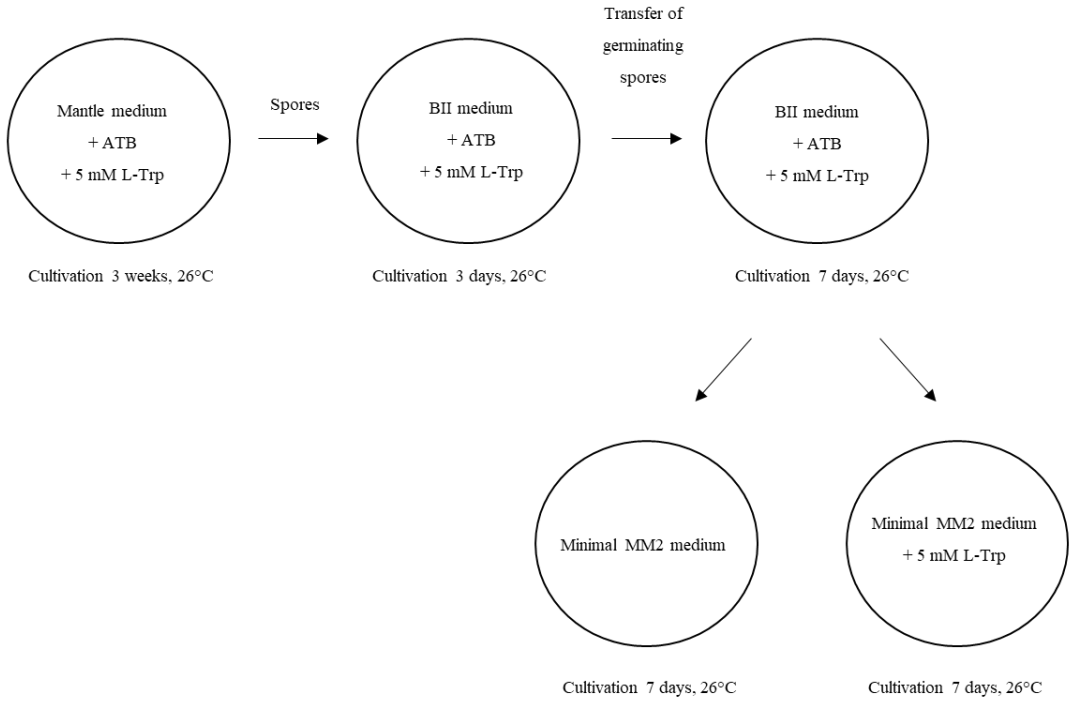

Fig. 46 Schema of the selection of homokaryons with a mutation in *TrpE*.
TrpE heterokaryons of *C. purpurea* 20.1 were selected by single spore isolation on media containing L-Trp and hygromycin (*CRIPSR/Cas9 TrpE*), phleomycin (*ΔTrpE*) or both (*Δ+CRISPR/Cas9 TrpE*), and then cultivated on minimal MM1 agar plates with or without L-Trp.

4.3.5.3 Trp auxotrophy

To check Trp auxotrophy, all generated *TrpE* homokaryons (*CRISPR/Cas9 TrpE*, *ΔTrpE*, and *Δ+CRISPR/Cas9 TrpE)* were cultivated on minimal MM2 agar plates with and without 5 mM L-Trp.

4.3.5.4 Pathogenicity assays

Pathogenicity assays were performed according to 3.2.3.4. Infections were performed according to Tenberge *et al*. (1996) by piercing ears with a needle and syringe containing WT and *CRISPR/Cas9 TrpE, ΔTrpE*, and *Δ+CRISPR/Cas9 TrpE C. purpurea* 20.1 conidial suspension (10^6 conidia/mL) harvested from MM2 agar plates supplemented with 5 mM L-Trp.

4.3.6 Sequencing of CRISPR/Cas9 mutations in *TrpE* heterokaryons

Parts of *TrpE* around the PAM sequence was amplified from gDNA of T6 and T16 *CRISPR/Cas9 TrpE C. purpurea* 20.1 heterokaryons using Phusion High-Fidelity DNA polymerase (Tab. 1, 2) and primers PCR_TrpE_fw and PCR_TrpE_rev (631 bp) (Tab. 36). To clone these amplicons into *pDRIVE* (Fig. 19) (see 3.2.4.5.3.1), A overhangs were created by the addition of GoTaq G2 Flexi DNA polymerase into the PCR mixture in the final elongation step. Plasmid DNA isolated from *E. coli* TOP10 clones resistant to *Bsa*AI cleavage were sequenced by commercial service (SEQme).

4.3.7 Recycling of AMA1-based plasmid

To obtain *CRISPR/Cas9 TrpE C. pupurea* 20.1 homokaryons that lost the *pFC332:TrpE*, single spore isolation (see 3.3.3.2) using agar plates without selection pressure was performed (Fig. 47).

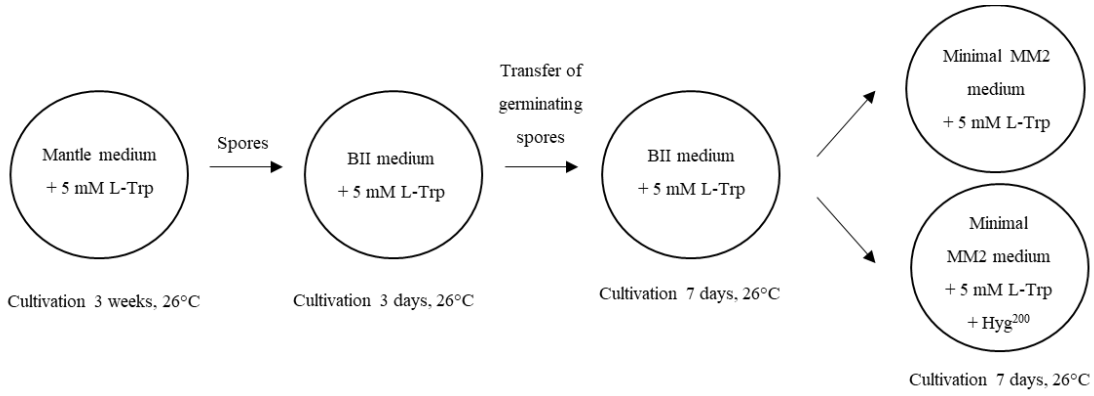

Fig.47 Schema of the selection of *CRISPR/Cas9 TrpE* homokaryons of *C. purpurea* 20.1 sensitive to hygromycin.

4.4 Results

4.4.1 Vectors construction

4.4.1.1 USER cloning

Together, two CRISPR/Cas9 vectors targeting *pyr4* (CPUR_06934.1) and *TrpE* (CPUR_05013.1) that encode orotidine-5´-phosphate decarboxylase and α-subunit of anthranilate synthase, respectively were prepared using USER cloning method (4.2.1.1). SgRNA backbone was together with *pyr4* or *TrpE* protospacer amplified from *pFC334* (Fig. 48a, c) and then cloned into *pFC332* digested with *Pac*I and *NtBbcv*I. Plasmids isolated from *E. coli* TOP10 ampicillin-resistant clones were confirmed by restriction analysis and then sequenced (Fig. 48b, d).

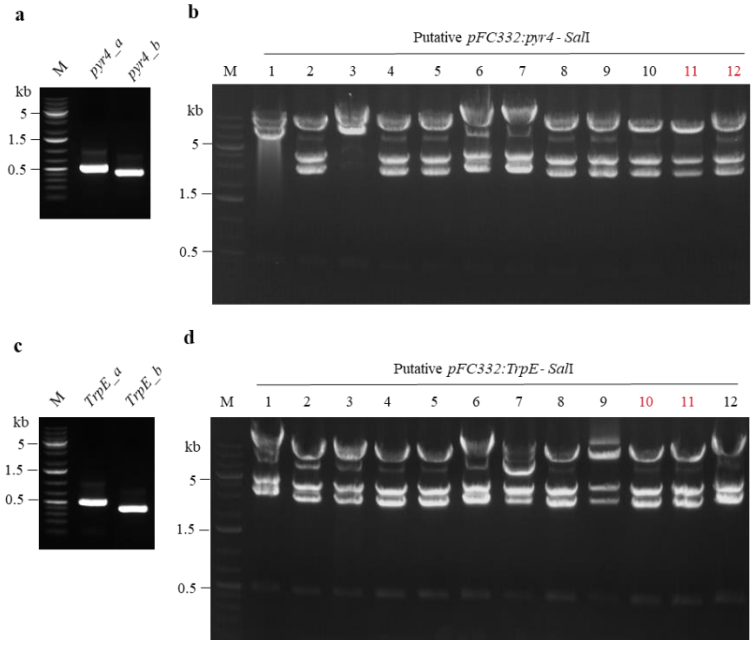

Fig. 48 Cloning of *pFC332:pyr4* and *pFC332:TrpE*.
(a) Amplification of sgRNA in two parts with Phusion High-Fidelity DNA polymerase and primers PgpdA_fw and pFC334_pyr4_rev (545 bp), and pFC334_pyr4_fw and TtrpC_rev (424 bp). Primers contained 20 bp of protospacer sequence targeting *pyr4*. As a template, *pFC334* was used. M - 1 kb Plus DNA ladder.
(b) *Sal*I-digestion of putative plasmids *pFC332:pyr4* isolated from *E. coli* TOP10 (expected bands: 9,297 bp; 3,945 bp; 2,761 bp, and 465 bp), M - 1 kb DNA ladder.
Plasmids 11 and 12 (red) were sequenced.
(c) Amplification of sgRNA in two parts with Phusion High-Fidelity DNA polymerase and primers PgpdA_fw and pFC334_TrpE_rev (545 bp), and pFC334_TrpE_fw and TtrpC_rev (424 bp). Primers contained 20 bp of protospacer sequence targeting *TrpE*. As a template, *pFC334* was used M - 1 kb Plus DNA ladder.
(d) *Sal*I-digestion of putative plasmids *pFC332:TrpE* isolated from *E. coli* TOP10 (expected bands: 9,297 bp; 3,945 bp; 2,761 bp, and 465 bp), M - 1 kb DNA ladder.
Plasmids 10 and 11 (red) were sequenced.

4.4.1.2 Yeast recombinational cloning

Vector *pRS426:ΔTrpE2* for deletion of α-subunit of anthranilate synthase (CPUR_05013.1) was prepared using yeast recombinational cloning (4.2.1.2). 5´and 3´flanking regions of *TrpE* and phleomycin resistance cassette were amplified from gDNA of *C. purpurea* 20.1 and *pRS426_CpBle*, respectively (Fig. 49a, b). Obtained DNA amplicons were cloned into *Xho*I+*Eco*RI-digested *pRS426* (Fig. 49c). Plasmids isolated from *E. coli* TOP10 ampicillin-resistant colonies were confirmed by restriction analysis and then sequenced (Fig. 49d).

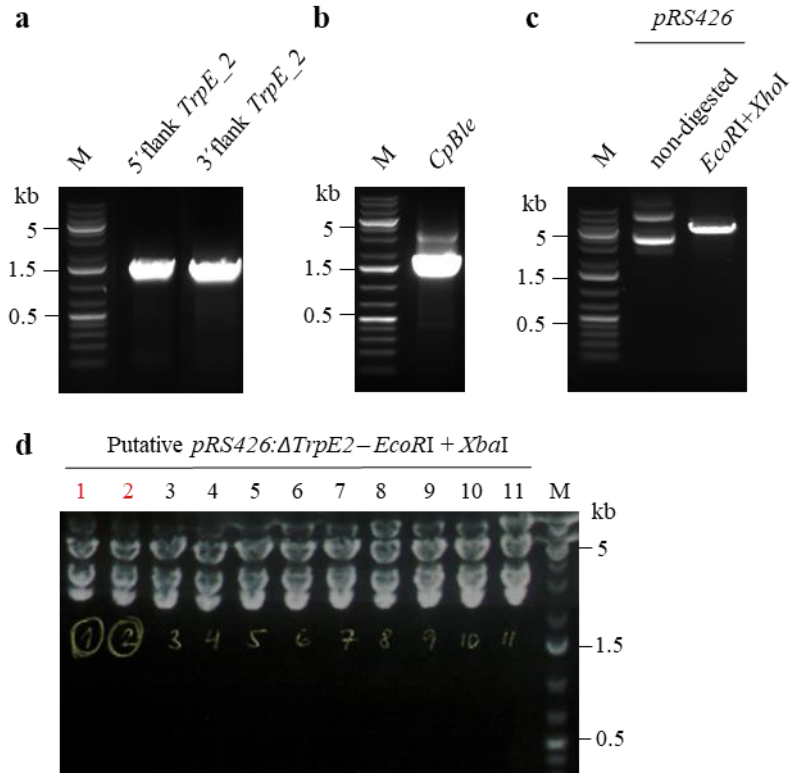

Fig. 49 Cloning of *pRS426:ΔTrpE2*.
(a) Amplification of phleomycin resistance cassette (1,847 bp) from *pRS426_CpBle* using Phusion High-Fidelity DNA polymerase and primers Cpble1F and Cpble1R. M - 1 kb Plus DNA ladder.
(b) Amplification of 5´flanking (1,547 bp) and 3´flanking (1,500 bp) regions of *TrpE* from gDNA of WT *C. purpurea* 20.1 using Phusion High-Fidelity DNA polymerase and primers *Eco*RI_5F_TrpE2 and 5R_TrpE2, 3F_TrpE2 and 3R_TrpE2_*Eco*RI. M - 1 kb Plus DNA ladder.
(c) Digestion of *pRS426* (5,756 bp) with enzymes *Xho*I and *Eco*RI. The non-digested plasmid was used as a control. M - 1 kb Plus DNA ladder.
(d) *Eco*RI+*Xba*I-digestion of putative plasmids *pRS426:ΔTrpE2* isolated from *E. coli* TOP10 (expected bands: 4,900 bp; 3,131 bp, and 2,375 bp), M - 1 kb DNA ladder.
Plasmids 1 and 2 (red) were sequenced.

4.4.2 Generation and characterization of *C. purpurea* 20.1 transformants expressing Cas9

4.4.2.1 Detection of *Cas9* at DNA level

By transforming protoplasts of *C. purpurea* 20.1 with *pFC332* (Nødvig *et al*., 2015) (4.3.2), mutants constitutively expressing *Cas9* were prepared. Together, gDNA was isolated from 30 putative *OE:Cas9 C. purpurea* 20.1 transformants that were resistant to hygromycin; the presence of *Cas9* and *hph* was checked by diagnostic PCR (4.2.3.1).

For further analyses only three independent mutants (marked as T1, T3, and T4) were selected; homokaryons were selected by single spore isolation (4.2.3.2) and confirmed again by diagnostic PCR (Fig. 50).

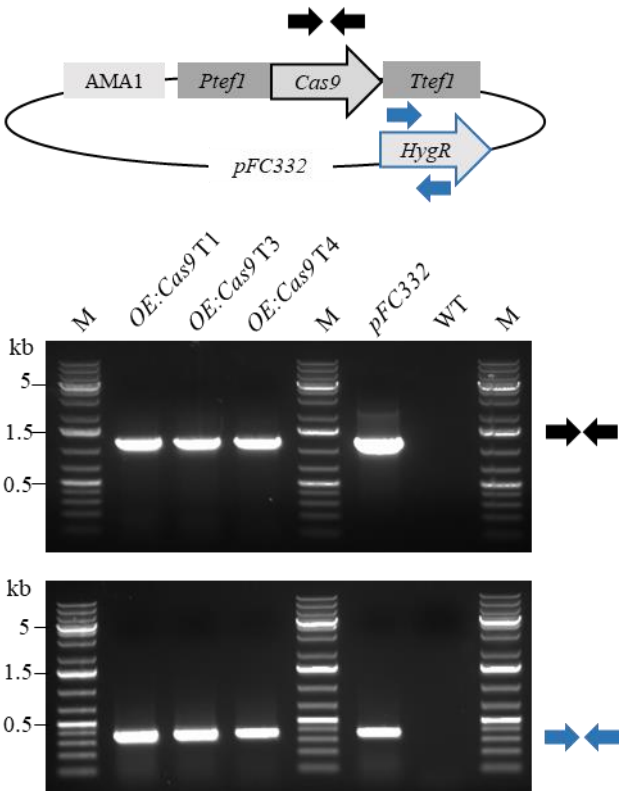

Fig. 50 Diagnostic PCR of *OE:Cas9* mutants of *C. purpurea* 20.1
Presence of AMA-1 based *pFC332* in three independent *OE:Cas9* mutants of *C. purpurea* 20.1 (T1, T3, and T4) was confirmed by diagnostic PCR using primers dia_Cas9_fw and dia_Cas9_rev (1,203 bp) (upper panel) and hph_fw and hph_rev (366 bp) (lower panel). The *pFC332* and gDNA isolated from WT of *C. purpurea* 20.1 were used as the positive and negative control, respectively; M, 1 kb Plus DNA ladder.

4.4.2.2 Detection of Cas9 at RNA level

RNA was isolated from lyophilized mycelia of *OE:Cas9 C. purpurea* 20.1 and WT; the expression of *Cas9* was confirmed in all transformants by RT-PCR (4.2.3.3) (Fig. 51).

.

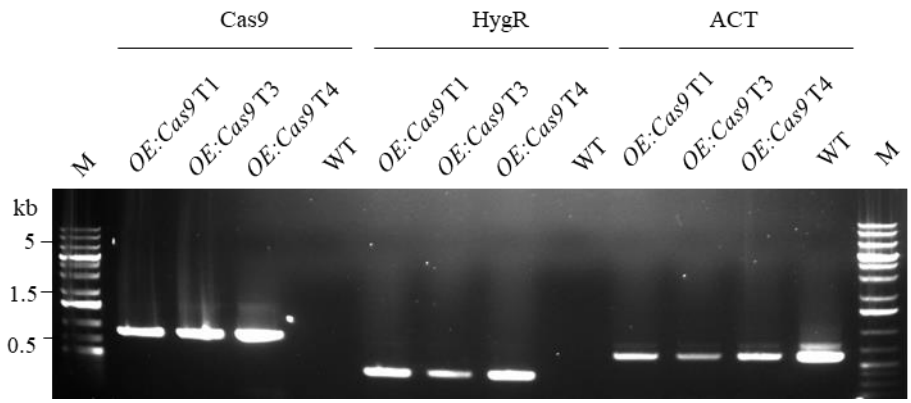

Fig. 51 RT-PCR of WT and *OE:Cas9 C. purpurea* 20.1 homokaryons.
Presence of Cas9, hygromycin resistance cassette (HygR), and γ-actin (ACT) in three independent *OE:Cas9* mutants of *C. purpurea* 20.1 (T1, T3, and T4) was confirmed by RT-PCR using primers Cas9_RT-PCR_fw and Cas9_RT-PCR_rev, hph_fw and hph_rev, γ-actin_RT-PCR_fw and γ-actin_RT-PCR_rev, respectively. gDNA from WT *C. purpurea* 20.1 was used as the negative control in the case of detection of expression of Cas9 and hygromycin resistance; M, 1 kb Plus DNA ladder.

4.4.2.3 Stress assays

To test stress sensitivity, *OE:Cas9 C. purpurea* 20.1 were, together with WT, cultivated on minimal MM2 agar plates supplemented with different concentrations of stress agents Congo red, hydrogen peroxide, and fungin (4.2.3.4). After 7, 10, and 14 days, the colony diameter was measured and no changes in phenotype were observed between WT and *C. purpurea* 20.1 mutants (Fig. 52-54).

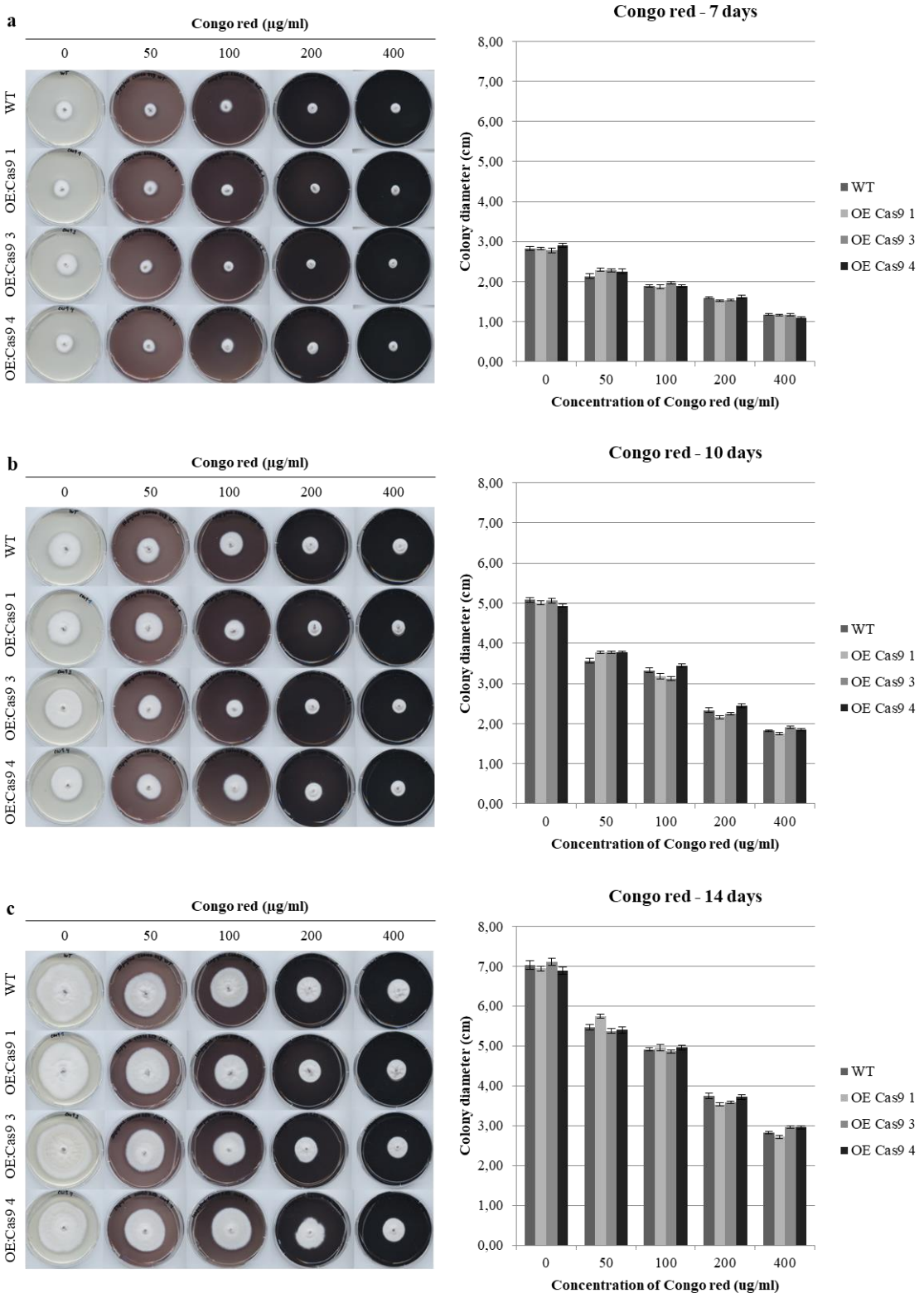

Fig. 52 Growth comparison of WT and *OE:Cas9* mutants of *C. purpurea* 20.1 on minimal MM2 agar plates supplemented with Congo red in different concentrations.
Colony diameter was determined after 7 (a), 10 (b), and 14 (c) days. The non-parametric Kruskal-Wallis ANOVA followed by multiple comparisons of mean ranks was used to compare the differences between groups. Data comparing differences between WT and individual transformants are shown (all not significant).

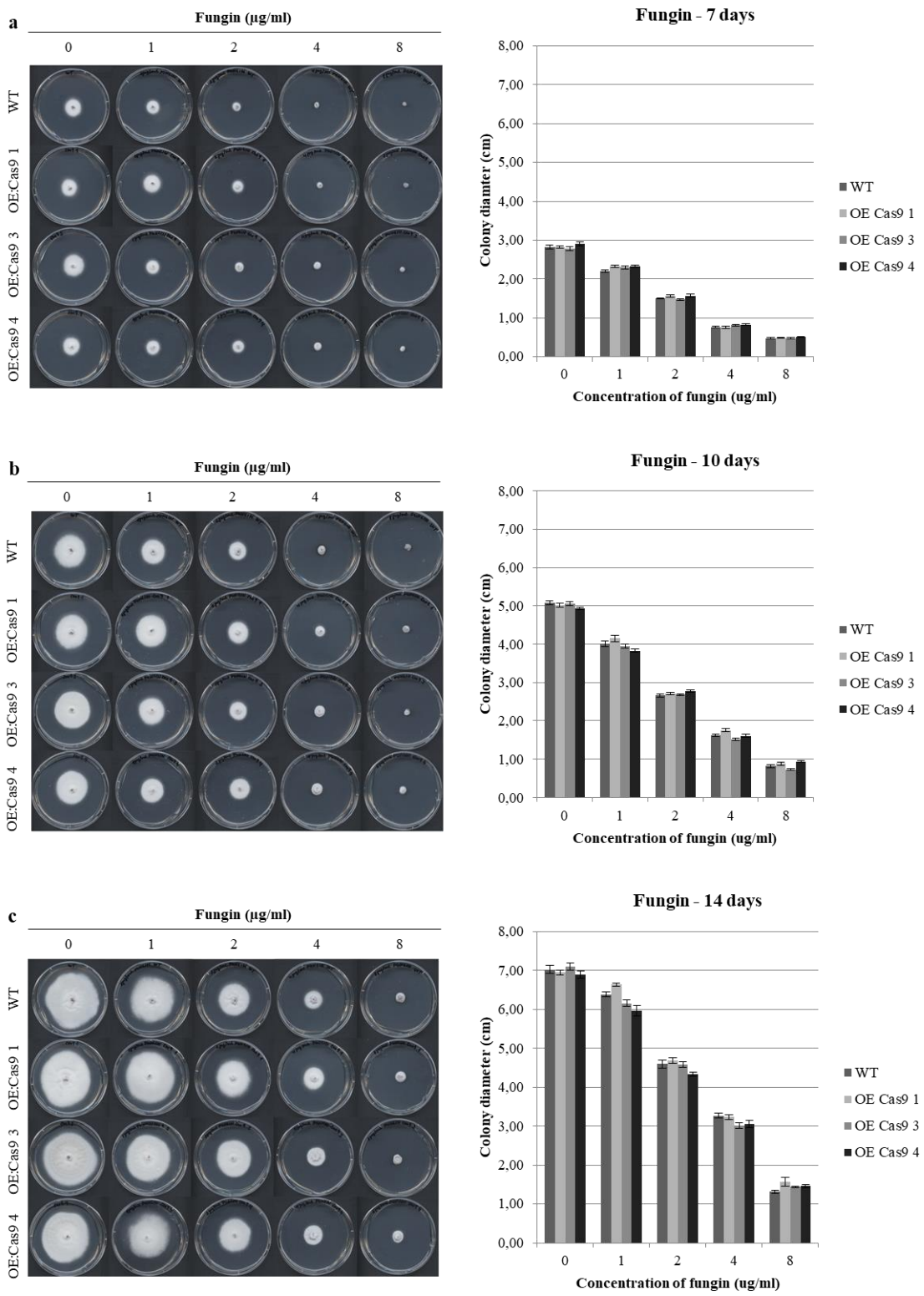

Fig. 53 Growth comparison of WT and *OE:Cas9* mutants of *C. purpurea* 20.1 on minimal MM2 agar plates supplemented with fungin in different concentrations.
Colony diameter was determined after 7 (a), 10 (b), and 14 (c) days. The non-parametric Kruskal-Wallis ANOVA followed by multiple comparisons of mean ranks was used to compare the differences between groups. Data comparing differences between WT and individual transformants are shown (all not significant).

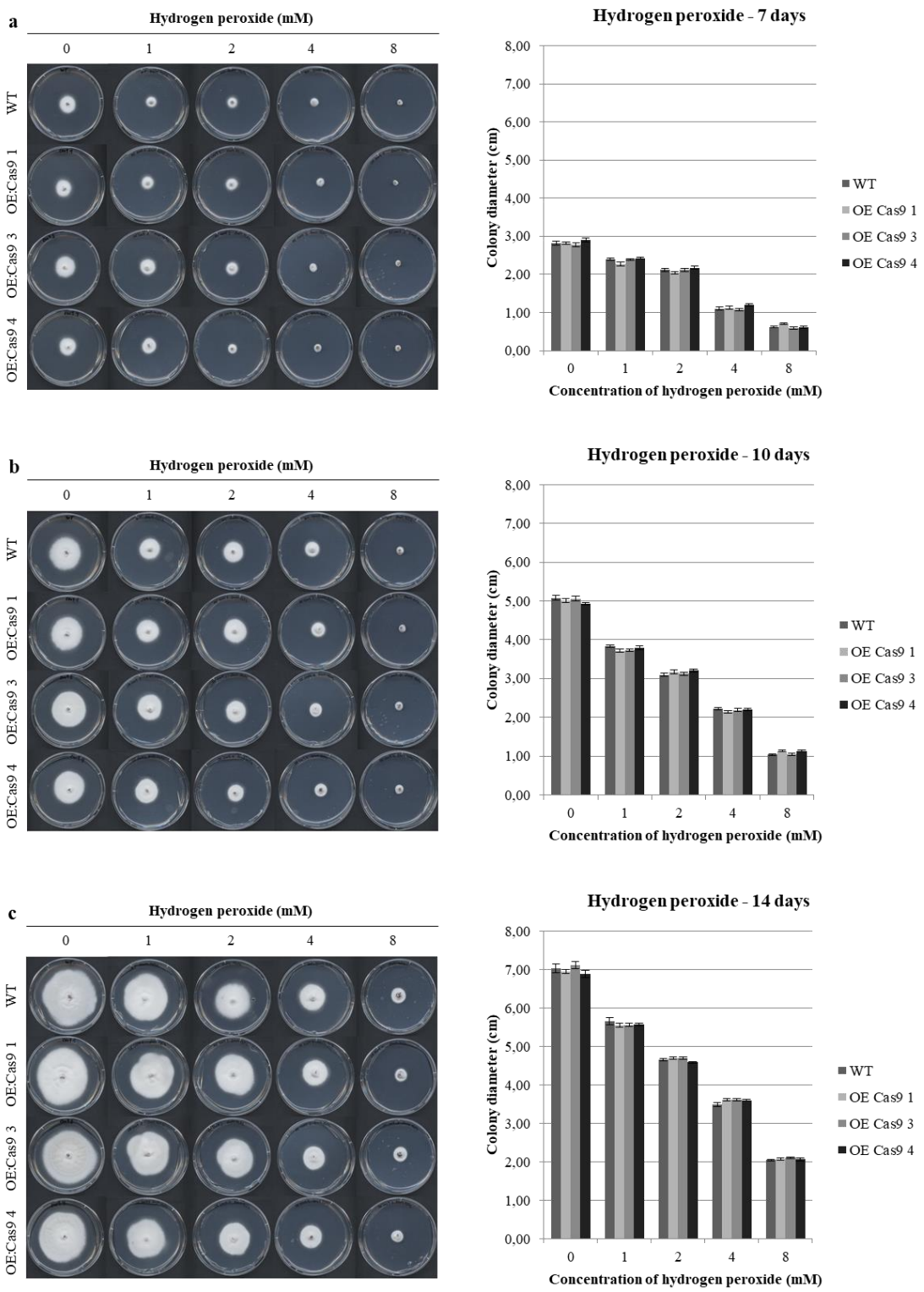

Fig. 54 Growth comparison of WT and *OE:Cas9* mutants of *C. purpurea* 20.1 on minimal MM2 agar plates supplemented with hydrogen peroxide in different concentrations.
Colony diameter was determined after 7 (a), 10 (b), and 14 (c) days. The non-parametric Kruskal-Wallis ANOVA followed by multiple comparisons of mean ranks was used to compare the differences between groups. Data comparing differences between WT and individual transformants are shown (all not significant).

4.4.2.4 Pathogenicity assays

Male sterile rye plants were inoculated with conidia of *OE:Cas9 C. purpurea* 20.1 and WT (4.2.3.5). In all cases, honeydew started to be produced approximately 7 dpi, sphacelia began to form a week later, and at the end of infection, sclerotia were formed (Fig. 55).

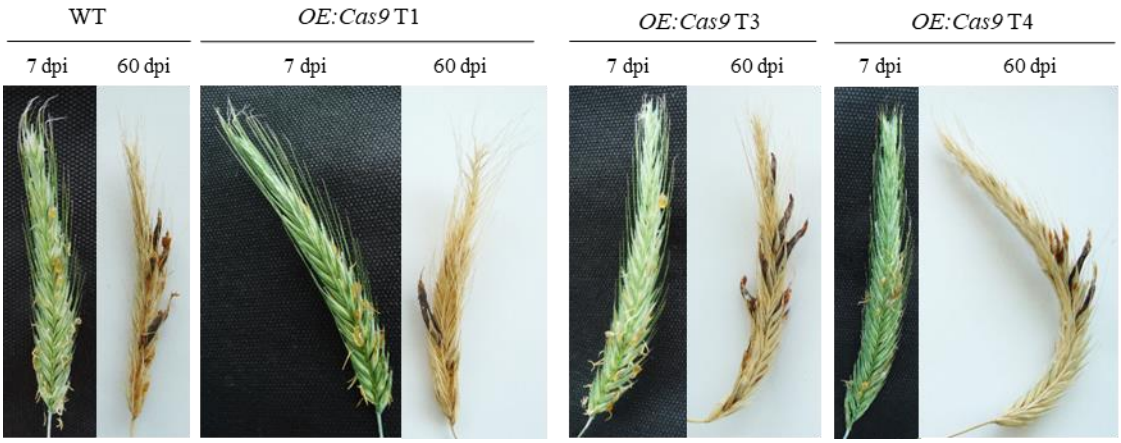

Fig. 55 Infection of male-sterile rye plants by WT and *OE:Cas9 C. purpurea* 20.1 conidia. Pictures were taken 7 dpi (production of honeydew) and 60 dpi (sclerotia).

4.4.3 Generation and characterization of *C. purpurea* 20.1 transformants with a mutation in *pyr4* prepared by CRISPR/Cas9

Firstly, to test the efficiency of CRISPR/Cas9 in *C. purpurea* 20.1, *pyr4* gene (CPUR_06934.1) encoding orotidine 5´-phosphate decarboxylase involved in pyrimidine biosynthesis was targeted. As CRISPR/Cas9 target site in *pyr4* contains the *Nco*I restriction site (Fig. 56a), *C. purpurea* 20.1 transformants were screened by PCR-RFLP analysis (4.2.4.1). In total, only three independent *pyr4* heterokaryons (marked as *CRISPR/Cas9 pyr4* T27, T31, and T255) out of 405 primary hygromycin resistant transformants were obtained after protoplasts transformation (Fig. 56b). *CRISPR/Cas9 pyr4* homokaryons were subsequently selected by single spore isolation on media containing hygromycin followed by the cultivation of fungi on minimal MM1 media with and without 10 mM uridine (4.2.4.2). In total, only one uridine auxotroph out of 283 transformants derived from T27 was obtained, likewise one out of 157 from T31, and two out of 254 from T255 were selected (Tab. 38).

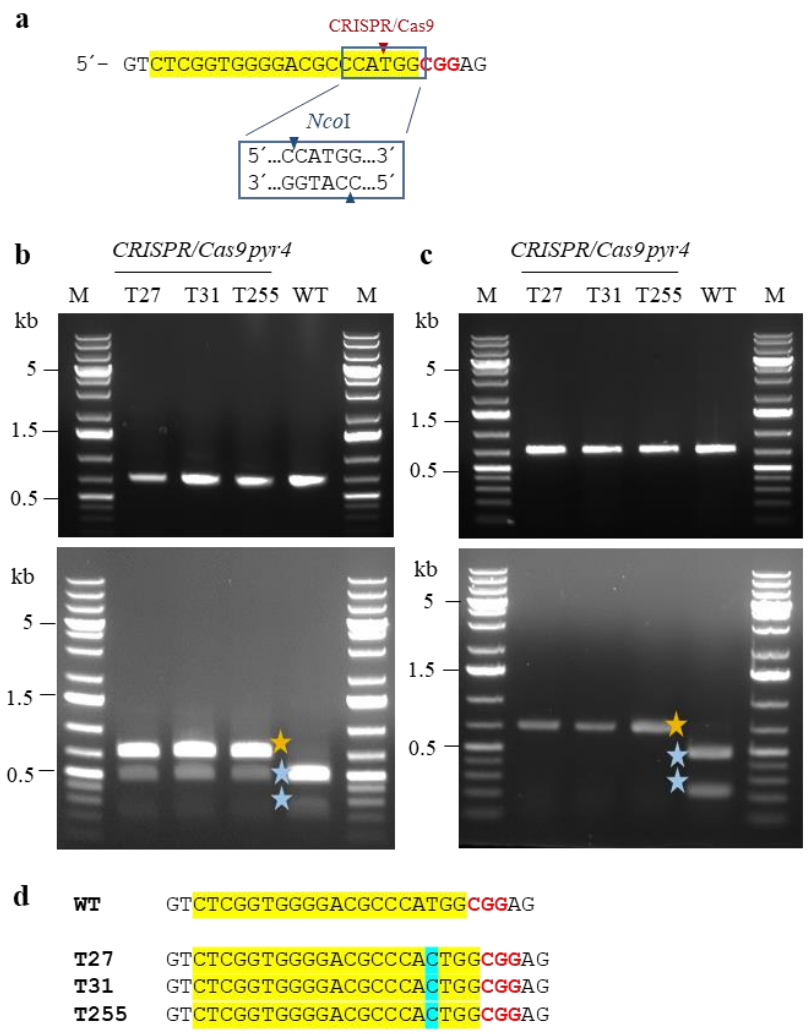

Fig. 56 Characterization of *CRISPR/Cas9 pyr4* homo- and hetero- karyons of *C. purpurea* 20.1.
(a) Design of *pyr4* protospacer including the *Nco*I restriction site needed for PCR-RFLP analysis.
(b) PCR-RFLP analysis of *CRISPR/Cas9 pyr4* heterokaryons (T27, T31, and T255): upper panel, PCR with primers PCR_pyr4_fw and PCR_pyr4_rev; lower panel, restriction of PCR product by *Nco*I (two blue asterisks (482 bp and 223 bp), amplified part of non-mutated *pyr4* cleaved by *Nco*I; orange asterisk (706 bp), amplified part of *pyr4* resistant to *Nco*I cleavage containing a mutation; M, 1 kb Plus DNA ladder.
(c) PCR-RFLP analysis of *CRISPR/Cas9 pyr4* homokaryons (T27, T31, and T255): upper panel, PCR with primers PCR_pyr4_fw and PCR_pyr4_rev; lower panel, restriction of PCR product by *Nco*I (two blue asterisks (482 bp and 223 bp), amplified part of non-mutated *pyr4* cleaved by *Nco*I; orange asterisk (706 bp), amplified part of *pyr4* resistant to *Nco*I cleavage containing a mutation. WT: wild type, M, 1 kb Plus DNA ladder.
(d) Sequencing results of the region around PAM in *CRISPR/Cas9 pyr4* homokaryons.
In (A) and (D), the PAM sequence is indicated in red bold characters, while the targeted site for Cas9 is highlighted in yellow.

Tab. 38 Efficiency of single spore isolation in the case of selection of *CRISPR/Cas9 pyr4 C. purpurea* 20.1 homokaryons.

	In total	Uridine auxotrophs	Efficiency (%)
T27	283	1	0.35
T31	157	1	0.64
T255	254	2	0.79

After single spore isolation, one *CRISPR/Cas9 pyr4* homokaryon derived from each heterokaryon was checked again by PCR-RFLP analysis (Fig. 56c); amplicons were sequenced (Fig. 56d). The same mutations, an addition of cytidine 3 bp upstream the PAM sequence, were detected in all three independent *CRISPR/Cas9 pyr4* homokaryons.

Concerning the phenotype, all three *CRISPR/Cas9 pyr4* homokaryons showed uridine auxotrophy (data not shown), however, they were drastically impaired in the growth, and unfortunately, it was impossible to cultivate or store them.

4.4.4 Generation and characterization of *C. purpurea* 20.1 transformants with a mutation in *TrpE* prepared by CRISPR/Cas9, HR, and CRISPR/Cas9-mediated HDR

4.4.4.1 Mutations in *TrpE* mutants

The second selected target for application of CRISPR/Cas9 in *C. purpurea* 20.1 was the *TrpE* (CPUR_05013.1) encoding the α-subunit of anthranilate synthase involved in Trp biosynthesis (Wang *et al*., 2016). In the case of the mutating *TrpE*, the *Bsa*AI restriction site was included in the designed CRISPR/Cas9 target sequence (Fig. 57a). After *C. purpurea* 20.1 transformation, ten independent *TrpE* heterokaryons (marked as *CRISPR/Cas9 TrpE* T6, T16, T37, T40, T93, T248, T262, T275, T290, and T321) out of 364 primary transformants resistant to hygromycin were selected by PCR-RFLP analysis (4.2.5.1) (Fig. 57b). *TrpE* homokaryons were obtained by single spore isolation on media containing hygromycin and subsequent cultivations on minimal MM2 media with and without 5 mM L-Trp (4.2.5.2) (Fig. 58, Tab. 39), and in the end, one chosen *CRISPR/Cas9 TrpE* homokaryon derived from each heterokaryon was again confirmed by PCR-RFLP analysis (Fig. 57c).

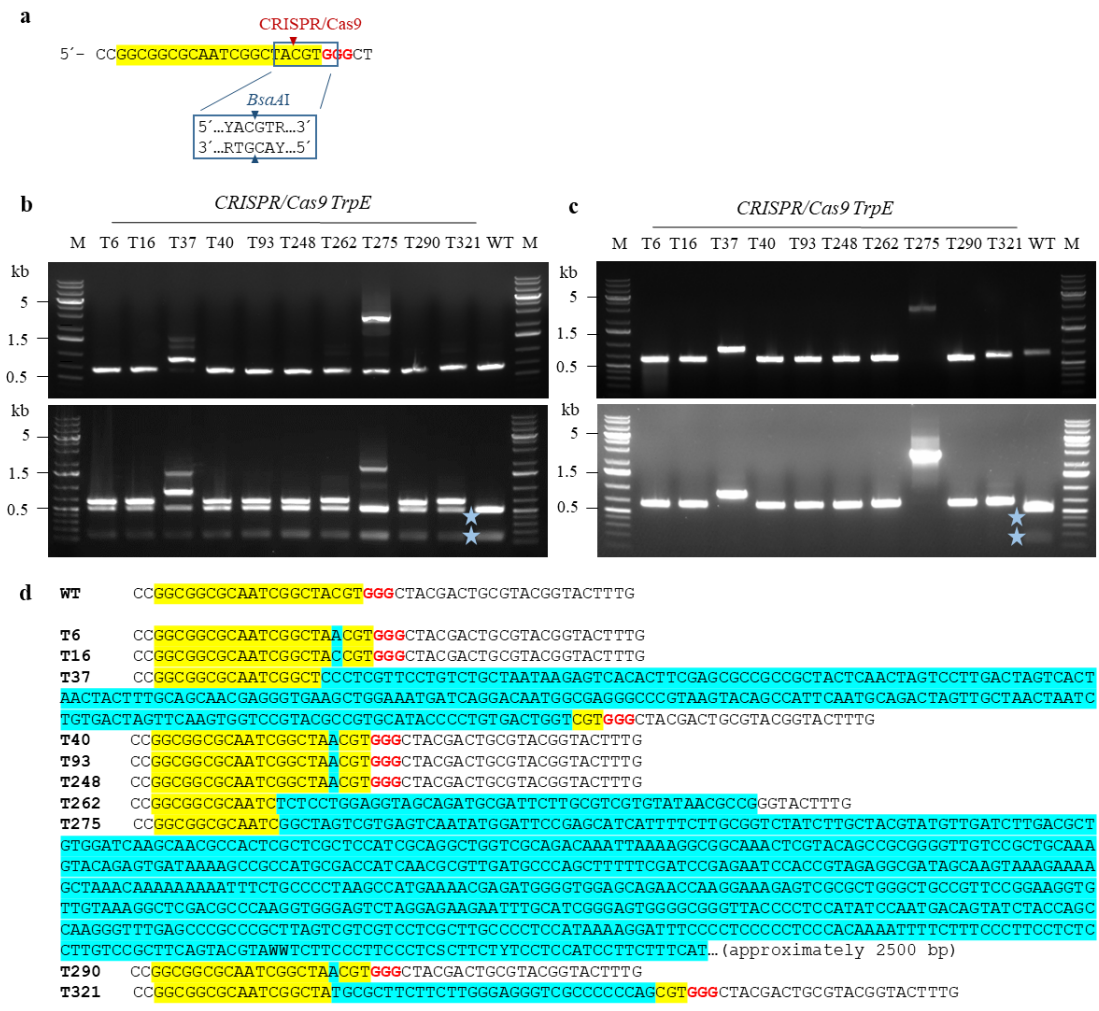

Fig. 57 Characterization of *CRISPR/Cas9 TrpE* heterokaryons of *C. purpurea* 20.1.
(a) Design of *TrpE* protospacer with *Bsa*AI restriction site needed for PCR-RFLP analysis.
(b) PCR-RFLP analysis of *CRISPR/Cas9 TrpE* heterokaryons (T6, T16, T37, T40, T93, T248, T262, T275, T290, and T321): upper panel, PCR with primers PCR_TrpE_fw and PCR_TrpE_rev; lower panel, restriction of PCR product by *Bsa*AI (blue asterisks (504 bp and 127 bp), amplified part of non-mutated *TrpE* cleaved by *Bsa*AI; bands of size ≥ 631 bp, amplified part of *TrpE* resistant to *Bsa*AI cleavage containing a mutation). WT: wild type; M, 1 kb Plus DNA ladder.
(c) PCR-RFLP analysis of *CRISPR/Cas9 TrpE* homokaryons (T6, T16, T37, T40, T93, T248, T262, T275, T290, and T321): upper panel, PCR with primers PCR_TrpE_fw and PCR_TrpE_rev; lower panel, restriction of PCR product by *Bsa*AI (blue asterisks (504 bp and 127 bp), amplified part of non-mutated *TrpE* cleaved by *Bsa*AI; bands of size ≥ 631 bp, amplified part of *TrpE* resistant to *Bsa*AI cleavage containing a mutation); M, 1 kb Plus DNA ladder.
(d) Sequencing results of the region around PAM in *CRISPR/Cas9 TrpE* homokaryons.
In (A) and (D), the PAM sequence is indicated in red bold characters, while the targeted site for Cas9 is highlighted in yellow.

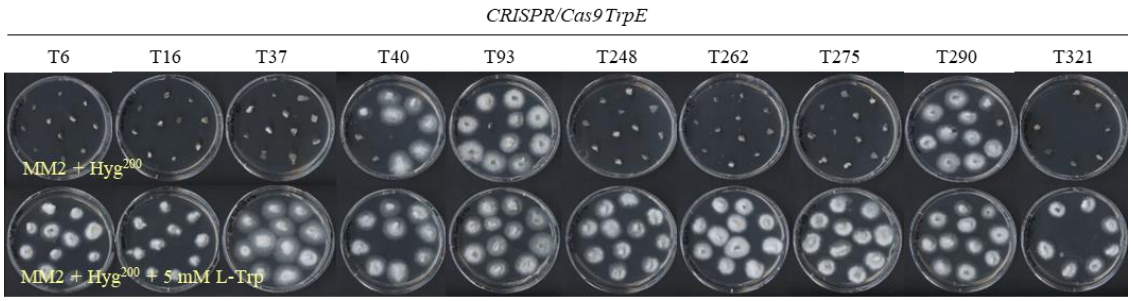

Fig. 58 Selection of CRISPR/Cas9 *TrpE C. purpurea* 20.1 homokaryons.
Heterokaryons of *C. purpurea* 20.1 with a mutation in *TrpE* gene were selected by single spore isolation on media containing L-Trp and hygromycin and then cultivated on minimal MM2 agar plates with or without L-Trp.

Tab. 39 Efficiency of single spore isolation in the case of selection of CRISPR/Cas9 *TrpE C. purpurea* 20.1 homokaryons.

	In total	Tryptophan auxotrophs	Efficiency (%)
T6	11	11	100
T16	10	10	100
T37	11	11	100
T40	9	2	22
T93	11	1	9
T248	11	11	100
T262	11	11	100
T275	11	11	100
T290	11	1	9
T321	7	7	100

As in the case of *CRISPR/Cas9 TrpE* heterokaryons, *TrpE* region around the PAM was amplified from genomic DNA isolated from homokaryons and sequenced (Fig. 57d). Whereas the same nucleotide, adenosine, was detected in five mutants (T6, T40, T93, T248, and T290), cytidine was present in T16 mutant. Apart from these mutations, insertions of 31 bp and > 2 kb occurred in mutants T321 and T275, respectively. Moreover, a combination of insertion (222 bp and 46 bp) and deletion (1 bp and 25 bp) occurred in T37 and T262 mutants, respectively.

Except for CRISPR/Cas9 directed mutagenesis of *TrpE*, the knock-out of this gene was performed also by CRISPR/Cas9-mediated HDR and by the classical knock-out approach mediated by HR. *TrpE* replacement vector used for both methods was prepared by yeast recombinational cloning (4.2.1.2).

Concerning CRISPR/Cas9-mediated HDR, four independent *TrpE* heterokaryons (marked as *Δ+CRISPR/Cas9 TrpE* T9, T50, T64, and T102) out of 116 primary transformants resistant to hygromycin and phleomycin were obtained after *C. purpurea* 20.1 transformation (4.2.2); these mutants were confirmed by diagnostic PCR (4.2.5.1).

Subsequently, *TrpE* homokaryons were selected by single spore isolation on media containing both hygromycin and phleomycin and subsequent cultivations on minimal MM2 media with and without 5 mM L-Trp (4.2.5.2) (Fig. 60, Tab. 40). Replacement of *TrpE* by phleomycin resistance cassette was again confirmed in all chosen *Δ+CRISPR/Cas9 TrpE* homokaryons by diagnostic PCR (Fig. 59b).

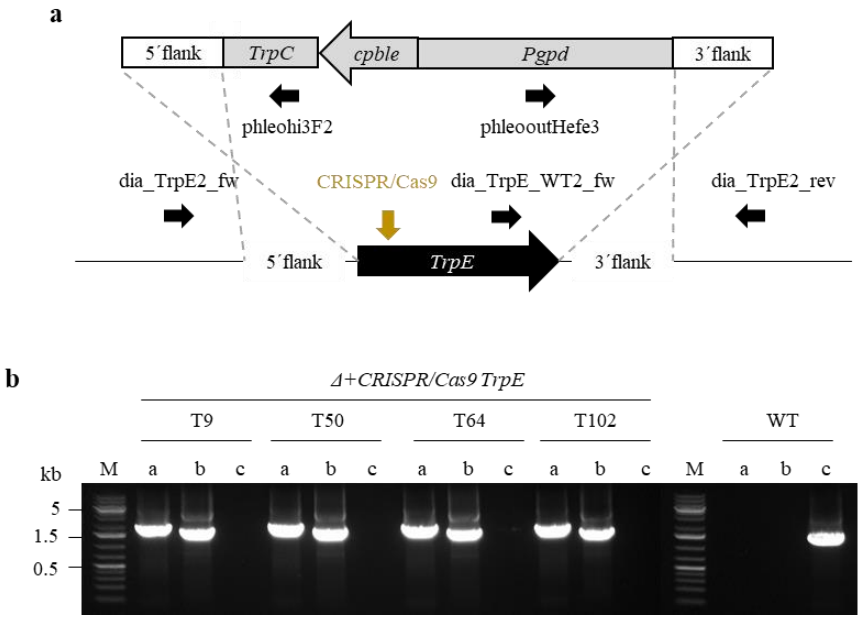

Fig. 59 Confirmation of *Δ+CRISPR/Cas9 TrpE* homokaryons of *C. purpurea* 20.1 prepared by CRISPR/Cas9-mediated HDR by diagnostic PCR.
(a) Homologous recombination of *TrpE* replacement vector. Three different sets of primers (dia_TrpE2_fw and phleohi3F2, phleooutHefe3 and dia_TrpE2_rev, dia_TrpE_WT2_fw and dia_TrpE2_rev) were used for diagnostic PCR.
(b) Integration of *TrpE* replacement vector in four independent *Δ+CRISPR/Cas9 TrpE* transformants (T9, T50, T64, and T102) confirmed by diagnostic PCR. Fragments were amplified with following primers: a, dia_TrpE2_fw and Phleohi3F2; b, PhleooutHefe3 and dia_TrpE2_rev; c, dia_TrpE_WT2_fw and dia_TrpE2_rev. WT: wild type; M: 1 kb Plus DNA ladder.

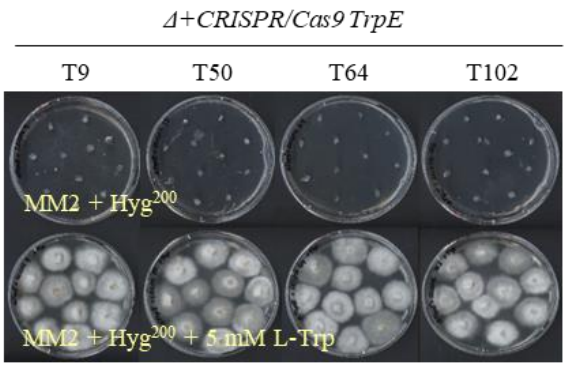

Fig. 60 Selection of *Δ+CRISPR/Cas9 TrpE C. purpurea* 20.1 homokaryons.
Heterokaryons of *Δ+CRISPR/Cas9 TrpE C. purpurea* 20.1 were selected by single spore isolation on media containing L-Trp and hygromycin and phleomycin, and then cultivated on minimal MM2 agar plates with or without L-Trp.

Tab. 40 Efficiency of single spore isolation in the case of selection of *Δ+CRISPR/Cas9 TrpE C. purpurea* 20.1 homokaryons.

	In total	Tryptophan auxotrophs	Efficiency (%)
T9	11	11	100
T50	11	11	100
T64	11	11	100
T102	11	11	100

In the case of HR-mediated gene knock-out, six independent *TrpE* heterokaryons (marked as *ΔTrpE* T42, T94, T95, T181, T200, and T326) out of 384 primary transformants resistant to phleomycin were obtained after *C. purpurea* 20.1 transformation (4.2.2); these mutants were confirmed by diagnostic PCR (4.2.5.1) (Fig. 61a).

Subsequently, *TrpE* homokaryons were selected by single spore isolation on media containing phleomycin and subsequent cultivations on minimal MM2 media with and without 5 mM L-Trp (4.2.5.2) (Fig. 62, Tab. 41). Replacement of *TrpE* by phleomycin resistance cassette was again confirmed in all chosen *ΔTrpE* homokaryons by diagnostic PCR (Fig. 61b).

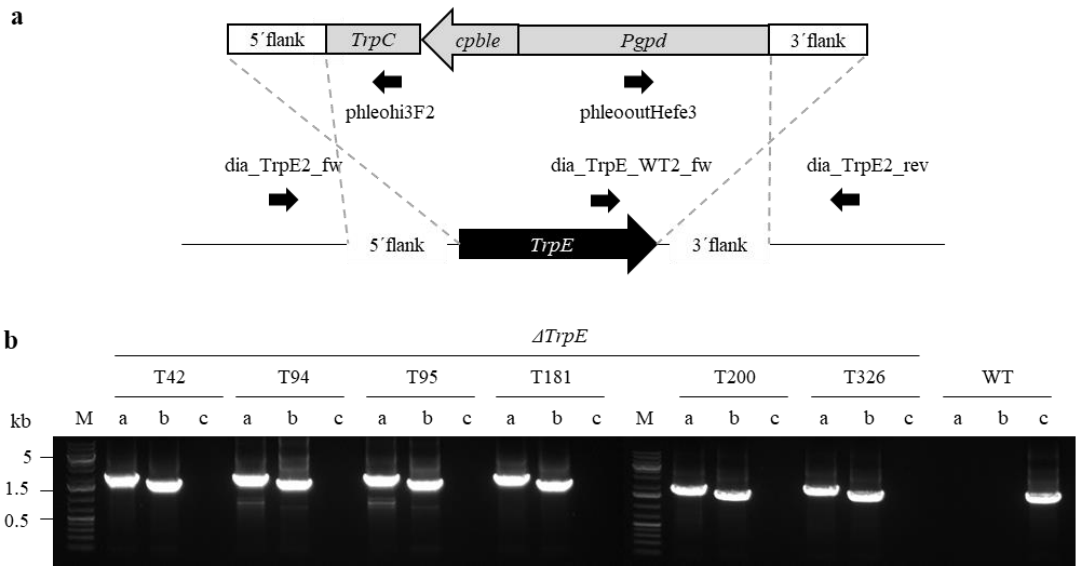

Fig. 61 Confirmation of *Δ+CRISPR/Cas9 TrpE* homokaryons of *C. purpurea* 20.1 prepared by classical gene knock-out approach based on HR by diagnostic PCR.
(a) Homologous recombination of *TrpE* replacement vector. Three different sets of primers (dia_TrpE2_fw and phleohi3F2, phleooutHefe3 and dia_TrpE2_rev, dia_TrpE_WT2_fw and dia_TrpE2_rev) were used for diagnostic PCR.
(b) Integration of *TrpE* replacement vector in six independent *ΔTrpE C. purpurea* 20.1 (T42, T94, T95, T181, T200, and T326) confirmed by diagnostic PCR. Fragments were amplified with the following primers: a, dia_TrpE2_fw and Phleohi3F2; b, PhleooutHefe3 and dia_TrpE2_rev; c, dia_TrpE_WT2_fw and dia_TrpE2_rev (M, 1 kb Plus DNA ladder).

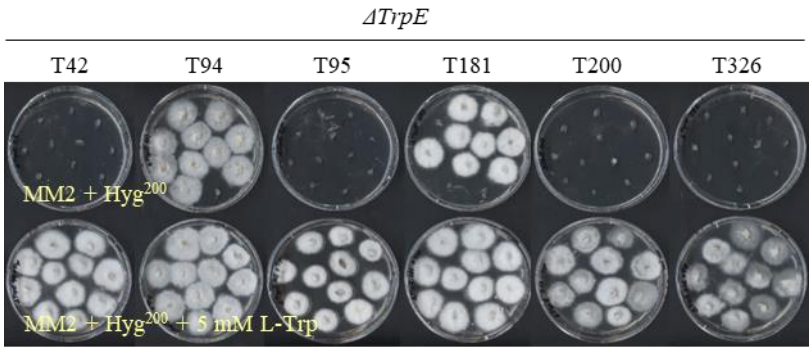

Fig. 62 Selection of *ΔTrpE C. purpurea* 20.1 homokaryons.
Heterokaryons of *ΔTrpE C. purpurea* 20.1 were selected by single spore isolation on media containing L-Trp and phleomycin and then cultivated on minimal MM2 agar plates with or without L-Trp.

Tab. 41 Efficiency of single spore isolation in the case of selection of *ΔTrpE C. purpurea* 20.1 homokaryons.

	In total	Tryptophan auxotrophs	Efficiency (%)
T42	11	11	100
T94	11	1	9
T95	11	11	100
T181	11	3	27
T200	11	11	100
T326	11	11	100

4.4.4.2 Trp auxotrophy

Concerning the phenotype, all selected *TrpE* homokaryons (*CRISPR/Cas9 TrpE*, *Δ+CRISPR/Cas9 TrpE*, and *ΔTrpE*) exhibited Trp auxotrophy (4.2.5.3) (Fig. 63).

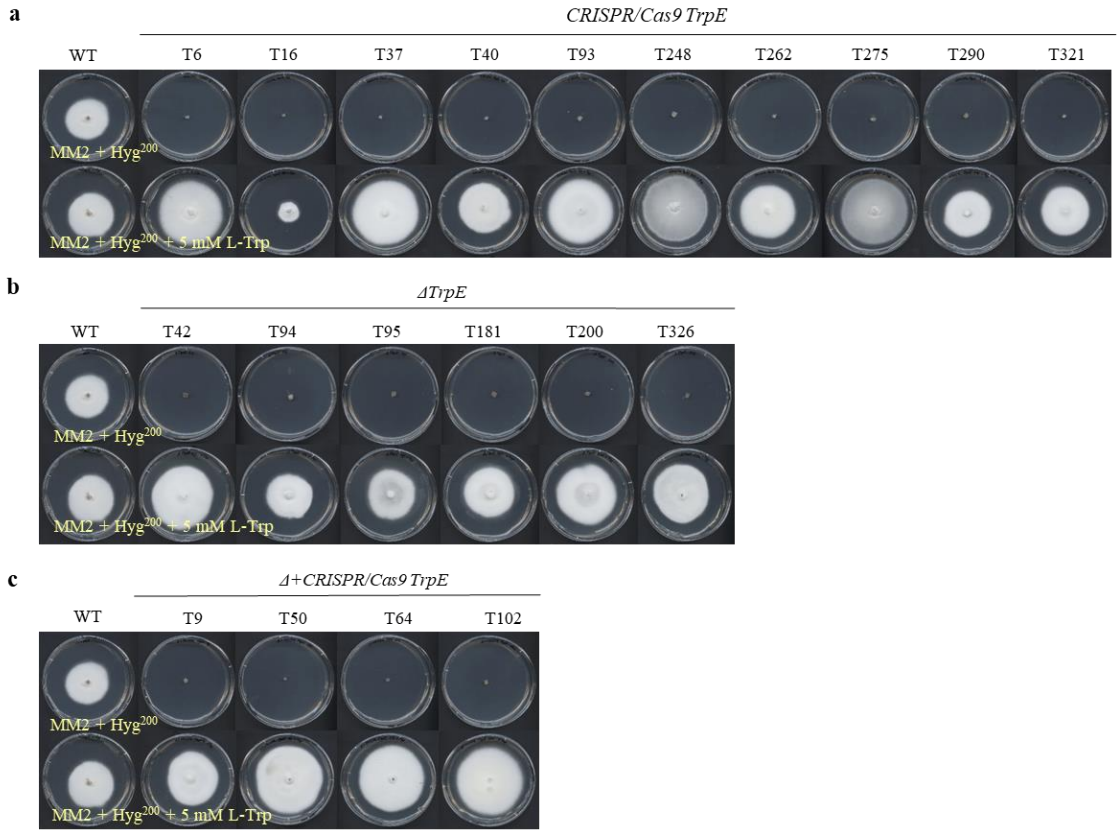

Fig. 63 Cultivation of *CRISPR/Cas9 TrpE*, *Δ+CRISPR/Cas9 TrpE*, and *ΔTrpE C. purpurea* 20.1 homokaryons together with WT on minimal MM2 agar plates with and without 5 mM L-Trp.

4.4.4.3 Pathogenicity assays

All selected *TrpE* homokaryons (*CRISPR/Cas9 TrpE*, *Δ+CRISPR/Cas9 TrpE*, and *ΔTrpE*) were used to infect male-sterile rye plants (4.2.5.4). Only in the case of WT *C. purpurea* 20.1 a production of honeydew, formation of sphacelia, and then sclerotia could be observed approximately 7, 14, and 21 dpi, respectively (Fig. 64).

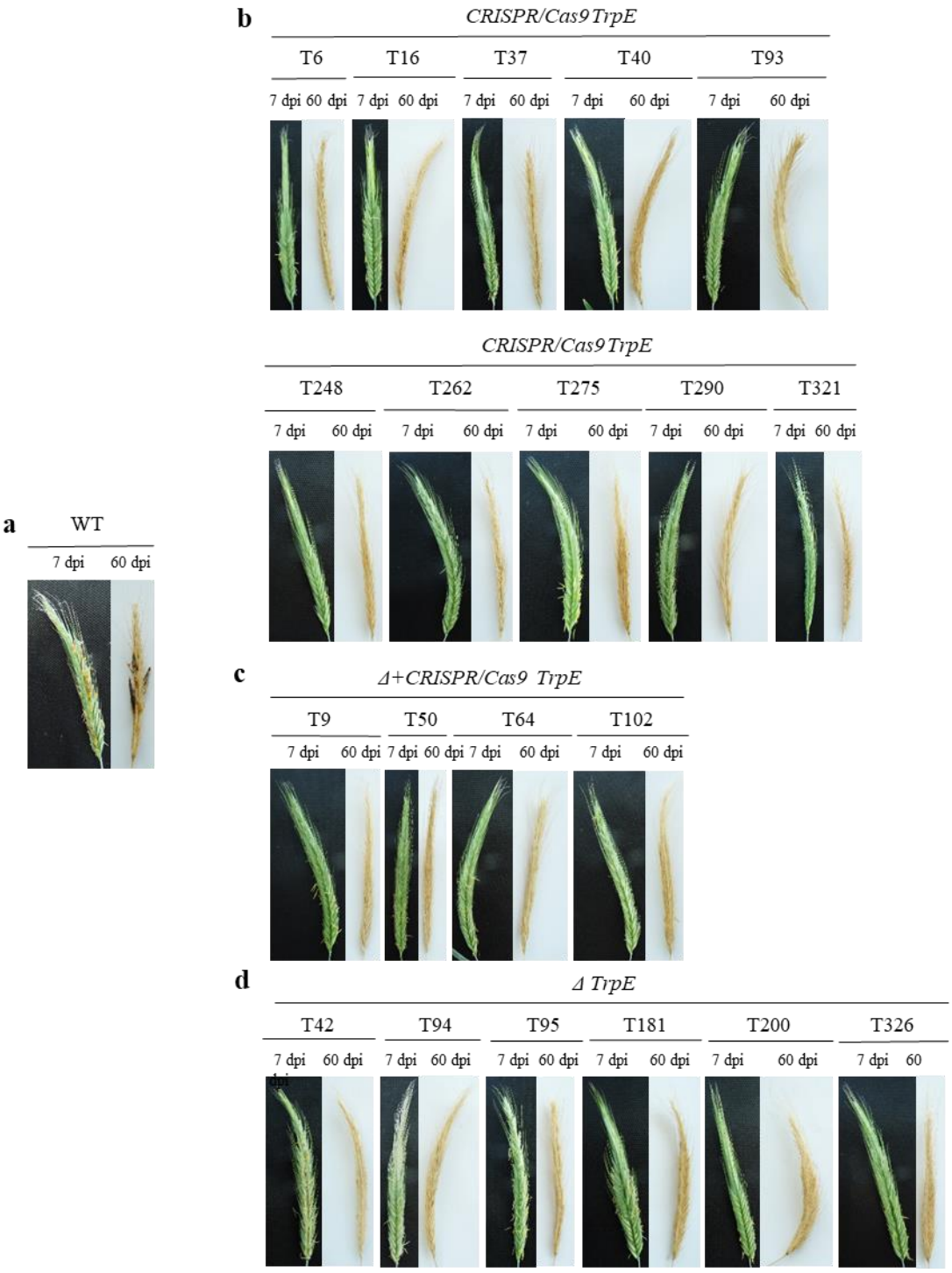

Fig. 64 Infection of rye plants with *C. purpurea* 20.1 transformants containing a mutation in *TrpE*.
(a) Rye florets inoculated with conidia of WT and *TrpE* mutants generated by CRISPR/Cas9 (*CRISPR/Cas9*
(b) Rye florets inoculated with conidia of *TrpE* mutants generated by CRISPR/Cas9 (*CRISPR/Cas9 TrpE* T6, T16, T37, T40, T93, T248, T262, T275, T290, and T321).
(c) Rye florets inoculated with conidia of *TrpE* mutants generated by CRISPR/Cas9-mediated HDR (*Δ+CRISPR/Cas9 TrpE* T9, T50, T64, and T102).
(d) Rye florets inoculated with conidia of *TrpE* mutants generated by gene knock-out based on HR (*ΔTrpE* T42, T94, T95, T181, T200, and T326).
Photos were taken after 7 dpi (production of honeydew) and 60 dpi (sclerotia).

4.4.5 Sequencing of mutations in CRISPR/Cas9 *TrpE* heterokaryons

TrpE region around the PAM sequence was amplified from the gDNA of two independent *TrpE* heterokaryons (T6 and T16), cloned into *pDRIVE* vector, and the ligation mixture was transformed into *E. coli* (4.2.6). Seven and five randomly selected *E. coli* TOP10 clones resistant to *BsaA*I restriction (Fig. 65, 66) derived from T6 and T16 heterokaryons respectively were sequenced. According to the results, two clones derived from T6 and two clones derived from T16 contained thymidine and five clones derived from T6 and three clones derived from T16 contained adenosine inserted 3 bp upstream of the PAM sequence.

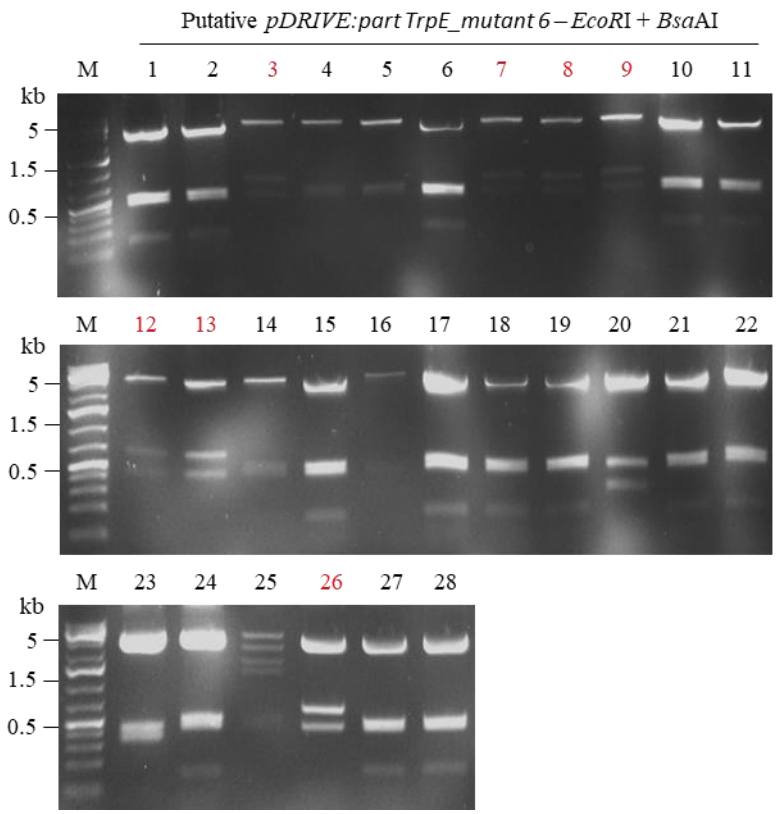

Fig. 65 Digestion of putative *pDRIVE:part_TrpE_mutant 6* plasmids with restriction endonucleases *Eco*RI and *Bsa*AI (expected bands: 3,332 kb, 631 bp, and 445 bp).
M – 1 kb Plus DNA ladder
Plasmids 3, 7, 8, 9, 12, 13, and 26 (red) were sequenced.

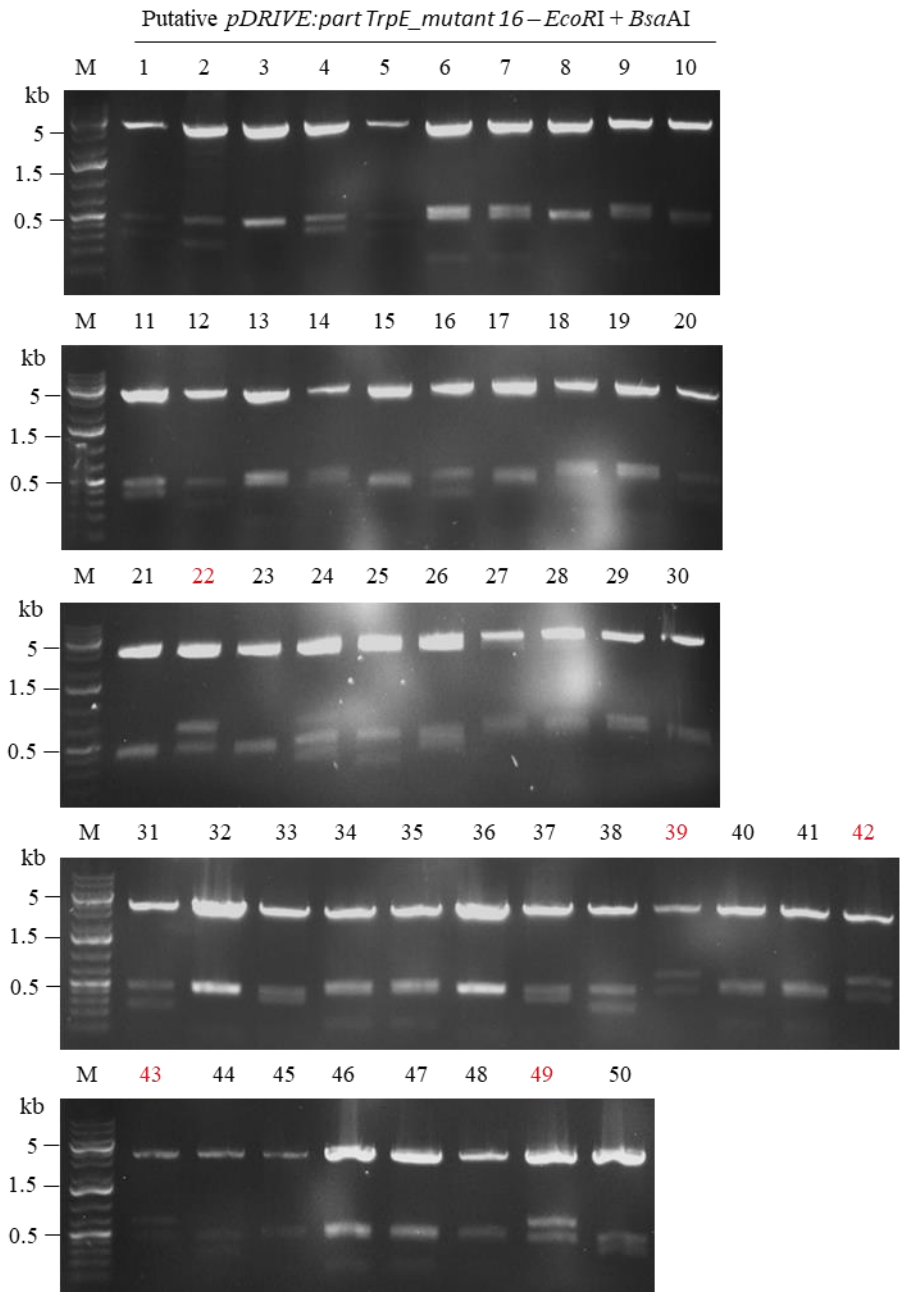

Fig. 66 Digestion of putative *pDRIVE:part_TrpE_mutant 16* plasmids with restriction endonucleases *Eco*RI and *Bsa*AI (expected bands: 3,332 kb, 631 bp, and 445 bp).
M – 1 kb Plus DNA ladder.
Plasmids 22, 39, 42, 43, and 49 (red) were sequenced.

4.4.6 Recycling of AMA-1 based plasmid

Firstly, Trp auxotrophy and resistance to hygromycin were confirmed in all selected *TrpE* homokaryons T40, T93, T248, and T321 (Fig. 67).

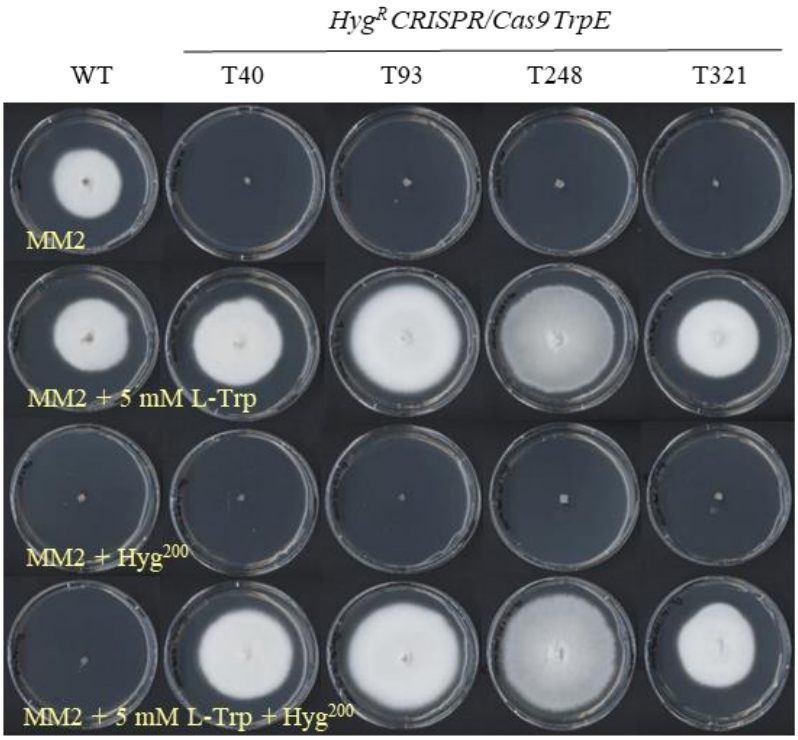

Fig. 67 Growth of four independent *CRISPR/Cas9 TrpE C. purpurea* 20.1 homokaryons resistant to hygromycin (T40, T93, T248, and T321) together with WT on minimal MM2 agar plates with different supplements as indicated.

After that, single spore isolation on media without antibiotics and subsequent cultivation on minimal MM2 media supplemented with 5 mM L-Trp and with and without hygromycin were performed (4.2.7).

C. purpurea 20.1 mutants sensitive to hygromycin appeared immediately after the first round of single spore isolation (Fig. 68, Tab. 42). To ensure that the isolates sensitive to hygromycin indeed represent *CRISPR/Cas9 TrpE C. purpurea* 20.1 homokaryons and not WT, eleven hygromycin sensitive isolates per each mutant were cultivated on four different media (Fig. 69). As expected, all isolates except two derived from T93 mutant, exhibited Trp auxotrophy and remained sensitive to hygromycin. The sensitivity to hygromycin and Trp auxotrophy of selected *CRISPR/Cas9 TrpE* homokaryons (T40, T93, T248, and T321) can be seen in Fig. 70.

Tab. 42 Efficiency of single spore isolation in the case of selection of hygromycin resistant *CRISPR/Cas9 TrpE C. purpurea* 20.1 homokaryons.

	In total	Sensitive to Hyg	Efficiency (%)
T40	50	32	64
T50	44	18	41
T64	54	11	20
T102	33	27	82

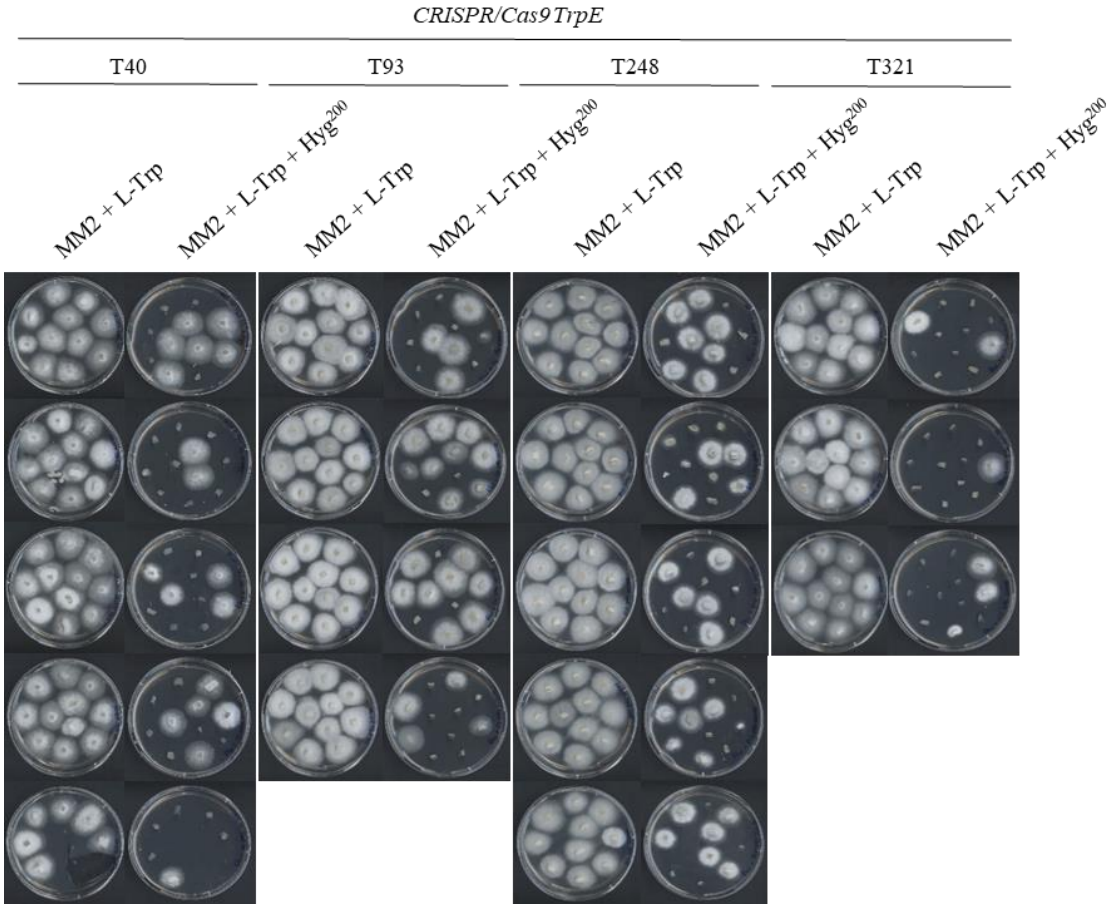

Fig. 68 Growth of *C. purpurea* 20.1 mutants obtained by single spore isolation on minimal MM2 agar plates containing L-Trp with and without hygromycin.

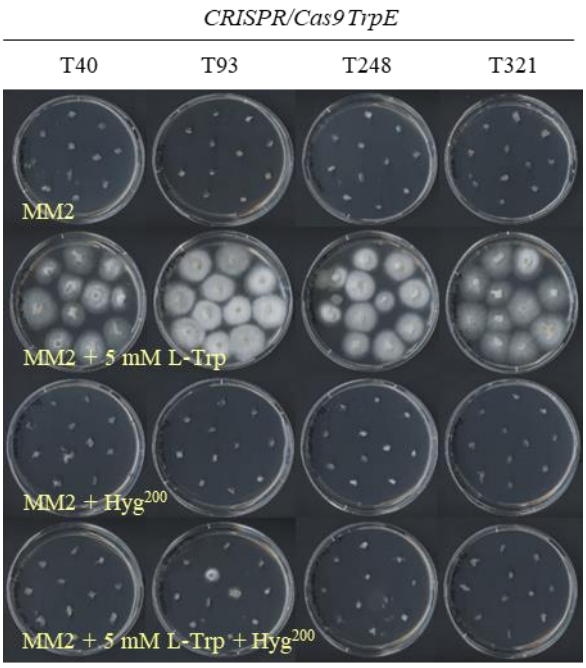

Fig. 69 Growth of fungi derived from four independent *CRISPR/Cas9 TrpE C. purpurea* 20.1 homokaryons (T40, T93, T248, and T321) obtained after single spore isolation without selection pressure on minimal MM2 agar plates with different supplements as indicated.

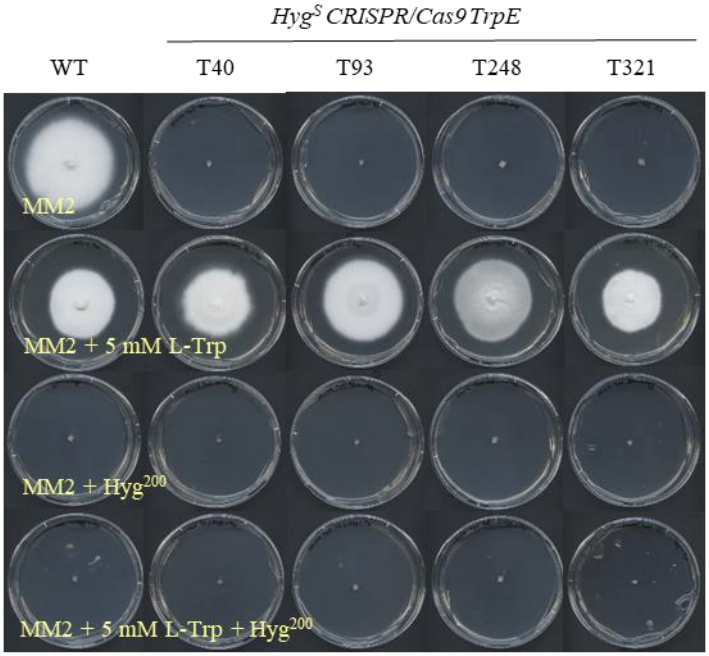

Fig. 70 Removal of AMA1-based plasmid *pFC332:TrpE* from *CRISPR/Cas9 TrpE C. purpurea* 20.1 homokaryons

Cultivation of *CRISPR/Cas9 TrpE C. purpurea* 20.1 homokaryons (T40, T93, T248, and T321) selected by single spore isolation on medium without selection pressure together with WT on minimal MM2 agar plates with different supplements as indicated.

4.5 Discussion

4.5.1 Generation and characterization of *OE:Cas9 C. purpurea* 20.1

Before developing a genome editing protocol for ergot, it was necessary to obtain *Cas9* gene overexpressing line, in which the accumulation of Cas9 enzyme did not interfere with the normal development of the fungus. To check whether the expression of *Cas9* has some effect on the phenotype of *C. purpurea* 20.1, transformants expressing *Cas9* under the strong constitutive promoter *tef1* from *Aspergillus nidulans* (Nødvig *et al*., 2015) were prepared.

The presence of the *Cas9* in these mutants was firstly verified at the DNA level by diagnostic PCR (Fig. 50); moreover, its successful transcription into RNA was confirmed by RT-PCR (Fig. 51). In general, the production of Cas9 in fungi is usually confirmed by western blot using an anti-Cas9 antibody (Liu *et al*., 2015a; Chen *et al*., 2018). Alternatively, the *Cas9* is fused to a gene that encodes a green fluorescent protein (GFP); thus, its production and even the localization can be checked by fluorescence microscopy (Liu *et al*., 2015a; Zheng *et al*., 2017). Another option represents a fusion of the *Cas9* with tags such as Myc-tag (Chen *et al*., 2017) or FLAG-tag (Katayama *et al*., 2016), thus commercially available antibodies against these tags can be used. However, as it has been reported earlier that *pFC332* vector containing *Cas9* gene has effectively worked not only in *Aspergillus* sp. (Kuivanen *et al*., 2016; Nødvig *et al*., 2015; van Leeuwe *et al*., 2019; Kadooka *et al*., 2020) but also in other filamentous fungi including *A. alternata* (Wenderoth *et al*., 2017), *T. atroroseus* (Nielsen *et al*., 2017), and *P. subrubescens* (Salazar-Cerezo *et al*., 2020), we decided to use this vector directly without any further modifications and the production of Cas9 protein was not checked.

To test stress sensitivity (Fuller *et al*., 2015), *OE:Cas9 C. purpurea* 20.1 transformants were, together with WT, cultivated on agar plates supplemented with different concentrations of Congo red, a secondary diazo dye that binds to polysaccharide fibrils in the cell wall (Vannini *et al*., 1983), hydrogen peroxide as a reactive oxygen species that induce oxidative stress damage (Ward *et al*., 1987) and fungin, an anti-fungal agent that disrupts ionic exchange through the cell membrane (Kia *et al*., 2018). As expected, no significant changes in phenotype were observed after 7, 10, and 14 days between WT and *C. purpurea* mutants (Fig. 52-54).

Moreover, generated mutants were together with WT inoculated on male-sterile rye plants. According to the results, a honeydew, sphacelia, and also sclerotia were formed during the infection process in the case of all *OE:Cas9* transformants and WT, thus confirming that the expression of *Cas9* did not interfere with fungal growth and development (Fig. 55).

4.5.2 Generation of CRISPR/Cas9 mutants in *C. purpurea* 20.1

In this work, we used *C. purpurea* strain 20.1, which genome has already been sequenced (Schardl *et al*., 2013), for CRISPR/Cas9 directed mutagenesis. While protoplasts prepared from this fungus are multinucleate and their transformation usually results in heterokaryotic mutations, its spores are uninucleate, thus homokaryons can be obtained by single spore isolation. Unfortunately, this method is laborious and time-consuming especially when the mutation does not produce an easily observable phenotype or mutants cannot be selected based on their resistance to fungicide or other specific compounds.

Because we decided to mutate *pyr4* and *TrpE* genes encoding orotidine 5′-phosphate decarboxylase involved in pyrimidine biosynthesis and α-subunit of anthranilate synthase involved in Trp biosynthesis, respectively, a robust screening method to reveal CRISPR/Cas9 mutations in *C. purpurea* had to be developed. For this reason, PCR-RFLP analysis based on the amplification of DNA fragment around the PAM sequence and its subsequent restriction was used. This method has already been performed in plants (Liu *et al*., 2015b; Osakabe *et al*., 2016; Ueta *et al*., 2017), oomycete *Phytophtora sojae* (Fang and Tyler, 2016), and phytopathogenic fungus *Leptosphaeria maculans* (Idnurm *et al*., 2017). Compared to other advanced methods such as sequencing-based techniques (e.g. amplicon next- sequencing, NGS (Bell *et al*., 2014); tracking indels by decomposition, TIDE (Etard *et al*., 2017); indel detection by amplification analysis, IDEAA (Lonowski *et al*., 2017)) or denaturation-based methods (e.g. high-resolution melting, HRM (Samarut *et al*., 2016); single-stranded conformational polymorphism, SSCP (Zheng *et al*., 2016); mismatch-sensitive endonucleases T7/Surveyor (Huang *et al*., 2012), PCR-RFLP analysis is inexpensive and does not require special equipment, cloning step prior to sequencing or additional denaturation/renaturation steps. On the other hand, it is quite laborious when hundreds of mutants have to be screened, and most importantly, it requires a suitable restriction site within the target sequence.

4.5.2.1 Targeting *pyr4* gene

First, to test the efficiency of CRISPR/Cas9 in *C. purpurea* 20.1, *pyr4* gene (CPUR_06934.1) encoding orotidine 5´-phosphate decarboxylase (EC 4.1.1.23) involved in pyrimidine biosynthesis was targeted. This enzyme catalyzing the decarboxylation of orotidine monophosphate (OMP) to uridine monophosphate (UMP) (Silverman and Groziak, 1982) has already been mutated in many different filamentous fungi including *Aspergillus* sp. (van Hartingsveldt *et al*., 1987; de Ruiter-Jacobs *et al*., 1989; Weidner *et al*., 1998), *Penicillium chrysogenum* (Díez *et al*., 1987) and *Trichoderma reesei* (Smith *et al*., 1991). Moreover, this gene has already been mutated in *C. purpurea* strain T5 and as expected, obtained *pyr4* mutants showed uridine auxotrophy and were resistant to 5-FOA (Smit and Tudzynski, 1992), however, since 1992 they have never been used for further experiments.

As CRISPR/Cas9 *pyr4* target site contains the *Nco*I restriction site (Fig. 56a) *CRISPR/Cas9 pyr4* heterokaryons were selected by PCR-RFLP analysis (Fig. 56b). In this case, very low (< 1 %) transformation efficiency was observed. Together three independent *CRISPR/Cas9 pyr4* homokaryons were obtained by single spore isolation and confirmed by PCR-RFLP analysis (Fig. 56c). Surprisingly, also, in the case of single spore isolation, very low efficiency (< 1 %) was observed (Tab. 38). On the other hand, a similar result has been shown for *Fusarium graminearum* where RNAseq analysis of *FgOs1* transformant containing Cas9 and sgRNA that was not exposed to fludioxonil has revealed the efficiency of homokaryon isolation in the range of 1-10 % (Gardiner and Kazan, 2018).

Concerning the data from Sanger DNA sequencing, the same mutations, an addition of cytidine 3 bp upstream the PAM sequence, were detected in all three independent *CRISPR/Cas9 pyr4* homokaryons (Fig. 56d). The position of this mutation correlates with other CRISPR/Cas9 mutations reported in the literature as Cas9 induces mutations mostly 3-4 bp upstream of PAM sequence (Fuller *et al*., 2015; Katayama *et al*., 2016; Nødvig *et al*., 2015). Moreover, the same mutation, 1 bp deletion, has also been detected for example in two independent transformants of *Rhizopus delemar* (Bruni *et al*., 2019).

As expected, the insertion of one nucleotide led to a frameshift and resulted in uridine auxotrophy of the mutants. Nevertheless, the *CRISPR/Cas9 pyr4* homokaryons were drastically impaired in their growth compared to *pyr4* heterokaryons and WT; their

mycelium was transparent, and unfortunately, it was impossible to cultivate or store them. This was surprising as *C. purpurea* uridine auxotrophs lacking OMPD activity have been already prepared previously (Smit and Tudzynski, 1992). However, in this case, a different fungal strain, T5, was used for transformation and although this mutation was complemented by OMPD genes of *C. purpurea*, *A. niger*, and *N. crassa*, the mutated sequence in *pyr4* gene has never been characterized (Smit and Tudzynski, 1992).

4.5.2.2 Targeting *TrpE* gene

The second selected target for application of CRISPR/Cas9 in *C. purpurea* 20.1 was the *TrpE* gene (CPUR_05013.1) that encodes the putative α-subunit of anthranilate synthase (EC: 4.1.3.27) involved in Trp biosynthesis (Wang *et al*., 2016). In filamentous fungi, the Trp biosynthesis is ensured by four genes (*TrpB, TrpC, TrpD,* and *TrpE*), encoding three different enzymatic components that catalyze the five sequential reactions leading to the final product (Hütter and DeMoss, 1967). Fungal anthranilate synthase catalyzing the conversion of chorismic acid to anthranilic acid consists of two subunits: the α-subunit encoded by *TrpE* gene and the β-subunit, a trifunctional peptide that contains also phosphoribosylanthranilate isomerase and indole-3-glycerol-phosphate synthase, all encoded by *TrpC* gene (Hütter *et al*., 1986). Compared to the β-subunit, the α-subunit contains a chorismate binding site and Trp-feedback inhibition domain, thus it can synthesize anthranilic acid independently in the presence of high levels of ammonia (Crawford and Eberly, 1986). Moreover, *TrpE* knock-out mutants of *Aspergillus fumigatus* exhibited Trp auxotrophy (Wang *et al*., 2016).

As the *Bsa*AI restriction site was included in the designed CRISPR/Cas9 target sequence (Fig. 57a) transformants were screened by PCR-RFLP analysis (Fig. 57b). Together, ten independent *CRISPR/Cas9 TrpE* heterokaryons were prepared, thus provide the transformation efficiency of 2.75 %. After, the *CRISPR/Cas9 TrpE* homokaryons were obtained (Fig. 58, Tab. 39) and verified again by PCR-RFLP analysis (Fig. 57c); moreover, mutations in *TrpE* gene were sequenced (Fig. 57d).

Correspondingly to *CRISPR/Cas9 pyr4* mutants described above, mutations were located mostly 3 bp upstream of the PAM sequence. Interestingly, except for 1 bp insertion, insertion of larger DNA fragments and their combination with deletion occurred. Concerning the phenotype, all ten *CRISPR/Cas9 TrpE* homokaryons showed Trp auxotrophy (Fig. 63a).

Although the CRISPR/Cas9 transformation efficiencies were quite low in the case of targeting both genes, *pyr4* and *TrpE*, obtained *CRISPR/Cas9* homokaryons showed expected phenotypes, uridine, and tryptophan auxotrophy, respectively. Although CRISPR/Cas9 system based on the same principle thus containing sgRNA flanked by two ribozymes has provided quite high transformation efficiencies in *Aspergilllus* sp. (Nødvig *et al*., 2015) and in *A. alternata* (Wenderoth *et al*., 2017), any transformants have been selected in fungus *Cordyceps militaris* (Chen *et al*., 2018). Although the expression of sgRNA cassette was confirmed in this fungus by qPCR and the production of Cas9 was successfully detected by western blot analysis and its localization was confirmed by fluorescence microscopy as it was fused with GFP, most probably sgRNA cassette did not generate functional sgRNA. Concerning CRISPR/Cas9 in *C. purpurea*, we did not check the expression of sgRNA and its production as we successfully obtained CRISPR/Cas9 mutants. However, to increase the transformation efficiency in this ergot fungus *in vitro* synthesized sgRNA (Kuivanen *et al*., 2016; Kuivanen *et al*., 2017; Chen *et al*., 2018) could be used in the future instead of the self-processing system or higher amount of CRISPR/Cas9 plasmid could be utilized for protoplasts transformation. Alternatively, exposure time to Cas9 could be prolonged as it has already been demonstrated in *Aspergillus* sp. (Nødvig *et al*., 2015), *A. alternata* (Wenderoth *et al*., 2017), and also in *U. maydis* (Schuster *et al*., 2018) that CRISPR/Cas9 transformation efficiency can be increased by prolonging culturing of fungi on media under selection pressure.

Interestingly, it has been demonstrated that different mutations can occur in CRISPR/Cas9 heterokaryons when Cas9 is constitutively expressed (Gardiner and Kazan, 2018). To test if different mutations occurred also in *C. purpurea* heterokaryons, *TrpE* region around the PAM sequence was amplified from the genomic DNA of two independent *CRISPR/Cas9 TrpE* heterokaryons, cloned into *pDRIVE* vector and sequenced (Fig. 65, 66). Surprisingly, sequencing data confirmed this hypothesis; two different mutations have been detected in *E. coli* clones derived from both *CRISPR/Cas9 TrpE* heterokaryons. Moreover, while selected *TrpE* homokaryon T16 used for PCR-RFLP analysis and further experiments contained cytidine inserted 3 bp upstream of the PAM, only thymidine and adenosine were detected in all five randomly selected *E. coli* clones derived from T16 heterokaryon. Most probably, too few *E. coli* clones were sequenced to reveal all CRISPR/Cas9 mutations that occurred in this heterokaryon.

4.5.3 Knock-out of *TrpE* in *C. purpurea* 20.1 generated by HR and CRISPR/Cas9-mediated HDR

In general, it has been shown that the HIF can be increased in yeasts and filamentous fungi when a double-strand break is introduced into the target gene (Arras *et al*., 2016; Pohl *et al*., 2016). Thus, CRISPR/Cas9-mediated HDR has already been developed and used for gene targeting in filamentous fungi (Kuivanen *et al*., 2016; Pohl *et al*., 2016; Liu *et al*., 2017; Zheng *et al*., 2017). In this method, components for CRISPR/Cas9 are co-transformed into fungal protoplasts together with HR repair template containing a selection marker, thus any gene regardless of its function can be targeted and the mutation can be easily confirmed by diagnostic PCR. In this case, HIF also depends on the size of flanking regions. For example, the highest HIF has occurred in *P. sojae* when donor DNA containing 1 kb flanking regions were used for transformation (Fang and Tyler, 2016); on the other hand, flanking regions with a size of 30-60 bp have yielded quite a lot of positive transformants in *Aspergillus* sp. (Nødvig *et al*., 2015) and *P. chrysogenum* (Pohl *et al*., 2016). Although donor DNA is usually introduced in double-stranded form as a circular or linearized plasmid, single-stranded DNA oligonucleotides have also been successfully used (Nødvig *et al*., 2018).

To show that *CRISPR/Cas9 TrpE* homokaryons behave in the same way as transformants obtained by the gene-knock-out approach when the target gene is completely replaced by a resistance cassette, *TrpE* gene was deleted in *C. purpurea* 20.1 also by CRISPR/Cas9-mediated HDR and by classical approach mediated by HR.

Concerning CRISPR/Cas9-mediated HDR and HR-mediated gene knock-out, four independent *Δ+CRISPR/Cas9 TrpE* heterokaryons (transformation efficiency 3.45 %) and six independent *ΔTrpE* heterokaryons (transformation efficiency 1.45 %), respectively were selected after *C. purpurea* 20.1 protoplasts transformation. All *TrpE* homokaryons were selected by single spore isolation (Fig. 60, 62, Tab. 40, 41) and verified by diagnostic PCR (Fig. 59, 61). As *CRISPR/Cas9 TrpE* homokaryons, all these mutants exhibited Trp auxotrophy (Fig. 63b, c).

As expected, HR-mediated gene knock-out provided the lowest transformation efficiency, but the efficiency well correlates with 1-2 % reported earlier (Oeser *et al*., 2002). On the other hand, the transformation efficiency of CRISPR/Cas9-mediated HDR was the highest but still very low. This was not so surprising as the efficiency of HDR-based editing relies not only on the design of Cas9 and sgRNA but also on the

length of the homology arms and efficiencies of the NHEJ and HR pathways in selected organisms.

4.5.4 Infections of rye plants with *C. purpurea* 20.1 *TrpE* mutants

Finally, all prepared *TrpE* mutants were inoculated on male-sterile rye plants (Fig. 64). Surprisingly, only in the case of WT *C. purpurea* 20.1 a production of honeydew, formation of sphacelia, and then sclerotia could be observed approximately 7, 14, and 21 dpi, respectively. As all these mutants behave phenotypically the same as WT except for Trp auxotrophy, it can be concluded that the virulence phenotype was caused by the mutation in *TrpE* gene. Most probably, Trp auxotrophs were non-infectious because of decreased levels of auxins, plant hormones previously detected in *C. purpurea* 20.1 (Hinsch *et al*., 2015) that are predominantly synthesized in fungi from L-Trp. Besides, it is well documented that these compounds are involved in plant-pathogen interactions (Yamada, 1993).

4.5.5 Recycling of AMA1-based plasmid

In this work, either *pFC332*:*pyr4* or *pFC332*:*TrpE* containing autonomously replicating sequence AMA1, was introduced into *C. purpurea* 20.1 solely for performing CRISPR/Cas9 directed mutagenesis, so it would be useful to remove them from the mutant strains. Although this type of vector was not used for *C. purpurea* transformation before, in other fungi it can be lost by repeated culturing on a non-selective medium (Nødvig *et al*., 2015; Weyda *et al*., 2017). Therefore, we decided to cultivate four randomly selected independent *CRISPR/Cas9 TrpE* homokaryons of *C. purpurea* 20.1 on media without hygromycin.

After, Trp auxotrophy and resistance to hygromycin were confirmed in four selected *TrpE* homokaryons (Fig. 67), single spore isolation on media without antibiotic, and subsequent cultivation on minimal media supplemented with L-Trp and with and without hygromycin were performed (Fig. 68, Tab. 42). Surprisingly, compared to published work on *Aspergillus carbonarius* where hygromycin-sensitive transformants were obtained after three rounds of single spore isolation (Weyda *et al*., 2017), *C. purpurea* mutants sensitive to hygromycin appeared immediately after the first round with efficiency ranging from 20 to 82 %. The sensitivity to hygromycin and Trp auxotrophy of selected *CRISPR/Cas9 TrpE* homokaryons was also confirmed (Fig. 69).

By the cultivation process described above, we demonstrated that the autonomously replicating vector *pFC332:TrpE* used to perform CRISPR/Cas9 directed mutagenesis can be fully removed from *C. purpurea* 20.1 genome (Fig. 70). This brings forward an opportunity to design a mutation strategy for virtually any gene without changing the selection marker. According to our knowledge, so far only hygromycin and phleomycin resistance cassettes have been used for *C. purpurea* 20.1 transformant selection (Hinsch *et al*., 2015; Kind *et al*., 2018), thus by using this approach *C. purpurea* transformant containing mutations in three or even more genes could be prepared by CRISPR/Cas9 with AMA1-based plasmid.

5 Genetic transformation of fungi from the genus *Fusarium*

5.1 Introduction

Fusarium graminearum (teleomorph *Gibberella zeae*), previously also known as *F. graminearum* group 2 is a homothallic pathogenic fungus that infects mostly wheat and barley with Fusarium head blight (FHB) disease and maize with Fusarium stalk or ear rot disease. *Fusarium pseudograminearum* (teleomorph *Gibberella coronicola*) previously also known as *F. graminearum* group 1 is a haploid heterothallic pathogenic fungus that also causes Fusarium head blight of crops; moreover, it infects wheat and barley with a disease known as crown rot. In contrast to *F. graminearum* and *F. pseudograminearum*, fungi from *Fusarium oxysporum* species complex (FOSC) colonize more than 120 plant species including cotton, banana, and tomato and cause vascular wilts, crown rot, foot rot and root rot; moreover, human pathogenic and non-pathogenic strains were identified in this complex. For example, *F. oxysporum* f. sp. *medicaginis* infects *Medicago* plants.

In this part of work, we decided to transform *F. graminearum*, *F. pseudograminearum*, and *F. oxysporum* f. sp. *medicaginis* with green and red reporter genes. In the future, *F. graminearum* and *F. pseudograminearum* mutants will be inoculated on WT barley plants (*Hordeum vulgare*) and plants with inactivated or downregulated mitogen-activated proteinkinases HvMPK3 or HvMPK6 prepared by CRISPR/Cas9 or RNAi, respectively.*F. oxysporum* f. sp. *medicaginis* mutants will be inoculated on WT alfalfa plants (*Medicago sativa*) and plants with downregulated or upregulated mitogen-activated proteinkinases SIMKK or GFP-SIMK prepared by RNAi or overexpression, respectively. Plant-fungus interactions will be monitored using novel microscopic techniques.

5.2 Material

5.2.1 Buffers and solutions

Transformation of *F. graminearum* and *F. pseudograminearum*

50% PEG 4000

- 20.9 ml 60% PEG 4000, 0.25 ml 1 M Tris, 1.25 ml 1 M calcium chloride, 2.7 ml sterile distilled water

1x STC

- 24 ml 2 M sorbitol, 0.4 ml 1M Tris, 2 ml 1 M calcium chloride, 13.6 ml distilled water

2x STC

- 10 ml 3 M sorbitol, 0.25 ml 1M Tris, 1.25 ml 1 M calcium chloride, 1 ml distilled water

1M Tris

- 121.1 g Tris, made up to 1 l with distilled water, pH adjusted to 7.5 with hydrochloric acid, autoclaved for 20 min at 120 °C

1 M calcium chloride

- 1.47 g calcium chloride in 10 ml distilled water, sterilized through 0.45 µm filter

2 M sorbitol

- 364.34 g sorbitol, made up to 1 l with distilled water, autoclaved for 20 min at 120 °C

3 M sorbitol

- 546.51 g sorbitol, made up to 1 l with distilled water, autoclaved for 20 min at 120 °C

Complete agar

- 10 g glucose, 2 g meat peptone, 1 g casamino acids, 1 g yeast extract, 50 ml salt solution, 1 ml vitamins, 2 ml trace elements, made up to 1 l with distilled water, 15 g agar, autoclaved for 20 min at 120 °C

Enzyme solution

- 250 mg driselase from Basidiomycetes sp., 1 mg chitinase *from Streptomyces griseus*, 100 mg lyzing enzyme from *Trichoderma harzianum* resuspended in 20 ml of 1.2 M potassium chloride, sterilized through 0.45 µm filter

KCl buffer

- 89.46 g potassium chloride, made up to 1 l with distilled water, autoclaved for 20 min at 120 °C

Mung bean soup

- 8 g mung beans were boiled in 500 ml distilled water for 20 min, the solution was filtered through Miracloth membrane and the volume was adjusted to 800 ml with distilled water, autoclaved for 20 min at 120 °C

Regeneration agar

- 239.9 g sucrose, 0.5 g yeast extract, made up to 1 l with distilled water, 20 g agar, autoclaved for 20 min at 120 °C

Salt solution

- 10.4 g potassium chloride, 10.4 g magnesium sulphate heptahydrate, 30.4 g potassium dihydrogen phosphate, made up to 1 l with distilled water autoclaved for 20 min at 120 °C

Trace elements

- 1 g ferrous sulphate heptahydrate, 0.15 g cupric sulphate pentahydrate, 1.61 g zinc sulphate heptahydrate, 0.1 g manganese sulphate hydrate, 0.1 g ammonium molybdate tetrahydrate, made up to 1 l with sterile distilled water

Vitamins

- 25 mg biotin, 2.5 g nicotinic acid, 0.8 PABA, 1 g pyridoxine hydrochloride, made up to 50 ml with sterile distilled water

YPD medium

- 3 g yeast extract, 10 g meat peptone, 20 g glucose, made up to 1 l with distilled water, autoclaved for 20 min at 120 °C

Transformation of *F. oxysporum* f. sp. *medicaginis*

Darken medium

- 15 g corn steep solids, 30 g sucrose, 1 g ammonium sulphate, 7 g calcium carbonate, made up to 1 l with distilled water, autoclaved for 20 min at 120 °C

Enzyme solution

- 200 mg lysing enzyme from *Trichoderma harzianum*, 150 mg driselase from Basidiomycetes sp., 10 mg BSA, 10 mg yatalase, 50 ml $KCl/CaCl_2$ buffer, sterilized through 0.45 µm filter

ICI medium

- 10 g fructose, 0.5 g potassium dihydrogen phosphate, 1 g magnesium sulphate heptahydrate, 2 ml trace elements, 1 g ammonium sulphate, made up to 1 l with distilled water, autoclaved for 20 min at 120 °C

$KCl/CaCl_2$ buffer

- 35.97 g potassium chloride, 2.94 g calcium chloride, made up to 400 ml with distilled water, autoclaved for 20 min at 120 °C

Single spore isolation

V8 agar

- 2 g calcium carbonate, 200 ml V8 juice, 800 ml distilled water, 15 g agar, autoclaved for 20 min at 120 °C

5.2.2 Organisms

- *Fusarium graminearium* cultivated at 20 °C or 26 °C in the dark.
- *Fusarium pseudograminearum* cultivated at 20 °C or 26 °C in the dark.
- *Fusarium oxyysporum* f. sp. *medicaginis* cultivated at 30 °C or 26 °C in the dark.

5.2.3 Plasmids

- *pNDN-OGG* (Schumacher, 2012)
- *pNDN-ODT* (Schumacher, 2012)
- *pNDH-OCT* (Schumacher, 2012)

5.3 Methods

5.3.1 Transformation of *F. graminearum* and *F. pseudograminearum*

F. graminearum and *F. pseudograminearum* were cultivated in 100 ml of mung bean soup for 3 days at 20 °C and 140 rpm. After the cultivation, the culture was filtered through the glass wool and centrifuged for 5 min (3000 rpm, room temperature). Conidia were resuspended in 1 ml of sterile distilled water and used to inoculate 100 ml of YPD medium; cultivation overnight at 30 °C and 180 rpm.

The next day, mycelium was filtered through the Miracloth membrane, washed with sterile distilled water and KCl buffer. For protoplast generation, only a pea-size amount of mycelium was transferred into 10 ml of enzyme solution containing lysing enzyme, driselase, and chitinase. After 3 h at 30 °C and 90 rpm, the enzyme-protoplast solution was run over the frit and the flow-through was centrifuged for 10 min (3000 rpm, 4 °C). The pellet was washed with 5 ml KCl buffer, centrifugation 10 min (3000 rpm, 4 °C). Finally, protoplasts were resuspended in 1x STC buffer.

In 10 ml glass tube, 50 µl (5 µg) *pNDN-OGG* (Fig. 71) or *pNDH-OCT* (Fig. 72), 50 µl of 2x STC, 50 µl of protoplasts and 50 µl of 50% PEG were mixed. After 25 min on ice, samples were mixed with 1.6 ml of 50% PEG and transferred into new glass tubes. After 10 min at RT 3.2 ml of 1x STC were added. Samples were shortly mixed using a vortex and transferred into 100 ml of Regeneration agar that was subsequently poured into five Petri dishes. After 4 h at RT, four plates containing Regeneration agar were overlaid with 10 ml of new Regeneration agar. This time, agar contained antibiotic nourseothricin (Jena Bioscience) (*pNDN-OGG*) or hygromycin (InvivoGen) (*pNDH-OCT*) in the concentration of 300 µg/ml, so the final concentration of antibiotic in Petri dishes was 100 µg/ml. The fifth Petri dish with Regeneration agar served as a control.

After 5 days at 20 °C, fungi resistant to nourseothricin or hygromycin appeared. Mycelia were transferred into Complete agar plates containing nourseothricin or hygromycin in the final concentration of 100 µg/ml.

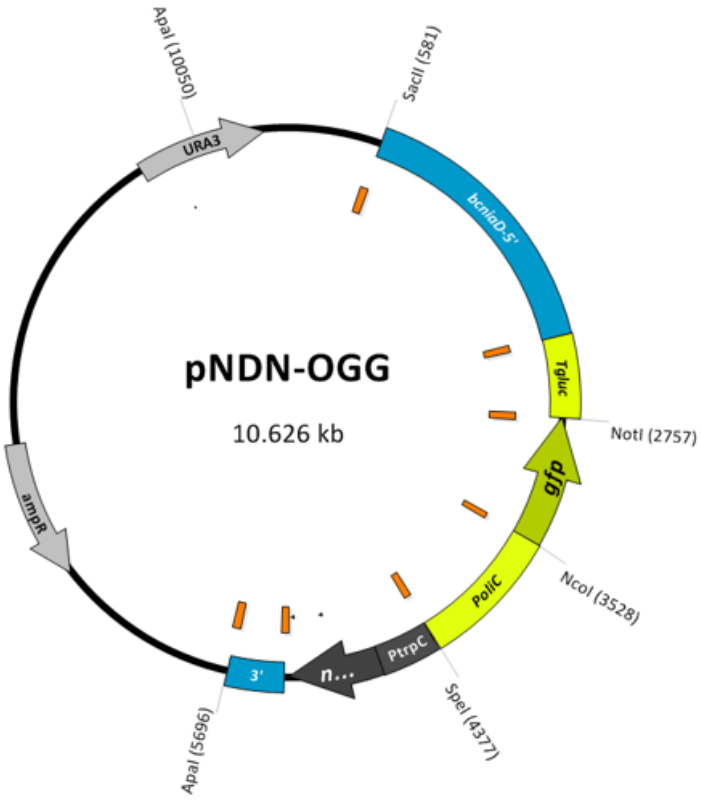

Fig. 71 ***pNDN-OGG*** **containing** ***gfp*** **and resistance to nourseothricin (Schumacher, 2012).**

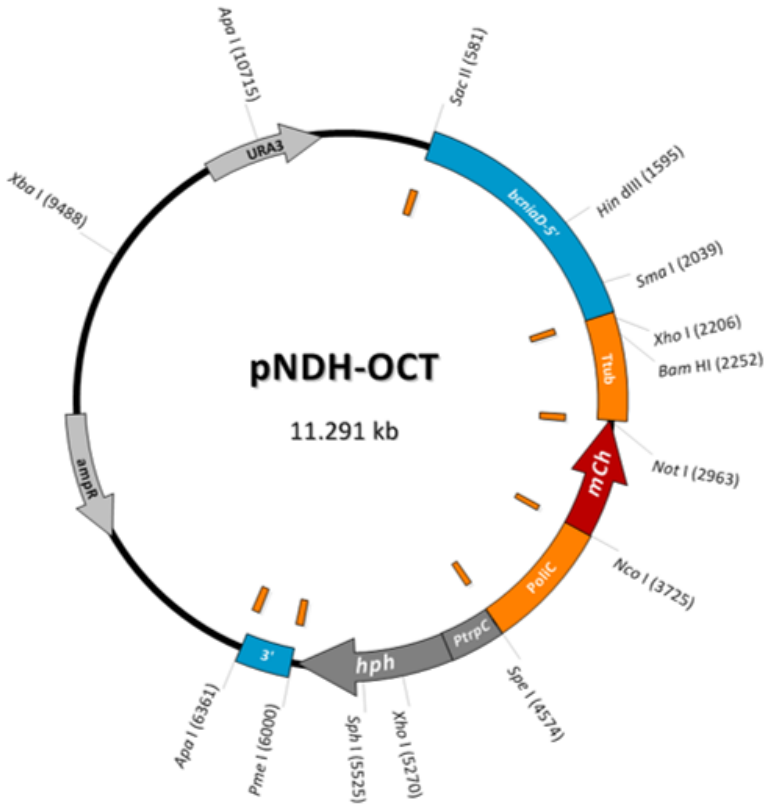

Fig. 72 ***pNDH-OCT*** **containing** ***mCherry*** **and resistance to hygromycin (Schumacher, 2012).**

5.3.2 Transformation of *F. oxysporum* f. sp. *medicaginis*

F. oxysporum f. sp. *medicaginis* was cultivated in 100 ml of Darken medium for 3 days at 30 °C and 180 rpm. Subsequently, 500 µl of the pre-culture was used for inoculation of 100 ml ICI medium; cultivation took place at 30 °C and 180 rpm no longer than 16 h.

After the cultivation, mycelium was filtered through the Miracloth membrane, washed with sterile distilled water and $KCl/CaCl_2$ buffer. For protoplast generation, only a pea-size amount of mycelium was transferred into 10 ml of enzyme solution containing lysing enzyme, driselase, and yatalase. After 3 h at 30 °C and 90 rpm, the enzyme-protoplast solution was run over the frit and the flow-through was centrifuged for 10 min (3000 rpm, 4 °C). The pellet was washed with 5 ml of $KCl/CaCl_2$ buffer and centrifuged for 10 min (3000 rpm, 4 °C). Protoplasts were resuspended in 1x STC buffer.

In 10 ml glass tube, 50 µl (10 µg) of *pNDN-OGG* (Fig. 71) or *pNDN-ODT* (Fig. 73), 50 µl of 2x STC, 50 µl of protoplasts and 50 µl of 50% PEG were mixed. After 25 min on ice, samples were mixed with 1.6 ml of 50% PEG and transferred into new glass tubes. After 10 min at room temperature 3.2 ml of 1x STC were added. Samples were shortly mixed using a vortex and transferred into 100 ml of Regeneration agar that was subsequently poured into five Petri dishes. After 4 h at RT, four plates containing regeneration agar were overlaid with 10 ml of new Regeneration agar. This time, agar contained antibiotic nourseothricin (Jena Bioscience) in the concentration of 300 µg/ml, so the final concentration of antibiotic in Petri dishes was 100 µg/ml. The fifth Petri dish with Regeneration agar served as a control.

After 5 days at 30 °C, fungi resistant to nourseothricin appeared. Mycelia were transferred into Complete agar plates containing nourseothricin in the final concentration of 100 µg/ml.

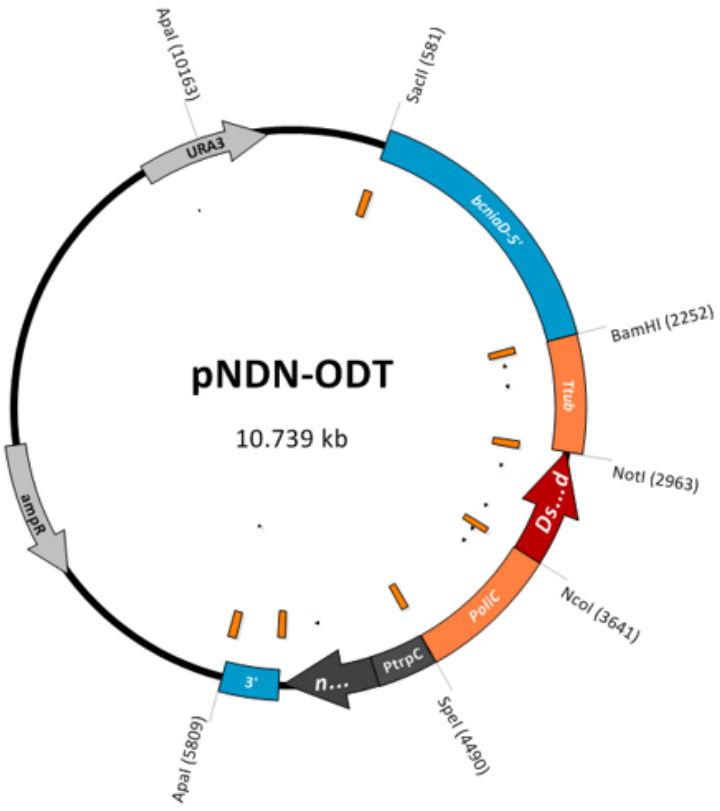

Fig. 73 *pNDN-ODT* containing *dsRED* and resistance to nourseothricin (Schumacher, 2012).

5.3.3 Selection of obtained transformants using diagnostic PCR

Genomic DNA was isolated from lyophilized mycelia of *F. graminearum*, *F. pseudograminearum*, and *F. oxysporum* f. sp. *medicaginis* according to 3.3.3.1.1.

The presence of *pNDN-OGG* in *OE:gfp F. graminearum* transformants and *pNDH-OCT* in *OE:mCherry F. graminearum* transformants was confirmed by diagnostic PCR using GoTaq G2 Flexi DNA polymerase (Tab. 9, 10) and primers PoliC_fw and Tgluc_rev (1,295 bp) and PoliC_fw and Ttub_rev, respectively (1,593 bp) (Tab. 42).

Tab. 42 Sequences of primers used for diagnostic PCR of *ΔTrpE*^{TrpE} *C. purpurea* 20.1.

Primer	Sequence
PoliC_fw	5´-CCCGGAAACTCAGTCTCCTT-3´
TgluC_rev	5´-GTCTTCCGCTAAAACACCCC-3´
Ttub_rev	5´-GAGGTGTGAGCATGGAAGTGATG-3´

The presence of *pNDN-OGG* in *OE:gfp F. pseudograminearum* transformants and *pNDH-OCT* in *OE:mCherry F. pseudograminearum* transformants was confirmed by diagnostic PCR using GoTaq G2 Flexi DNA polymerase (Tab. 9, 10) and primers PoliC_fw and Tgluc_rev (1,295 bp) and PoliC_fw and Ttub_rev, respectively (1,593 bp) (Tab. 42).

The presence of *pNDN-OGG* in *OE:gfp F. oxysporum* f. sp. *medicaginis* transformants and *pNDN-ODT* in *OE:dsRED F. oxysporum* f. sp. *medicaginis* transformants was confirmed by diagnostic PCR using GoTaq G2 Flexi DNA polymerase (Tab. 9, 10) and primers PoliC_fw and Tgluc_rev (1,295 bp) and PoliC_fw and Ttub_rev, respectively (1,509 bp) (Tab. 42).

5.3.4 Single spore isolation

Homokaryotic mutants of *F. graminearum*, *F. pseudograminearum*, and *F. oxysporum* f. sp. *medicaginis* were obtained by single spore isolation.

In the case of *F. graminearum* and *F. pseudograminearum*, fungi were cultivated in 50 ml Mung bean medium for 5 days at 20 °C and 140 rpm. After, the cultures were filtered through glass wool and centrifuged for 10 min (3000 rpm, 4 °C). Conidia were resuspended in 1 ml of sterile distilled water and sprayed on Complete agar plates containing hygromycin or nourseothricin in the final concentration of 100 µg/ml.

In the case of *F. oxysporum* f. sp. *medicaginis*, fungi were cultivated on V8 agar plates for 7 days, 16 h light 20 °C/ 8 h dark 16 °C. After 7 days, conidia were harvested from agar plates, filtered through glass wool, and centrifuged for 10 min (3000 rpm, 4 °C). Conidia were resuspended in 1 ml of sterile distilled water and sprayed on complete agar plates containing nourseothricin in the final concentration of 100 µg/ml.

5.3.5 Fluorescence microscopy

WT, *OE:gfp*, and *OE:mCherry F. graminearum*, *OE:gfp*, and *OE:mCherry F. pseudograminearum*, and *OE:gfp*, and *OE:dsRED F. oxysporum* f. sp. *medicaginis* were each cultivated in 50 ml of YPG medium with nourseothricin or hygromycin. After 3 days at 26 °C and 180 rpm, 1 ml of the pre-culture was used to inoculate 50 ml of YPG without antibiotics. After overnight cultivation at 26 °C and 180 rpm, 10 µl of each culture was taken to examine the fluorescence. Fluorescence microscopy was performed with a Zeiss AxioScope microscope equipped with a Zeiss AxioCam 305 camera. GFP

fluorescence was examined using an excitation wavelength of 488 nm and an emission wavelength of 509 nm, mCherry fluorescence was examined using an excitation wavelength of 587 nm and an emission wavelength of 610 nm, dsRED fluorescence was examined using an excitation wavelength of 533 nm and an emission wavelength of 583 nm. Image analysis was performed using ZEN 2.6 lite software.

5.4 Results

5.4.1 Transformants derived from *F. graminearum*

Protoplasts of *F. graminearum* were transformed with *pNDN-OGG* and *pNDH-OCT* (5.2.1).

In the case of transformation of *F. graminearium* with *pNDN-OGG* gDNA was isolated from 20 putative transformants resistant to nourseothricin, presence of the transgene was verified by diagnostic PCR (5.2.3). For further experiments three transformants marked as *OE:gfp* 3, 4, 5 were selected; homokaryons (Fig. 74a) were obtained by single spore isolation (5.2.4) and confirmed again by diagnostic PCR (5.2.3) (Fig. 74b). Subsequently, gfp fluorescence was checked using fluorescence microscopy in all obtained mutants. As a negative control, WT *F. graminearum* was used (Fig. 75).

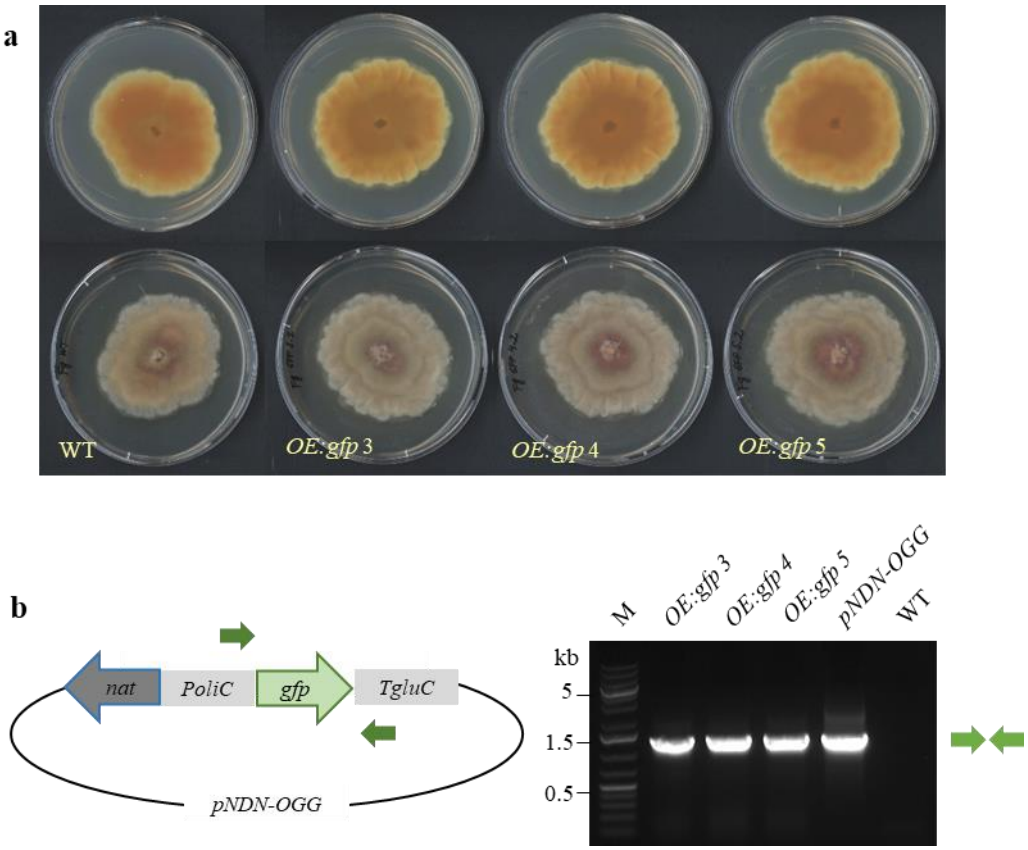

Fig. 74 *F. graminearum* transformants expressing *gfp*.
(a) Three independent transformants *OE:gfp* 3, 4, 5 on PDA agar.
(b) Integration of *pNDN-OGG* in three independent *OE:gfp F. graminearum* transformants confirmed by diagnostic PCR using primers PoliC_fw and Tgluc_rev (1,295 bp), positive control – *pNDN-OGG*, negative control – WT, M – 1 kb Plus DNA ladder.

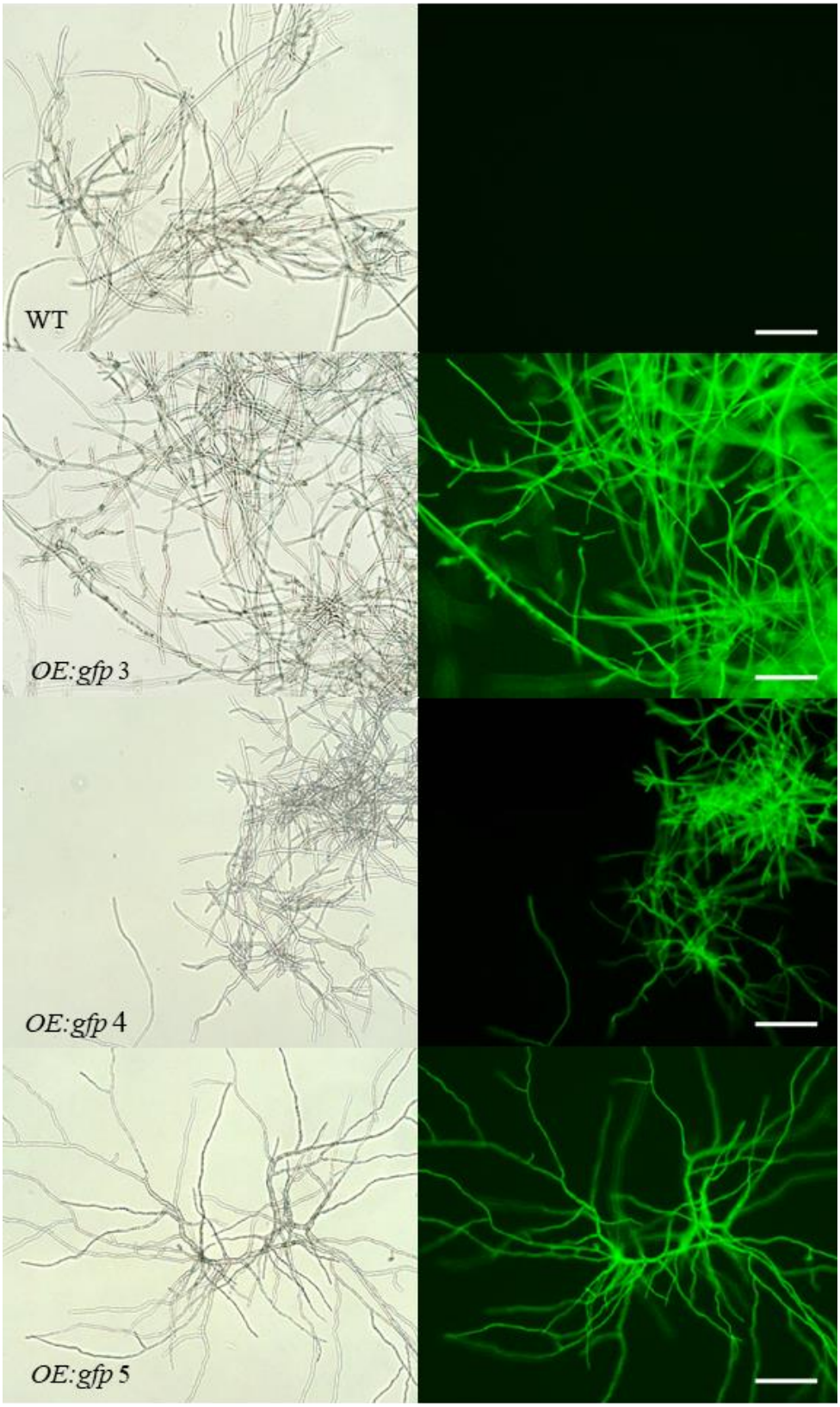

Fig. 75 Detection of GFP signal in *OE:gfp F. graminearum* using fluorescence microscopy. As a negative control, WT *F. graminearum* was used. The bar represents 200 µm.

In the case of transformation of *F. graminearium* with *pNDH-OCT* gDNA was isolated from 20 putative transformants resistant to hygromycin, presence of the transgene was verified by diagnostic PCR (5.2.3). For further experiments three transformants marked as *OE:mCherry* 2, 3, 4 were selected; homokaryons (Fig. 76a) were obtained by single spore isolation (5.2.4) and confirmed again by diagnostic PCR (5.2.3) (Fig. 76b). After, mCherry fluorescence was checked using fluorescence microscopy in all obtained mutants. As a negative control, WT *F. graminearum* was used (Fig. 77).

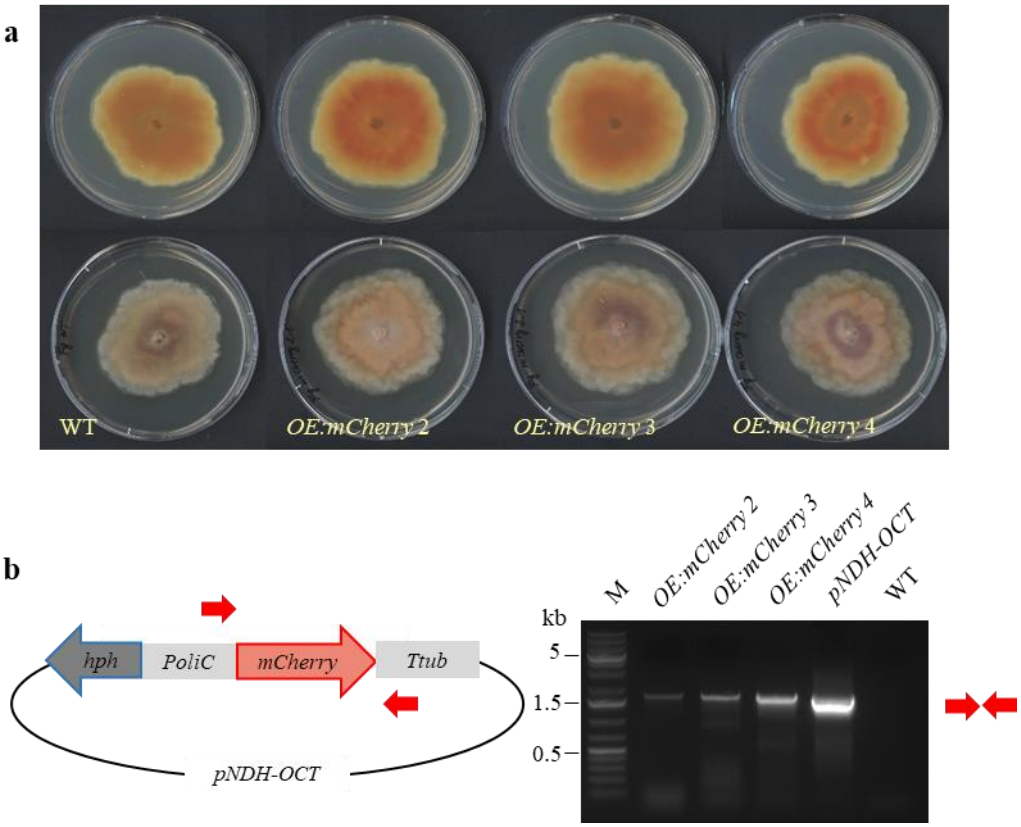

Fig. 76 *F. graminearum* transformants expressing *mCherry*.
(a) Three independent transformants *OE:mCherry* 2, 3, 4 on PDA agar.
(b) Integration of *pNDH-OCT* in three independent *OE:mCherry F. graminearum* transformants confirmed by diagnostic PCR using primers PoliC_fw and Ttub_rev (1,593 bp), positive control – *pNDH-OCT*, negative control – WT, M – 1 kb Plus DNA ladder.

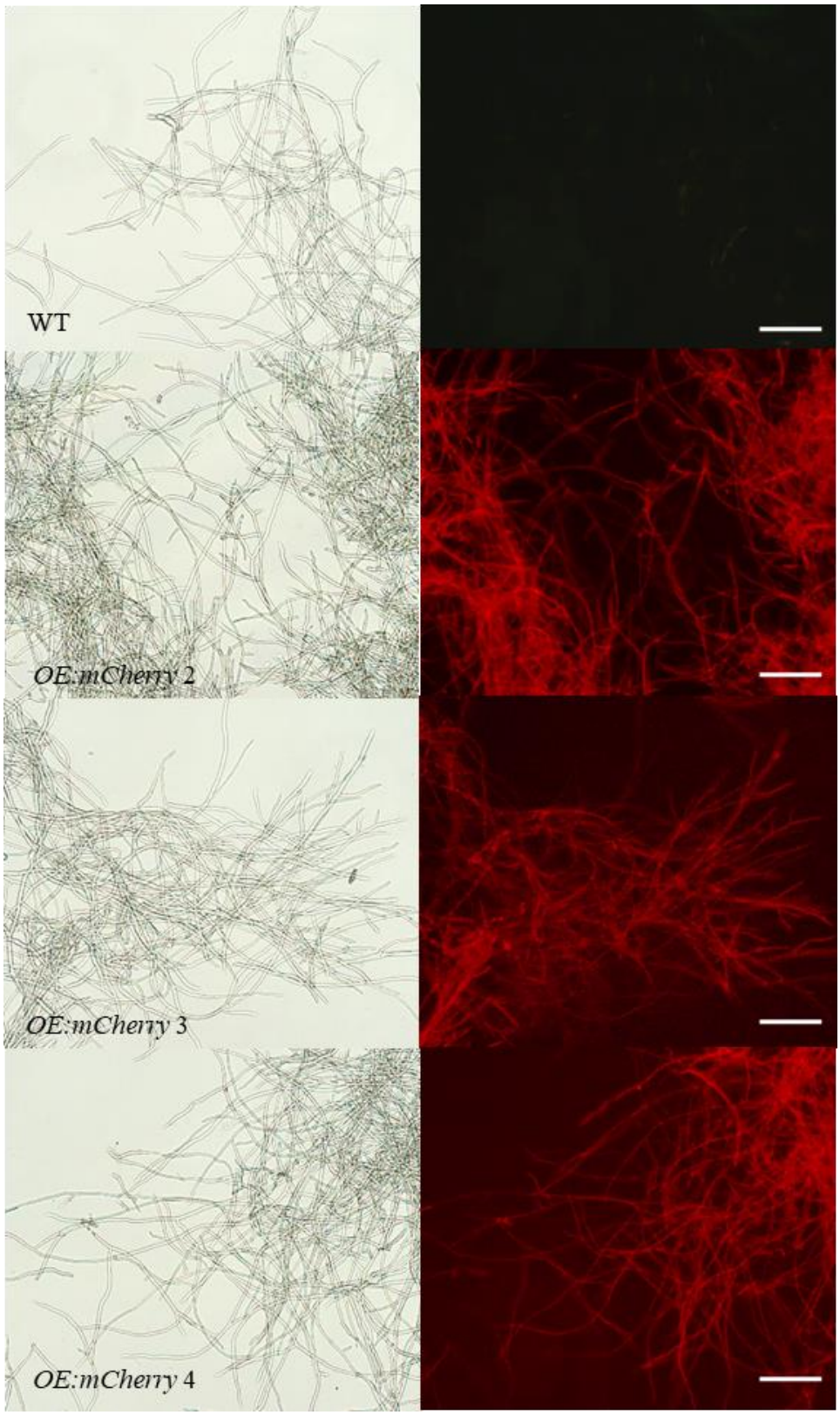

Fig. 77 Detection of mCherry signal in *OE:mCherry F. graminearum* using fluorescence microscopy. As a negative control, WT *F. graminearum* was used. The bar represents 200 µm.

5.4.2 Transformants derived from *F. pseudograminearum*

Protoplasts of *F. pseudograminearum* were transformed with *pNDN-OGG* and *pNDH-OCT* (5.2.1).

In the case of transformation of *F. pseudograminearium* with *pNDN-OGG* gDNA was isolated from 20 putative transformants resistant to nourseothricin, presence of the transgene was verified by diagnostic PCR (5.2.3). For further experiments three transformants marked as *OE:gfp* 1, 2, 6 were selected; homokaryons (Fig. 78a) were obtained by single spore isolation (5.2.4) and confirmed again by diagnostic PCR (5.2.3) (Fig. 78b). Subsequently, gfp fluorescence was checked using fluorescence microscopy in all obtained mutants. As a negative control, WT *F. pseudograminearum* was used (Fig. 79).

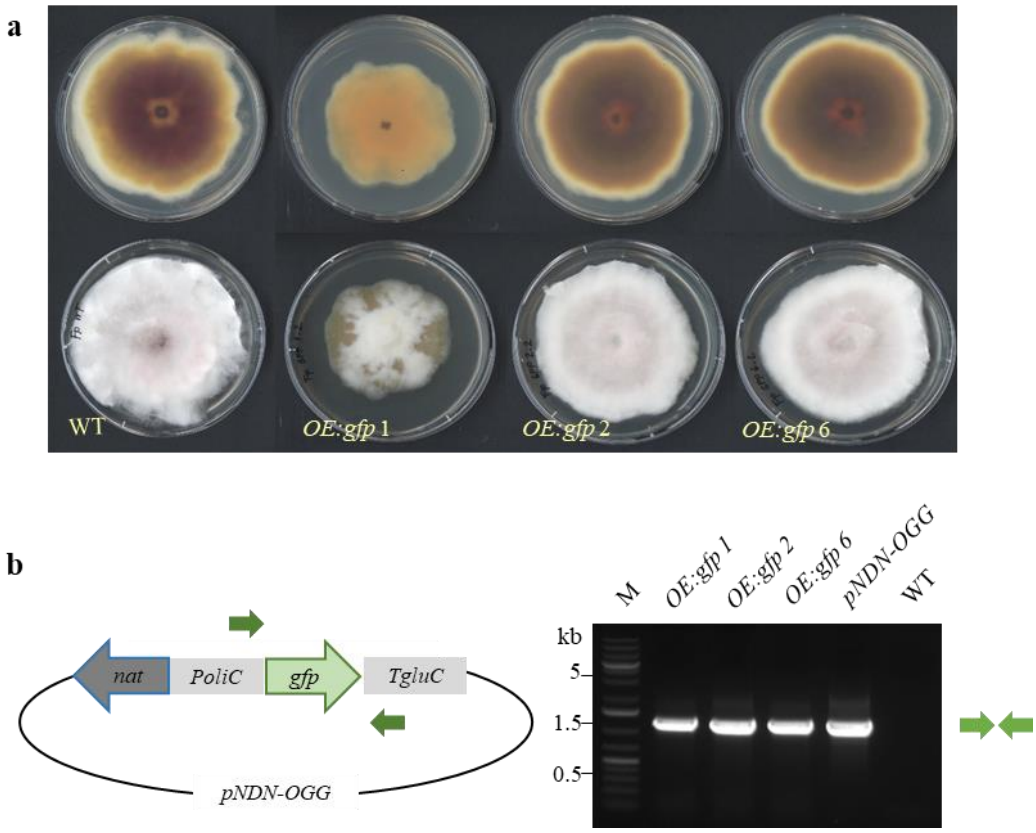

Fig. 78 *F. pseudograminearum* transformants expressing *gfp*.
(a) Three independent transformants *OE:gfp* 1, 2, 6 on PDA agar.
(b) Integration of *pNDN-OGG* in three independent *OE:gfp F. pseudograminearum* transformants confirmed by diagnostic PCR using primers PoliC_fw and Tgluc_rev (1,295 bp), positive control – *pNDN-OGG*, negative control – WT, M – 1 kb Plus DNA ladder.

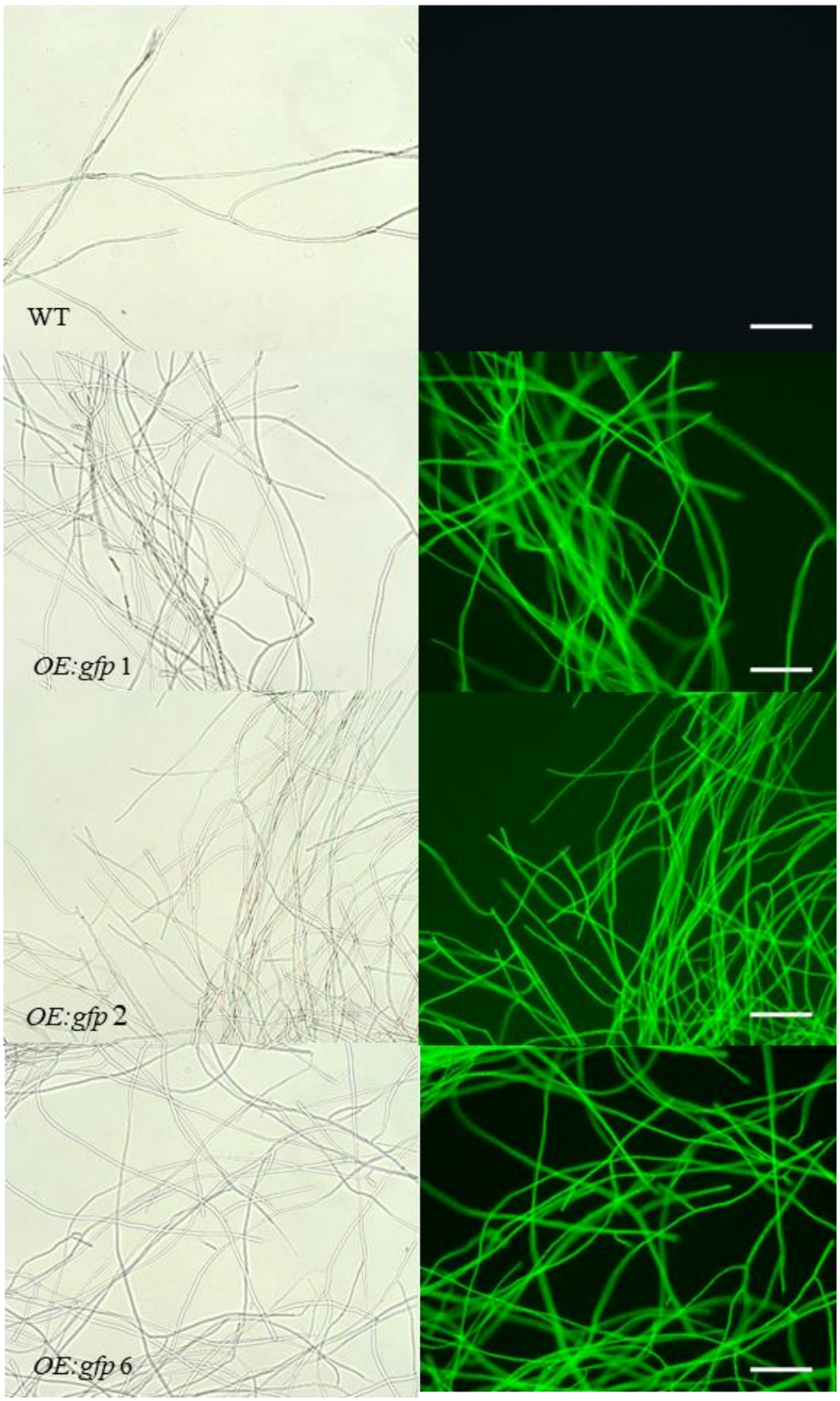

Fig. 79 Detection of GFP signal in *OE:gfp F. pseudograminearum* using fluorescence microscopy. As a negative control, WT *F. pseudograminearum* was used. The bar represents 200 µm.

In the case of transformation of *F. pseudograminearium* with *pNDH-OCT* gDNA was isolated from 20 putative transformants resistant to hygromycin, presence of the transgene was verified by diagnostic PCR (5.2.3). For further experiments three transformants marked as *OE:mCherry* 2, 3, 4 were selected; homokaryons (Fig. 80a) were obtained by single spore isolation (5.2.4) and confirmed again by diagnostic PCR (5.2.3) (Fig. 80b). Subsequently, mCherry fluorescence was checked using fluorescence microscopy in all obtained mutants. As a negative control, WT *F. pseudograminearum* was used (Fig. 81).

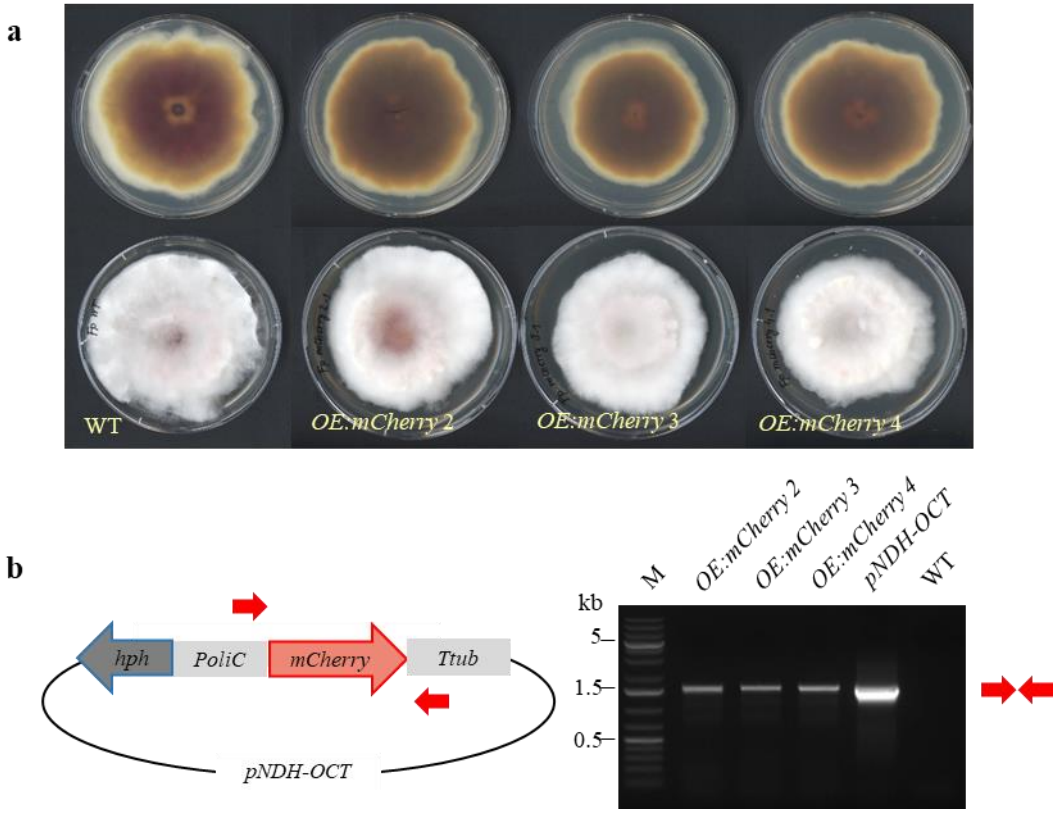

Fig. 80 *F. pseudograminearum* transformants expressing *mCherry*.
(a) Three independent transformants *OE:mCherry* 2, 3, 4 on PDA agar.
(b) Integration of *pNDH-OCT* in three independent *OE:mCherry F. pseudograminearum* transformants confirmed by diagnostic PCR using primers PoliC_fw and Ttub_rev (1,593 bp), positive control – *pNDH-OCT*, negative control – WT, M – 1 kb Plus DNA ladder.

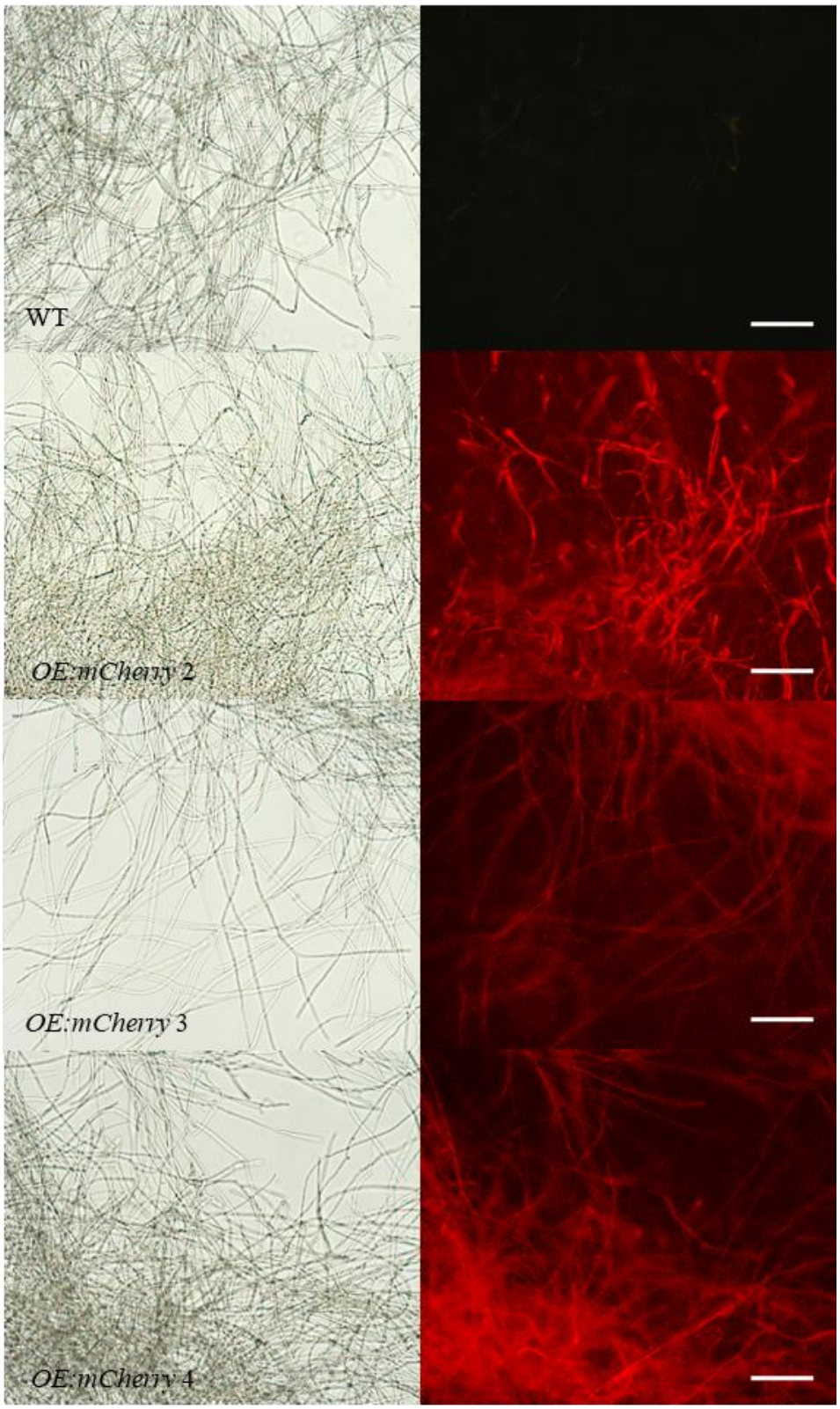

Fig. 81 Detection of mCherry signal in *OE:mCherry F. pseudograminearum* using fluorescence microscopy.
As a negative control, WT *F. pseudograminearum* was used. The bar represents 200 µm.

5.4.3 Transformants derived from *F. oxysporum* f. sp. *medicaginis*

Protoplasts of *F. pseudograminearum* were transformed with *pNDN-OGG* and *pNDN-ODT* (5.2.1).

In the case of transformation of *F. oxysporum* f. sp. *medicaginis* with *pNDN-OGG* gDNA was isolated from 20 putative transformants resistant to nourseothricin, presence of the transgene was verified by diagnostic PCR (5.2.3). For further experiments three transformants marked as *OE:gfp* 3, 4, 6 were selected; homokaryons (Fig. 82a) were obtained by single spore isolation (5.2.4) and confirmed again by diagnostic PCR (5.2.3) (Fig. 82b). Subsequently, gfp fluorescence was checked using fluorescence microscopy in all obtained mutants. As a negative control, WT *F. oxysporum* f. sp. *medicaginis* was used (Fig. 83).

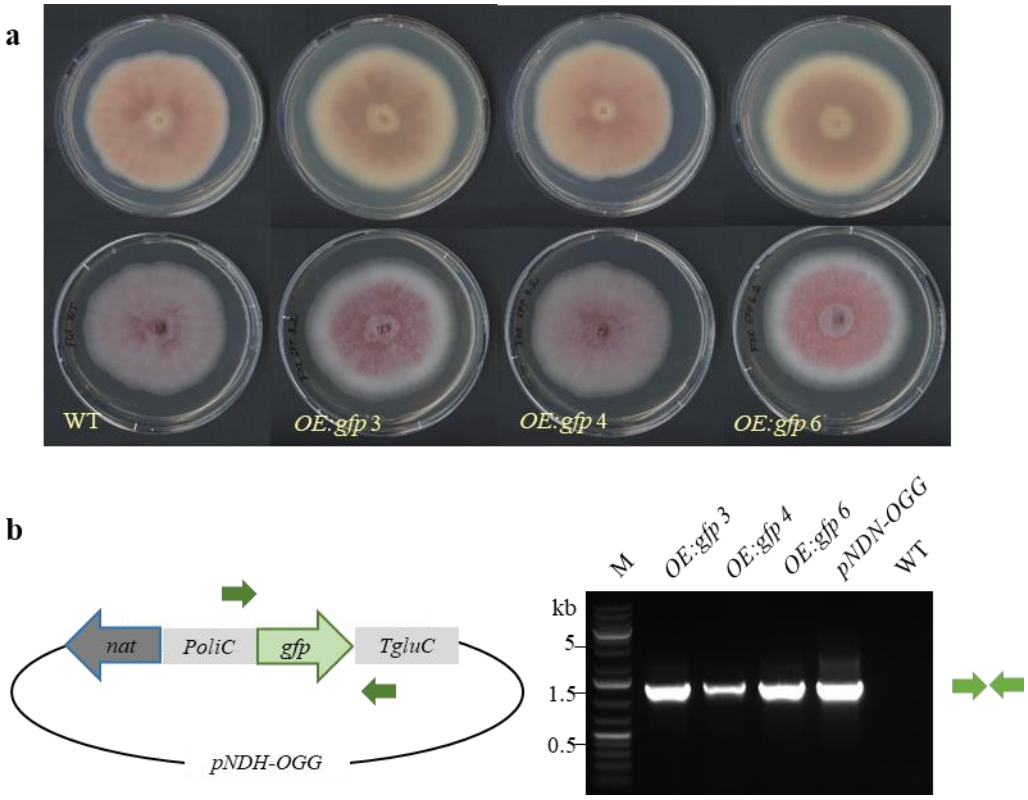

Fig. 82 *F. oxysporum* f. sp. *medicaginis* transformants expressing *gfp*.
(a) Three independent transformants *OE:gfp* 3, 4, 6 on PDA agar.
(b) Integration of *pNDN-OGG* in three independent *OE:gfp F. oxysporum* f. sp. *medicaginis* transformants confirmed by diagnostic PCR using primers PoliC_fw and Tgluc_rev (1,295 bp), positive control – *pNDN-OGG*, negative control – WT, M – 1 kb Plus DNA ladder.

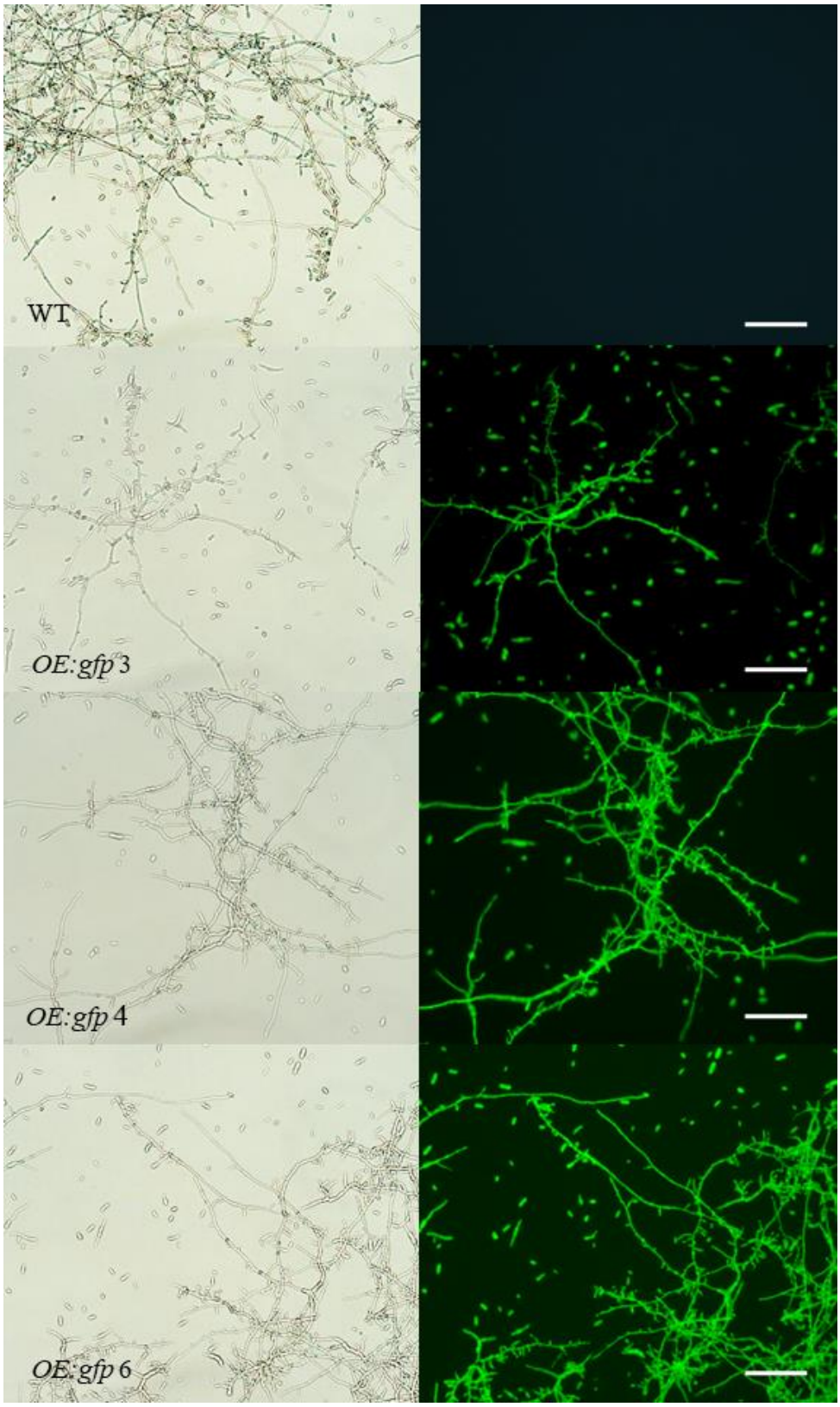

Fig. 83 Detection of GFP signal in *OE:gfp F. oxyssporum* f. sp. *medicaginis* using fluorescence microscopy.
As a negative control, WT *F. oxysporum* f. sp. *medicaginis* was used. The bar represents 200 µm.

In the case of transformation of *F. oxysporum* f. sp. *medicaginis* with *pNDN-ODT* gDNA was isolated from 20 putative transformants resistant to nourseothricin, presence of the transgene was verified by diagnostic PCR (5.2.3). For further experiments three transformants marked as *OE:dsRED* 1, 2, 4 were selected; homokaryons (Fig. 84a) were obtained by single spore isolation (5.2.4) and confirmed again by diagnostic PCR (5.2.3) (Fig. 84b). Subsequently, dsRED fluorescence was checked using fluorescence microscopy in all obtained mutants. As a negative control, WT *F. oxysporum* f. sp. *medicaginis* was used (Fig. 85).

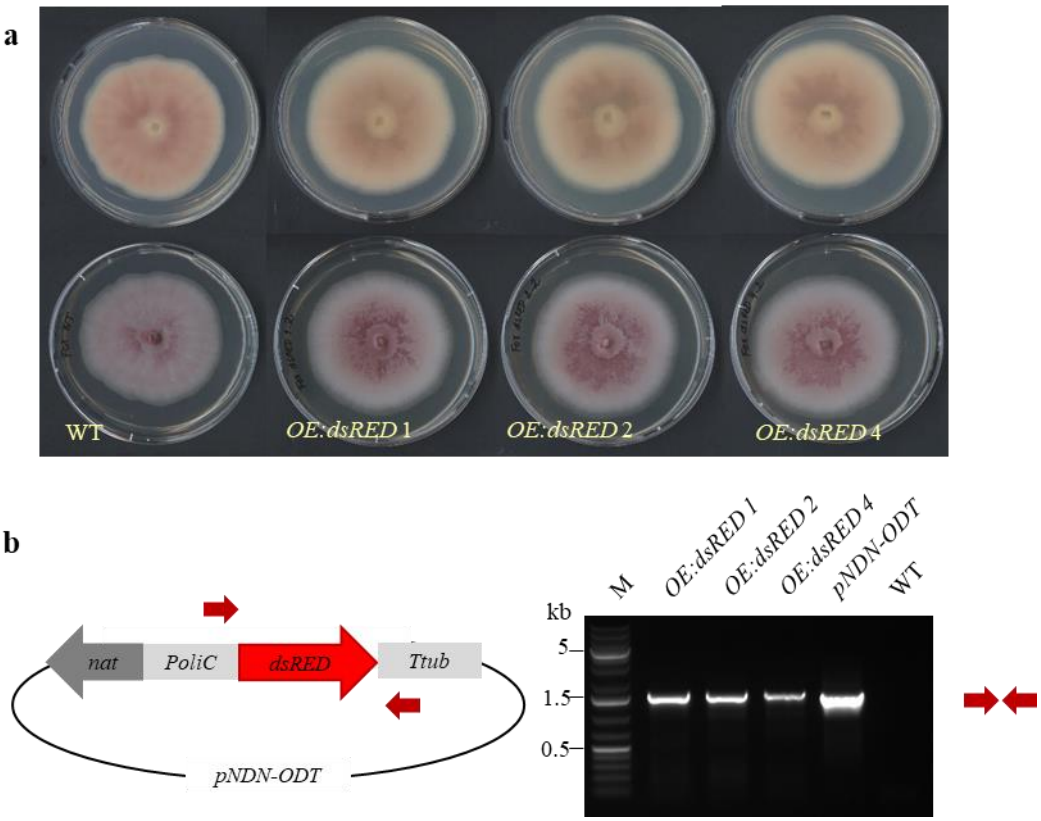

Fig. 84 *F. oxysporum* f. sp. *medicaginis* transformants expressing *dsRED*.
(a) Three independent transformants *OE:dsRED* 1, 2, 4 on PDA agar.
(b) Integration of *pNDN-ODT* in three independent *OE:dsRED F. oxysporum* f. sp. *medicaginis* transformants confirmed by diagnostic PCR using primers PoliC_fw and Ttub_rev (1,509 bp), positive control – *pNDN-ODT*, negative control – WT, M – 1 kb Plus DNA ladder.

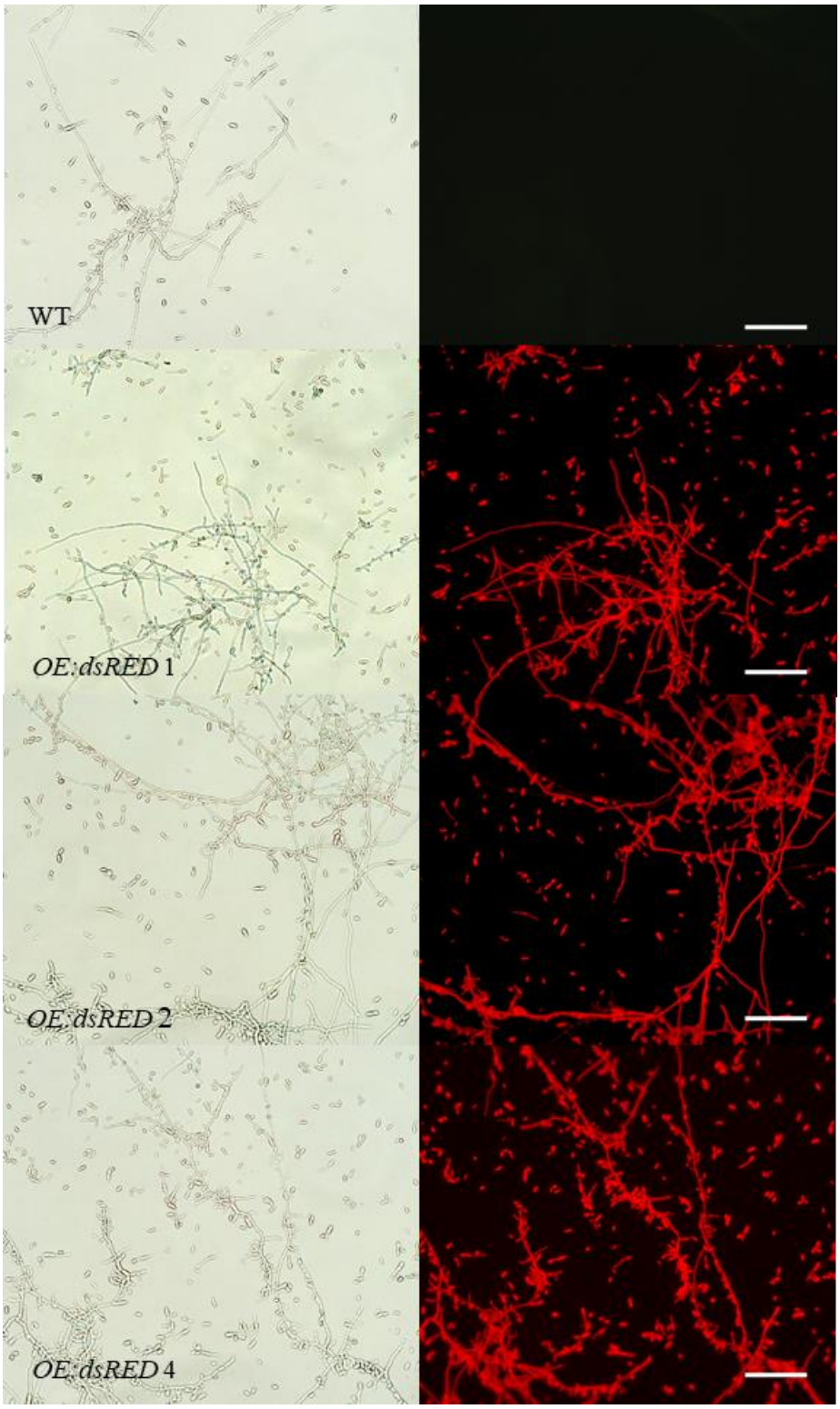

Fig. 85 Detection of dsRED signal in *OE:dsRED F. oxyssporum* f. sp. *medicaginis* using fluorescence microscopy.
As a negative control, WT *F. oxysporum* f. sp. *medicaginis* was used. The bar represents 200 μm.

5.5 Discussion

In this study, fungi from the genus *Fusarium* (*F. graminearum*, *F. pseudograminearum*, and *F. oxysporum* f. sp. *medicaginis*) were transformed with genes encoding red and green fluorescent proteins. These proteins allow us the study plant-pathogen interactions using fluorescence microscopy.

5.5.1 F. graminearum

F. graminearum, the main agent of Fusarium head blight on wheat, maize, and barley (Leplat *et al*., 2013) is usually transformed using protoplast-PEG mediated transformation (Moradi *et al*., 2013). Alternatively, *Agrobacterium*-mediated transformation can be used (Fradsen *et al*., 2006). As we wanted to transform *F. graminearum* with green and red reporter genes, we decided for genes encoding *gfp* and *dsRED*, respectively. Thus, vectors *pNDN-OGG* and *pNDN-ODT* (Schumacher, 2012) containing *gfp* and *dsRED* under the control of the strong constitutive *oliC* (subunit 9 of mitochondrial ATP synthase) promoter from *A. nidulans* (Bailey *et al*., 1989), respectively were used for *F. graminearum* transformation. Although these vectors have been originally prepared to study *Botrytis cinerea*, *pNDN-OGG* has already been successfully used to transform *F. fujikuroi* (Studt *et al*., 2013a, b).

After *F. graminearum* protoplast-PEG mediated transformation, mutants resistant to nourseothricin thus containing *pNDN-OGG* or *pNDN-ODT* were obtained. However, only mutants containing *pNDN-OGG* successfully expressed gfp. In the case of fungi containing *pNDN-ODT*, no dsRED fluorescence could be observed (data not showed). Thus, vector *pNDH-OCT* (Schumacher, 2012) containing mCherry was used in the second round of *F. graminearum* transformation. In general, the quantum yield of monomeric mCherry is usually smaller than in the case of tetrameric dsRED, but as mCherry is a monomer it can be more easily accepted by fungal protoplasts. As expected, mCherry fluorescence was successfully observed in all generated hygromycin-resistant *F. graminearum* transformants containing *pNDH-OCT*.

Concerning reporter lines of *F. graminearum*, the fungus expressing *gfp* under the constitutive *TEF* promoter encoding translation elongation factor from *Aureobasidium pullulans* has already been successfully generated and used to study the pattern of infection in *Arabidopsis thaliana* and barley spike tissue (Skadsen and Hohn, 2004). The same fungus has been also used to study the infection in wheat (Miller *et al*., 2004).

Besides *F. graminearum* expressing a red tag (*dsRED)* under the control of constitutive *gpdA* promoter has been generated by Ilgen *et al*. (2009). Moreover, this fungus contained *gfp* that was driven by the promoter of *TRI5* gene that encodes a trichodiene synthase involved in the biosynthesis of trichothecenes. In this case, the production of secondary metabolites was measured (Ilgen *et al*., 2009). In addition, reporter genes have been fused to a target gene and used to complement knock-out mutants (Bormann *et al.*, 2014) or these vectors have been used for localization studies (Haack *et al*., 2016; Chen *et al*., 2019b).

5.5.2 F. pseudograminearum

Concerning transformation of *F. pseudograminearum* causing Fusarium head blight and crown rot (Kazan and Gardiner, 2018) with vectors containing green and red reporter genes, completely the same situation as in *F. graminearum* was observed.

Firstly, protoplasts of this fungus were transformed with vectors *pNDN-OGG* and *pNDN-ODT* containing *gfp* and *dsRED*, respectively. As in the case of *F. graminearum* transformants, only *OE:gfp* mutants successfully expressed the green tag; no dsRED fluorescence was observed in nourseothricin-resistant *OE:dsRED F. pseudograminearum* mutants (data not shown). Thus, protoplasts of this fungus were transformed again, this time with the vector *pNDH-OCT* containing mCherry. In contrast to dsRED, mCherry fluorescence was observed in all generated hygromycin-resistant *F. pseudograminearum* transformants.

According to the literature, fusions of the target gene with *gfp* in *F. graminearum* have already been successfully generated and used for complementation and subsequent localization studies (Chen *et al*., 2019c; Kang *et al*., 2020; Zhang *et al*., 2020) or to study the regulation of cytokinin production (Blum *et al*., 2019). In addition, *mcherry* has already been also successfully transformed into *F. pseudograminearum* (Chen *et al*., 2019c).

5.5.3 F. oxysporum f. sp. medicaginis

As in the case of *F. graminearum* and *F. pseudograminearum* transformations, vectors *pNDN-OGG* and *pNDN-ODT* were used for PEG-protoplast mediated transformation of *F. oxysporum* f. sp. *medicaginis* that infects *Medicago* plants. Surprisingly, not only gfp

but also dsRED fluorescence were observed in all generated *OE:gfp* and *OE:dsRED* transformants, respectively.

Regarding the transformation of *F. oxysporum* f. sp. *medicaginis* this is the first time this fungus was transformed. Concerning the transformation process of *formae speciales* of *F. oxysporum,* both protoplast- and *Agrobacterium*-mediated transformations have already been used (Malardier *et al*., 1989; Mullins *et al*., 2001). Generated *F. oxyporum* mutants containing gfp or dsRED have already been successfully used as markers for studying the plant-pathogen interactions in many economically important plant species. For example, *F. oxysporum* f. sp. *cubense* and *F. oxysporum* f. sp. *radicis-lycopersici* infecting banana and melon, respectively were successfully transformed with vectors containing *gfp* (Nonomura *et al*., 2001; Visser *et al*., 2004; Li *et al*., 2011). Besides *dsRED* under the control of constitutive *gpdA* promoter has been used to generate reporter line of *F. oxysporum* f. sp. *lycopersici* and *F. oxysporum* f. sp. *dianthi* infecting tomato and carnation, respectively (Nahalkova and Fatehi, 2003; Sarrocco *et al*., 2007).

6 Conclusion

In the first part of this thesis that is focused on ergot fungus *C. purpurea*, it was demonstrated that the overexpression of two genes, *dmaW* encoding dimethylallyltryptophan synthase, an enzyme catalyzing the first pathway-specific step leading to EAs, and a mutated version of *TrpE* encoding α-subunit of anthranilate synthase involved in Trp biosynthesis, led to a significantly increased content of ergopeptines in *C. purpurea* P1 under inducing (low Pi) conditions. On the other hand, mutants overexpressing WT form of *TrpE* that is feedback inhibited by Trp did not have increased levels of anthranilic acid, Trp or ergotamine, and α-ergocryptine compared to WT. At non-inducing conditions (high Pi) under which WT does not produce EAs, both ergopeptines were detected in *OE:TrpE* and $OE{:}TrpE^{S76L}$, suggesting the involvement of Trp in the production of ergopeptines by an unknown mechanism.

The function of *TrpE* gene that has not been previously characterized in *C. purpurea* was confirmed using a knock-out mutant of this gene in *C. purpurea* 20.1 and complemented strain $\Delta TrpE^{TrpE}$. As expected, contrary to WT and $\Delta TrpE^{TrpE}$ strains, *ΔTrpE* strain showed Trp auxotrophy and was non-infectious, presumably due to a decreased content of auxins, plant hormones synthesized from Trp that are involved in plant-pathogen interaction.

In the second part of this thesis that is also focused on *C. purpurea*, it was shown that CRISPR/Cas9 can be used for directed mutagenesis in this ergot fungus. Heterokaryotic mutants containing a mutation in *pyr4* and *TrpE* genes encoding orotidine 5′-phosphate decarboxylase involved in pyrimidine biosynthesis and α-subunit of anthranilate synthase involved in Trp biosynthesis, confirmed by PCR-RFLP analysis, were obtained after *C. purpurea* protoplasts transformation. *Pyr4* and *TrpE* homokaryons showing uridine and tryptophan auxotrophy, respectively, were selected by single spore isolation followed by cultivation of fungi on minimal media with and without uridine or Trp. According to the data obtained from Sanger DNA sequencing, different mutations caused by CRISPR/Cas9 including insertions and their combination with deletions occurred in all *pyr4* and *TrpE* homokaryons. Moreover, almost all mutations were located 3 bp upstream of the PAM sequences.

As *pyr4* homokaryons were drastically impaired in the growth, removal of AMA1-based plasmid used for *CRISPR/Cas9* directed mutagenesis was carried out only for *TrpE* homokaryons. By cultivation of hygromycin resistant fungal mutants impaired

in *TrpE* on media without the antibiotic, vector-free *TrpE* mutants sensitive to hygromycin were obtained already after the first round of single spore isolation.

The transformation efficiencies of three methods (CRISPR/Cas9, CRISPR/Cas9-mediated HDR, and HR-mediated gene knock-out used for mutation of *TrpE* gene) were compared. As expected, the lowest transformation efficiency (1.45 %) was observed for HR-mediated gene knock-out. On contrary, CRISPR/Cas9-mediated HDR provided the highest transformation efficiency (3.45 %). Moreover, all *TrpE* mutants generated by these three methods including CRISPR/Cas9 showed Trp auxotrophy and were non-infectious when inoculated on male-sterile rye plants. This phenomenon was again likely caused by decreased auxin level.

In the third part of this thesis that is focused on fungi from the genus Fusarium, *F. graminearum*, *F. pseudograminearum*, and *F. oxysporum* f. sp. *medicaginis* were successfully each transformed with green and red reporter genes. The presence of vectors containing *gfp*, *mCherry*, or *dsRED* was confirmed with diagnostic PCR and the expression was checked by fluorescence microscopy.

In the future, *F. graminearum* and *F. pseudograminearum* mutants will be inoculated on WT barley plants and plants with inactivated or downregulated mitogen-activated proteinkinases HvMPK3 or HvMPK6 prepared by CRISPR/Cas9 or RNAi, respectively.*F. oxysporum* f. sp. *medicaginis* mutants will be inoculated on WT alfalfa plants and plants with downregulated or upregulated mitogen-activated proteinkinases SIMKK or GFP-SIMK prepared by RNAi or overexpression, respectively. Plant-fungus interactions will be monitored using novel microscopic techniques.

7 References

Adachi H., Tani S., Kanamasa S., Sumitani J.I., Kawaguchi T. (2009): Development of a homologous transformation system for *Aspergillus aculeatus* based on the *sC* gene encoding ATP-sulfurylase. *Bioscience, Biotechnology, and Biochemistry* **73**, 1197-1199. https://doi.org/10.1271/bbb.80772.

Ainsworthh G. C. (2008): *Ainsworth and Bisby´s Dictionary of the Fungi*. CABI, Wallingford, UK, 771 pages.

Albermann S., Linnemannstöns P., Tudzynski B. (2013): Strategies for strain improvement in *Fusarium fujikuroi*: overexpression and localization of key enzymes of the isoprenoid pathway and their impact on gibberellin biosynthesis. *Applied Microbiology and Biotechnology* **97**, 2979-2995. https://doi.org/10.1007/s00253-012-4377-5.

Aleksenko Y. A., Makarova N. A., Nikolaev I. V., Clutterbuck A. J. (1995): Integrative and replicative transformation of *Penicillium canescens* with a heterologous nitrate-reductase gene. *Current Genetics* **28**, 474-477. https://doi.org/10.1007/BF00310818.

Anaya N., Roncero M. I. G. (1991): Transformation of a methionine auxotrophic mutant of *Mucor circinelloides* by direct cloning of the corresponding wild type gene. *Molecular and General Genetics* **230**, 449-455. https://doi.org/10.1007/BF00280302.

Alic M., Kornegay J. R., Pribnow D., Gold M. H. (1989): Transformation by complementation of an adenine auxotroph of the lignin-degrading basidiomycete *Phanerochaete chrysosporium*. *Applied and Environmental Microbiology* **55**, 406-411. https://doi.org/ 10.1128/AEM.55.2.406-411.1989.

Allen N. K., Mirocha C. J., Weaver G., Aakhus-Allen S. A. N. D. R. A., Bates F. (1981): Effects of dietary zearalenone on finishing broiler chickens and young turkey poults. *Poultry Science* **60**, 124-131. https://doi.org/10.3382/ps.0600124.

Aloni R., Aloni E., Langhans M., Ullrich C. I. (2006a): Role of cytokinin and auxin in shaping root architecture: regulating vascular differentiation, lateral root initiation, root apical dominance and root gravitropism. *Annals of Botany* **97**, 883-93. https://doi.org/10.1093/aob/mcl027.

Aloni R., Aloni E., Langhans M., Ullrich C. I. (2006b): Role of auxin in regulating *Arabidopsis* flower development. *Planta* **223**, 315-28. https://doi.org/10.1007/s00425-005-0088-9.

Amey R. C., Athey-Pollard A., Burns C., Mills P. R., Bailey A., Foster G. D. (2002): PEG-mediated and *Agrobacterium*-mediated transformation in the mycopathogen *Verticillium fungicola*. *Mycological Research* **106**, 4-11. https://doi.org/10.1017/S0953756201005251.

Amici A. M., Minghetti A., Scotti T., Spalla C., Tognoli L. (1966): Production of ergotamine by a strain of *Claviceps purpurea* (Fr.) Tul. *Experientia* **22**, 415-416. https://doi.org/10.1007/BF01901174.

Anne J., Peberdy J. F. (1975): Conditions for induced fusion of fungal protoplasts in polyethylene glycol solutions. *Archives of Microbiology* **105**, 201-205. https://doi.org/10.1007/BF00447138.

Antunes M. S. (2003): Characterizing a benzoic acid inducible promoter system from the fungus *Aspergillus niger*. Disertation thesis, Purdue University, West Lafayette, IN, USA.

Aoki T., O´Donnell K. (1999): Morphological and molecular characterization of *Fusarium pseudograminearum* sp. nov., formerly recognized as the Group 1 population of *F. graminearum*. *Mycologia* **91**, 597-609. https://doi.org/10.1080/00275514.1999.12061058.

Aoki T., Ward T. J., Kistler H. C., O´Donnell K. (2012): Systematics, phylogeny and trichothecene mycotoxin potential of *Fusarium* head blight cereal pathogens. *JSM Mycotoxins* **62**, 91-102. https://doi.org/10.2520/myco.62.91.

Arazoe T., Miyoshi K., Yamato T., Ogawa T., Ohsato S., Arie T., Kuwata S. (2015): Tailor-made CRISPR/Cas system for highly efficient targeted gene replacement in the rice blast fungus. *Biotechnology and Bioengineering* **112**, 2543-2549. https://doi.org/10.1002/bit.25662.

Arentshorst M., Niu J., Ram A. F. (2015): Efficient generation of *Aspergillus niger* knock out strains by combining NHEJ mutants and a split marker approach. In *Genetic Transformation Systems in Fungi* (van den Berg M. A. Maruthachalam K., eds.). Springer, Cham, Switzerland, pp. 263-272. https://doi.org/10.1007/978-3-319-10142-2_25.

Armstrong G. M, Armstrong J. K. (1981): *Formae speciales and races of Fusarium oxysporum causing wilt diseases.* Pennsylvania State University Press, State College, PA, USA, 391-399.

Arntz C., Tudzynski P. (1997): Identification of genes induced in alkaloid-producing cultures of *Claviceps* sp. *Current Genetics* **31**, 357-360. https://doi.org/10.1007/s002940050216.

Arras S. D., Chua S. M., Wizrah M. S., Faint J. A., Yap A. S., Fraser J. A. (2016): Targeted genome editing via CRISPR in the pathogen *Cryptococcus neoformans*. *PLoS One* **11**, e0164322. https://doi.org/10.1371/journal.pone.0164322.

Arst H. N., Cove D. J. (1973): Nitrogen metabolite repression in *Aspergillus nidulans*. *Molecular and General Genetics* **126**, 111-141. https://doi.org/10.1007/BF00330988.

Austin B., Hall R. M., Tyler B. M. (1990): Optimized vectors and selection for transformation of *Neurospora crassa* and *Aspergillus nidulans* to bleomycin and phleomycin resistance. *Gene* **93**, 157-162. https://doi.org/10.1016/0378-1119(90)90152-H.

Avalos J., Geever R. F., Case M. E. (1989): Bialaphos resistance as a dominant selectable marker in *Neurospora crassa*. *Current Genetics* **16**, 369-372. https://doi.org/10.1007/BF00340716.

Bae Y. S., Knudsen G. R. (2000): Cotransformation of *Trichoderma harzianum* with β-glucuronidase and green fluorescent protein genes provides a useful tool for monitoring fungal growth and activity in natural soils. *Applied and Environmental Microbiology* **66**, 810-815. https://doi.org/10.1128/AEM.66.2.810-815.2000.

Bailey A.M., Turner G., Brown J., Kerry-Williams S., Ward M., Punt P. J., van den Hondel C. A. M. J. J. (1989): Analysis of the oliC promoter of *Aspergillus nidulans*. *Foundation for Biotechnical and Industrial Fermentation Research* **6**, 101-109.

Barcellos F. G., Fungaro M. H. P., Furlaneto M. C., Lejeune B., Pizzirani-Kleiner A. A., Lúcio de Azevedo J. (1998): Genetic analysis of *Aspergillus nidulans* unstable transformants obtained by the biolistic process. *Canadian Journal of Microbiology* **44**, 1137-1141. https://doi.org/10.1139/w98-213.

Barrow K. D., Mantle P. G., Quigley F. R. (1974): Biosynthesis of dihydroergot alkaloids. *Tetrahedron Letters* **15**, 1557-1560. https://doi.org/10.1016/S0040-4039(01)93135-1.

Bassett A. R., Liu J. L. (2014): CRISPR/Cas9 and genome editing in Drosophila. *Journal of Genetics and Genomics* **41**, 7-19. https://doi.org/10.1016/j.jgg.2013.12.004.

Bell C. C., Magor G. W., Gillinder K. R., Perkins A.C. (2014): A high-throughput screening strategy for detecting CRISPR-Cas9 induced mutations using next-generation sequencing. *BMC Genomics* **15**, 1-7. https://doi.org/10.1186/1471-2164-15-1002.

Berges T., Barreau C. (1991): Isolation of uridine auxotrophs from Trichoderma reesei and efficient transformation with the cloned *ura3* and *ura5* genes. *Current Genetics* **19**, 359-365. https://doi.org/10.1007/BF00309596.

Beri R. K., Turner G. (1987): Transformation of *Penicillium chrysogenum* using the *Aspergillus nidulans amdS* gene as a dominant selective marker. *Current Genetics* **11**, 639-41. https://doi.org/10.1007/BF00393928.

Bigal M. E., Tepper S. J. (2003): Ergotamine and dihydroergotamine: a review. *Current Pain and Headache Reports* **7**, 55-62. https://doi.org/10.1007/s11916-003-0011-7.

Bitinaite J., Rubino M., Varma K. H., Schilldkraut I., Vaisvila R., Vaiskunaite R. (2007): USER™ friendly DNA engineering and cloning method by uracil excision. *Nucleic Acids Research* **35**, 1992-2002. https://doi.org/10.1093/nar/gkm041.

Blatzer M., Gsaller F., Abt B., Schrettl M., Specht T., Haas H. (2014): An endogenous promoter for conditional gene expression in *Acremonium chrysogenum*: The xylan and xylose inducible promoter xyl1P. *Journal of Biotechnology* **169**, 82-86. https://doi.org/10.1016/j.jbiotec.2013.11.003.

Blum A., Benfield A. H., Sørensen J. L., Nielsen M. R., Bachleitner S., Studt L., Beccari G., Covarelli L., Batley J., Gardiner D. M. (2019): Regulation of a novel Fusarium cytokinin in *Fusarium pseudograminearum*. *Fungal Biology* **123**, 255-266. https://doi.org/10.1016/j.funbio.2018.12.009.

Bogo A., Mantle P. G. (1999): *Claviceps africana* discovered in India. *Plant Disease* **83**, 79-79. https://doi.org/10.1094/PDIS.1999.83.1.79B.

Boretsky Y., Voronovsky A., Liuta-Tehlivets O., Hasslacher M., Kohlwein S. D., Shavlovsky G. M. (1999): Identification of an ARS element and development of a high efficiency transformation system for *Pichia guilliermondii*. *Current Genetics* **36**, 215-221. https://doi.org/10.1007/s002940050493.

Bormann J., Boenisch M. J., Brückner E., Firat D., Schäfer W. (2014): The adenylyl cyclase plays a regulátory role in the morphogenetic switch from vegetative to pathogenic lifestyle of *Fusarium graminearum* on wheat. *PloS One* **9**, e91135. https://doi.org/10.1371/journal.pone.0091135.

Bos C. J., Slakhorst S. M. (1981): Isolation of protoplasts from *Aspergillus nidulans* conidiospores. *Canadian Journal of Microbiology* **27**, 400-407. https://doi.org/10.1139/m81-061.

Bradford M. M. (1976): A rapid and sensitive method for the quantitation of microgram quantities of protein utilizing the principle of protein-dye binding. *Analytical Biochemistry* **72**, 248–254. https://doi.org/10.1006/abio.1976.9999.

Brauer K. L., Robbers J. E. (1987): Induced parasexual processes in Claviceps sp. strain SD58. *Applied and Environmental Microbiology* **53**, 70-73. https://doi.org/10.1128/AEM.53.1.70-73.1987.

Breakspear A., Langford K. J., Momany M., Assinder S. J. (2007): CopA: GFP localizes to putative Golgi equivalents in *Aspergillus nidulans*. *FEMS Microbiology Letters* **277**, 90-97. https://doi.org/10.1111/j.1574-6968.2007.00945.x.

Brzezinska-Rodak M., Klimek-Ochab M., Zymanczyk-Duda E. (2016): Enzyme-mediated protoplast formation of *Cuninghamella echinulata* – preliminary studies. *BioTechnologia. Journal of*

Biotechnology Computational Biology and Bionanotechnology **97**. https://doi.org/10.5114/bta.2016.58541.

Brückner B., Unkles S. E., Weltring K., *Kinghorn J. R. (1992): Transformation of Gibberella fujikuroi: effect of the Aspergillus* nidulans AMA1 sequence on frequency and integration. *Current Genetics* **22**, 313-316. https://doi.org/10.1007/BF00317927.

Bruni G. O., Zhong K., Lee S. C., Wang P. (2019): CRISPR-Cas9 induces point mutation in the mucormycosis fungus *Rhizopus delemar*. *Fungal Genetics and Biology* **124**, 1-7. https://doi.org/ 10.1016/j.fgb.2018.12.002.

Bushnell W. R., Hazen B. E., Pritsch C., Leonard K. (2003): Histology and physiology of *Fusarium* head blight. In *Fusarium Head Blight of Wheat and Barley* (Leonard, K. J., Bushnell, W. R., eds.). APS Press, St. Paul, MN, USA, pp. 44-83.

Buxton F. P., Gwynne D. I., Davies R. W. (1985): Transformation of *Aspergillus niger* using the *argB* gene of *Aspergillus nidulans*. *Gene* **37**, 207-214. https://doi.org/10.1016/0378-1119(85)90274-4.

Campbell E. I., Unkles S. E., Macro J. A., van den Hondel C., Contreras R., Kinghorn J. R. (1989): Improved transformation efficiency of *Aspergillus niger* using the homologous *niaD* gene for nitrate reductase. *Current Genetics* **16**, 53-56. https://doi.org/10.1007/BF00411084.

Cassady J. M., Li G. S., Spitzner E. B., Floss H. G., Clemens J. A. (1974): Ergot alkaloids. Ergolines and related compounds as inhibitors of prolactin release. *Journal of Medicinal Chemistry* **17**, 300-307. https://doi.org/10.1021/jm00249a009.

Cenis J. L. (1992): Rapid extraction of fungal DNA for PCR amplification. *Nucleic Acids Research* **20**, 2380. https://doi.org/10.1093/nar/20.9.2380.

Chanclud E., Morel J. B. (2016): Plant hormones: a fungal point of view. *Molecular Plant Pathology* **17**, 1289-1297. https://doi.org/10.1111/mpp.12393.

Chang K., Kurtz H. J., Mirocha C. J. (1979): Effects of the mycotoxin zearalenone on swine reproduction. *American Journal of Veterinary Research* **40**, 1260.

Chang P. K., Yu J., Bhatnagar D., Cleveland T. E. (2000): Characterization of the *Aspergillus parasiticus* major nitrogen regulatory gene, *areA*. *Biochimica et Biophysica Acta - Gene Structure and Expression* **1491**, 263-266. https://doi.org/10.1016/S0167-4781(00)00004-X.

Chen X., Stone M., Schlagnhaufer C., Romaine C. P. (2000): A fruiting body tissue method for efficient *Agrobacterium*-mediated transformation of *Agaricus bisporus*. *Applied and Environmental Microbiology* **66**, 4510-4513. https://doi.org/ 10.1128/AEM.66.10.4510-4513.2000.

Chen J., Lai Y., Wang L., Zhai S., Zou G., Zhou Z., Cui C., Wang S. (2017): CRISPR/Cas9-mediated efficient genome editing via blastospore-based transformation in entomopathogenic fungus *Beauveria bassiana*. *Scientific Reports* **7**, 45763. https://doi.org/10.1038/srep45763.

Chen B. X., Wei T., Ye Z.W., Yun F., Kang L. Z., Tang H. B., Guo L. Q., Lin J. F. (2018): Efficient CRISPR-Cas9 gene disruption system in edible-medicinal mushroom *Cordyceps militaris*. *Frontiers in Microbiology* **9**, 1157. https://doi.org/ 10.3389/fmicb.2018.01157.

Chen J. J., Han M. Y., Gong T., Qiao Y. M., Yang J. L., Zhu P. (2019a): Epigenetic modification enhances ergot alkaloid production of *Claviceps purpurea*. *Biotechnology Letters* **41**, 1439-1449. https://doi.org/10.1007/s10529-019-02750-x.

Chen L., Tong q., Zhang C., Ding K. (2019a): The transcription factor FgCrz1A is essetial for fungal development, virulence, deoxynivalenol biosynthesis and stress responses in *Fusarium graminearum*. *Current Genetics* **65**, 153-166. https://doi.org/10.1007/s00294-018-0853-5.

Chen L., Geng X., Ma Y., Zhao J., Chen W., Xing X., Shi Y., Sun B., Li H. (2019c): The ER lumenal Hsp70 protein FpLhs1 is important for conidiation and plant infection in *Fusarium pseudograminearum*. *Frontiers in Microbiology* **10**, 1401. https://doi.org/10.3389/fmicb.2019.01401.

Cheng C., Tsukagoshi N., Udaka S. (1990): Transformation of *Trichoderma viride* using the *Neurospora crassa pyr4* gene and its use in the expression of a Taka-amylase A gene from *Aspergillus oryzae*. *Current Genetics* **18**, 453-456. https://doi.org/10.1007/BF00309916.

Chi M. S., Mirocha C. J., Kurtz H. J., Weaver G. A., Bates F., Robinson T., Shimoda W. (1980): Effect of dietary zearalenone on growing broiler chicks. *Poultry Science* **59**, 531-536. https://doi.org/10.3382/ps.0590531.

Christianson T. W., Sikorski R. S., Dante M., Shero J. H., Hieter P. (1992): Multifunctional yeast high-copy-number shuttle vectors. *Gene* **110**, 119–122. https://doi.org/10.1016/0378-1119(92)90454-w.

Chulkin A. M., Vavilova E. A., Benevolenskij S. V. (2010): Transcriptional regulator of carbon catabolite repression *CreA* of filamentous fungus *Penicillium canescens*. *Molecular Biology* **44**, 596-605. https://doi.org/10.1134/S0026893310040151.

Chung K. R., Shilts T., Ertürk Ü., Timmer L. W., Ueng P. P. (2003): Indole derivatives produced by the fungus *Colletotrichum acutatum* causing lime anthracnose and postbloom fruit drop of citrus. *FEMS Microbiology Letters* **226**, 23-30. https://doi.org/10.1016/S0378-1097(03)00605-0.

Chung K. R., Lee M. H. (2015): Split-marker-mediated transformation and targeted gene disruption in filamentous fungi. In *Genetic Transformation Systems in Fungi* (van den Berg M. A, Maruthachalam K., eds.). Springer, Cham Switzerland, pp. 175-180. https://doi.org/10.1007/978-3-319-10503-1_15.

Christensen T., Woeldike H., Boel E., Mortensen S. B., Hjortshoej K., Thim L., Hansen M. T. (1988): High level expression of recombinant genes in *Aspergillus oryzae*. *Biotechnology* **6**, 1419-1422. https://doi.org/10.1038/nbt1288-1419.

Clark C. A., Valverde R. A., Wilder-Ayers J. A., Nelson P. E. (1990): *Fusarium lateritium*, causal agent of sweet potato chlorotic leaf distortion. *Phytopathology* **80**, 741-744.

Cole R. J., Dorner J. W., Lansden J. A., Cox R. H., Pape C., Cunfer B., Nicholson S. S., Bedell D. M. (1977): Paspalum staggers: isolation and identification of tremorgenic metabolites from sclerotia of *Claviceps paspali*. *Journal of Agricultural and Food Chemistry* **25**, 1197-1201. https://doi.org/ 10.1021/jf60213a061.

Colot H. V., Park G., Turner G. E., Ringelberg C., Crew C. M., Litvinkova L., Weiss R. L., Borkovich K. A., Dunlap J. C. (2006): A high-throughput gene knockout procedure for *Neurospora* reveals functions for multiple transcription factors. *Proceedings of the National Academy of Sciences USA* **103**, 10352-10357. https://doi.org/10.1073/pnas.0601456103.

Comino A., Kolar M., Schwab H., Sočič H. (1989): Heterologous transformation of *Claviceps purpurea*. *Biotechnology Letters* **11**, 389-392. https://doi.org/10.1007/BF01089469.

Cormack B. (1988): Green fluorescent protein as a reporter of transcription and protein localization in fungi. *Current Opinion in Microbiology* **1**, 406-410. https://doi.org/10.1016/S1369-5274(98)80057-X.

Correia T., Grammel N., Ortel I., Keller U., Tudzynski P. (2003): Molecular cloning and analysis of the ergopeptine assembly system in the ergot fungus *Claviceps purpurea*. *Chemistry and Biology* **10**, 1281-1292. https://doi.org/10.1016/j.chembiol.2003.11.013.

Cope R. B. (2018): Trichothecenes. In *Veterinary Toxicology, Basic and Clinical Principles, 3rd Edition* (Gupta R. C., ed.). Academic Press, Cambridge, MA, USA, pp. 1043-1053. https://doi.org/10.1016/B978-0-12-811410-0.00075-1.

Covert S. F., Kapoor P., Lee M. H., Briley A., Nairn C. J. (2001): *Agrobacterium tumefaciens*-mediated transformation of *Fusarium circinatum*. *Mycological Research* **105**, 259-264. https://doi.org/10.1017/S0953756201003872.

Couteaudier Y., Daboussi M. J., Eparvier A., Langin T., Orcival J. (1993): The GUS gene fusion system (*Escherichia coli* beta-D-glucuronidase gene), a useful tool in studies of root colonization by *Fusarium oxysporum*. *Applied and Environmental Microbiology* **59**, 1767-1773. https://doi.org/10.1128/AEM.59.6.1767-1773.1993.

Coyle C. M., Cheng J. Z., O'Connor S. E., Panaccione D. G. (2010): An old yellow enzyme gene controls the branch point between *Aspergillus fumigatus* and *Claviceps purpurea* ergot alkaloid pathways. *Applied and Environmental Microbiology* **76**, 3898-3903. https://doi.org/ 10.1128/AEM.02914-09.

Crawford I. P., Eberly L. (1986): Structure and regulation of the anthranilate synthase genes in *Pseudomonas aeruginosa*: I. Sequence of *trpG* encoding the glutamine amidotransferase subunit. *Molecular Biology and Evolution* **3**, 436–448. https://doi.org/10.1093/oxfordjournals.molbev.a040408.

Cress W. A., Chayet L. T., Rilling H. C. (1981): Crystallization and partial characterization of dimethylallyl pyrophosphate: L-tryptophan dimethylallyltransferase from *Claviceps* sp. SD58. *Journal of Biological Chemistry* **256**, 10917-10923. https://doi.org/10.1016/S0021-9258(19)68532-7.

Cui Y., Xu J., Cheng M., Liao X., Peng S. (2018): Review of CRISPR/Cas9 sgRNA design tools. *Interdisciplinary Sciences: Computational Life Sciences* **10**, 455-465. https://doi.org/10.1007/s12539-018-0298-z.

Cundliffe E., Cannon M., Davies J. (1974): Mechanism of inhibition of eukaryotic protein synthesis by trichothecene fungal toxins. *Proceedings of the National Academy of Sciences USA* **71**, 30-34. https://doi.org/10.1073/pnas.71.1.30.

Cuomo C. A., Güldener U., Xu J. R., Trail F., Turgeon B. G., Di Pietro A., Walton J. D., Ma L. J., Baker S. E., Rep M., Adam G., Antoniw J., Baldwin T., Calvo S., Chang Y. L., DeCaprio D., Gale L. R., Gnerre S., Goswami R. S., Hammond-Kosack K., Harris L. J., Hilburn K., Kennell J. C., Kroken S., Magnuson J. K., Mannhaupt G., Mauceli E., Mewes H. W., Mitterbauer R., Muehlbauer G., Münsterkötter M., Nelson D., O´Donnell K., Ouellet T., Qi W., Quesneville H., Roncero M. I. G., Seong K. Y., Tetko I. V., Urban M., Waalwijk C., Ward T. J., Yao J., Birren B. W., Kistler H. C.

(2005): The *Fusarium graminearum* genome reveals a link between localized polymorphism and pathogen specialization. *Science* **317**, 1400-1402. https://doi.org/10.1126/science.1143708.

Čudejková M. M., Vojta P., Valík J., Galuszka P. (2016): Quantitative and qualitative transcriptome analysis of four inductrial strains of *Claviceps purpurea* with respect to ergot alkaloid production. *New Biotechnology* **33**, 743-754. https://doi.org/10.1016/j.nbt.2016.01.006.

da Silva Ferreira M. E., Kress M. R., Savoldi M., Goldman M. H., Härtl A., Heinekamp T., Brakhage A. A., Goldman G. H. (2006): The *akuBKU80* mutant deficient for nonhomologous end joining is a powerful tool for analyzing pathogenicity in *Aspergillus fumigatus*. *Eukaryotic Cell* **5**, 207-211. https://doi.org/ 10.1128/EC.5.1.207-211.2006.

Davis R. D., Moore N. Y., Kochman J. K. (1996): Characterization of a population of *Fusarium oxysporum* f. sp. *vasinfectum* causing wilt of cotton in Australia. *Australian Journal of Agricultural Research* **47**, 1143-1156. https://doi.org/10.1071/AR9961143.

De Battista J. P., Bacon C. W., Severson R., Plattner R. D., Bouton J. H. (1990): Indole acetic acid production by the fungal endophyte of tall fescue. *Agronomy Journal* **82**, 878-80. https://doi.org/10.2134/agronj1990.00021962008200050006x.

De Groot M. J., Bundock P., Hooykaas P. J., Beijersbergen A. G. (1998): *Agrobacterium tumefaciens*-mediated transformation of filamentous fungi. *Nature Biotechnology* **16**, 839-842. https://doi.org/10.1038/nbt0998-839.

de Gouvêa P. F., Soriani F. M., Malavazi I., Savoldi M., de Souza Goldman M. H., Loss O., Bignell E., da Silva Ferreira M. E., Goldman G. H. (2008): Functional characterization of the *Aspergillus fumigatus* PHO80 homologue. *Fungal Genetics and Biology* **45**, 1135-1146. https://doi.org/10.1016/j.fgb.2008.04.001.

De Lucas R. J., Domínguez A. I., Higuero Y., Martínez Ó., Romero B., Mendoza A., Garcia-Bustos F. J., Laborda F. (2001): Development of a homologous transformation system for the opportunistic human pathogen *Aspergillus fumigatus* based on the *sC* gene encoding ATP sulfurylase. *Archives of Microbiology* **176**, 106-113. https://doi.org/ 10.1007/s002030100299.

de Ruiter-Jacobs Y. M., Broekhuijsen M., Unkles S. E., Campbell E. I., Kinghorn J. R., Contreras R., Pouwels P. H., van den Hondell C. A. (1989): A gene transfer system based on the homologous pyrG gene and efficient expression of bacterial genes in *Aspergillus oryzae*. *Current Genetics* **16**, 159-163. https://doi.org/10.1007/BF00391472.

De Saeger S., Van Peteghem C. (1996): Dipstick enzyme immunoassay to detect *Fusarium* T-2 toxin in wheat. *Applied and Environmental Microbiology* **62**, 1880-1884.

Deng H., Gao R., Liao X., Cai Y. (2017): Genome editing in *Shiraia bambusicola* using CRISPR-Cas9 system. *Journal of Biotechnology* **259**, 228-234. https://doi.org/10.1016/j.jbiotec.2017.06.1204.

Desai K., Sullards M. C., Allegood J., Wang E., Schmelz E. M., Hartl M., Humpf H. U., Liotta D. C., Peng Q., Merrill Jr A. H. (2002): Fumonisins and fumonisin analogs as inhibitors of ceramide synthase and inducers of apoptosis. *Biochimica et Biophysica Acta – Molecular and Cell Biology of Lipids* **1585**, 188-192. https://doi.org/10.1016/S1388-1981(02)00340-2.

Desjardins A. E., Hohn T. M., McCormick S. P. (1993): Trichothecenes biosynthesis in Fusarium species: chemistry, genetics, and significance. *Microbiology and Molecular Biology Review* **57**, 595-604.

d'Enfert C. (1996): Selection of multiple disruption events in *Aspergillus fumigatus* using the orotidine-5′-decarboxylase gene, *pyrG*, as a unique transformation marker. *Current Genetics* **30**, 76-82. https://doi.org/10.1007/s002940050103.

Diez B., Alvarez E., Cantoral J. M., Barredo J. L., Martin J. F. (1987): Selection and characterization of *pyrG* mutants of *Penicillium chrysogenum* lacking orotidine-5′-phosphate decarboxylase and complementation by the *pyr4* gene of *Neurospora crassa*. *Current Genetics* **12**, 277-282. https://doi.org/10.1007/BF00435290.

Dignani M. C., Anaissie E. (2004): Human fusariosis. *Clinical Microbiology and Infection* **10**, 67-75. https://doi.org/10.1111/j.1470-9465.2004.00845.x.

Ding Y., Williams R. M., Sherman D. H. (2008): Molecular analysis of a 4-dimethylallyltryptophan synthase from *Malbranchea aurantiaca*. *Journal of Biological Chemistry* **283**, 16068-16076. https://doi.org/10.1074/jbc.M801991200.

Diolez A., Langin T., Gerlinger C., Brygoo Y., Daboussi M. J. (1993): The *nia* gene of *Fusarium oxysporum*: isolation, sequence and development of a homologous transformation system. *Gene* **131**, 61-67. https://doi.org/10.1016/0378-1119(93)90669-T.

Doherty A. J., Jackson S. P. (2001): DNA repair: how Ku makes ends meet. *Current Biology* **11**, R920-R924. https://doi.org/10.1016/S0960-9822(01)00555-3.

Döll S., Dänicke S. (2011): The Fusarium toxins deoxynivalenol (DON) and zearalenone (ZON) in animal feeding. *Preventive Veterinary Medicine* **102**, 132-145. https://doi.org/10.1016/j.prevetmed.2011.04.008.

Dooijewaard-Kloosterziel A. M., Sietsma J. H., Wouters J. T. M. (1973): Formation and regeneration of *Geotrichum candidum* protoplasts. *Microbiology* **74**, 205-209. https://doi.org/10.1099/00221287-74-2-205.

Dopstadt J., Neubauer L., Tudzynski P., Humpf H. U. (2016): The epipolythiodiketopiperazine gene cluster in *Claviceps purpurea*: Dysfunctional-cytochrome p450 enzyme prevents formation of the previously unknown clapurines. *PloS One* **11**, e01158945. https://doi.org/10.1371/journal.pone.0158945.

Dorcey E., Urbez C., Blázquez M. A., Carbonell J., Perez-Amador M. A. (2009): Fertilization-dependent auxin response in ovules triggers fruit development through the modulation of gibberellin metabolism in *Arabidopsis*. *The Plant Journal* **58**, 318-332. https://doi.org/10.1111/j.1365-313X.2008.03781.x.

Doudna J. A., Charpentier E. (2014): The new frontier of genome engineering with CRISPR-Cas9. *Science* **346**, 6213. https://doi.org/10.1126/science.1258096.

Eckert S. E., Kübler E., Hoffmann B., Braus G. H. (2000): The tryptophan synthase-encoding *trpB* gene of *Aspergillus nidulans* is regulated by the cross-pathway control system. *Molecular and General Genetics* **263**, 867-876. https://doi.org/10.1007/s004380000250.

Edel-Hermann V., Lecomte C. (2019): Current status of *Fusarium oxysporum formae speciales* and races. *Phytopathology* **109**, 512-530. https://doi.org/10.1094/PHYTO-08-18-0320-RVW.

Erge D., Schumann B., Gröger D. (1984): Influence of tryptophan and related compounds on ergot alkaloid formation in *Claviceps purpurea* (Fr.) Tul. *Zeitschrift für Allgemeine Mikrobiologie* **24**, 667-678. https://doi.org/10.1002/jobm.19840241002.

Esser K., Tudzynski P. (1978): Genetics of the ergot fungus *Claviceps purpurea*: I. Proof of a monoecious life cycle and segregation patterns for mycelial morphology and alkaloid production. *Theoretical and Applied Genetics* **53**, 145-149. https://doi.org/10.1007/BF00273574.

Etard C., Joshi S., Stegmaier J., Mikut R., Strähle U. (2017): Tracking of indels by DEcomposition is a simple and effective method to assess efficiency of guide RNAs in zebrafish. *Zebrafish* **14**, 586–588. https://doi.org/10.1089/zeb.2017.1454.

Fadl-Allah E., Stack M., Goth R., Bean G. (1997): Production of fumonisins B1, B2 and B3 by *Fusarium proliferatum* isolated from rye grains. *Mycotoxin Research* **13**, 43. https://doi.org/10.1007/BF02945061.

Fairhead C., Llorente B., Denis F., Soler M., Dujon B. (1996): New vectors for combinatorial deletions in yeast chromosomes and for gap-repair cloning using 'split-marker'recombination. *Yeast* **12**, 1439-1457. https://doi.org/10.1002/(SICI)1097-0061(199611)12:14<1439::AID-YEA37>3.0.CO;2-O.

Fan X., Qiu R., Liu L., Tang G. (2001): Study on the molecular basis of glucoamylase overproduction of a mutant strain *Aspergillus niger* T21. *Science in China Series C: Life Sciences* **44**, 287-293. https://doi.org/10.1007/BF02879335.

Fandohan P., Hell K., Marasas W. F. O., Wingfield M. J. (2003): Infection of maize by *Fusarium* species and contamination with fumonisin in Africa. *African Journal of Biotechnology* **2**, 570-579. https://doi.org/10.5897/AJB2003.000-1110.

Fang Y., Tyler B. M. (2016): Efficient disruption and replacement of an effector gene in the oomycete *Phytophthora sojae* using CRISPR/Cas9. *Molecular Plant Pathology* **17**, 127-139. https://doi.org/10.1111/mpp.12318.

Fernández-Bodega Á., Álvarez-Álvarez R., Liras P., Martín J. F. (2017): Silencing of a second dimethylallyltryptophan synthase of *Penicillium roqueforti* reveals a novel clavine alkaloid gene cluster. *Applied Microbiology and Biotechnology* **101**, 6111-6121. https://doi.org/10.1007/s00253-017-8366-6.

Fierro F., Kosalková K., Gutiérrez S., Martín J. F. (1996): Autonomously replicating plasmids carrying the AMA1 region in *Penicillium chrysogenum*. *Current Genetics* **29**, 482-489. https://doi.org/10.1007/BF02221518.

Fitze D., Wiepning A., Kaldorf M., Ludwig-Müller J. (2005): Auxins in the development of an arbuscular mycorrhizal symbiosis in maize. *Journal of Plant Physiology* **162**, 1210-1219. https://doi.org/10.1016/j.jplph.2005.01.014.

Fitzgerald A. M., Mudge A. M., Gleave A. P., Plummer K. M. (2003): *Agrobacterium* and PEG-mediated transformation of the phytopathogen *Venturia inaequalis*. *Mycological Research* **107**, 803-810. https://doi.org/10.1017/S0953756203008086.

Flaherty J. E., Weaver M. A., Payne G. A., Woloshuk C. P. (1995): A beta-glucuronidase reporter gene construct for monitoring aflatoxin biosynthesis in *Aspergillus flavus*. *Applied and Environmental Microbiology* **61**, 2482-2486. https://doi.org/10.1128/AEM.61.7.2482-2486.1995.

Florea S., Panaccione D. G., Schardl C. L. (2017): Ergot alkaloids of the family *Clavicipitaceae*. *Phytopathology* **107**, 504-518. https://doi.org/10.1094/PHYTO-12-16-0435-RVW.

Floss H. G., Mothes U. (1964): Über den Einfluss von Tryptophan und analogen Verbindungen auf die Biosynthese von Clavinalkaloiden in saprophytischer Kultur. *Archiv für Mikrobiologie* **48**, 231-221. German. https://doi.org/10.1007/BF00408592.

Forsyth L. M., Smith L. J., Aitken E. A. (2006): Identification and characterization of non-pathogenic *Fusarium oxysporum* capable of increasing and decreasing Fusarium wilt severity. *Mycological Research* **110**, 929-935. https://doi.org/10.1016/j.mycres.2006.03.008.

Fradsen R. J. N., Nielsen N. J., Maolanon N., Sørensen J. C., Olsson S., Nielsen J., Giese H. (2006): The biosynthetic pathway for aurofusarn in *Fusarium graminearum* reveals a close link between the napthoquinones and naphthopyrones. *Molecular Microbiology* **61**, 1069-1080. https://doi.org/10.1111/j.1365-2958.2006.05295.x.

Frederickson D. E., Mantle P. G., De Milliano W. A. (1991): *Claviceps africana* sp. nov.; the distinctive ergot pathogen of sorghum in Africa. *Mycological Research* **95**, 1101-1107. https://doi.org/10.1016/S0953-7562(09)80555-8.

Frisvad J. C., Smedsgaard J., Samson R. A., Larsen T. O., Thrane U. (2007): Fumonisin B2 production by *Aspergillus niger*. *Journal of Agriculture and Food Chemistry* **55**, 9727-9732. https://doi.org/10.1021/jf0718906.

Fuchs J. G., Moënne-Loccoz Y., Défago G. (1997): Nonpathogenic *Fusarium oxysporum* strain Fo47 induces resistence to *Fusarium* wilt in tomato. *Plant Disease* **81**, 492-496. https://doi.org/10.1094/PDIS.1997.81.5.492.

Fuentes S. F., Maria D. L., Ullstrup A. J., Rodriguez A. E. (1964): *Claviceps gigantea*, a new pathogen of Maize in Mexico. *Phytopathology* **54**, 379-381.

Fuller K. K., Chen S., Loros J. J., Dunlap J. C. (2015): Development of the CRISPR/Cas9 system for targeted gene disruption in *Aspergillus fumigatus*. *Eukaryotic Cell* **14**, 1073-1080. https://doi.org/10.1128/EC.00107-15.

Gajecka M., Zielonka L., Gajecki M. (2015): The effect of low monotonic doses of zearalenone on selected reproductive tissues in pre-pubertal female dogs – a review. *Molecules* **20**, 20669-20687. https://doi.org/10.3390/molecules201119726.

Gale L. R., Chen L. F., Hernick C. A., Takamura K., Kistler H. C. (2002): Population analysis of *Fusarium graminearum* from wheat fields in eastern China. *Phytopathology* **92**, 1315-1322. https://doi.org/10.1094/PHYTO.2002.92.12.1315.

Gale L. R., Bryant J. D., Calvo S., Giese H., Katan T., O´Donnell K., Suga H., Taga M., Usgaard T. R., Ward T. J., Kistler H. C. (2005): Chromosome complement of the fungal plant pathogen *Fusarium graminearum* based on genetic and physical mapping and cytological observations. *Genetics* **171**, 985-1001. https://doi.org/10.1534/genetics.105.044842.

Gardiner D. M., McDonald M. C., Covarelli L., Solomon P. S., Rusu A. G., Marshall M., Kazan K., Chakraborty S., McDonald B. A., Manners J. M. (2012): Comparative pathogenomics reveals horizontally acquired novel virulence genes in fungi infecting cereal hosts. *PLoS Pathology* **8**, e1002952. https://doi.org/10.1371/journal.ppat.1002952.

Gardiner D. M., Kazan K. (2018): Selection is required for efficient Cas9-mediated genome editing in *Fusarium graminearum*. *Fungal Biology* **122**, 131-137. https://doi.org/10.1016/j.funbio.2017.11.006.

Gardiner D. M., Benfield A: H., Stiller J., Stephen S., Aiken K., Liu C., Kazan K. (2018): A high-resolution genetic map of the cereal crown rot pathogen *Fusarium pseudograminearum* provides a near-complete genome assembly. *Molecular Plant Pathology* **19**, 217-226. https://doi.org/10.1111/mpp.12519.

Garre V., Torres-Martínez S. (1996): Mutants of *Phycomyces blakesleeanus* defective in acetyl-CoA synthetase. *Fungal Genetics and Biology* **20**, 70-73. https://doi.org/10.1006/fgbi.1996.0011.

Gasiunas G., Barrangou R., Horvath P., Siksnys V. (2012): Cas9–crRNA ribonucleoprotein complex mediates specific DNA cleavage for adaptive immunity in bacteria. *Proceedings of the National Academy of Sciences USA* **109**, E2579-E2586. https://doi.org/10.1073/pnas.1208507109.

Gebler J. C., Poulter C. D. (1992): Purification and characterization of dimethylallyl tryptophan synthase from *Claviceps purpurea*. *Archives of Biochemistry and Biophysics* **296**, 308-13. https://doi.org/10.1016/0003-9861(92)90577-J.

Gems D., Johnstone I. L., Clutterbuck A. J. (1991): An autonomously replicating plasmid transforms *Aspergillus nidulans* at high frequency. *Gene* **98**, 61-67. https://doi.org/10.1016/0378-1119(91)90104-J.

Giesbert S., Schuerg T., Scheele S., Tudzynski P. (2008): The NADPH oxidase Cpnox1 is required for full pathogenicity of the ergot fungus *Claviceps purpurea*. *Molecular Plant Pathology* **9**, 317-327. https://doi.org/10.1111/j.1364-3703.2008.00466.x.

Gilbert J., Tekauz A. (2000): Recent developments in research on Fusarium head blight of wheat in Canada. *Canadian Journal of Plant Pathology* **22**, 1-8. https://doi.org/10.1080/07060660009501155.

Goetz K. E., Coyle C. M., Cheng J. Z., O'Connor S. E., Panaccione D. G. (2011): Ergot cluster-encoded catalase is required for synthesis of chanoclavine-I in *Aspergillus fumigatus*. *Current Genetics* **57**, 201. https://doi.org/10.1007/s00294-011-0336-4.

Goldman G. H., Van Montagu M., Herrera-Estrella A. (1990): Transformation of *Trichoderma harzianum* by high-voltage electric pulse. *Current Genetics* **17**, 169-174. https://doi.org/10.1007/BF00312863.

Goosen T., van Engelenburg F., Debets F., Swart K., Bos K., van den Broek H. (1989): Tryptophan auxotrophic mutants in *Aspergillus niger*: inactivation of the trpC gene by cotransformation mutagenesis. *Molecular and General Genetics* **219**, 282-288. https://doi.org/10.1007/BF00261189.

Gordon A., McCartney C., Knox R. E., Ereful N., Hiebert C. W., Konkin D. J., Hsueh Y., Bhadauria V., Sgrol M., O´Sullivan D. M., Hadley C., Boyd L. A., Menzles J. G. (2020): Genetic and transcriptional dissection of resistence to *Claviceps purpurea* in the durum wheat cultivar Greenshank. *Theoretical and Applied Genetics* **133**, 1873-1886. https://doi.org/10.1007/s00122-020-03561-9.

Goswami R. S. (2012): Targeted gene replacement in fungi using a split-marker approach. In *Plant fungal pathogens*. Humana Press, Totowa, NJ, USA, 255-269. https://doi.org/10.1007/978-1-61779-501-5_16.

Graf R., Mehmann B., Braus G. H. (1993): Analysis of feedback-resistant anthranilate synthases from *Saccharomyces cerevisiae*. *Journal of Bacteriology* **175**, 1061-1068. https://doi.org/10.1128/JB.175.4.1061-1068.1993

Gravelat F. N., Askew D. S., Sheppard D. C. (2012): Targeted gene deletion in *Aspergillus fumigatus* using the hygromycin-resistance split-marker approach. In *Host-Fungus Interactions* (pp. 119-130). Humana Press. https://doi.org/10.1007/978-1-61779-539-8_8.

Grawunder U., Wilm M., Wu X., Kulesza P., Wilson T. E., Mann M., Lieber M. R. (1997): Activity of DNA ligase IV stimulated by complex formation with XRCC4 protein in mammalian cells. *Nature* **388**, 492-495. https://doi.org/10.1038/41358.

Gromadzka K., Waskiewicz A., Chelkowski J., Golinski P. (2008): Zearalenone and its metabolites: occurence, detection, toxicity and guidelines. *World Mycotoxin Journal* **1**, 209-220. https://doi.org/10.3920/WMJ2008.x015.

Gruber F., Visser J., Kubicek C. P., De Graaff L. H. (1990): The development of a heterologous transformation system for the cellulolytic fungus *Trichoderma reesei* based on a *pyrG*-negative mutant strain. *Current Genetics* **18**, 71-76. https://doi.org/10.1007/BF00321118.

Gunasekaran M., Weber D. J. (1972): Auxin production of three phytopathogenic fungi. *Mycologia* **64**, 1180-1183. https://doi.org/10.1080/00275514.1972.12019366.

Güldener U., Mannhaupt G., Münsterkötter M., Haase D., Oesterheld M., Stümpflen V., Mewes H. W., Adam G. (2006): FGDB: a comprehensive fungal genome resource on the plant pathogen *Fusarium graminearum*. *Nucleic Acids Research* **34**, D456-D458. https://doi.org/10.1093/nar/gkj026.

Haack F. S., Poehlein A., Kröger C., Voigt C: A., Piepenbring M., Bode H. B., Daniel R., Schäfer W., Streit W. R. (2016): Molecular keys to the Janthinobacterium and Duganella spp. Interaction with the plant pathogen *Fusarium graminearum*. *Frontiers in microbiology* **7**, 1668. https://doi.org/10.3389/fmicb.2016.01668.

Haarmann T., Machado C., Lübbe Y., Correia T., Schardl C. L., Panaccione D. G., Tudzynski P. (2005): The ergot alkaloid gene cluster in *Claviceps purpurea*: extension of the cluster sequence and intra species evolution. *Phytochemistry* **66**, 1312-1320. https://doi.org/10.1016/j.phytochem.2005.04.011.

Haarmann T., Ortel I., Tudzynski P., Keller U. (2006): Identification of the cytochrome P450 monooxygenase that bridges the clavine and ergoline alkaloid pathways. *ChemBioChem* **7**, 645-652. https://doi.org/10.1002/cbic.200500487.

Haarmann T., Lorenz N., Tudzynski P. (2008): Use of a nonhomologous end joining deficient strain (*Δku70*) of the ergot fungus *Claviceps purpurea* for identification of a nonribosomal peptide synthetase gene involved in ergotamine biosynthesis. *Fungal Genetics and Biology* **45**, 35-44. https://doi.org/10.1016/j.fgb.2007.04.008.

Haarmann T., Rolke Y., Giesbert S., Tudzynski P. (2009): Ergot: from witchcraft to biotechnology. *Molecular Plant Pathology* **10**, 563-577. https://doi.org/10.1111/j.1364-3703.2009.00548.x.

Hammarsten O., Chu G. (1998): DNA-dependent protein kinase: DNA binding and activation in the absence of Ku. *Proceedings of the National Academy of Sciences USA* **95**, 525-30. https://doi.org/10.1073/pnas.95.2.525.

Harris S. D. (2005): Morphogenesis in germinating *Fusarium graminearum* macroconidia. *Mycologia* **97**, 880-887. https://doi.org/10.1080/15572536.2006.11832779.

Havemann J., Vogel D., Loll B., Keller U. (2014): Cyclolization of D-lysergic acid alkaloid peptides. *Chemistry and Biology* **21**, 146-155. https://doi.org/10.1016/j.chembiol.2013.11.008.

Heinstein P. F., Lee S. I., Floss H. G. (1971): Isolation of dimethylallylpyrophosphate: tryptophan dimethylallyl transferase from the ergot fungus (Clavicepsspec.). *Biochemical and Biophysical Research Communications* **44**, 1244-1251. https://doi.org/10.1016/s0006-291x(71)80219-x.

Hellberg H. A. (1958): On the photo-transformation of ergot alkaloids. *Acta Chemica Scandinavica* **12**, 678-683. https://doi.org/10.3891/acta.chem.scand.11-0219

Hillocks R. J. (1992): *Fusarium* wilt. In *Cotton Diseases* (Hillocks R. J., ed.). CABI, Wallingford, UK, pp. 127-160.

Hinsch J, Tudzynski P. (2015): *Claviceps*: The ergot fungus. In *Molecular Biology of Food and Water Borne Mycotoxigenic and Mycotic Fungi* (Paterson R. R. M., Lima N., eds.). CRC Press, Boca Raton, FL, USA, pp. 229-250.

Hinsch J., Vrabka J., Oeser B., Novák O., Galuszka P., Tudzynski P. (2015): *De novo* biosynthesis of cytokinins in the biotrophic fungus *Claviceps purpurea*. *Environmental Microbiology* **17**, 2935-2951. https://doi.org/10.1111/1462-2920.12838.

Hinsch J., Galuszka P., Tudzynski P. (2016): Functional characterization of the first filamentous fungal tRNA-isopentenyltransferase and its role in the virulence of *Claviceps purpurea*. *New Phytologist* **211**, 980-992. https://doi.org/10.1111/nph.13960.

Hitchcock A. S., Chase A. (1951): *Manual of the grasses of the United States*. US Department of Agriculture, Washington, D.C, USA, 1040 pages.

Honda Y., Matsuyama T., Irie T., Watanabe T., Kuwahara M. (2000): Carboxin resistance transformation of the homobasidiomycete fungus *Pleurotus ostreatus*. *Current Genetics* **37**, 209-212. https://doi.org/10.1007/s002940050521.

Hong S. B., Peebles C. A., Shanks J. V., San K. Y., Gibson S. I. (2006): Expression of the Arabidopsis feedback-insensitive anthranilate synthase holoenzyme and tryptophan decarboxylase genes in *Catharanthus roseus* hairy roots. *Journal of Biotechnology* **122**, 28–38. https://doi.org/10.1016/j.jbiotec.2005.08.008.

Hoof J. B., Nødvig C. S., Mortensen U. H. (2018): Genome editing: CRISPR-Cas9. In *Fungal Genomics* (de Vries R. P., Grigoriev I. V., Tsang A., eds.), Humana Press, Totowa, NJ, USA, pp. 119-132. https://doi.org/10.1007/978-1-4939-7804-5_11.

Horng J. S., Chang P. K., Pestka J. J., Linz J. E. (1990): Development of a homologous transformation system for *Aspergillus parasiticus* with the gene encoding nitrate reductase. *Molecular and General Genetics* **224**, 294-296. https://doi.org/10.1007/BF00271564.

Hsu P. D., Scott D. A., Weinstein J. A., Ran F. A., Konermann S., Agarwala V., Li Y., Fine E. J., Wu X., Shalem O., Cradick T. J. (2013): DNA targeting specificity of RNA-guided Cas9 nucleases. *Nature Biotechnology* **31**, 827-832. https://doi.org/10.1038/nbt.2647.

Huang M. C., Cheong W. C., Lim L. S., Li. M. H. (2012): A simple, high sensitivity mutation screening using Ampligase mediated T7 endonuclease I and Surveyor nuclease with microfluidic capillary electrophoresis. *Electrophoresis* **33**, 788-796. https://doi.org/10.1002/elps.201100460.

Hulvová H., Galuszka P., Frébortová J., Frébort I. (2013): Parasitic fungus Claviceps as a source for biotechnological production of ergot alkaloids. *Biotechnology Advances* **31**, 79-89. https://doi.org/10.1016/j.biotechadv.2012.01.005.

Hütter R., DeMoss J. A. (1967): Organization of the tryptophan pathway: a phylogenetic study of the fungi. *Journal of Bacteriology* **94**, 1896–1907.

Hütter R., Niederberger P., DeMoss J. A. (1986): Tryptophan biosynthetic genes in eukaryotic microorganisms. *Annual Reviews in Microbiology* **40**, 55-77. https://doi.org/10.1146/annurev.mi.40.100186.000415.

Idnurm A., Urquhart A. S., Vummadi D. R., Chang S., Van de Wouw A. P., López-Ruiz F. J. (2017): Spontaneous and CRISPR/Cas9-induced mutation of the osmosensor histidine kinase of the canola pathogen *Leptosphaeria maculans*. *Fungal Biology and Biotechnology* **4**, 12. https://doi.org/10.1186/s40694-017-0043-0.

Ilgen P., Hadeler B., Maier F. J., Schäfer W. (2009): Developing kernel and rachis node induce the trichothecene pathway of *Fusarium graminearum* during wheat head infection. *Molecular Plant-Microbe Interactions* **22**, 899-908. https://doi.org/10.1094/MPMI-22-8-0899.

Isakeit T., Odvody G. N., Shelby R. A. (1998): First report of sorghum ergot caused by *Claviceps africana* in the United States. *Plant Disease* **82**, 592. https://doi.org/10.1094/PDIS.1998.82.5.592A.

Ishino Y., Shinagawa H., Makino K., Amemura M., Nakata A. (1987): Nucleotide sequence of the *iap* gene, responsible for alkaline phosphatase isozyme conversion in *Escherichia coli*, and identification of the gene product. *Journal of Bacteriology* **169**, 5429-5433. https://doi.org/ 10.1128/jb.169.12.5429-5433.1987.

Itoh H., Miura A., Matsui M., Arazoe T., Nishida K., Kumagai T., Arita M., Tamano K., Machida M., Shibata T. (2018): Knockout of the SREBP system increases production of the polyketide FR901512 in filamentous fungal sp. No. 14919 and lovastatin in *Aspergillus terreus* ATCC20542. *Applied Microbiology and Biotechnology* **102**, 1393-405. https://doi.org/10.1007/s00253-017-8685-7.

Jameson P. E. (2000): Cytokinins and auxins in plant-pathogen interactions – An overview. *Plant Growth Regulation* **32**, 369-380. https://doi.org/10.1023/A:1010733617543.

Jarvis W. R., Shoemaker R. A. (1978): Taxonomic status of *Fusarium oxysporum* causing foot and root rot of tomato. *Phytopathology* **68**, 1679-1680.

Ji F., Xu J., Liu X., Yin X., Shi J. (2014): Natural occurance of deoxynivalenol and zearalenone in wheat from Jiangsu province, China. *Food Chemistry* **157**, 393-397.

Ji L. J., Kong L. X., Li Q. S., Wang L. S., Chen D., Ma P. (2016): First report of *Fusarium pseudograminearum* causing *Fusarium* head blight of wheat in Hebei Province, China. *Plant Disease* **100**, 220-220. https://doi.org/10.1094/PDIS-06-15-0643-PDN.

Jin F. J., Maruyama J. I., Juvvadi P. R., Arioka M., Kitamoto K. (2004): Adenine auxotrophic mutants of *Aspergillus oryzae*: development of a novel transformation system with triple auxotrophic hosts. *Bioscience, Biotechnology, and Biochemistry* **68**, 656-662. https://doi.org/10.1271/bbb.68.656.

Jinek M., Chylinski K., Fonfara I., Hauer M., Doudna J. A., Charpentier E. A. (2012): programmable dual-RNA–guided DNA endonuclease in adaptive bacterial immunity. *Science*. **337**, 816-821. https://doi.org/ 10.1126/science.1225829.

Jørgensen S. H., Frandsen R. J., Nielsen K. F., Lysøe E., Sondergaard T. E., Wimmer R., Giese H., Sørensen J. L. (2014): *Fusarium graminearum* PKS14 is involved in orsellinic acid and orcinol synthesis. *Fungal Genetics and Biology* **70**, 24-31. https://doi.org/10.1016/j.fgb.2014.06.008.

Jungehülsing U., Arntz C., Smit R., Tudzynski P. (1994): The *Claviceps purpurea* glyceraldehyde-3-phosphate dehydrogenase gene: cloning, characterization, and use for the improvement of a dominant selection system. *Current Genetics* **25**, 101-106. https://doi.org/10.1007/bf00309533.

Kadooka C., Yamaguchi M., Okutsu K., Yoshizaki Y., Takamine K., Katayama T., Maruyama J. I., Tamaki H., Futagami T. (2020): A CRISPR/Cas9-mediated gene knockout systém in *Aspergillus luchuensis* mut. Kawachii. *Bioscience, Biotechnology, and Biochemistry* **84**, 2179-2183. https://doi.org/10.1186/s40694-019-0076-7.

Kallela K., Ettala E. (1984): The oestrogenic Fusarium toxin (zearalenone) in hay as a cause of early abortions in the cow. *Nordisk Veterinaermedicin* **36**, 305-309.

Kang S., Metzenberg R. L. (1990): Molecular analysis of nuc-1+, a gene controlling phosphorus acquisition in *Neurospora crassa*. *Molecular and Cellular Biology* **10**, 5839-5848. https://doi.org/ 10.1128/MCB.10.11.5839.

Kang R., Li G., Zhang M., Zhang P., Wang L., Zhang Y., Chen L., Yuan H., Ding S., Li H. (2020): Expression of *Fusarium pseudograminearum* FpNPS9 in wheat plant and its function in pathogenicity. *Current Genetics* **66**, 229-243. https://doi.org/10.1007/s00294-019-01017-2.

Katayama T., Tanaka Y., Okabe T., Nakamura H., Fujii W., Kitamoto K., Maruyama J. I. (2016): Development of a genome editing technique using the CRISPR/Cas9 system in the industrial filamentous fungus *Aspergillus oryzae*. *Biotechnology Letters* **38**, 637-642. https://doi.org/ 10.1007/s10529-015-2015-x.

Katayama T., Nakamura H., Zhang Y., Pascal A., Fujii W., Maruyama J. (2018): Forced recycling of an AMA1-based genome-editing plasmid allows for efficient multiple gene deletion/integration in the industrial filamentous fungus *Aspergillus oryzae*. *Applied and Environmental Microbiology* **85**, e01896-18. https://doi.org/10.1128/AEM.01896-18.

Katayama T., Nakamura H., Zhang Y., Pascal A., Fujii W., Maruyama J. I. (2019): Forced recycling of an AMA1-based genome-editing plasmid allows for efficient multiple gene deletion/integration in the industrial filamentous fungus *Aspergillus oryzae*. *Applied and Environmental Microbiology* **85**, e01896-18. https://doi.org/ 10.1128/AEM.01896-18.

Kazan K., Manners J. M. (2009): Linking development to defense: auxin in plant–pathogen interactions. *Trends in Plant Science* **14**, 373-382. https://doi.org/10.1016/j.tplants.2009.04.005.

Kazan K., Gardiner D. M. (2018): Fusarium crown rot caused by *Fusarium pseudograminearum* in cereal crops: recent progress and future prospects. *Molecular Plant Pathology* **19**, 1547-1562. https://doi.org/10.1111/mpp.12639.

Keller U., Zocher R., Kleinkauf H. (1980): Biosynthesis of ergotamine in protoplasts of *Claviceps purpurea*. *Microbiology* **118**, 485-494. https://doi.org/10.1099/00221287-118-2-485.

Kelly J. M., Hynes M. J. (1985): Transformation of *Aspergillus niger* by the *amdS* gene of *Aspergillus nidulans*. *The EMBO Journal* **4**, 475-479. https://doi.org/10.1002/j.1460-2075.1985.tb03653.x.

Kemppainen B. W., Riley R. T., Pace J. G. (1988): Skin absorption as a route of exposure for aflatoxin and trichothecenes. *Journal of Toxicology: Toxin reviews* **7**, 95-120. https://doi.org/10.3109/15569548809059728.

Khalaj V., Eslami H., Azizi M., Rovira-Graells N., Bromley M. (2007): Efficient downregulation of *alb1* gene using an AMA1-based episomal expression of RNAi construct in *Aspergillus fumigatus*. *FEMS Microbiology Letters* **270**, 250-254. https://doi.org/10.1111/j.1574-6968.2007.00680.x.

Kia A., McAvoy K., Krishnamurthy K., Trotti D., Pasinelli P. (2018): Astrocytes expressing ALS-linked mutant FUS induce motor neuron death through release of tumor necrosis factor-alpha. *Glia* **66**, 1016–1033. https://doi.org/10.1002/glia.23298.

Kidrič J., Kocjan D., Hadži D. (1986): The biologically active conformation of ergot alkaloids. *Experientia* **42**, 327-328. https://doi.org/10.1007/BF01942524.

Kim J. C., Kang H. J., Lee D. H., Lee Y. W., Yoshizawa T. (1993): Natural occurance of Fusarium mycotoxins (trichothecenes and zearalenone) in barely and corn in Korea. *Applied and Environmental Microbiology* **59**, 3798-3802. https://doi.org/10.1128/AEM.59.11.3798-3802.1993.

Kind S., Hinsch J., Vrabka J., Hradilová M., Majeská-Čudejková M., Tudzynski P., Galuszka P. (2018): Manipulation of cytokinin level in the ergot fungus *Claviceps purpurea* emphasizes its contribution to virulence. *Current Genetics* **64**, 1303-1319. https://doi.org/10.1007/s00294-018-0847-3.

King R., Urban M., Hammond-Kosack M. C., Hassani-Pak K., Hammond-Kosack K. E. (2015): The completed genome sequence of the pathogenic ascomycete fungus *Fusarium graminearum*. *BMC Genomics* **16**, 544. https://doi.org/10.1186/s12864-015-1756-1.

Kistler H. C., Benny U. K. (1988): Genetic transformation of the fungal plant wilt pathogen, *Fusarium oxysporum*. *Current Genetics* **13**, 145-149. https://doi.org/10.1007/BF00365649.

Klein T. M., Wolf E. D., Wu R., Sanford J. C. (1987): High-velocity microprojectiles for delivering nucleic acids into living cells. *Nature* **327**, 70-73. https://doi.org/10.1038/327070a0.

Kobel H., Sanglier J. J. (1973): Qualitative changes in the alkaloid spectrum of *Claviceps purpurea* after mutation. *Genetics of Industrial Microorganisms* **2**, 421-425. https://doi.org/10.1007/BF00273873.

Kolar M., Punt P. J., van den Hondel C. A., Schwab H. (1988): Transformation of *Penicillium chrysogenum* using dominant selection markers and expression of an *Escherichia coli lacZ* fusion gene. *Gene* **62**, 127-134. https://doi.org/10.1016/0378-1119(88)90586-0.

Kos A., Kuijvenhoven J., Wernars K., Bos C. J., Van den Broek H. W. J., Pouwels P. H., Van den Hondel C. A. M. J. J. (1985): Isolation and characterization of the *Aspergillus niger trpC* gene. *Gene* **39**, 231-238. https://doi.org/10.1016/0378-1119(85)90317-8.

Kozák L., Szilágyi Z., Vágó B., Kakuk A., Tóth L., Molnár I., Pócsi I. (2018): Inactivation of the indole-diterpene biosynthetic gene cluster of *Claviceps paspali* by *Agrobacterium*-mediated gene replacement. *Applied Microbiology and Biotechnology* **102**, 3255-3266. https://doi.org/10.1007/s00253-018-8807-x.

Krappmann S., Sasse C., Braus G. H. (2006): Gene targeting in *Aspergillus fumigatus* by homologous recombination is facilitated in a nonhomologous end-joining-deficient genetic background. *Eukaryotic Cell* **5**, 212-215. https://doi.org/ 10.1128/EC.5.1.212-215.2006.

Krupinski V. M., Robbers J. E., Floss H. G. (1976): Physiological study of ergot: induction of alkaloid synthesis by tryptophan at the enzymatic level. *Journal of Bacteriology* **125**, 158-165.

Krska R., Crews C. (2008): Significance, chemistry and determination of ergot alkaloids: A review. *Food Additives and Contaminants* **25**, 722-731. https://doi.org/10.1080/02652030701765756.

Křen V., Pažoutová S., Sedmera P., Rylko V., Řeháček Z. (1986): High-production mutant *Claviceps purpurea* 59 accumulating secoclavines. *FEMS Microbiology Letters* **37**, 31-34. https://doi.org/10.1111/j.1574-6968.1986.tb01761.x.

Křen V., Cvak L. (1999): *Ergot: the genus Claviceps*. CRC Press, Boca Raton, FL, USA, 503 pages.

Kuck U., Hoff B. (2006): Application of the nourseothricin acetyltransferase gene (nat1) as dominant marker for the transformation of filamentous fungi. *Fungal Genetics Newsletter* **53**, 9. https://doi.org/10.4148/1941-4765.1106.

Kuivanen J., Wang Y. M., Richard P. (2016): Engineering *Aspergillus niger* for galactaric acid production: elimination of galactaric acid catabolism by using RNA sequencing and CRISPR/Cas9. *Microbial Cell Factories* **15**, 210. https://doi.org/10.1186/s12934-016-0613-5.

Kuivanen J., Arvas M., Richard, P. (2017): Clustered genes encoding 2-keto-l-gulonate reductase and l-idonate 5-dehydrogenase in the novel fungal d-glucuronic acid pathway. *Frontiers in Microbiology*, **8**, 225. https://doi.org/10.3389/fmicb.2017.00225.

Kulkarni G. B., Sanjeevkumar S., Kirankumar B., Santoshkumar M., Karegoudar T. B. (2013): Indole-3-acetic acid biosynthesis in *Fusarium delphinoides* strain GPK, a causal agent of Wilt in Chickpea. *Applied Biochemistry and Biotechnology* **169**, 1292-1305. https://doi.org/10.1007/s12010-012-0037-6.

Lamprecht S. C., Tewoldemedhin Y. T., Botha W. J., Calitz F. J. (2011): *Fusarium graminearum* species complex associated with maize crowns and roots in the KwaZulu-Natal province of South Africa. *Plant Disease* **95**, 1153-1158. https://doi.org/10.1094/PDIS-02-11-0083.

Langley P., Shuttleworth A., Sidebottom P. J., Wrigley S. K., Fisher P. J. (1990): A trichothecene from *Spicellum roseum*. *Mycological Research* **94**, 705-706. https://doi.org/10.1016/S0953-7562(09)80672-2.

Leath K. T., Kendall W. A. (1978): Fusarium root rot of forage species: pathogenicity and host range. *Phytopathology* **68**, 826-831

Lebrun B., Tardivel C., Félix B., Abysique A, Troadec J. D., Gaigé S., Dallaporta M. (2015): Dysregulation of energy balance by trichothecene mycotoxins: Mechanisms and prospects. *Neurotoxicology* **49**, 15-27. https://doi.org/10.1016/j.neuro.2015.04.009.

Lee S. L., Floss H. G., Heinstein P. (1976): Purification and properties of dimethylallylpyrophosphate: tryptophan dimethylallyl transferase, the first enzyme of ergot alkaloid biosynthesis in *Claviceps*. sp. SD 58. *Archives of Biochemistry and Biophysics* **177**, 84-94. https://doi.org/10.1016/0003-9861(76)90418-5.

Leonard K. J., Bushnell W. R. (2003): *Fusarium Head Blight of Wheat and Barley*. APS Press, St. Paul, MN, USA, 512 pages.

Leplat J., Friberg H., Abid M., Steinberg C. (2013): Survival of *Fusarium graminearum*, the causal agent of Fusarium head blight. A review. *Agronomy for Suistable Development* **33**, 97-111. https://doi.org/10.1007/s13593-012-0098-5.

Leslie J. F., Summerell B. A. (2006): *The Fusarium Laboratory Manual*. Blackwell Publishing, Hoboken, NJ, USA, 369 pages.

Li C., Chen S., Zuo C., Sun Q., Ye Q., Yi G., Huang B. (2011): The use of GFP-transformed isolates to study infection of banana with *Fusarium oxysporum* f. sp. *cubense* race 4. *European Journal of Plant Pathology* **131**, 327-340. https://doi.org/10.1007/s10658-011-9811-5.

Li Y., Burns K. A., Arao Y., Luh C. J., Korach K. S. (2012a): Differential estrogenic actions of endocrine-disrupting chemicals bisphenol A, bisphenol AF, and zearalenone through estrogen receptor α and β *in vitro*. *Environmental Health Perspectives* **120**, 1029-1035. https://doi.org/10.1289/ehp.1104689.

Li H. L., Yuan H. X., Fu B., Xing X. P., Sun B. J., Tang W. H. (2012b): First report of *Fusarium pseudograminearum* causing srown rot of wheat in Henan, China. *Plant Disease* **96**, 1065-1065. https://doi.org/10.1094/PDIS-01-12-0007-PDN.

Liang L., Li J., Cheng L., Ling J., Luo Z., Bai M., Xie B. (2014): A high efficiency gene disruption strategy using a positive–negative split selection marker and electroporation for *Fusarium oxysporum*. *Microbiological Research* **169**, 835-843. https://doi.org/10.1016/j.micres.2014.03.004.

Lieberman A., Kupersmith M., Estey E., Goldstein M. (1976): Treatment of Parkinson's disease with bromocriptine. *New England Journal of Medicine* **295**, 1400-1404. https://doi.org/ 10.1056/NEJM197612162952504 .

Li Y., Fan Y., Xia B., Xiao Q., Wang Q., Sun W., Zhang H., He C. (2017): The immunosuppressive characteristics of FB1 by inhibition of maturation and function of BMDCs. *International Immunopharmacology* **47**, 206-211. https://doi.org/10.1016/j.intimp.2017.03.031.

Liu R., Chen L., Jiang Y., Zhou Z., Zou G. (2015a): Efficient genome editing in filamentous fungus *Trichoderma reesei* using the CRISPR/Cas9 system. *Cell Discovery* **1**, 1-11. https://doi.org/10.1038/celldisc.2015.7.

Liu W., Zhu X., Lei M., Xia Q., Botella J. R., Zhu J. K., Mao Y. (2015b): A detailed procedure for CRISPR/Cas9-mediated gene editing in *Arabidopsis thaliana*. *Science Bulletin* **60**, 1332-1347. https://doi.org/10.1007/s11434-015-0848-2.

Liu Q., Gao R., Li J., Lin L., Zhao J., Sun W., Tian C. (2017): Development of a genome-editing CRISPR/Cas9 system in thermophilic fungal *Myceliophthora species* and its application to hyper-cellulase production strain engineering. *Biotechnology for Biofuels* **10**, 1-14. https://doi.org/10.1186/s13068-016-0693-9.

Logrieco A., Ferracane R., Haidukowsky M., Cozzi G., Visconti A., Ritieni A. (2009): Fumonisin B2 production by Aspergillus niger from grapes and natural accurence in must. *Food Additives and Contaminants* **26**, 1495-1500. https://doi.org/10.1080/02652030903148322.

Lohmeyer M., Dierkes W., Rehm H. J. (1990): Influence of inorganic phosphate and immobilization on *Claviceps purpurea*. *Applied Microbiology and Biotechnology* **33**, 196-201. https://doi.org/10.1007/BF00176524.

Lombard L., Houbraken J., Decock C., Samson R. A., Meeijer M., Réblová M., Groenewald J. Z., Crous P. W. (2016): Generic hyper-diversity in Stachybotriaceae. *Persoonia: Molecular Phylogeny and Evolution of Fungi* **36**, 156. https://doi.org/10.3767/003158516X691582.

Lonowski L.A., Narimatsu Y., Riaz A., Delay C. E., Yang Z., Niola F., Duda K., Ober E. A., Clausen H., Wandall H. H., Hansen S. H., Bennett E. P., Frödin M. (2017): Genome editing using FACS enrichment of nuclease-expressing cells and indel detection by amplicon analysis. *Nature Protocols* **12**, 581–603. https://doi.org/10.1038/nprot.2016.165.

Lorenz N., Haarmann T., Pažoutová S., Jung M., Tudzynski P. (2009): The ergot alkaloid gene cluster: functional analyses and evolutionary aspects. *Phytochemistry* **70**, 1822-1832. https://doi.org/10.1016/j.phytochem.2009.05.023.

Lorenz N., Olšovská J., Šulc M., Tudzynski P. (2010): Alkaloid cluster gene *ccsA* of the ergot fungus *Claviceps purpurea* encodes chanoclavine I synthase, a flavin adenine dinucleotide-containing oxidoreductase mediating the transformation of N-methyl-dimethylallyltryptophan to chanoclavine I. *Applied and Environmental Microbiology* **76**, 1822-1830. https://doi.org/10.1128/AEM.00737-09.

Lorito M., Hayes C. K., DiPietro A., Harman G. E. (1993): Biolistic transformation of *Trichoderma harzianum* and *Gliocladium virens* using plasmid and genomic DNA. *Current Genetics* **24**, 349-356. https://doi.org/10.1007/BF00336788.

Lucas M., Guédon Y., Jay-Allemand C., Godin C., Laplaze L. (2008): An auxin transport-based model of root branching in *Arabidopsis thaliana*. *PLoS One* **3**, e3673. https://doi.org/10.1371/journal.pone.0003673.

Lünne F., Niehaus E. M., Lipinski S., Kunigkeit J., Kalinina S. A., Humpf H. U. (2020): Identification of the polyketide synthase PKS7 responsible for the production of lecanoric acid and ethyl lecanorate in *Claviceps purpurea*. *Fungal Genetics and Biology* **145**, 103481. https://doi.org/10.1016/j.fgb.2020.103481.

Ma Y., Pannicke U., Schwarz K., Lieber M. R. (2002): Hairpin opening and overhang processing by an Artemis/DNA-dependent protein kinase complex in nonhomologous end joining and V (D) J recombination. *Cell* **108**, 781-794. https://doi.org/10.1016/S0092-8674(02)00671-2.

Ma B., Mayfield M. B., Gold M. H. (2003): Homologous expression of *Phanerochaete chrysosporium* manganese peroxidase, using bialaphos resistance as a dominant selectable marker. *Current Genetics* **43**, 407-414. https://doi.org/10.1007/s00294-003-0418-z.

Maaroufi K., Chekir L., Creppy E. E., Ellouz F., Bacha H. (1996): Zearalenone induces modifications of haematological and biochemical parameters in rats. *Toxicon* **34**, 535-540. https://doi.org/10.1016/0041-0101(96)00008-6.Magbanua J. P., Ogawa N., Harashima S., Oshima Y. (1997): The transcriptional activators of the PHO regulon, Pho4p and Pho2p, interact directly with each other and with components of the basal transcription machinery in *Saccharomyces cerevisiae*. *The journal of Biochemistry* **121**, 1182-1189. https://doi.org/10.1093/oxfordjournals.jbchem.a021713.

Malardier L., Daboussi M. J., Julien J., Roussel F., Scazzocchio C., Brygoo Y. (1989): Cloning of the nitrate reductase gene (*niaD*) of *Aspergillus nidulans* and its use for transformation of *Fusarium oxysporum*. *Gene* **78**, 147-156. https://doi.org/10.1016/0378-1119(89)90322-3.

Mann D. F., Floss H. G. (1977): Purification and properties of anthranilate synthetase from the ergot fungus, *Claviceps* spec., strain SD 58. *Lloydia* **40**, 136.

Manstretta V., Rossi V. (2016): Effects of temperature and moisture on development of *Fusarium graminearum* perithecia in maize stalk residues. *Applied and Environmental Microbiology* **82**, 184-191. https://doi.org/10.1128/AEM.02436-15.

Mantle P. G., Nisbet L. J. (1976): Differentiation of *Claviceps purpurea* in axenic culture. *Microbiology* **93**, 321-334. https://doi.org/10.1099/00221287-93-2-321.

Maor R., Puyesky M., Horwitz B. A., Sharon A. (1998): Use of green fluorescent protein (GFP) for studying development and fungal-plant interaction in *Cochliobolus heterostrophus*. *Mycological Research* **102**, 491-496. https://doi.org/10.1017/S0953756297005789.

Maor R., Haskin S., Levi-Kedmi H., Sharon A. (2004): In planta production of indole-3-acetic acid by *Colletotrichum gloeosporioides* f. sp. *aeschynomene*. *Applied and Environmental Microbiology* **70**, 1852-1854. https://doi.org/ 10.1128/AEM.70.3.1852-1854.2004.

Marin S., Magan N., Serra J., Ramos A. J., Canela R., Sanchis V. (1999): Fumonisin B1 production and growth of *Fusarium moniliforme* and *Fusarium proliferatum* on maize, wheat, and barley grain. *Journal of Food Science* **64**, 921-924. https://doi.org/10.1111/j.1365-2621.1999.tb15941.x.

Martin J. D., Dumoulin J. G. (1953): Use of intravenous ergometrine to prevent post-partum haemorrhage. *British Medical Journal* **1**, 643. https://doi.org/10.1136/bmj.1.4811.643.

Matsuda F., Yamada T., Miyazawa H., Miyagawa H., Wakasa K. (2005): Characterization of tryptophan-overproducing potato transgenic for a mutant rice anthranilate synthase alpha-subunit gene (*OASA1D*). *Planta* **222**, 535–545. https://doi.org/10.1007/s00425-005-1565-x.

Matsu-ura T., Baek M., Kwon J., Hong C. (2015): Efficient gene editing in *Neurospora crassa* with CRISPR technology. *Fungal Biology and Biotechnology* **2**, 4. https://doi.org/10.1186/s40694-015-0015-1.

Matsuzaki M., Tatsumi R., Kita K. (2017): Protoplast generation from the ascofuranone-producing fungus *Acremonium sclerotigenum*. *Cytologia* **82**, 317-320. https://doi.org/10.1508/cytologia.82.317.

Matuschek M., Wallwey C., Xie X., Li S. M. (2011): New insights into ergot alkaloid biosynthesis in *Claviceps purpurea*: an agroclavine synthase *EasG* catalyses, via a non-enzymatic adduct with reduced glutathione, the conversion of chanoclavine-I aldehyde to agroclavine. *Organic and Biomolecular Chemistry* **9**, 4328-4335. https://doi.org/10.1039/C0OB01215G.

Matuschek M., Wallwey C., Wollinsky B., Xie X., Li S. M. (2012): In vitro conversion of chanoclavine-I aldehyde to the stereoisomers festuclavine and pyroclavine controlled by the second reduction step. *RSC Advances* **9**, 3662-3669. https://doi.org/ 10.1039/C2RA20104F .

Matz M. V., Fradkov A. F., Labas Y. A., Savitsky A. P., Zaraisky A. G., Markelov M. L., Lukyanov S. A. (1999): Fluorescent proteins from nonbioluminescent *Anthozoa* species. *Nature Biotechnology* **17**, 969-973. https://doi.org/10.1038/13657.

McCormick S. P., Stanley A. M., Stover N. A., Alexander N. J. (2011): Trichothecenes: from simple to complex mycotoxins. *Toxins* **3**, 802-814. https://doi.org/10.3390/toxins3070802.

Metzger U., Schall C., Zocher G., Unsöld I., Stec E., Li S. M., Heide L., Stehle T. (2009): The structure of dimethylallyl tryptophan synthase reveals a common architecture of aromatic prenyltransferases in fungi and bacteria. *Proceedings of the National Academy of Sciences USA* **106**, 14309-14314. https://doi.org/10.1073/pnas.0904897106.

Mey G., Oeser B., Lebrun M. H., Tudzynski P. (2002a): The biotrophic, non-appressorium-forming grass pathogen *Claviceps purpurea* needs a Fus3/Pmk1 homologous mitogen-activated protein kinase for colonization of rye ovarian tissue. *Molecular Plant-Microbe Interactions* **15**, 303-312. https://doi.org/10.1094/MPMI.2002.15.4.303.

Mey G., Held K., Scheffer J., Tenberge K. B., Tudzynski P. (2002b): CPMK2, an SLT2-homologous mitogen-activated protein (MAP) kinase, is essential for pathogenesis of *Claviceps purpurea* on rye: evidence for a second conserved pathogenesis-related MAP kinase cascade in phytopathogenic fungi. *Molecular Microbiology* **46**, 305-318. https://doi.org/10.1046/j.1365-2958.2002.03133.x.

Meyer, V., Mueller D., Strowig T., Stahl U. (2003): Comparison of different transformation methods for *Aspergillus giganteus*. *Current Genetics* **43**, 371-377. https://doi.org/10.1007/s00294-003-0406-3.

Meyer V. (2008): Genetic engineering of filamentous fungi - progress, obstacles and future trends. *Biotechnology Advances* **26**, 177-185. https://doi.org/10.1016/j.biotechadv.2007.12.001.

Michielse C. B., Hooykaas P. J., Van Den Hondel C. A., Ram A. F. (2008): *Agrobacterium*-mediated transformation of the filamentous fungus *Aspergillus awamori*. *Nature Protocols* **3**, 1671. https://doi.org/10.1038/nprot.2008.154.

Miller J. D., Ewen M. A. (1997): Toxic effects of deoxynivalenol on ribosomes and tissues of the spring wheat cultivars Frontana and Casavant. *Natural Toxins* **5**, 234-237. https://doi.org/10.1002/(SICI)1522-7189(1997)5:6<234::AID-NT3>3.0.CO;2-Q.

Miller S. S., Chabot D. M., Oullet T., Harris L. J., Fedak G. (2004): Use of *Fusarium graminearum* strain transformed with green fluorescent protein to study infection in wheat (*Triticum aestivum*). *Canadian Journal of Plant Pathology* **26**, 453-463. https://doi.org/10.1080/07060660409507165.

Miller S. S., Reid L. M., Harris L. J. (2007): Colonization of maize by *Fusarium graminearum*, the causative organism of gibberella ear rot. *Botany* **85**, 369-376. https://doi.org/10.1139/B07-027.

Mirocha C. J., Christensen C. M., Nelson G. H. (1969): Biosynthesis of the fungal estrogen F-2 and a naturally occurring derivative (F-3) by *Fusarium moniliforme*. *Applied Microbiology* **17**, 482.

Mirocha C. J., Abbas H. K., Windels C. E., Xie X. (1989): Variation in deoxynivalenol, 15-acetyldeoxynivalenol, 3-acetyldeoxynivalenol, and zearalenone production by *Fusarium graminearum* isolates. *Applied and Environmental Microbiology* **55**, 1315-1316. https://doi.org/10.1128/AEM.55.5.1315-1316.1989.

Mishra N. C., Szabo G., Tatum E. L. (1973): Nucleic acid-induced genetic changes in *Neurospora*. In *The Role of RNA in Reproduction and Development, Proceedings of the AAAS Symposium* (Niu M. C., Segal S. J., eds.), American Elsevier Pub. Co., New York, NY, USA, pp. 259-268.

Mlynarčíková E. (2015): The deletion of *CpiaaH* gene in the phytopathogenic fungus *Claviceps purpurea*. Diploma thesis, Palacký University, Olomouc, Czech Republic.

Mojica F. J., Díez-Villaseñor C., Soria E., Juez G. (2000): Biological significance of a family of regularly spaced repeats in the genomes of Archaea, Bacteria and mitochondria. *Molecular Microbiology* **36**, 244-246. https://doi.org/10.1046/j.1365-2958.2000.01838.x.

Mojica F. J., Díez-Villaseñor C., García-Martínez J., Almendros C. (2009): Short motif sequences determine the targets of the prokaryotic CRISPR defence system. *Microbiology* **155**, 733-740. https://doi.org/10.1099/mic.0.023960-0.

Moolhuijzen P. M., Manners J. M., Wilcox S. A., Bellgard M. I., Gardiner D. M. (2013): Genome sequences of six wheat-infecting fusarium species isolates. *Genome Announcements* **1**, e0067013. https://doi.org/10.1128/genomeA.00670-13.

Moore P. M., Peberdy J. F. (1976): Release and regeneration of protoplasts from the conidia of *Aspergillus flavus*. *Transactions of the British Mycological Society* **66**, 421-425. https://doi.org/10.1016/S0007-1536(76)80211-2.

Moradi S., Sanjarian F., Safaie N., Mousavi A., Bakhshi Khaniki G. R. (2013): A modified method for transformation of *Fusarium graminearum. Journal of Crop Protection* **2**, 297-304.

Moskowitz M. A. (1992): Neurogenic versus vascular mechanisms of sumatriptan and ergot alkaloids in migraine. *Trends in Pharmacological Sciences* **13**, 307-311. https://doi.org/10.1016/0165-6147(92)90097-P.

Muday G. K. (2001): Auxins and tropisms. *Journal of Plant Growth Regulation* **20**, 226-243. https://doi.org/ 10.1007/s003440010027.

Mullins E. D., Chen X., Romaine P., Raina R., Geiser D. M., Kang S. (2001): *Agrobacterium*-mediated transformation of *Fusarium oxysporum*: an efficient tool for insertional mutagenesis and gene transfer. *Phytopathology* **91**, 173-180. https://doi.org/10.1094/PHYTO.2001.91.2.173.

Munkwold G. P., Carson T., Thoreson D. (1997): Outbreak of ergot (*Claviceps purpurea*) in Iowa barley. *Plant Disease* **81**, 830-830. https://doi.org/10.1094/PDIS.1997.81.7.830A.

Murray G. M., Brennan J. P. (2009): Estimating disease losses to the Australian wheat industry. *Australasian Plant Pathology* **38**, 558-570. https://doi.org/10.1071/AP09053.

Murray J. J., Raid R., Miller C. F., Sandoya Miranda G. V. (2020): First report of *Fusarium oxysporum* f. sp. *lactucae* causing vascular wilt of lettuce in Florida. *Plant Disease* **104**, 3069. https://doi.org/10.1094/PDIS-12-19-2625-PDN.

Musser S. M., Plattner R. D. (1997): Fumonisin composition in cultures of *Fusarium moniliforme, Fusarium proliferatum*, and *Fusarium nygami*. *Journal of Agricultural and Food Chemistry* **45**, 1169-1173. https://doi.org/10.1021/jf960663t.

Nagy G., Szebenyi C., Csernetics Á., Vaz A. G., Tóth E. J., Vágvölgyi C., Papp T. (2017): Development of a plasmid free CRISPR-Cas9 system for the genetic modification of *Mucor circinelloides*. *Scientific Reports* **7**, 1-10. https://doi.org/10.1038/s41598-017-17118-2.

Nahalkova J., Fatehi J. (2003): Red fluorescent protein (DsRed2) as a novel reporter in *Fusarium oxysporum* f. sp. *lycopersici*. *FEMS Microbiology Letters* **225**, 305-309. https://doi.org/10.1016/S0378-1097(03)00534-2.

Nakamura T., Kawanabe Y., Takiyama E., Takahashi N., Murayama T. (1978): Effects of auxin and gibberellin on conidial germination in *Neurospora crassa*. *Plant and Cell Physiology* **19**, 705-709. https://doi.org/10.1093/oxfordjournals.pcp.a075642.

Nakamura T., Tomita K., Kawanabe Y., Murayama T. (1982): Effect of auxin and gibberellin on conidial germination in *Neurospora crassa* II. "Conidial density effect" and auxin. *Plant and Cell Physiology* **23**, 1363-1369. https://doi.org/10.1093/oxfordjournals.pcp.a076483.

Nathues E., Joshi S., Tenberge K. B., von den Driesch M., Oeser B., Bäumer N., Mihlan M., Tudzynski P. (2004): CPTF1, a CREB-like transcription factor, is involved in the oxidative stress response in the phytopathogen *Claviceps purpurea* and modulates ROS level in its host *Secale cereale*. *Molecular Plant-Microbe Interactions* **17**, 383-393. https://doi.org/10.1094/MPMI.2004.17.4.383.

Navarrete K., Roa A., Vaca I., Espinosa Y., Navarro C., Chávez R. (2009): Molecular characterization of the *niaD* and *pyrG* genes from *Penicillium camemberti*, and their use as transformation markers. *Cellular and Molecular Biology Letters* **14**, 692-702. https://doi.org/: 10.2478/s11658-009-0028-y.

Nayak T., Szewczyk E., Oakley C. E., Osmani A., Ukil L., Murray S. L., Hynes M. J., Osmani S. A., Oakley B. R. (2006) A versatile and efficient gene-targeting system for *Aspergillus nidulans*. *Genetics* **172**, 1557-1566. https://doi.org/10.1534/genetics.105.052563.

Nelson P. E., Toussoun T. A., Marasas W. F. O. (1983): *Fusarium Species: an Illustrated Manual for Identification*. Pennsylvania State University Press, State College, PA, USA, 193 pages.

Neubauer L., Dopstadt J., Humpf H. U., Tudzynski P. (2016): Identification and characterization of the ergochrome gene cluster in the plant pathogenic fungus *Claviceps purpurea*. *Fungal Biology and Biotechnology* **3**, 1-14. https://doi.org/10.1186/s40694-016-0020-z.

Nielsen M. L., Isbrandt T., Rasmussen K. B., Thrane U., Hoof J. B., Larsen T. O., Mortensen U. H. (2017): Genes linked to production of secondary metabolites in *Talaromyces atroroseus* revealed using CRISPR-Cas9. *PloS One* **12**, e0169712. https://doi.org/10.1371/journal.pone.0169712.

Ninomiya Y., Suzuki K., Ishii C., Inoue H. (2004): Highly efficient gene replacements in *Neurospora* strains deficient for nonhomologous end-joining. *Proceedings of the National Academy of Sciences USA* **101**, 12248-12253. https://doi.org/10.1073/pnas.0402780101.

Nishimasu H., Ran F. A., Hsu P. D., Konermann S., Shehata S. I., Dohmae N., Ishitani R., Zhang F., Nureki O. (2014): Crystal structure of Cas9 in complex with guide RNA and target DNA. *Cell* **156**, 935-949. https://doi.org/10.1016/j.cell.2014.02.001.

Noël T., Simoneau P., Labarére J. (1995): Heterologous transformation of *Agrocybe aegerita* with a bacterial neomycin-resistance gene fused to a fungal promoter-like DNA sequence. *Theoretical and Applied Genetics* **90**, 1019-1027. https://doi.org/10.1007/BF00222916.

Nødvig C. S., Nielsen J. B., Kogle M. E., Mortensen U. H. (2015): A CRISPR-Cas9 system for genetic engineering of filamentous fungi. *PloS One* **10**, e0133085. https://doi.org/10.1371/journal.pone.0133085.

Nødvig C. S., Hoof J. B., Kogle M. E., Jarczynska Z. D., Lehmbeck J., Klitgaard D. K., Mortensen U. H. (2018): Efficient oligo nucleotide mediated CRISPR-Cas9 gene editing in Aspergilli. *Fungal Genetics and Biology* **115**, 78-89. https://doi.org/ 10.1016/j.fgb.2018.01.004.

Nonomura T., Matsuda Y., Takasugi M., Ootani T., Hasegawa T., Miyajima K., Hatasa T., Toyoda H. (2001): A monitoring systém for green fluorescence protein gene-transformed *Fusarium oxysporum* in melon seedlings. *Journal of General Plant Pathology* **67**, 273-280. https://doi.org/10.1007/PL00013029.

Novák O., Hényková E., Sairanen I., Kowalczyk M., Pospíšil T., Ljung K. (2012): Tissue-specific profiling of the *Arabidopsis thaliana* auxin metabolome. *The Plant Journal* **72**, 523-536. https://doi.org/10.1111/j.1365-313X.2012.05085.x.

Oakley B. R., Rinehart J. E., Mitchell B. L., Oakley C. E., Cannona C., Gray G. L., May G. S. (1987): Cloning, mapping and molecular analysis of the *pyrG* (orotidine-5'-phosphate decarboxylase) gene of *Aspergillus nidulans*. *Gene* **61**, 385-399. https://doi.org/10.1016/0378-1119(87)90201-0.

Obanor F., Neate S., Simpfendorfer S., Sabburg R., Wilson P., Chakraborty S. (2013): *Fusarium graminearum* and *Fusarium pseudograminearum* caused the 2010 head blight epidemics in Australia. *Plant Pathology* **62**, 79-91. https://doi.org/10.1111/j.1365-3059.2012.02615.x.

Oda K., Terado S., Toyoura R., Fukuda H., Kawauchi M., Iwashita K. (2016): Development of a promoter shutoff system in *Aspergillus oryzae* using a sorbitol-sensitive promoter. *Bioscience, Biotechnology, and Biochemistry* **80**, 1792-1801. https://doi.org/10.1080/09168451.2016.1189313.

O´Donnell K., Kistler H. C., Tacke B. K.., Casper H. H. (2000): Gene genealogies reveal global phylogeographic structure and reproductive isolation among lineages of *Fusarium graminearum*, the fungus causing wheat scab. *Proceedings of the National Academy of Sciences USA* **97**, 7905-7910. https://doi.org/10.1073/pnas.130193297.

O´Donnell K., Sarver B. A., Brandt M., Chang D. C., Noble-Wang J., Park B. J., Sutton D. A., Benjamin L., Padhye A., Geiser D. M., Ward T. J. (2007): Phylogenetic diversity and microsphere array-based genotyping of human pathogenic fusaria, including isolates from the multistate contact lens-associated US keratitis outbreaks of 2005 and 2006. *Journal of Clinical Microbiology* **45**, 2235-2248. https://doi.org/10.1128/JCM.00533-07.

O'Donnell K., Rooney A. P., Proctor R. H., Brown D. W., McCormick S. P., Ward T. J., Frandsen R. J., Lysøe E., Rehner S. A., Aoki T., Robert V. A., Crous P. W., Groenewald J. Z., Kang S., Geiser D. M. (2013): Phylogenetic analyses of RPB1 and RPB2 support a middle Cretaceous origin for a clade comprising all agriculturally and medically important fusaria. *Fungal Genetics and Biology* **52**, 20-31. https://doi.org/10.1016/j.fgb.2012.12.004.

Oeser B., Heidrich P. M., Müller U., Tudzynski P, Tenberge K. B. (2002): Polygalacturonase is a pathogenicity factor in the *Claviceps purpurea*/rye interaction. *Fungal Genetics and Biology* **36**, 176-186. https://doi.org/10.1016/S1087-1845(02)00020-8.

Oeser B., Kind S., Schurack S., Schmutzer T., Tudzynski P., Hinsch J. (2017): Cross-talk of the biotrophic pathogen *Claviceps purpurea* and its host *Secale cereale*. *BMC Genomics* **18**, 273. https://doi.org/10.1186/s12864-017-3619-4.

Oka T., Katafuchi T., Fukuda K., Ekino K., Goto M., Nomura Y. (2014): Purification of the GfsA-3x FLAG protein expressed in *Aspergillus nidulans*. *Bio-protocol* **4**, e1222. https://doi.org/ 10.21769/BioProtoc.1222.

Olivain C., Alabouvette C. (1999): Process of tomato root colonization by a pathogenic strain of *Fusarium oxysporum* f. sp. *lycopersici* in comparison with a non-pathogenic strain. *The New Phytologist* **141**, 497-510. https://doi.org/10.1046/j.1469-8137.1999.00365.x.

Oñate-Sánchez L., Vicente-Carbajosa J. (2008): DNA-free RNA isolation protocols for *Arabidopsis thaliana*, including seeds and siliques. *BMC Research Notes* **1**, 93. https://doi.org/10.1186/1756-0500-1-93.

Orbach M. J., Porro E. B., Yanofsky C. (1986): Cloning and characterization of the gene for beta-tubulin from a benomyl-resistant mutant of *Neurospora crassa* and its use as a dominant selectable marker. *Molecular and Cellular Biology* **6**, 2452-2461. https://doi.org/ 10.1128/MCB.6.7.2452.

Oren L., Ezrati S., Cohen D., Sharon A. (2003): Early events in the *Fusarium verticillioides*-maize interaction characterized by using a green fluorescent protein-expressing transgenic isolate. *Applied and Environmental Microbiology* **69**, 1695-1701. https://doi.org/ 10.1128/AEM.69.3.1695-1701.2003.

Orlando B., Barrier-Guillot B., Gourdain E., Maumene C. (2010): Identification of agronomic factors that influence the levels of T-2 and HT-2 toxins in barley grown in France. *World Mycotoxin Journal* **3**, 169-174. https://doi.org/10.3920/WMJ2009.1191.

Ortel I., Keller U. (2009): Combinatorial assembly of simple and complex D-lysergic acid alkaloid peptide classes in the ergot fungus *Claviceps purpurea*. *Journal of Biological Chemistry* **284**, 6650-6660. https://doi.org/ 10.1074/jbc.M807168200.

Osakabe Y., Watanabe T., Sugano S. S., Ueta R., Ishihara R., Shinozaki K., Osakabe K. (2016): Optimization of CRISPR/Cas9 genome editing to modify abiotic stress responses in plants. *Scientific Reports* **6**, 26685. https://doi.org/10.1038/srep26685.

Otsuka H., Quigley F. R., Gröger D., Anderson J. A., Floss H. G. (1980): *In vivo* and *in vitro* evidence for N-methylation as the second pathway-specific step in ergoline biosynthesis1. *Planta Medica* **40**, 109-119. https://doi.org/ 10.1055/s-2008-1074947.

Ozeki K., Kyoya F. F., Hizume K., Kanda A., Hamachi M. (1994): Transformation of intact *Aspergillus niger* by electroporation. *Bioscience, Biotechnology, and Biochemistry* **58**, 2224-2227. https://doi.org/10.1271/bbb.58.2224.

Özarslandan M., Akgül D. S. (2020): First report of *Fusarium oxysporum* f. sp. *cubense* race 4 causing fusarium wilt disease of banana in Turkey. *Plant Disease* **104**, 974. https://doi.org/10.1094/PDIS-09-19-1881-PDN.

Palencia E. R., Mitchell T. R., Snook M. E., Glenn A. E., Gold S., Hinton D. M., Riley R. T., Bacon C. W. (2014): Analyses of black *Aspergillus* species of peanut and maize for ochratoxins and fumonisins. *Journal of Food Protection* **77**, 805-813. https://doi.org/10.4315/0362-028X.JFP-13-321.

Panaccione D. G., McKiernan M., Hanau R. M. (1988): *Colletotrichum graminicola* transformed with homologous and heterologous benomyl-resistance genes retains expected pathogenicity to corn. *Molecular Plant-Microbe Interaction* **1**, 113-120. https://doi.org/10.1094/MPMI-1-113.

Pancaldi D., Tonti S., Prodi A., Salomoni D., Dal Pra M., Nipoti P., Aberti I., Pisi A. (2010): Survey of the main causal agents of fusarium head blight of durum wheat around Bologna, northern Italy. *Phytopathologia Mediterranea* **49**, 258-266. https://doi.org/10.14601/Phytopathol_Mediterr-3442.

Pažoutová S., Tudzynski P. (1999): *Claviceps* sp. PRL 1980 (ATCC 26245), 59 and Pepty 695/ch-I: their true story. *Mycological Research* **103**, 1044-1048. https://doi.org/10.1017/S0953756298008132.

Pažoutová S., Bandyopadhyay R., Frederickson D. E., Mantle P. G., Frederiksen R. A. (2000): Relations among sorghum ergot isolates from the Americas, Africa, India, and Australia. *Plant Disease* **84**, 437-442. https://doi.org/10.1094/PDIS.2000.84.4.437.

Pažoutová S. (2001): The phylogeny and evolution of the genus *Claviceps*. *Mycological Research* **105**, 275-283. https://doi.org/10.1017/S0953756201003562.

Pažoutová S., Kolařík M., Odvody G. N., Fredereckson D. E., Olšovská J., Man P. (2008): A new species complex including *Claviceps fusiformis* and *Claviceps hirtella*. *Fungal Diversity* **31**, 95-110.

Peleg Y., Addison R., Aramayo R., Metzenberg R. L. (1996): Translocation of *Neurospora crassa* transcription factor NUC-1 into the nucleus is induced by phosphorus limitation. *Fungal Genetics and Biology* **20**, 185-191. https://doi.org/10.1006/fgbi.1996.0034.

Piacentini K. C., Savi G. D., Pereira M. E., Scussel V. M. (2015): Fungi and the natural accurence of deoxynivalenol and fumonisins in malting barely (*Hordeum vulgare* L.). *Food Chemistry* **187**, 204-209. https://doi.org/10.1016/j.foodchem.2015.04.101.

Píchová K., Pažoutová S., Kostovčík M., Chudíčková M., Stodůlková E., Novák P., Flieger M., van der Linde E., Kolařík M. (2018): Evolutionary history of ergot with a new infrageneric classification (*Hypocreales: Clavicipitaceae: Claviceps*). *Molecular Phylogenetics and Evolution* **123**, 73-87. https://doi.org/10.1016/j.ympev.2018.02.013.

Pierri L., Pitman I. H., Rae I. D., Winkler D. A., Andrews P. R. (1982): Conformational analysis of the ergot alkaloids ergotamine and ergotaminine. *Journal of Medicinal Chemistry* **25**, 937-942. https://doi.org/10.1021/jm00350a010.

Pleadin J., Sokolović M., Perši N., Zadravec M., Jaki V., Vulić A. (2012): Contamination of maize with deoxynivalenol and zearalenone in Croatia. *Food Control* **28**, 94-98. https://doi.org/10.1016/j.foodcont.2012.04.047.

Ploetz R. C. (2006): Fusarium wilt of banana is caused by several pathogens referred to as *Fusarium oxysporum* f. sp. *cubense*. *Phytopathology* **96**, 653-656. https://doi.org/10.1094/PHYTO-96-0653.

Pohl C., Kiel J. A., Driessen A. J., Bovenberg R. A., Nygard Y. (2016): CRISPR/Cas9 based genome editing of *Penicillium chrysogenum*. *ACS Synthetic Biology* **5**, 754-764. https://doi.org/10.1021/acssynbio.6b00082.

Portnoy T., Margeot A., Linke R., Atanasova L., Fekete E., Sándor E., Hartl L., Karaffa L., Druzhinina I. S., Seiboth B., Le Crom S. (2011): The CRE1 carbon catabolite repressor of the fungus *Trichoderma reesei:* a master regulator of carbon assimilation. *BMC Genomics* **12**, 269. https://doi.org/10.1186/1471-2164-12-269.

Punt P. J., Oliver R. P., Dingemanse M. A., Pouwels, P. H., van den Hondel C. A. (1987): Transformation of *Aspergillus* based on the hygromycin B resistance marker from *Escherichia coli*. *Gene* **56**, 117-124. https://doi.org/10.1016/0378-1119(87)90164-8.

Qin H., Xiao H., Zou G., Zhou Z., Zhong J. J. (2017): CRISPR-Cas9 assisted gene disruption in the higher fungus *Ganoderma* species. *Process Biochemistry* **56**, 57-61. https://doi.org/10.1016/j.procbio.2017.02.012.

Ramamoorthy V., Govindaraj L., Dhanasekaran M., Vetrivel S., Kumar K. K., Ebenezar E. (2015): Combination of driselase and lysing enzyme in one molar potassium chloride is effective for the production of protoplasts from germinated conidia of *Fusarium verticillioides*. *Journal of Microbiological Methods* **111**, 127-134. https://doi.org/10.1016/j.mimet.2015.02.010.

Reineke G., Heinze B., Schirawski J., Buettner H., Kahmann R, Basse C. W. (2008): Indole-3-acetic acid (IAA) biosynthesis in the smut fungus *Ustilago maydis* and its relevance for increased IAA levels in infected tissue and host tumour formation. *Molecular Plant Pathology* **9**, 339-355. https://doi.org/10.1111/j.1364-3703.2008.00470.x.

Riederer B., Han M., Keller U. (1996): D-Lysergyl peptide synthetase from the ergot fungus *Claviceps purpurea*. *Journal of Biological Chemistry* **271**, 27524-27530. https://doi.org/ 10.1074/jbc.271.44.27524.

Riley R. T., Voss K. A., Yool H. S., Gelderblom W. C., Merrill A. H. (1994): Mechanism of fumonisin toxicity and carcinogenesis. *Journal of Food Protection* **57**, 528-535. https://doi.org/10.4315/0362-028X-57.6.528.

Robbers J. E., Robertson L. W., Hornemann K. M., Jindra A., Floss H. G. (1972): Physiological studies on ergot: further studies on the induction of alkaloid synthesis by tryptophan and its inhibition by phosphate. *Journal of Bacteriology* **112**, 791-796. https://doi.org/10.1128/JB.112.2.791-796.1972.

Robinson M., Sharon A. (1999): Transformation of the bioherbicide *Colletotrichum gloeosporioides* f. sp. *aeschynomene* by electroporation of germinated conidia. *Current Genetics* **36**, 98-104. https://doi.org/10.1007/s002940050478.

Robinson S. L., Panaccione D. G. (2014): Heterologous expression of lysergic acid and novel ergot alkaloids in *Aspergillus fumigatus*. *Applied and Environmental Microbiology* **80**, 6465-6472. https://doi.org/ 10.1128/AEM.02137-14.

Robinson S. L., Panaccione D. G. (2015): Diversification of ergot alkaloids in natural and modified fungi. *Toxins* **7**, 201-218. https://doi.org/10.3390/toxins7010201.

Rolke Y., Tudzynski P. (2008): The small GTPase Rac and the p21-activated kinase Cla4 in *Claviceps purpurea*: interaction and impact on polarity, development and pathogenicity. *Molecular Microbiology* **68**, 405-423. https://doi.org/10.1111/j.1365-2958.2008.06159.x.

Roncero M. I., Jepsen L. P., Strøman P., van Heeswijck R. (1989): Characterization of a *leuA* gene and an ARS element from *Mucor circinelloides*. *Gene* **84**, 335-343. https://doi.org/10.1016/0378-1119(89)90508-8.

Ruijter G. J., Visser J. (1997): Carbon repression in *Aspergilli*. *FEMS Microbiology Letters* **151**, 103-114. https://doi.org/10.1111/j.1574-6968.1997.tb12557.x.

Ruiz-Roldán M. C., Köhli M., Roncero M. I. G., Philippsen P., Di Pietro A., Espeso E. A. (2010): Nuclear Dynamics during germination, conidiation, and hyphal fusion of *Fusarium oxysporum*. *Eukaryotic Cell* **9**, 1216-1224. https://doi.org/ 10.1128/EC.00040-10.

Salazar-Cerezo S., Kun R. S., de Vries R. P., Garrigues S. (2020): CRISPR/Cas9 technology enables the development of the filamentous ascomycete fungus *Penicillium subrubescens* as a new industrial enzyme producer. *Enzyme and Microbial Technology* **133**, 109463. https://doi.org/10.1016/j.enzmictec.2019.109463.

Samarut É., Lissouba A., Drapeau P. (2016): A simplified method for identifying early CRISPR-induced indels in zebrafish embryos using High Resolution Melting analysis. *BMC Genomics* **17**, 1-6. https://doi.org/10.1186/s12864-016-2881-1.

Sánchez O., Aguirre J. (1996): Efficient transformation of *Aspergillus nidulans* by electroporation of germinated conidia. *Fungal Genetics Reports* **43**, 48-51. https://doi.org/10.4148/1941-4765.1317.

Saremi H., Ammarellou A., Jafary H. (2007): Incidence of crown rot disease of wheat caused by *Fusarium pseudograminearum* as a new soil born fungal species in north west Iran. *Pakistan Journal of Biological Sciences* **10**, 3606-3612. https://doi.org/10.3923/pjbs.2007.3606.3612.

Sarrocco S., Falaschi N., Vergara M., Nicoletti F., Vannacci G. (2007): Use of *Fusarium oxysporum* f. sp. *dianthi* transformed with marker genes to follow colonization of carnation roots. *Journal of Plant Plant Pathology* **1**, 47-54. http://dx.doi.org/10.4454/jpp.v89i1.723.

Schardl C. L., Young C. A., Hesse U., Amyotte S. G., Andreeva K., Calie P. J., Fleetwood D. J., Haws D. C., Moore N., Oeser B., Panaccione D. G., Schweri K. K., Voisey C. R., Farman M. L., Jaromczyk J. W., Roe B. A., O´Sullivan D. M., Scott B., Tudzynski P., An Z., Arnaudova E. G., Bullock C. T., Charlton N. D., Chen L., Cox M., Dinkins R. D., Florea S., Glenn A. E., Gordon A., GüR. D., Khan A. K., Leistner E., Leuchtmann A., Li C., Liu J., Liu J., Liu M., Mace W., Machado C., Nagabhyru P., Pan J., Schmid J., Sugawara K., Steiner U., Takach J. E., Tanaka E., Webb J. S., Wilson E. V., Wiseman J. L., Yoshida R., Zeng Z. (2013): Plant-symbiotic fungi as chemical engineers: multi-genome analysis of the *Clavicipitaceae* reveals dynamics of alkaloid loci. *PLoS Genetics* **9**, e1003323. https://doi.org/10.1371/journal.pgen.1003323.

Schechtman M. G., Yanofsky C. (1983): Structure of the trifunctional *trp-1* gene from *Neurospora crassa* and its aberrant expression in *Escherichia coli*. *Journal of Molecular and Applied Genetics* **2**, 83.

Scheffer J., Chen C., Heidrich P., Dickman M. B., Tudzynski P. (2005): A CDC42 homologue in *Claviceps purpurea* ais involed in vegetative differentiation and is essential for pathogenicity. *Eukaryotic Cell* **4**, 1228-1238. https://doi.org/10.1128/EC.4.7.1228-1238.2005.

Schumacher J. (2012): Tools for *Botrytis cinerea*: new expression vectors make the gray mold fungus more accessible to cell biology approaches. *Fungal Genetics and Biology* **49**, 483-497. https://doi.org/10.1016/j.fgb.2012.03.005.

Schmauder H. P., Gröger D. (1976): Zur Charakterisierung der Anthranilat-Synthetase bei Claviceps. *Biochemie und Physiologie der Pflanzen* **169**, 471-486. https://doi.org/10.1016/S0015-3796(17)30897-1.

Schumann B., Erge D., Maier W., Gröger D. (1982): A new strain of *Claviceps purpurea* accumulating tetracyclic clavine alkaloids. *Planta Medica* **45**, 11-14. https://doi.org/ 10.1055/s-2007-971231.

Schuster M., Schweizer G., Reissmann S., Kahmann R. (2016): Genome editing in *Ustilago maydis* using the CRISPR–Cas system. *Fungal Genetics and Biology* **89**, 3-9. https://doi.org/10.1016/j.fgb.2015.09.001.

Schuster M., Schweizer G., Kahmann R. (2018): Comparative analyses of secreted proteins in plant pathogenic smut fungi and related basidiomycetes. *Fungal Genetics and Biology* **112**, 21-30. https://doi.org/10.1016/j.fgb.2016.12.003.

Schürmann J., Buttermann D., Herrmann A., Giesbert S., Tudzynski P. (2013): Molecular characterization of the NADPH oxidase complex in the ergot fungus *Claviceps purpurea*: CpNox2 and CpPls1 are important for a balanced host-pathogen interaction. *Molecular Plant-Microbe Interactions* **26**, 1151-1164. https://doi.org/10.1094/MPMI-03-13-0064-R.

Seo J. A., Proctor R. H., Plattner R. D. (2001): Characterization of four clustered and coregulated genes associated with fumonisin biosynthesis in *Fusarium verticillioides. Fungal Genetics and Biology* **34**, 155-165. https://doi.org/10.1006/fgbi.2001.1299.

Seo S., Pokhrel A., Coleman J. J. (2020): The genome sequence of five genotypes of *Fusarium oxysporum* f. sp. *vasinfectum*: A resource for studies on Fusarium wilt of cotton. *Molecular Plant-Microbe Interactions* **33**, 138-40. https://doi.org/10.1094/MPMI-07-19-0197-A.

Shaner N. C., Campbell R. E., Steinbach P. A., Giepmans B. N., Palmer A. E., Tsien R. Y. (2004): Improved monomeric red, orange and yellow fluorescent proteins derived from *Discosoma* sp. red fluorescent protein. *Nature Biotechnology* **22**, 1567-1572. https://doi.org/10.1038/nbt1037.

Shapiro R. S., Chavez A., Porter C. B., Hamblin M., Kaas C. S., DiCarlo J. E., Zeng G., Xu X., Revtovich A. V., Kirienko N. V., Wang Y. (2018): A CRISPR–Cas9-based gene drive platform for genetic interaction analysis in *Candida albicans*. *Nature Microbiology* **3**, 73-82. https://doi.org/10.1038/s41564-017-0043-0.

Sharma K. K., Kuhad R. C. (2010): Genetic transformation of lignin degrading fungi facilitated by *Agrobacterium tumefaciens*. *BMC Biotechnology* **10**, 1-8. https://doi.org/10.1186/1472-6750-10-67.

Sharma N., Sharma V. K., Manikyam H. K., Krishna A. B. (2016): Ergot alkaloids: a review on therapeutic applications. *European Journal of Medicinal Plants* **14**, 1-17. https://doi.org/10.9734/EJMP/2016/25975.

Shi T. Q., Gao J., Wang W. J., Wang K. F., Xu G. Q., Huang H., Ji X. J. (2019): CRISPR/Cas9-based genome editing in the filamentous fungus *Fusarium fujikuroi* and its application in strain

engineering for gibberellic acid production. *ACS Synthetic Biology* **8**, 445-454. https://doi.org/10.1021/acssynbio.8b00478.

Shimomura O., Johnson F. H., Saiga Y. (1962): Extraction, purification and properties of aequorin, a bioluminescent protein from the luminous hydromedusan, Aequorea. *Journal of Cellular and Comparative Physiology* **59**, 223-239. https://doi.org/10.1002/jcp.1030590302.

Sibanda B. L., Critchlow S. E., Begun J., Pei X. Y., Jackson S. P., Blundell T. L., Pellegrini L. (2001): Crystal structure of an Xrcc4–DNA ligase IV complex. *Nature Structural and Molecular Biology* **8**, 1015-1019. https://doi.org/10.1038/nsb725.

Silverman R. B., Groziak M. P. (1982): Model chemistry for a covalent mechanism of action of orotidine 5'-phosphate decarboxylase. *Journal of the American Chemical Society* **104**, 6434–6439. https://doi.org/10.1021/ja00387a047.

Skadsen R. W., Hohn T. M. (2004): Use of *Fusarium graminearum* transformed with gfp to follow infection patterns in barely and Arabidopsis. *Physiological and Molecular Plant Pathology* **64**, 45-53. https://doi.org/10.1016/j.pmpp.2004.04.003.

Smit R., Tudzynski P. (1992): Efficient transformation of *Claviceps purpurea* using pyrimidine auxotrophic mutants: cloning of the OMP decarboxylase gene. *Molecular and General Genetics* **234**, 297-305. https://doi.org/10.1007/BF00283850.

Smith J. L., Bayliss F. T., Ward M. (1991): Sequence of the cloned *pyr4* gene of *Trichoderma reesei* and its use as a homologous selectable marker for transformation. *Current Genetics* **19**, 27-33. https://doi.org/10.1007/BF00362084.

Smith D. J., Shappell N. W. (2002): Epimerization of ergopeptine alkaloids in organic and aqueous solvents. *Journal of Animal Science* **80**, 1616-1622. https://doi.org/10.2527/2002.8061616x.

Somma S., Petruzzella A. L., Logrieco A. F., Meca G., Cacciola O. S., Moretti A. (2014): Phylogenetic analyses of Fusarium gramminearum strains from cereals in Italy, and characterization of their molecular and chemical chemotypes. *Crop and Pasture Science* **65**, 52-60. https://doi.org/10.1071/CP13314.

Sørensen L. Q., Lysøe E., Larsen J. E., Khorsand-Jamal P., Nielsen K. F., Frandsen R. J. N. (2014): Genetic transformation of *Fusarium avenaceum* by *Agrobacterium tumefaciens* mediated transformation and the development of a USER-Brick vector construction system. *BMC Molecular Biology* **15**, 15. https://doi.org/10.1186/1471-2199-15-15.

Spagnolo L., Rivera-Calzada A., Pearl L. H., Llorca O. (2006): Three-dimensional structure of the human DNA-PKcs/Ku70/Ku80 complex assembled on DNA and its implications for DNA DSB repair. *Molecular Cell* **22**, 511-519. https://doi.org/10.1016/j.molcel.2006.04.013.

Stanković S., Lević J., Ivanović G., Tančić S. (2012): Fumonisin B1 and its co-occurrence with other fusariotoxins in naturally-contaminated wheat grain. *Food Control* **23**, 384-388. https://doi.org/10.1016/j.foodcont.2011.08.003.

Stoll A. Highly active preparation of ergot and process of makingsame. US1394233A, 1921. https://patents.google.com/patent/US1394233A/en.

Strnadová K. (1964): UV-mutanten bei *Claviceps purpurea. Planta Medica* **12**, 521-527.

Strnadová K. (1967): Der Alkaloidgehalt und der Alkaloidtyp auxotropher UV-Mutanten des Mutterkorns (*Claviceps purpurea* [FR.] TUL.) bei parasitischer Kultur auf Roggen. *Flora oder Allgemeine botanische Zeitung. Abt. A, Physiologie und Biochemie* **157**, 517-523. https://doi.org/10.1016/S0367-1836(17)30069-1.

Strnadová K. (1976): A method of preparation and application of nitrous acid as a mutagen in *Claviceps purpurea. Folia Microbiologica* **21**, 455-458. https://doi.org/10.1007/BF02876936.

Strnadová K., Kybal J. (1976): Morphological changes of *Claviceps purpurea* induced by the mutagenic effect of nitrous acid. *Planta Medica* **30**, 395-398.

Studt L., Humpf H. U., Tudzynski B. (2013a): Signaling governed by G proteins and cAMP is crucial for growth, secondary metabolism and sexual development in *Fusarium fujikuroi*. *PloS One* **8**, e58185. https://doi.org/10.1371/journal.pone.0058185.

Studt L., Schmidt F. J., Jahn L., Sieber C. M., Connolly L. R., Niehaus E. M., Freitag M., Humpf H. U., Tudzynski B. (2013b): Two histone deacetylases, FfHda1 and FfHda2, are important for *Fusarium fujikuroi* secondary metabolism and virulence. *Applied and Environmental Microbiology* **79**, 7719-7734. https://doi.org/ 10.1128/AEM.01557-13 .

Sugui J. A., Chang Y. C., Kwon-Chung K. J. (2005): *Agrobacterium tumefaciens*-mediated transformation of *Aspergillus fumigatus*: an efficient tool for insertional mutagenesis and targeted gene disruption. *Applied and Environmental Microbiology* **71**, 1798-1802. https://doi.org/ 10.1128/AEM.71.4.1798-1802.2005.

Summerell B. A., Salleh B., Leslie J. F. (2003): A utilitarian approach to Fusarium identification. *Plant Disease* **87**, 117-128. https://doi.org/10.1094/PDIS.2003.87.2.117.

Sutton J. C. (1982): Epidemiology of wheat head blight and maize ear rot caused by *Fusarium graminearum*. *Canadian Journal of Plant Pathology* **4**, 195-209. https://doi.org/10.1080/07060668209501326.

Suzuki C. A., Hierlihy L., Barker M., Curran I., Mueller R., Bondy G. S. (1995): The effects of fumonisin B1 on several markers of nephrotoxicity in rats. *Toxicology and Applied Pharmacology* **133**, 207-214. https://doi.org/10.1006/taap.1995.1143.

Taj-Aldeen S. J., Gene J., Bozom I. A., Buzina W., Cano J. F., Guarro J. (2006): Gangrenous necrosis of the diabetic foot caused by *Fusarium acutatum*. *Medical Mycology* **44**, 547-552. https://doi.org/10.1080/13693780500543246.

Takahashi T., Masuda T., Koyama Y. (2006): Enhanced gene targeting frequency in *ku70* and *ku80* disruption mutants of *Aspergillus sojae* and *Aspergillus oryzae*. *Molecular Genetics and Genomics* **275**, 460-470. https://doi.org/10.1007/s00438-006-0104-1.

Tekauz A., McCallum B., Gilbert J. (2000): Fusarium head blight of barely in western Canada. *Canadian Journal of Plant Pathology* **22**, 9-16. https://doi.org/10.1080/07060660009501156.

Tekauz A., McCallum B., Ames N., Fetch J. M. (2004): Fusarium head blight of oat - current status in western Canada. *Canadian Journal of Plant Pathology* **26**, 473-479. https://doi.org/10.1080/07060660409507167.

Tenberge, K. B., Homann, V., Oeser, B., Tudzynski, P. (1996): Structure and expression of two polygalacturonase genes of *Claviceps purpurea* oriented in tandem and cytological evidence for pectinolytic enzyme activity during infection of rye. *Phytopthology* **86**, 1084-1097.

Thompson W. L., Wannemachel Jr R. W. (1990): In vivo effects of T-2 mycotoxin on synthesis of proteins and DNA in rat tissues. *Toxicology and Applied Pharmacology* **105**, 483-491. https://doi.org/10.1016/0041-008X(90)90151-J.

Tilburn J. Scazzocchio C., Taylor G. G., Zabicky-Zissman J. H., Lockington R. A., Davies R. W. (1983): Transformation by integration in *Aspergillus nidulans*. *Gene* **26**, 205-221. https://doi.org/10.1016/0378-1119(83)90191-9

Tilburn J., Sarkar S., Widdick D. A., Espeso E. A., Orejas M., Mungroo J., Penalva M. A., Arst H. N. (1995): The *Aspergillus PacC* zinc finger transcription factor mediates regulation of both acid-and alkaline-expressed genes by ambient pH. *The EMBO Journal* **14**, 779-790. https://doi.org/10.1002/j.1460-2075.1995.tb07056.x.

Tommassen J., de Geus P., Lugtenberg B., Hackett J., Reeves P. (1982): Regulation of the pho regulon of *Escherichia coli* K-12. *Journal of Molecular Biology* **157**, 265-274. https://doi.org/10.1016/0022-2836(82)90233-9.

Trail F. (2009): For blighted waves of grain: *Fusarium graminearum* in the postgenomics era. *Plant Physiology* **149**, 103-110. https://doi.org/10.1104/pp.108.129684.

Trapp S. C., Hohn T. M., McCormick S., Jarvis B. B. (1998): Characterization of the gene cluster for biosynthesis of macrocyclic trichothecenes in *Myrothecium roridum*. *Molecular and General Genetics* **257**, 421-432. https://doi.org/10.1007/s004380050666.

Tsai H. F., Wang H., Gebler J. C., Poulter C. D., Schardl C. L. (1995): The *Claviceps purpurea* gene encoding dimethylallyltryptophan synthase, the committed step for ergot alkaloid biosynthesis. *Biochemical and Biophysical Research Communications* **216**, 119-125. https://doi.org/10.1006/bbrc.1995.2599.

Tsai F. Y., Brotherton J. E., Widholm J. M. (2005): Overexpression of the feedback-insensitive anthranilate synthase gene in tobacco causes tryptophan accumulation. *Plant Cell Reports* **23**, 548–556. https://doi.org/10.1007/s00299-004-0849-0.

Tsukuda T., Carleton S., Fotheringham S., Holloman W. K. (1988): Isolation and characterization of an autonomously replicating sequence from *Ustilago maydis*. *Molecular and Cellular Biology* **8**, 3703-3709. https://doi.org/ 10.1128/MCB.8.9.3703.

Tsavkelova E., Oeser B., Oren-Young L., Israeli M., Sasson Y., Tudzynski B., Sharon A. (2012): Identification and functional characterization of indole-3-acetamide-mediated IAA biosynthesis in plant-associated *Fusarium* species. *Fungal Genetics and Biology* **49**, 48-57. https://doi.org/10.1016/j.fgb.2011.10.005.

Tsukiboshi T., Shimanuki T., Koga H. (2001): *Claviceps sorghicola* and *C. africana*, the ergot pathogens of sorghum, and their cultural control in Japan. *Japan Agricultural Research Quarterly* **35**, 221-226. https://doi.org/10.6090/jarq.35.221.

Tudzynski P., Esser K., Gröschel H. (1982): Genetics of the ergot fungus *Claviceps purpurea*. *Theoretical and Applied Genetics* **61**, 97-100. https://doi.org/10.1007/BF00273873.

Tudzynski P., Hölter K., Correia T., Arntz C., Grammel N., Keller U. (1999): Evidence for an ergot alkaloid gene cluster in *Claviceps purpurea*. *Molecular and General Genetics* **261**, 133-41. https://doi.org/10.1007/s004380050950.

Tudzynski P., Scheffer J. A. N. (2004): Claviceps purpurea: molecular aspects of a unique pathogenic lifestyle. *Molecular Plant Pathology* **5**, 377-388. https://doi.org/10.1111/j.1364-3703.2004.00237.x.

Ueta R., Abe C., Watanabe T., Sugano S.S., Ishihara R., Ezura H., Osakabe Y., Osakabe K. (2017): Rapid breeding of parthenocarpic tomato plants using CRISPR/Cas9. *Scientific Reports* **7**, 1-8. https://doi.org/10.1038/s41598-017-00501-4.

Ulaganathan K., Goud S., Reddy M., Kayalvili U. (2017): Genome engineering for breaking barriers in lignocellulosic bioethanol production. *Renewable and Sustainable Energy Reviews* **74**, 1080-1107. https://doi.org/10.1016/j.rser.2017.01.028.

Unsöld I. A., Li S. M. (2005): Overproduction, purification and characterization of FgaPT2, a dimethylallyltryptophan synthase from *Aspergillus fumigatus*. *Microbiology* **151**, 1499-1505. https://doi.org/10.1099/mic.0.27759-0.

van Bakel J. M. M., Kerstens J. A. (1970): Footrot in asparágus caused by *Fusarium oxysporum* f. sp. *asparagi*. *Netherlands Journal of Plant Pathology* **76**, 320-325. https://doi.org/10.1007/BF03041363.

vann de Walle J., Sergent T., Piront N., Toussaint O., Schneider Y. J., Larondelle Y. (2010): Deoxynivalenol affects in vitro intestinal epithelial cell barrier integrity through inhhibition of protein synthesis. *Toxicology and Applied Pharmacology* **245**, 291-298. https://doi.org/10.1016/j.taap.2010.03.012.

van Engelenburg F., Smit R., Goosen T., van den Broek H., Tudzynski P. (1989): Transformation of *Claviceps purpurea* using a bleomycin resistance gene. *Applied Microbiology and Biotechnology* **30**, 364-370. https://doi.org/10.1007/BF00296625.

van Hartingsveldt W., Mattern I. E., van Zeijl C. M., Pouwels P. H., van den Hondel C. A. (1987): Development of a homologous transformation system for *Aspergillus niger* based on the *pyrG* gene. *Molecular and General Genetics* **206**, 71-75. https://doi.org/10.1007/BF00326538.

van Heeswijck R. (1986): Autonomous replication of plasmids in *Mucor* transformants. *Carlsberg Research Communications* **51**, 433. https://doi.org/10.1007/BF02907316 .

van Leeuwe T. M., Arentshorst M., Ernst T., Alazi E., Punt P. J., Ram A. F. (2019): Efficient marker free CRISPR/Cas9 genome editing for functional analysis of gene families in filamentous fungi. *Fungal Biology and Biotechnology* **6**, 13. https://doi.org/10.1186/s40694-019-0076-7.

Vanegas K. G., Jarczynska Z. D., Strucko T., Mortensen U. H. (2019): Cpf1 enables fast and efficient genome editing in *Aspergilli*. *Fungal Biology and Biotechnology* **6**, 6. https://doi.org/10.1186/s40694-019-0069-6.

Vannini G. L., Poli F., Donini A., Pancaldi S. (1983): Effects of Congo red on wall synthesis and morphogenesis in *Saccharomyces cerevisiae*. *Plant Science Letters* **31**, 9-17. https://doi.org/10.1016/0304-4211(83)90125-6.

Varadarajalu L. P., Punekar N. S. (2005): Cloning and use of *sC* as homologous marker for *Aspergillus niger* transformation. *Journal of Microbiological Methods* **61**, 219-224. https://doi.org/10.1016/j.mimet.2004.11.022.

Vining L. C. (1970): Effect of tryptophan on alkaloid biosynthesis in cultures of a *Claviceps* species. *Canadian Journal of Microbiology* **16**, 473-480. https://doi.org/10.1139/m70-080.

Visser M., Gordon T. R., Wingfield B. D., Wingfield M. J., Viljoen A. (2004): Transformation of *Fusarium oxysporum* f. sp. *cubense*, causal agent of Fusarium wilt of banana, with the green fluorescent protein (GFP) gene. *Australasian Plant Pathology* **33**, 69-75. https://doi.org/10.1071/AP03084.

Vyas V. K., Barrasa M. I., Fink G. R. (2015): A Candida albicans CRISPR system permits genetic engineering of essential genes and gene families. *Science Advances* **1**, e1500248. https://doi.org/10.1126/sciadv.1500248.

Walker J. R., Corpina R. A., Goldberg J. (2001a): Structure of the *Ku* heterodimer bound to DNA and its implications for double-strand break repair. *Nature* **412**, 607-614. https://doi.org/10.1038/35088000.

Walker S. L., Leath S., Hagler Jr W. M., Murphy J. P. (2001b): Variation among isolates of *Fusarium graminearum* associated with *Fusarium* head blight in North Carolina. *Plant Disease* **85**, 404-410. https://doi.org/10.1094/PDIS.2001.85.4.404.

Wallwey C., Matuschek M., Li S. M. (2010): Ergot alkaloid biosynthesis in *Aspergillus fumigatus*: conversion of chanoclavine-I to chanoclavine-I aldehyde catalyzed by a short-chain alcohol dehydrogenase FgaDH. *Archives of Microbiology* **192**, 127-134. https://doi.org/10.1007/s00203-009-0536-1.

Walzel B., Riederer B., Keller U. (1997): Mechanism of alkaloid cyclopeptide synthesis in the ergot fungus *Claviceps purpurea*. *Chemistry and Biology* **4**, 223-230. https://doi.org/10.1016/S1074-5521(97)90292-1.

Wang P. M., Choera T., Wiemann P., Pisithkul T., Amador-Noguez D., Keller N. P. (2016): *TrpE* feedback mutants reveal roadblocks and conduits toward increasing secondary metabolism in *Aspergillus fumigatus*. *Fungal Genetics and Biology* **89**, 102–113. https://doi.org/10.1016/j.fgb.2015.12.002.

Wang Q., Cobine P. A., Coleman J. J. (2018): Efficient genome editing in *Fusarium oxysporum* based on CRISPR/Cas9 ribonucleoprotein complexes. *Fungal Genetics and Biology* **117**, 21-29. https://doi.org/10.1016/j.fgb.2018.05.003.

Ward J. F., Evans J. W., Limoli C. L., Calabro-Jones P. M. (1987): Radiation and hydrogen peroxide induced free radical damage to DNA. *The British Journal of Cancer* **55**, 105-112.

Waśkiewicz A., Gromadzka K., Wiśniewska H., Goliński P. (2008): Accumulation of zearalenone in genotypes of spring wheat after inoculation with *Fusarium culmorum*. *Cereal Research Communications* **36**, 401-403.

Weidner G., d'Enfert C., Koch A., Mol P. C., Brakhage A. A. (1998): Development of a homologous transformation system for the human pathogenic fungus *Aspergillus fumigatus* based on the pyrG gene encoding orotidine 5′-monophosphate. *Current Genetics* **33**, 378-385. https://doi.org/10.1007/s002940050350.

Wernars K., Goosen T., Wennekes B. M., Swart K., van den Hondel C. A., van den Broek H. W. (1987): Cotransformation of *Aspergillus nidulans*: a tool for replacing fungal genes. *Molecular and General Genetics MGG* **209**, 71-77. https://doi.org/10.1007/BF00329838.

Wenderoth M., Pinecker C., Voß B., Fischer R. (2017): Establishment of CRISPR/Cas9 in *Alternaria alternata*. *Fungal Genetics and Biology* **101**, 55-60. https://doi.org/10.1016/j.fgb.2017.03.001.

Weyda I., Yang L., Vang J., Ahring B. K., Lübeck M., Lübeck P. S. (2017): A comparison of *Agrobacterium*-mediated transformation and protoplast-mediated transformation with CRISPR-Cas9 and bipartite gene targeting substrates, as effective gene targeting tools for *Aspergillus carbonarius*. *Journal of Microbiological Methods* **135**, 26-34. https://doi.org/10.1016/j.mimet.2017.01.015.

Whitehead M. P., Unkles S. E., Ramsden M., Campbell E. I., Gurr S. J., Spence D., van den Hondel C., Contreras R., Kinghorn J. R. (1989): Transformation of a nitrate reductase deficient mutant of *Penicillium chrysogenum* with the corresponding *Aspergillus niger* and *A. nidulans niaD* genes. *Molecular and General Genetics MGG* **216**, 408-411. https://doi.org/10.1007/BF00334383.

Wilkins K., Nielsen K. F., Din S. U. (2003): Patterns of volatile metabolites and nonvolatile trichothecenes produced by isolates of *Stachybotrys*, *Fusarium*, *Trichoderma*, *Trichothecium* and *Memnoniella*. *Environmental Science and Pollution Research* **10**, 162. https://doi.org/10.1065/espr2002.05.118.

Winston F., Dollaerd C., Ricupero-Hovasse S. L. (1995): Construction of a set of convenient *Saccharomyces cerevisiae* strains that are isogenic to S288C. *Yeast* **11**, 53-55. https://doi.org/10.1002/yea.320110107.

Wright M. C., Philippsen P. (1991): Replicative transformation of the filamentous fungus *Ashbya gossypii* with plasmids containing *Saccharomyces cerevisiae* ARS elements. *Gene* **109**, 99-105. https://doi.org/10.1016/0378-1119(91)90593-Z.

Xu F., Song Y. L., Wang J. M., Liu L. L., Zhao K. (2017): Occurence of *Fusarium* crown rot caused by *Fusarium pseudograminearum* on barley in China. *Plant Disease* **101**, 837-837. https://doi.org/10.1094/PDIS-10-16-1436-PDN.

Yamada T. (1993): The role of auxin in plant-disease development. *Annual Review of Phytopathology* **31**, 253-273. https://doi.org/10.1146/annurev.py.31.090193.001345.

Yang J. Y., Wang G. X., Liu J. L., Fan J. J., Cui S. (2007): Toxic effects of zearalenone and its derivatives α-zearalenol on male reproductive systém in mice. *Reproductive Toxicology* **24**, 381-387. https://doi.org/10.1016/j.reprotox.2007.05.009.

Yang K., Liang L., Ran F., Liu Y., Li Z., Lan H., Gao P., Zhuang Z., Zhang F., Nie X., Yirga S. K. (2016): The DmtA methyltransferase contributes to *Aspergillus flavus* conidiation, sclerotial production, aflatoxin biosynthesis and virulence. *Scientific Reports* **6**, 1-3. https://doi.org/10.1038/srep23259.

Yang X., Liu P., Cui Y., Xiao B., Liu M., Song M., Huang W., Li Y. (2020): Review of the reproductive toxicity of T-2 toxin. *Journal of Agricultural and Food Chemistry* **68**, 727-734. https://doi.org/10.1021/acs.jafc.9b07880.

Yao Y., An C., Evans D., Liu W., Wang W., Wei G., Ding N., Houk K. N., Gao, S. S. (2019): Catalase involved in oxidative cyclization of the tetracyclic ergoline of fungal ergot alkaloids. *Journal of the American Chemical Society* **44**, 17517-17521. https://doi.org/10.1021/jacs.9b10217.

Yoo S., Dynan W. S. (1999): Geometry of a complex formed by double strand break repair proteins at a single DNA end: recruitment of DNA-PKcs induces inward translocation of Ku protein. *Nucleic Acids Research* **27**, 4679-4686. https://doi.org/10.1093/nar/27.24.4679.

Young L. G., Ping H., King G. J. (1990): Effects of feeding zearalenone to sows on rebreeding and pregnancy. *Journal of Animal Science* **68**, 15-20. https://doi.org/10.2527/1990.68115x.

Yoshizawa T., Jin Y. Z. (1995): Natural occurrence of acetylated derivatives of deoxynivalenol and nivalenol in wheat and barley in Japan. *Food Additives and Contaminants* **12**, 689-694. https://doi.org/10.1080/02652039509374358.

Zhang C., Meng X., Wei X., Lu L. (2016): Highly efficient CRISPR mutagenesis by microhomology-mediated end joining in *Aspergillus fumigatus*. *Fungal Genetics and Biology* **86**, 47-57. https://doi.org/10.1016/j.fgb.2015.12.007.

Zhang Y., Wang L., Liang S., Zhang P., Kang R., Zhang M., Wang M., Chen L., Yuan H., Ding S., Li H. (2020): FpDep1, a component of Rpd3L histone deacetylase complex, is important for vegetative development, ROS accumulation, and pathogenesis in *Fusarium pseudograminearum*. *Fungal Genetics and Biology* **135**, 103299. https://doi.org/10.1016/j.fgb.2019.103299.

Zheng X., Yang S., Zhang D., Zhong Z., Tang X., Deng K., Zhou J., Qi Y., Zhang Y. (2016): Effective screen of CRISPR/Cas9-induced mutants in rice by single-strand conformation polymorphism. *Plant Cell Reports* **35**, 1545–1554. https://doi.org/10.1007/s00299-016-1967-1.

Zheng Y. M., Lin F. L., Gao H., Zou G., Zhang J. W., Wang G. Q., Chen G. D., Zhou Z. H., Yao X. S., Hu D. (2017): Development of a versatile and conventional technique for gene disruption in filamentous fungi based on CRISPR-Cas9 technology. *Scientific Reports* **7**, 1-10. https://doi.org/10.1038/s41598-017-10052-3.

Zheng X., Zheng P., Zhang K., Cairns T. C., Meyer V., Sun J., Ma Y. (2018): 5S rRNA promoter for guide RNA expression enabled highly efficient CRISPR/Cas9 genome editing in *Aspergillus niger*. *ACS Synthetic Biology* **8**, 1568-1574. https://doi.org/10.1021/acssynbio.7b00456.

8 Abbreviations

ΔTrpE	mutants lacking *TrpE* prepared by HR
Δ+CRISPR/Cas9 TrpE	mutants lacking *TrpE* prepared by CRISPR/Cas9-mediated HDR
4-DMAT	4-(γ,γ)-dimethylallyltryptophan
ade2	gene encoding phosphoribosylaminoimidazole carboxylase involved in purine biosynthesis
adeA	gene encoding phosphoribosylaminoimidazolesuccinocarboxamide synthase involved in purine biosynthesis
adeB	gene encoding phosphoribosylaminoimidazole carboxylase involved in purine biosynthesis
albA	gene encoding polyketide synthase involved in the biosynthesis of green conidial pigment
AMA1	autonomous maintenance in *Aspergillus*
AMT	*Agrobacterium*-mediated transformation
argB	gene encoding ornithine carbamoyltransferase involved in arginine biosynthesis
ARSs	autonomously replicating sequences
carB	gene encoding phytoene dehydrogenase involved in the biosynthesis of β-carotene
cloA	gene encoding NAPDH-dependent cytochrome P450 involved in ergot alkaloid biosynthesis
clr2	gene encoding a transcription factor that regulates xylanase genes
CPUR_05013.1	*TrpE* gene encoding α-subunit of anthranilate synthase
CPUR_04075.1	*easH* gene encoding dioxygenase
CPUR_04076.1	*dmaW* gene encoding DMAT synthase
CPUR_04077.1	*easG* gene encoding reductase
CPUR_04078.1	*easF* gene encoding DMAT N-methyltransferase
CPUR_04079.1	*easE* gene encoding chanoclavine-I-synthase
CPUR_04080.1	*easD* gene encoding chanoclavine-I-dehydrogenase
CPUR_04081.1	*easC* gene encoding catalase
CPUR_04082.1	*cloA* gene encoding NADPH-dependent cytochrome P450
CPUR_04083.1	*lpsB* gene encoding nonribosomal lysergyl peptide synthetase LPS2
CPUR_04084.1	*easA* gene encoding chanoclavine-I-aldehyde oxidoreductase
CR	crown rot
CRISPR/Cas	Clustered Regularly Interspaced Short Palindromic Repeat/CRISPR Activated System
CRISPR/Cas9 pyr4	mutants with a mutation in *pyr4* prepared by CRISPR/Cas9
CRISPR/Cas9 TrpE	mutants with a mutation in *TrpE* prepared by CRISPR/Cas9
crRNA	CRISPR RNA
DBS	double-stranded DNA break
DMAPP	dimethylallyl diphosphate
dmaW	gene encoding DMAT synthase involved in ergot alkaloid biosynthesis
DNA-PK	DNA-dependent protein kinase
DON	deoxynivalenol
dpi	days post inoculation
EA	ergot alkaloids
easA	gene encoding chanoclavine-I aldehyde oxidoreductase involved in ergot alkaloid biosynthesis
easC	gene encoding catalase/decarboxylase involved in ergot alkaloid biosynthesis
easD	gene encoding chanoclavine-I dehydrogenase involved in ergot alkaloid biosynthesis
easE	gene encoding chanoclavine-I synthase involved in ergot alkaloid biosynthesis

easF	gene encoding DMAT *N*-methyltransferase involved in ergot alkaloid biosynthesis
easG	gene encoding reductase involved in ergot alkaloid biosynthesis
easH1	gene encoding dioxygenase involved in ergot alkaloid biosynthesis
ER	ear rot
FHB	*Fusarium* head blight or scab
FOSC	*Fusarium oxysporum* species complex
fw	forward
GA	gibberellin acid
gDNA	genomic DNA
gRNA	guide RNA
GUS	gene encoding β-glucuronidase
*hcp*A	gene encoding nonribosomal peptide synthases involved in the biosynthesis of penicillin
HDR	homologous directed repair
HDV	hepatitis delta virus
HH	hammerhead
HIF	homologous integration frequency
HR	homologous recombination
HRM	high-resolution melting
IAA	indole-3-acetic acid
IAAId	indole-3-acetaldehyde
IAM	indole-3-acetamide
IAN	indole-3-acetonitrile
IDEAA	indel detection by amplification analysis
IPTG	isopropyl β-D-1-thiogalactopyranoside
IPyA	indole-3-pyruvic acid
lacZ	gene encoding β-galactosidase
lae1	gene encoding a methyltransferase involved in the asexual development and pathogenesis
lovF	gene encoding diketide synthase involved in the biosynthesis of lovastatin
lpsA1	gene encoding nonribosomal lysergyl peptide synthetase LPS1 involved in ergot alkaloid biosynthesis
lpsA2	gene encoding nonribosomal lysergyl peptide synthetase LPS4 involved in ergot alkaloid biosynthesis
lpsB	gene encoding nonribosomal lysergyl peptide synthetase LPS2 involved in ergot alkaloid biosynthesis
lpsC	gene encoding nonribosomal lysergyl peptide synthetase LPS3 involved in ergot alkaloid biosynthesis
MUG	4-methylumbelliferyl-β-D-glucuronide
neo	neomycin phosphotransferase gene
NGS	next generation sequencing
NHEJ	non-homologous end-joining
niaD	gene encoding nitrate reductase
NIV	nivalenol
NLS	nuclear localization signal
OE:Cas9	mutants expressing Cas9
OE:gfp	mutants expressing gfp
OE:gfp_dmaW	mutants expressing dimethylallyltryptophan synthase fused with gfp
OE:TrpE	mutants expressing WT form of α-subunit of anthranilate synthase
OE:TrpE^{S76L}	mutants expressing Trp-resistant form of α-subunit of anthranilate synthase
PAM	protospacer adjacent motifs

*pcb*AB	gene encoding alpha-aminoadipyl-cysteinyl-valine (ACV) synthetase involved in the biosynthesis of penicillin
PCR-RFLP	PCR restriction length polymorphism
*pen*DE	gene encoding acetyl-CoA:isopenicillin N-acetyltransferase involved in the biosynthesis of penicillin
pks17	gene encoding polyketide synthetase involved in the biosynthesis of green conidial pigment
PMT	protoplast-mediated transformation
PNPG	p-nitrophenyl-β-D-glucuronide
pyr4/pyrG	gene encoding orotidine 5´-phosphate decarboxylase involved in pyrimidine biosynthesis
rev	reverse
*roq*A	gene encoding nonribosomal peptide synthases involved in the biosynthesis of penicillin
RR	root rot
RT	room temperature
sC	gene encoding ATP-sulphurylase
sgRNA	single guide RNA
SM cluster	secondary metabolite cluster
SSCP	single-stranded conformational polymorphism
SV40NLS	nuclear localization signal from Simian virus 40
TAM	tryptamine
tracrRNA	transactivating CRISPR RNA
TIDE	tracking indels by decomposition
TrpB	gene encoding tryptophan synthase involved in Trp biosynthesis
TrpC	gene encoding a trifunctional peptide involved in Trp biosynthesis constisting of β-subunit od anthtranilate synthase, phosphoribosylanthranilate isomerase and indole-3-glycerol-phosphate synthase
TrpD	gene encoding anthranilate phosphoribosyltransferase involved in Trp biosynthesis
TrpE	gene encoding α-subunit od anthtranilate synthase involved in Trp biosynthesis
vib1	gene encoding a transcription factor involved in cellulose production
WT	wild type
X-gal	5-bromo-4-chloro-3-indolyl-β-D-galactopyranoside
X-Gluc	5-bromo-4-chloro-3-indolyl glucuronide
yA	gene encoding p-diphenol oxidase involved in the biosynthesis of green conidial pigment
ZEA	zearalenone

9 List of publications

Kind S., Hinsch J., Vrabka J., Hradilová M., Majeská-Čudejková M., Tudzynski P., Galuszka P. (2018): Manipulation of cytokinin level in the ergot fungus *Claviceps purpurea* emphasizes its contribution to virulence. *Current Genetics* **64**, 1-17. https://doi.org/10.1007/s00294-018-0847-3. IF – 3.574.

Vrabka J., Niehaus E. M., Münsterkötter M., Proctor R. H., Brown D. W., Novák O., Pěnčík A., Tarkowská D., Hromadová K., Hradilová M., Oklešťková J., Oren-Young L., Idan Y., Sharon A., Maymon M., Elazar M., Freeman S., Güldener U., Tudzynski B., Galuszka P., Bergougnoux V. (2019): Production and role of hormones during interaction of *Fusarium* species with maize (*Zea mays* L.) seedlings. *Frontiers in Plant Science* **9**, 1936. https://doi.org/10.3389/fpls.2018.01936. IF – 3.677.

Králová M., Bergougnoux V., Frébort I. (2021): CRISPR/Cas9 genome editing in ergot fungus *Claviceps purpurea*. *Journal of Biotechnology* **325**, 341-354. https://doi.org/10.1016/j.jbiotec.2020.09.028. IF – 3.503.

Králová M., Frébortová J., Pěnčík A., Frébort I. (2021): Overexpression of Trp-related genes in *Claviceps purpurea* leading to increased ergot alkaloid production. *New Biotechnology* **61**, 69-79. https://doi.org/10.1016/j.nbt.2020.11.003. IF – 4.674.